PhD Programme in Food Systems

Department of Food, Environmental and Nutritional Sciences (DeFENS)

Chemistry and Biochemistry

XXXIV Cycle

Biocatalytic and fermentative approaches for the production of added value compounds using wild type and genetically modified acetic acid bacteria

Pietro Cannazza

R12389

Tutor: Prof. Francesco Molinari

Dean: Prof. Diego Mora

2020/2021

Table of contents

Abstract

This PhD thesis is divided into four chapters that report the development of different microbial biocatalysts aimed at the valorization of food and biotechnological industrial by-products. The experimental parts are preceded by an introduction aimed to give a background on the impact of biocatalysis on green chemistry and, more generally on circular economy, together with a systematic review of the main molecular biology approaches employed to genetically engineer acetic acid bacteria.

The second chapter reports the optimization of a biocatalytic system for the regioselective hydroxylation of different terpenes employing a *Mycobacterium sp.* CYP153A6 monoxygenase. In chapter 3 and in chapter 4 is described the development of different recombinant acetic acid bacteria strains, aimed at the production of highly added value products, such as perillic acid, starting from limonene, a cheap and highly available substrate derived from the agro-food industry. Limonene was employed as a pure compound (chapter 3) or via fermentation of orange peel wastes (chapter 4). The last chapter deals with the isolation and characterization of a bacterial cellulose (BC) producer strain, namely *Komagataeibacter rhaeticus ENS9b,* able to produce BC from acetate and crude glycerol, a by-product from the biodiesel production process.

Abbreviations

AAB: Acetic acid bacteria
DH: Dehydrogenase
ADH Alcohol Dehydrogenase
ALDH: Aldehyde dehydrogenase
GLDH: Glucose Dehydrogenase
GRAS: Generally Recognized As Safe
ORF: Open Reading Frame
QPS: Qualified presumption of safety
LPS: Lipopolysaccharide
NICE: Nisin-controlled expression
UV: Ultraviolet
PA: Perillyl alcohol
PAL: Perillyl aldehyde
PAC: Perillic acid
PQQ: Pyrroloquinoline quinone
PPP: Pentose Phosphate Pathway
EDP: Entner–Doudoroff pathway
Fdh: Formate Dehydrogenase
BCsA: Bacterial cellulose synthase subunit A
BCsB: Bacterial cellulose synthase sub. B
BCsC: Bacterial cellulose synthase subunit C
BCsD: Bacterial cellulose synthase subunit A
CE: Circular economy
LBA: Lactobionic acid

Chapter 1

Introduction

Circular economy and green chemistry

The concept of “sustainable development” was introduced for the first time in 1987 by the World Commission on Environment and Development (WCED) with the report “Our Common Future” or “Brundtland Report” which defined the sustainability concept as “The development that meets the needs of the present generation without compromising the needs of future generations to meet their own needs”. With this report, the main concepts regarding sustainability were pointed out together with the main causes of environmental issues which were attributed to the non-sustainable production of northern countries and to the poverty of southern regions (Brundtland 1987).

After the first reports about the sustainability of industrial production at the end of the 80s the sensitivity of society to environmental issues started to rise and the first reports regarding environmental issues were published, with particular interest in the environmental impact of chemical manufactures. From the mid-80s, it was emphasized the importance of reducing the environmental impact of “stoichiometric” processes technologies in fine and bulk organic chemical manufacturers due to excessive amounts of inorganic wastes and pushed to replace them with cleaner, catalytic alternatives. The E factor was propounded to point out the unacceptability, in terms of environmental impact, of the traditional chemical industries. This parameter describes the amount of by-products produced per kg of final product and goes beyond the concept of selectivity (yield of product divided by the amount of employed substrate) which does not consider the amount of waste generated in a process (R. A. Sheldon, 1997 and R. A. Sheldon, 1996).

Within the sustainability concept, only in 1998 the term “Green chemistry”, already introduced in the previous years by chemicals manufacture as “clean chemistry”, was spawned by Anastas (Anastas P. T., Warner, J. C., eds Green Chemistry: Theory and Practice, 2013). Anastas systematized the main

concept of green chemistry through twelve fundamental principles which are here reported in Table 1.

Twelve fundamental principles of green chemistry
1. Waste prevention instead of remediation
2. Atom efficiency
3. Less hazardous materials
4. Safer products by design
5. Innocuous solvents and auxiliaries
6. Energy efficient by design
7. Preferably renewable raw materials
8. Shorter synthesis (avoid derivatization)
9. Catalytic rather than stoichiometric reagents
10. Design products for degradation
11. Analytical methodologies for pollution prevention
12. Inherently safer processes

***Table 1**: The principles of green chemistry (Anastas, 2013)*

The concept of sustainability is strictly correlated to the industrial model of circular economy (CE). CE was defined (Ellen Macarthur Foundation, 2013) as “an industrial economy that is restorative or regenerative by intention and design” and it represents the opposite and the solution of the linear economy model which is based on production, consumption and waste (Figure 1) (*TOWARDS THE CIRCULAR ECONOMY, 2013*).

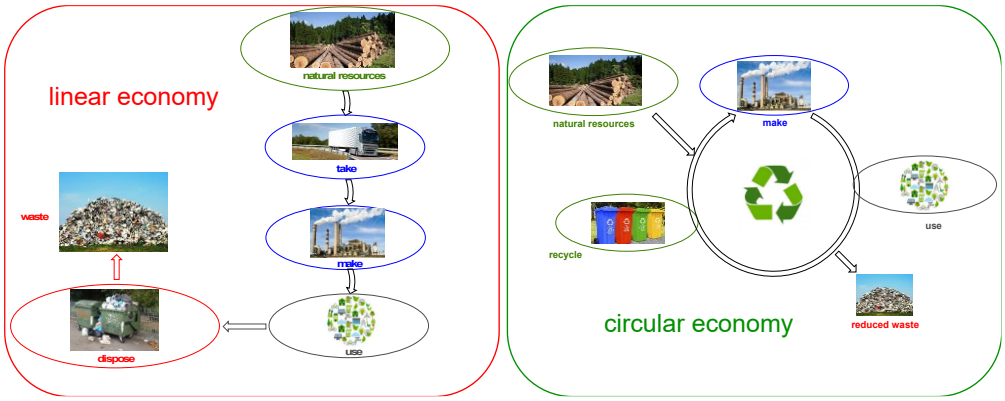

Figure 1. *Schematic representation of linear and circular economy models*

On the contrary, CE was born with the observation that fossil resources are limited and with the intention to build a new economic model based on the concept of reuse of natural resources along the manufacturing processes. In this sense, CE is also defined as the "Realization of closed loop material flow in the whole economic system" (Geng & Doberstein, 2010). CE is based on the main concept of minimization of the inputs (intended as feedstocks and energy), the wastes and the emissions during a manufacturing process by the auto regeneration of the resources. The CE concept relies on three main concepts which are reported here:

1) preservation of the natural capital;
2) optimization of resources yields meaning;
3) improvement of system effectiveness.

Preservation of the natural capital implies the cautious utilization of limited resources such as fossil fuels and the simultaneous push to the development and exploitation of alternative renewable energy resources. The latter two points overcome the concept of waste valorization with the idea of designing an industrial process specifically tailored to prevent leakages of raw materials to maximize resources utilization.

Biocatalysis

Within the framework of green chemistry, biocatalysis is considered a potentially sustainable complement to conventional synthesis. Biocatalysis is defined as the employment of whole cells or isolated enzymes to catalyze chemical reactions (Woodley, 2020). Chemical reactions performed with biocatalysts are called biotransformation or bioconversion; biotransformations are carried out under mild reaction conditions, usually without the employment of troublesome organic solvent, heavy metal catalysts and harsh reaction conditions (Patel, 2016)**.** Biocatalysts catalyze chemical reactions often in a chemo-, regio- and stereoselective manner and are progressively replacing chemical processes in some industries (S. Wu et al., 2021). Besides the clear benefits deriving from safety and selectivity above described, another advantage is the possibility to prepare improved biocatalysts exploiting the rapid increase of useful bioinformatics tools, the robotization of canonical laboratory procedures which enable fast screening of molecules or enzymes, and the development of highly efficient mutagenesis methods. The improvement of a biocatalyst is based on the concept of tailoring the biocatalyst according to the process needs in terms of substrate specificity, reaction environment and technological needs (Bell et al., 2021). If historically biocatalytic operations along an industrial process were designed according to the characteristics of employed enzymes and microorganisms, in newly born processes biocatalysts often are engineered to maximize process productivity before the industrial facility assessment (Devine et al., 2018) (Table 2).

Advantages	Disadvantages
Possibility to link consecutive enzymatic steps	Requirement of certain parameters: pH, temperature, ionic strength, substrate concentrations
Chemo -, regio-, enantioselectivity	Enzymes have their highest catalytic activity in water
Methods to engineer biocatalysts	Enzymes sometimes require expensive cofactors
Very efficient catalysts	Inhibition by substrates or products
Catalysis of a wide spectrum of reactions	Catalyst recovery and reuse
Absence of heavy metals, hazardous reagents/solvents	

***Table 2**. Common pros and cons of biocatalysis* (Faber, 2011).

Acetic acid bacteria: their utilization through the centuries, from vinegar production to modern biocatalysts

The utilization of AAB throughout human history, has always been linked with the production of vinegar and similar fermented beverages or foods. Generally speaking, all types of vinegar are derived from a two-step fermentation process. The first step, namely alcoholic fermentation, is operated by yeasts while the second fermentation step, called acetic fermentation is due to AAB. The oldest traces of fermented food and beverages date back to the Neolithic period (8500 – 4000 A.C.). In the mountain “Zagros” Persian region were found large urns containing residues of wine production. Obviously, the oldest traces of fermented fruits came from spontaneous fermentation of acid- and sugar rich substrates such as fruit juices. These kinds of natural culture media are naturally colonized by acid tolerant yeasts, lactic acid bacteria (LAB) and AAB. Different microbial strains, depending on the nature and origin of the sugar rich original substrate might be involved in vinegar production. Among all the AAB genera, *Acetobacter* and *Komagataeibacter* (previously *Gluconacetobacter)* are the ones most employed for vinegar industrial production and as well the mostly found genera in spontaneous fermentation of alcoholic substrates (Wilkins et al., 2007).

Wine and vinegar are currently defined and recognized as separate products, each characterized by peculiar characteristics since they are derived from two separate processes. Differently, the same differentiation presumably was not clear in the ancient times because the microorganisms responsible for the fermentation were already colonizing the fruits employed for wort production and because of the sequentiality of the two fermentation steps. However, a primordial differentiation from wine and vinegar was probably known. Traces of clay in the fermentation vessels probably demonstrate that the acid fermentation by AAB might be prevented by adding natural preservatives which stopped or delayed AAB growth and the consequent acidification of wines or similar alcoholic beverages.

Egyptians were probably the first society to employ vinegar as an actual food. The fact that wine when exposed to air can easily be transformed into a sour product called “HmD” or “Hemedj” was well established in egyptian society. In ancient times HmD and similar sour products were employed as food preservatives or consumed mixed with water as a beverage. Hippocrates, nowadays considered as the father of Medicine, used to give vinegar as an effective remedy against respiratory diseases such as cold and cough and even for wound and sore healing. It can be affirmed that vinegar was commonly used in all the ancient cultures for different purposes. Due to its high acidity it was employed as part of the diet as a beverage, dressing agent, food preservative and sometimes even as corrosive and a solubilizing agent (Solieri Lisa, 2009).

Then, from the Middle ages moving forward to the Renaissance, new utilization of vinegar got popular. During the Middle ages it was employed to chill and clear firing iron-made cannons and, during the bubonic plague that broke out in 1665 in London, it was employed as a systematic method to disinfect hands and coins to limit the spread of the Plague pandemic. Together with new employment of vinegar, due to the increased demand for the product, the first large scale production was started in 1934 in Orleans, hence the name “Orleans method” of the production process. In this kind of production, which

at the time was kept secret, the fermentation was taking place in wooden casks and regularly the main part of the vinegar (85%) was replaced by fresh wine to keep a product storage in the production mall. The process can be defined as one of the first continuous industrial processes since the fermentation process is never stopped even if the time required to recover the desired product may exceed several months.

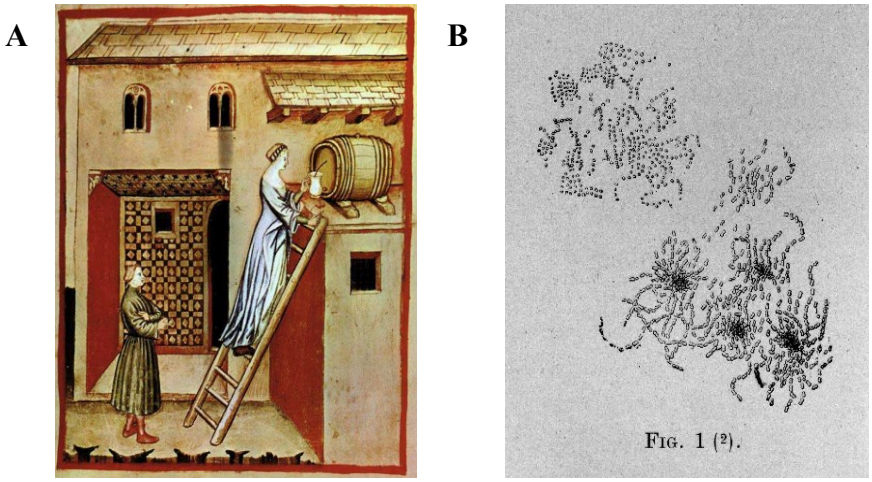

***Figure 2**. **A**: Lady climbing a ladder and drawing Vinegar from a cask, Tacuinum Sanitatis Casanatense,1450 circa. **B:** Earlier representation of AAB isolated by Louis Pasteur, Mémoire sur la fermentation acétique* (Pasteur, 1864).

The first findings about the bacteria involved in vinegar fermentation date back to the XVIII century with the advent of microbiology. In 1822 Christian Persoon was the first to identify a microbe, called *Mycoderma aceti*, as the responsible of this kind of fermentation. At the end of the 19th century Louis Pasteur with the publication of his studies in 1864 established the reasons for the production of acetic acid from sugars corroborating Persoon's findings which were still debated within the scientific community. The French scientist described for the first time the microbial growth of a microbe and, with a scientific methodology which today we would call "microbiology", he isolated AAB strains able to ferment ethanol into acetic acid. "*Mycoderma pasteurianum*" and "*Bacterium kützingianum*" were the names of the strains he isolated respectively from the mother of vinegar and from beer (Pasteur,

1864). In 1720 it was proposed for the first time a fast fermentation process called *Boerhave method* which required 3-4 weeks of fermentation to get the desired product. Boerhave's intuition was to increase the surface area of the fermenter in contact with air employing wood curls in the fermentation casks. During the industrial revolution taking advantage of Pasteur's finding and of increased industrialization of productive processes, quicker fermentation processes employing AAB were developed. Then, with the automatization of industrial processes and thanks to new scientific findings, many innovations were quickly applied in industrial vinegar production. The most important improvement in industrial vinegar manufacture probably dates back to 1929, when forced aeration was introduced in the fermentation vessels. Modern fermentation called submerged cultures are carried out in stainless-steel agitated tanks where AAB are entrapped in the fermentation medium and receive oxygen from the bottom of the fermenter with a rotating aerator. Modern fermenters contain up to 500 hL of culture medium and allow to reach the required acidity in less than 24 hours (Solieri Lisa, 2009).

Other industrial applications

Acetic acid bacteria, other than vinegar production, are exploited at industrial level to produce many molecules and added value materials. Here are reported the most significant ones from an industrial perspective.

Vitamin C

AAB due to their peculiar ability to perform incomplete oxidation or "oxidative fermentation" of carbon substrates have been widely employed in the biotechnological industry for the production of carboxylic acid and ketones. In particular, *Gluconobacter* strains are used for the regio- and stereo-selective oxidation of chiral and prochiral alcohol and sugars. A clear example of AAB usefulness at industrial level is the oxidation of D-sorbitol to L-sorbose in the ascorbic acid (vitamin C) production process. (Matsushita k., Toyama h., Tonouchi n. 2016). Vitamin C is a crucial molecule for human and animal nutrition. It is involved in the synthesis of collagen in connective tissue and its

deficiency is the cause of scurvy. In addition, it is employed as an antioxidant in the food and pharmaceutical industry. Vitamin C annual production is estimated at about 100.000 tons and is made with the so-called Reichstein process introduced in 1934 by F. Hoffmann-La Roche. The process includes a microbial step catalyzed by *G. oxydans* for the regioselective oxidation of D-sorbitol to L-sorbose and six chemical reaction steps (figure 2) (Deppenmeier, hoffmeister, and Prust 2002). Vit C synthesis starts with the reduction by hydrogenation of D-glucose to D-sorbitol, followed by *G. oxydans* oxidation to L-sorbose crystallization and protection with acetone to form sorbose diacetone. Sorbose diacetone is then oxidized by a platinum catalyst and deprotected to give 2-keto-L-gluonic acid. Then, after esterification with methanol and lactonization, the final product is produced (Matsushita k., Toyama h., Tonouchi n. 2016).

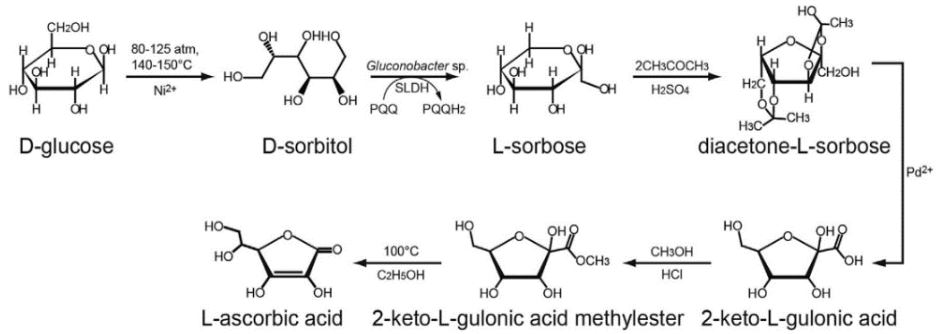

Figure 3: *Reichstein process for L-ascorbic acid production from D-glucose* (Wang et al., 2018)

Gluconic acid and keto-gluconic acid

D-gluconic acid (GA), 2-keto-D-gluconic acid (2KGA), 5-keto-D-gluconic (5KGA) and 2,5-diketo-D-gluconic acid (2,5 KGA) are the oxidation products derived from D-glucose oxidation by *Gluconobacter* strains. 2KGA, 5KGA and 2,5KGA are naturally produced by *Gluconobacter* strains and the regioselectivity of the reaction is dependent on the employed strain. Glucose oxidation products find numerous applications in the food, pharmaceutical, and chemical industry. GA is employed as a food additive as an acidity

regulator (E574), as an ingredient for multiple formulations such as quinine gluconate and ferrous gluconate employed, respectively, for malaria and anemia treatments. 2KGA is a building block in the stereoselective synthesis of heterocyclic, while 5KGA is a precursor of the synthesis of alimentary industry-relevant compounds, such as tartaric acid and xylaric acid (Saichana et al. 2015 and Matsushita k., Toyama h., Tonouchi n. 2016).

Dihydroxyacetone

1,3-dihydroxyacetone (DHA) is a commercially important chemical compound employed in the pharmaceutical industry. It has a wide range of applications, being found in cosmetics as tanning agent formulations and is an important precursor building block for various surfactants and fine chemicals such as 1,2-propylene glycol or lactic acid and surfactants. *Gluconobacter oxydans* is the strain industrially employed to produce dihydroxyacetone (DHA) from glycerol. Glycerol, the feedstock of the reaction is a cheap and highly available molecule derived as a by-product from the biodiesel production and from hydrolysis of triglycerides (Saichana et al. 2015 and Matsushita k., Toyama h., Tonouchi n. 2016). The oxidative reaction carried out by *Gluconobacter oxydans* is catalyzed by a membrane-bound, PQQ dependent glycerol dehydrogenase (Deppenmeier et al., 2002).

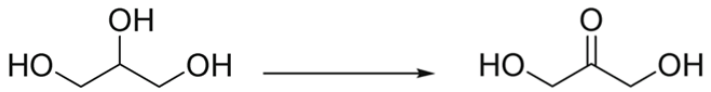

Figure 4: *Dihydroxyacetone from glycerol catalyzed by Gluconobacter oxydans*

Lactobionic acid

Lactobionic acid (4-O-β-galactopyranosyl-D-gluconic acid or LBA) is an aldonic sugar acid derived from galactose by a membrane-bound PQQ-GDH from Acetobacter species found is milk fermenting AAB such as *Acetobacter orientalis* KYG22 and *Gluconobacter cerinus* UTBC-427 (Alonso, Rendueles, and Díaz 2013 and Deppenmeier, Hoffmeister, and Prust 2002). LBA is

employed as an antioxidant, stabilizing and chelating agent in pharmaceutical and food formulations. *Gluconobacter cerinus* is the strain currently employed, (with a patented process) as a microbial platform for industrial production of LBA (Alonso et al., 2013)**.**

Exo-polysaccharides: Bacterial cellulose, dextran and fructan

Many acetic acid bacteria strains are known to produce exopolysaccharides from a wide range of carbon sources. Dextran (or Levan) is a polymer produced by some AAB strains made by glucose monomers linked by α-1,6 glycosidic bonds. Fructosyltransferases (Ftfs) is the enzyme which catalyses the polymerization of the glyocosidic branch. *Gluconobacter frateurii, Gluconobacter cerinus, Kozakia baliensis and Neoasaia chiangmaiensis* are the AAB strains demonstrated to secrete large quantities of dextran (Jakob et al., 2013). Hydrocolloids such as levan and bacterial cellulose are employed in many industrial applications for their high water-retention capacity and physical properties. More detailed information about bacterial cellulose will be later reported in chapter 5.

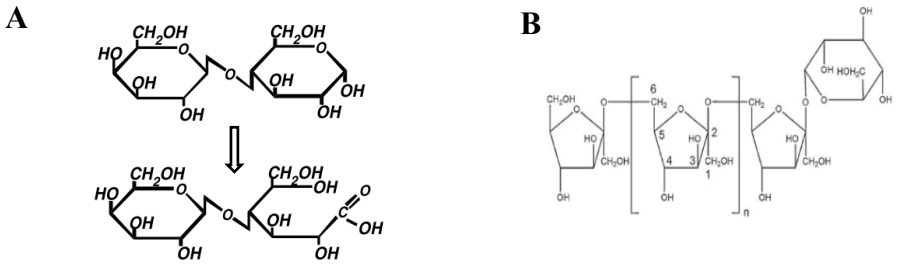

Figure 5. A**:** *Lactobionic acid from lactose catalyzed by Gluconobacter cerinus (Alonso 2013)* ***B:*** *Proposed structure of dextran produced by G. frateurii, G. cerinus, N. chiangmaiensis and K. baliensis proposed by Jakob* (Jakob et al., 2013).

Acetic acid bacteria: unconventional microbial hosts for gene expression

Thanks to the availability of tailor-made expression systems and cheap oligonucleotide synthesis services, nowadays the expression of recombinant proteins has become an accessible task in terms of time, equipment, and affordability. Historically, researchers have utilized as host chassis, model organisms such as *E. coli, B. subtilis*, S*accharomyces cerevisiae* and mammalian cells due to the high accessibility of ready-to-use molecular biology tools, well-established expression procedures and the deep knowledge of their complete genomes as their physiological and biochemical characteristics (Schmidt, 2004). Decades of biotechnological studies on genetic elements, metabolic and proteomic aspects of those organisms led to a deep spread in biotechnological industries of those above-mentioned expression systems.

Today *E. coli* and mammalian cells are the most utilized organisms for recombinant protein expression; they are found in laboratory-scale utilization and in industrial production of biopharmaceutical products. Most of the vaccines, biomolecules, peptides are produced with typical host organisms. If historically *E. coli* was the main character in the industrial scenario for the production of biomolecules, more recently mammalian expression systems are overtaking bacterial recombinant production especially in monoclonal antibodies production. According to the “Biopharmaceutical benchmarks 2018”, the main part of new biopharmaceutical active ingredients launched on the market from January 2014 to July 2018 were recombinant proteins (62 of the 71), which 84% was expressed in mammalian cell lines against remaining that was produced using *E. coli* and *S. cerevisiae* (Walsh 2018, Legastelois et al. 2017).

If the use of classical expression systems is certainly simpler, sometimes the employment of unconventional organisms can be advantageous for some applications compared to traditional recombinant hosts. The use of non-model

hosts allows to exploit the natural features of the organism and to achieve biotechnological applications that would be tricky with classical recombinant host-strains. Non-*E. coli* bacteria, plant cells, filamentous fungi and insect cells are the most studied unconventional host organisms. The main advantages of those atypical systems are the enhanced folding together specific activity of expressed heterologous proteins, the physiological peculiarities of the hosts such as high resistance to extreme conditions and the legislative status (GRAS) of the host organism, an aspect that is always considered for the use of recombinants in food manufactures.

Among yeast-based expression systems, *Pichia pastoris* is becoming the most promising host organism for the expression of basidiomycetous and ascomycetous oxidoreductases. Thanks to this yeast, elevated extracellular expression of glycosylated and highly functional enzymes can be reached, his genetic manipulation is quite established and fermentation steps can be easily scaled at semi-industrial level (Spohner et al., 2015). Moreover, *P. pastoris* was recently recognized as safe, achieving GRAS status by FDA that approved his use for recombinant protein expression therefore today is used for the industrial production of numerous enzymes (Macauley-Patrick et al., 2005).

The soft-rot filamentous fungus *Trichoderma reseei* is very attractive from an industrial point of view for the high amount of extracellular protein naturally secreted by the fungus. Cellulases, the most secreted proteins by *Trichoderma reseei*, allow good growth yields on raw agricultural and food industry residues degrading high molecular weight and insoluble polysaccharides (Jun et al., 2011). Those implications, with the ability to perform post-translational modifications, make this fungus a suitable host for the expression of recombinant proteins, especially cellulosic enzymes like cellobiose dehydrogenase (CDH), laccases, cellulases and lytic polysaccharide monooxygenases (LPMO); all enzymes naturally secreted by fungi to gain carbon sources from lignocellulosic substrates (Collén et al., 2005).

Food grade, “clean” recombinant lactic acid bacteria LAB are obtained by chromosomal integration and deletion, are currently utilized in food and pharma industries. *Lactococcus lactis* has become a model organism due to his extensive genetic and metabolic knowledge. Its inability to secrete lipopolysaccharide (LPS) or extracellular proteases, his capability to secrete a high amount of proteins and his GRAS status make this strain an excellent probiotic and make possible the expression or delivery of heterologous anti-inflammatory bioactives in the human gastrointestinal tract (Bron 2018 and Peterbauer 2011). The Nisin-controlled Gene Expression system (NICE) is probably the most used expression system for *L. lactis*, the strain is characterized by the genomic insertion of nisR and nisK genes, responsible for the regulation of nisin expression (Carvalho et al., 2017) and is considered the best expression system for food-grade recombinant LAB (Le Loir et al., 2005).

We have seen before how wide is the use of AAB as biocatalysts, but hitherto only a few examples of metabolically engineered AABs are used for practical scopes, both at academic and industrial levels. In the last few years, some research groups have started to utilize various AAB strains for the expression of recombinant proteins with different aims. The availability of genetic elements and transformation procedures until now are still fragmented, and even literature sources are few and sometimes even contradictory. This chapter is aimed to overview the peculiar characteristics of industrial appealing AAB and to analyze the main molecular biology techniques historically utilized for AAB, such as chromosomal integration systems, adaptive laboratory evolution methods and host vector transformation. The overall novelty and effectiveness as main issues in terms of safety, sustainability and possible applicability of the reported recombination systems will be underlined.

Advantages
Oxidation products are released into the culture media
Regioselectivity and enantioselectivity of (membrane) dehydrogenases
Generally recognized as safe (GRAS) strain
High resistance to environment characterized by high concentration of solutes and low pH
Easy scalability of fermentation processes for bulk production (strains already utilized in industrial processes)
Availability of many strains, wide range of physiological and morphological varieties
Fast genetic adaptation
Cellulose production
Disadvantages
Slow growth rate
Resistance of some strains to high antibiotic concentrations
Low availability of genetic toolkits for gene cloning and expression

Table 3 *Advantages and disadvantages in the utilization of AAB as microbial hosts for protein expression.*

Conventional breeding – laboratory adaptation

Classical mutagenesis consists of forcing natural breeding in microbial communities with physical or chemical treatments and isolating mutants carrying the desired phenotype. Mutation events are identified by researchers as “transversion” that occurs when a purine is replaced by another purine or a pyrimidine by another pyrimidine and “transition” when a purine is replaced by a pyrimidine (Freese, 1961). Even if this kind of mutagenesis is non-directional, non-specific and requires extensive screenings, it was deeply utilized for many microorganisms in laboratories and found fortune in industrial utilization because mutated strains can be adopted in large scale processes, including in the food industry, due to the maintenance of non-GMO and GRAS status after mutative treatments (J. X. Gao et al. 2017 and L. Gao et al. 2020). This technique was applied for the adaptation of AAB to different environmental stresses employing chemical and physical mutative agents. Canonical random mutations using UV treatment coupled with an acidic shock were carried out to obtain an *Acetobacter pasteurianus* mutant strain with higher resistance to acids and with enhanced acetic acid production (Qi et al., 2014). A similar approach was successfully employed to enhance *K. xylinus subsp. sucrofermentans* growth and BC production (Ishikawa et al., 1995). Similarly, UV mutagenesis was applied to increase BC productivity of *K. xylinus*, associated with an ethyl methanesulfonate (EMS) treatment, a chemical mutagenic agent that causes a single base pair change in genomic DNA (Hungund & Gupta, 2010).

To accelerate *Acetobacter* sp. phenotype evolution to improve ethanol and acetic acid tolerance, hydroxylamine hydrochloride and ultraviolet mutagenesis were coupled to gain an initial mutant library, whose genomes were then shuffled using the protoplast fusion technique (Y. X. Zhang et al., 2002 and Zheng et al. 2010). After three successive rounds of shuffling by protoplast fusion and subsequent screening on ethanol selective plates, mutants with significantly improved ethanol tolerance and acetic acid

production were found. Furthermore, the authors, using the mutant strains in a vinegar fermentation, detected an improvement of the flavor of the final product, an enhancement of the main volatile and non-volatile organic acids responsible for vinegar sour taste and of volatile flavor components such as acetate esters that were notably higher utilizing obtained mutant compared to the wild-type strain. Furthermore, finer approaches based on genome shuffling have been applied to generate hybrid strains with enhanced physiological capabilities (Chhabra & Keasling, 2019). The first protoplast fusion of an AAB strain was reported in 1992: an hybrid organism was constructed by an intergeneric protoplast fusion between *G. oxydans* and *Corynebacterium sp.* (Verma et al., 1992).

Adaptive laboratory evolution

AAB are known for their peculiar genetic instability that makes those microorganisms highly adaptive to new environments. The frequent mutations of the phenotypic tracts occurring along repetitive cultivations are caused by spontaneous genetic modifications that are very frequent in acetobacteraceae. Those events represent a hurdle for industrial employment that requires highly standardized fermentation parameters. These peculiar features of AAB have been always taken into account in vinegar manufacturing productions and this is the reason why new fermentation batches for traditional vinegar production are inoculated from old tanks (Azuma et al., 2009).

The mutation of physiological peculiarities has been often observed in *Acetobacter* and defined as “temporal acclimation” or “heritable adaptation”. A clear example of the phenomenon is presented by Ohomri who described the reduced acetic acid resistance and ethanol oxidizing ability of *Acetobacter aceti* when cultured in a liquid medium containing ethanol (Ohmori et al., 1982). A similar event was reported by Steel who reported the decreased ability of *K. xylinus* to produce BC when sub-cultivated in liquid medium (Steel & Walker, 1957). Those kinds of happenings during AAB daily cultivations

remained unexplained for decades until it was observed the transposition of multiple indigenous insertion sequence elements in a small genome characterized by a high information density (Kondo & Horinouchi, 1997).
The characteristic genetic instability of AAB was further explained by Azuma who showed in the genome of *Acetobacter pasteurianus* NBRC 3283 the presence of numerous motile elements such as 280 transposons and five genes with hyper-mutable tandem repeats (Azuma et al., 2009).

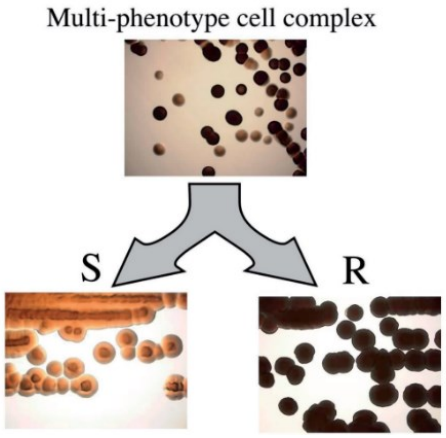

Figure 6*: Phenotypic variations of A. pasteurianus occurred along serial cultivation on Potato solid medium. A multi-phenotype cell texture is clearly visible (R; rough colony and S; smooth)* (Azuma et al., 2009).

Those findings led researchers to improve adaptive laboratory evolution techniques for AAB evolution utilizing stress conditions to introduce mutagenesis. Stress conditions were modulated and tailored depending on the desired mutations. A clear example of the utility of this technique was presented comparing *A. aceti* and *E. coli* growth and acidic resistance in long-term continuous cultures with increased acetate concentrations. After long cultivation in aerobic continuous culture, *E. coli* growth was slightly improved, unlike *A. aceti* that grew in presence of 20% higher acetate concentration compared to its wild type (Steiner & Sauer, 2003). Utilizing the same approach, increased ethanol resistance of *A. pasteurianus* was obtained (Zheng et al., 2015). Similarly, Matsutani increased thermotolerance of *A.*

pasteurianus by *in vitro* adaptation, growing the strain under high temperatures in acidic conditions enhancing fermentation abilities in the isolated strains. Ethanol oxidation and acetic acid-resistance were increased and the physiological mutations were explained by genomic mutations identified by next-generation sequencing analysis (Matsutani et al., 2013). Even if it has been proved that genetic instability and adaptive mutations of AAB are strictly correlated with the transposition of multiple indigenous insertion sequences and similar recombination events, sometimes the acquired or lost phenotypic characteristics of some AAB strains are still not well understood. For instance Hattori (Hattori et al., 2012) obtained an adapted *Gluconobacter* strain able to grow better and produce more L-sorbose compared to the reference strain at 38.5°C. The authors could not find any significant mutation that could explain the acquired phenotypic mutation, including the observation of Sorbose-DH ORF (gene coding for dehydrogenase responsible for sorbose oxidation) of mutated strains and analysis of the genes correlated to the biosynthesis and regulation of PQQ associated with GLDH.

Early attempts to transform acetic acid bacteria

Despite few molecular biology tools such as shuttle vectors suitable for genetic engineering studies of AAB being reported, the utilization of recombinant AAB strains has not spread at industrial and academic level. First molecular biology tools tailored for AAB dates to the 80', when first host-vector systems were constructed starting from native *G. oxydans* and *A. aceti* plasmids. Murooka was the first to attempt to engineer *Gluconobacter* strain by transferring a temperature sensitive plasmid carrying kanamycin resistance from *E. coli* into *G. suboxydans*. (Murooka et al., 1981). Few years later, Fukaya attested the presence of numerous plasmids in many AAB strains, whose modification led to the construction of the first engineered host vector for expression in *A. aceti* (Fukaya & Iwata, 1985, Uozumi & Beppu, 1985, Okumura et al., 1988 and Hayata, 2002) and later in *G. oxydans* (Onouchi et

al., 2003). Together with new expression vectors, novel transformation procedures were described and depending on the studied AAB strain various transformation methods were developed. Initially *A. aceti* strains were transformed with heat shock procedure after $CaCl_2$ or dimethylsulfoxide treatments (Fukaya et al., 2014, Uozumi & Beppu, 1985 and Fukaya et al., 2014), later similar transformation techniques, employing PEG 4.000 solution for cell-washing step, was applied for *Gluconobacter* transformation (Fukaya et al., 1985). AAB transformation efficiency was drastically increased using electroporation, a technique that overpassed over years traditional heat shock transformation methods due to the higher transformation efficiency obtained. On the other side, the drawback of this technique is that the operative conditions must be optimized for each AAB employed strain, because it has been observed that the usage of the same procedure for different AAB strains is often unsuccessful (Tayama et al., 1994 and Wong et al., 1990).

Gluconobacter genus

Great effort was spent by different research groups for the development of genetic engineering techniques suitable for the *Gluconobacter* genus, due to his importance at industrial level. The species is renowned for its ability to incompletely oxidize many substrates such as aliphatic alcohols, sugar and polyols into the corresponding aldehydes, ketones and carboxylic acids. This ability is connected to the presence of numerous dehydrogenases (DH) located on its membrane. More than 75 ORF related to DH were found in his genome. Usually, the oxidation of sugars and alcohols by AAB is associated only with transmembrane alcohol and aldehyde dehydrogenases, while periplasmic and soluble dehydrogenases are being responsible for crucial metabolic reactions.

Strains of *Gluconobacter oxydans* are generally recognized as safe (GRAS) and it is the only species among AAB and almost all gram-negative bacteria to be listed on the “qualified presumption of safety” QPS list by European Food Safety Authority (EFSA) (Lynch et al., 2019). Like almost all AAB, *G.*

oxydans is non-pathogenic for humans and animals, indeed in food industries it is considered a protechnological microorganism. The fast oxidation of sugars and alcohols by *Gluconobacter* species causes fast environment acidification and a depletion of substrates necessary for pathogenic and food-spoiling microorganisms. Only few *Gluconobacter* strains with possible pathogenic properties are reported, but the threat of the strains is not clear since the reported cases regarded immunocompromised individuals with a history of intravenous drug abuse (Lynch et al. 2019, Alauzet et al. 2010, Bassetti et al. 2013). G*luconobacter* genera strains have been frequently utilized as host strains for the expression of alcohol and aldehyde dehydrogenases. The expression of dehydrogenases in AAB is considered optimal because of the physiological natural predisposition to express different membrane associated enzymes (Kallnik et al., 2010). In AAB membrane dehydrogenases are strictly linked to the respiratory chain thanks to ubiquinone (UQ) cofactors based on PQQ prosthetic group, that transfer electrons to ubiquinone oxidase responsible of the reduction of O_2 to H_2O, with the release of 2 protons outside the cell membrane and ATP generation.

In this sense, it has been suggested that, unlike classical cellular metabolism where the substrates are usually used as electron donors for NADH regeneration and metabolic intermediates for anabolic reasons inside the cells, in AAB the destiny of electrons and the generation of intermediates from carbon substrates, are separated. The main part of the energy is derived from incomplete fermentation reactions, only less of the 10% of carbon sources are metabolized inside the cells and mainly utilized for biosynthesis of building blocks, while the main part of carbon substrates is oxidized outside the cells and the derived electrons are sent to ubiquinone oxidase. It was supposed that this metabolic feature could be a result of the adaptation of those microorganisms to environments characterized by high concentrations of solutes such as sugars and acids (Ninla Elmawati Falabiba et al., 2014). Because of the absence of phosphofructokinase, glycolysis in *G. oxydans* is interrupted, and glucose is usually catabolized through the pentose phosphate

pathway (PPP) and sometimes through the Entner-Doudoroff Pathway (EDP). This situation is found in all the AAB as well. Furthermore, ^{13}C-based metabolic flux analysis revealed that *G. oxydans* lacks of succinyl-CoA synthetase and succinate dehydrogenase. The result is an incomplete citric acid cycle and the consequent uncomplete oxidation of substrates to CO_2 and H_2O (Hanke et al., 2013).

Molecular biology as a valuable tool for *G. oxydans* metabolic engineering studies

Peters from Ehrenreich group in München Technische University was probably the first to establish a robust method for the genomic insertion and deletion of heterologous genes into AAB genomic DNA, studying the effect of multi-deletions of many membrane-bound dehydrogenases on *Gluconobater oxydans* 621H physiology and carbon utilization (Peters, Junker, et al., 2013). The author, using different substrates, concluded that even the complete deletion of all membrane-associated dehydrogenases does not represent a hurdle for the strain's growth. More recently researchers from the same research group studied native ADH promoters' strength developing a new molecular biology system for heterologous gene expression in *Gluconobacter* (Peters, Mientus, et al., 2013). Thanks to this tool they investigated substrate specificity of each membrane dehydrogenase found in the G*. oxydans* genome. Firstly, all G*. oxydans* dehydrogenases were contemporaneously deleted from *Gluconobacter* wild type obtaining a multidelected strain. Then, all the previously deleted *G. oxydans* dehydrogenases were singularly overexpressed using the multidelected-engineered strain (Mientus et al., 2017). Doing so, they were able to identify substrate specificity of G*. oxydans* DHs, allowing to distinguish activity and chemical specificity of those, a task that would be impossible using whole cells bioconversion due to the multiple present DH and because many DHs can oxidize the same substrates (Peters, Mientus, et al., 2013).

Kieflr utilized molecular biology techniques to overexpress and deplete metabolic enzymes in order to implement typical *G. oxydans* incomplete pathways (Kiefler et al., 2017). Author's goal was to complete the *G. oxydans* pathway to improve the growth yield on glucose aimed at the minimization of the costs of biomass production. The first rational was the overexpression of succinate dehydrogenase and succinyl-CoA synthetase for complementation of the TCA cycle and deletion of cytosolic glucose dehydrogenase (*gdhS*) and the membrane-bound glucose dehydrogenase (*gdhM*) genes to avoid incomplete oxidation in the culture medium of glucose to gluconic acid (Kiefler et al., 2015). The engineered strain by Kieflr was further implemented by deleting pyruvate decarboxylase gene for prevention of acetaldehyde formation and with a genomic expression of NADH dehydrogenase. Finally, the succinyl-CoA synthetase genes *sucCD* from *Gluconacetobacter diazotrophicus* was integrated and the membrane-associated glucose dehydrogenase was deleted. The final obtained strain resulted in a biomass yield increased by 60 % compared to wild type and acetate accumulation was completely shot down (Kiefler et al., 2017). Those works are a clear example of how molecular biology techniques could be useful tools to implement acetic acid bacteria metabolic pathways and to boost biomass production during fermentation.

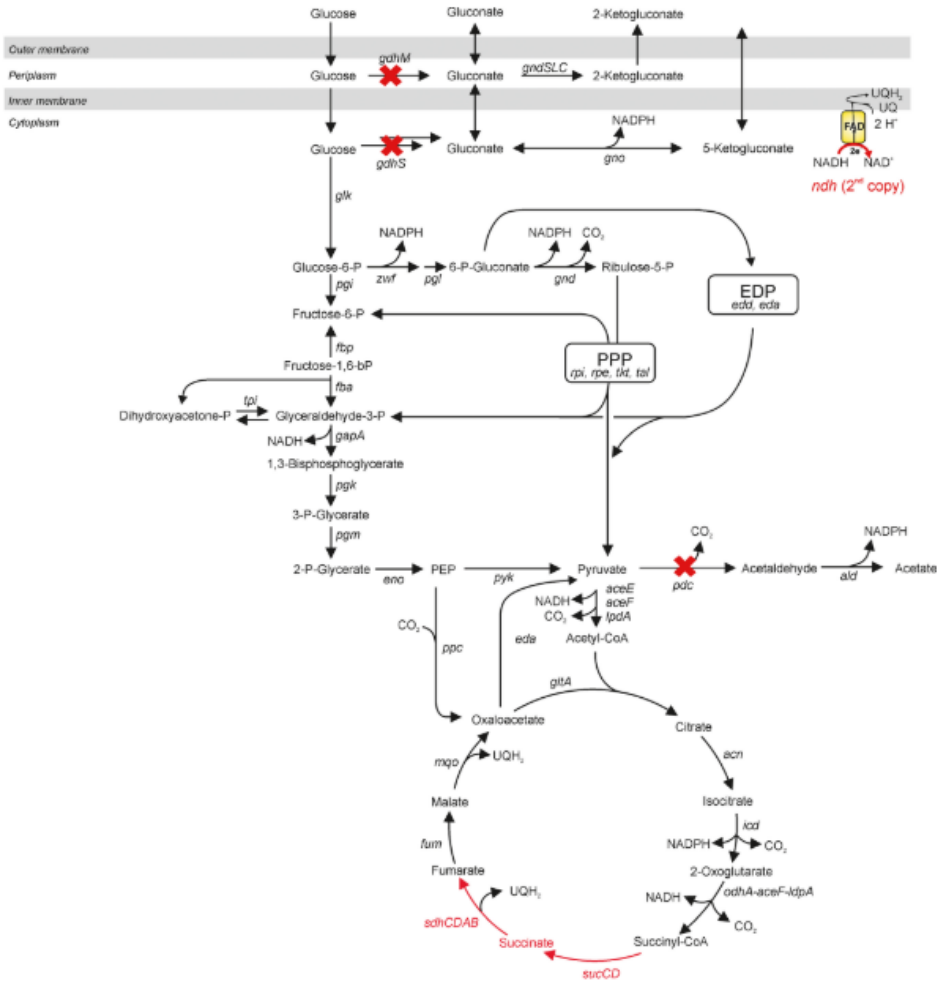

***Figure 7**: Implementation of glucose metabolism in G. oxydans. Red arrows represent introduced enzymes, red crosses represent deleted genes* (Kiefler et al., 2017).

Engineering of tailored plasmid vectors *for G. oxydans*

Schweigher group from Wisconsin University since 2010 set a point on the construction of molecular biology tools for AAB developing different plasmids for homologous and heterologous expression for *G. oxydans*. The construction of a tailored expression vectors for *G. oxydans* was possible using of a broad-host range vector (pBBR1MCS-2) with two constitutive promoters from *G. oxydans* ribosomal proteins for (Kallnik et al., 2010). Once assessed the strength of the two promoters, an useful and well described tool

for protein expression was obtained. The new genetic tool was then tested for the expression of the homologous membrane-bound PQQ-dependent glucose dehydrogenase (Meyer et al., 2013). Since the recombinant strain resulted with high GDH activity (13,300 mU/mg) and high rate of oxygen consumption (1,075±64 nmol O_2 min^{-1} mg^{-1}), the strain was proposed as a possible whole-cell biocatalyst for gluconate production. Similar GDH overexpression was previously reported by Merfort employing the same plasmid, but the attested activity of recombinant strain was lower due to the absence of a native *G. oxydans* promoter downstream the GDH gene (Merfort, Herrmann, Ha, et al., 2006).

The first genetic system for the expression in AAB of soluble cytoplasmic proteins was introduced by Kallnik (Kallnik et al., 2010). The ability to produce gluconic acid from glucose of *G. oxydans,* which was already enhanced by the overexpression of membrane associated dehydrogenases (Merfort, Herrmann, Bringer-Meyer, et al., 2006), was further implemented by Koshiow which developed a molecular biology system for the periplasmic expression of recombinant proteins (Kosciow et al., 2014). The authors constructed different plasmid vectors with many signal sequences downstream an alkaline phosphatase gene to assess the translocation efficiency of the selected leader sequences. Once the cytoplasmic translocation was assessed, alkaline phosphatase was replaced by an *E. coli* trehalose hydrolase and in such a way a *G. oxydans* strain able hydrolyze disaccharides was obtained. The same rationale was applied by Siemen (Siemen et al., 2018) that cloned a *Zymomonas mobilis* sucrose hydrolase (sacC) in G*luconobacter oxydans* strain SACC and coupled recombinant sacC *gluconobacter oxydans* strain with a recombinant *G. oxydans* expressing the *G. japonicus* fructose dehydrogenase (Fdh). The resulting microbial system could efficiently hydrolyze sucrose from sugar beet extract and oxidize the resulting fructose to the low-calorie sweetener 5-keto-fructose. Later, Blank from Schweiger research group, optimized a *G. oxydans* expression plasmids engineering a surface display system for the expression of recombinant enzymes anchored

outside the cell membrane (Blank & Schweiger, 2018). A chimeric *Pseudomonas aeruginosa* outer membrane porin F (OprF) connected with alkaline phosphatase (PhoA) with different cleavable linkers was expressed in *G. oxydans*. The expression of PhoA anchored outside the membrane was confirmed with a proteolytic cleavage of the linker and the system was tested using a wide list of flexible and rigid linkers. Even if the presence of the display system resulted in slightly increased recombinant PhoA activity, the system may represent a useful tool for genetic engineering of *G. oxydans* and for biocatalytic applications. Schwaiger was able to give a good impulse to AAB recombination study thanks to the new genetic engineering tools, describing many useful genetic elements for expression of cytoplasmic, periplasmic, membrane associated enzymes in *G. oxydans.* (The problem remains the availability of those tools since there are not any on-line platforms for their physical retrieval).

Characterization of genetic elements for AAB

As described by Mayer the characterization of promoter strength is crucial for the recombinant gene expression in AAB (Meyer et al., 2013). Since the strength of a defined promoter can vary depending on the host strain, the characterization of homologous and heterologous promoters is necessary for the construction of suitable expression vectors for AAB (Saito et al., 1997).
The traditional screening approaches aimed at the identification of native promoters and terminators consists in the amplification from (AAB) genome, the insertion of the putative regions in the expression system and finally the characterization of the obtained plasmid vector. The rationale of the technique is based on the construction of a “promoter probe plasmid” where a reporter gene is generally inserted between the presumed promoter and terminators. (Chavarrı et al., 2013). For AAB, as reporter genes have been utilized fluorescent proteins as GFP and mRFP (Teh et al. 2019, Florea, Hagemann, Santosa, Abbott, Micklem, et al. 2016) or enzymes such as phosphatase

(Blank & Schweiger, 2018) and glucose dehydrogenases (Merfort, Herrmann, Bringer-Meyer, et al., 2006).

Saito was the first to successfully apply this approach for the identification of suitable *G. oxydans* promoters. L-sorbose dehydrogenase (SDH) and L-sorbosone dehydrogenase (SNDH) homologous genes were overexpressed in *G. oxydans* tailoring the native T-100 and pHSG298 plasmids and *E. coli* Ptac, PL, and tufB promoters strength in *Gluconobacter* was investigated analyzing SDH and SNDH activity. Ptac promoter resulted to be the most effective in the conversion of D-sorbitol to 2-keto-L-gulonate (2-KLGA). Previously a similar attempt to overexpress a DH in *Acetobacer aceti* was done but according to the authors no improvements were observed (Inoue et al., 1989). Then, Merfort demonstrated again the efficiency of elongation factor TUtufB promoter comparing *G. oxydans* homologous pTuf promoter with a native *G. oxydans* GDH promoter (amplified from *G. oxydans* DSM 2343 genome). The two promoters were cloned upstream of a gluconate-5-dehydrogenases (ga5dh) in pBBR1MCS5 broad host vector. As expected, both the promoters resulted suitable for overexpression in *G. oxydans*, TUtufB showed a better expression of ga5dh with a higher oxidation of glucose to 5-keto-d-glucoconic acid (Merfort, Herrmann, Bringer-Meyer, et al., 2006).

The molecular manipulation of those plasmids was facilitated adding multiple cloning sites on the backbone (Schleyer et al., 2008) and implementing the copy number of pBBR1MCS-5 plasmid in G*luconobacter oxydans* by site-directed mutagenesis on the replication-control regions of the promoter at −10 and −35 positions and on the ribosome binding site (RBS) (Y. Y. Shi et al., 2015).

As anticipated above, Kallnik created new expression vectors for gene expression in *Gluconobacter spp* introducing the promoter regions of the genes encoding *G. oxydans* ribosomal proteins L35 and L13 into pBBR1MCS-2 plasmid. As reporter gene a β-d-glucuronidase was utilized and three expression vectors with different promoter strength (strong pBBR1p264,

moderate pBBR1p452 and weak pBBR1MCS-2) were proposed depending on the β-d-glucuronidase measured activity (Kallnik et al., 2010).

Then, a new promoter (gHp0169) for gene expression in *G. oxydans* was found by Shi. The promoter predicted region was amplified from *G. oxydans* DSM 2003 genomic DNA and characterized in pBBR1MCS5 plasmid upstream a GFP protein and a *G. oxydans* type II NADH dehydrogenase (NDH-2). DSM 2003 cells transformed with pBBR1pgHp0169-gfp plasmid carrying GFP gene downstream gHp0169 promoter showed high fluorescence and once the new promoter was compared with *E. coli* tufB promoter, higher NDH-2 activity was measured in presence of gHp0169 promoter (L. Shi et al., 2014).

More recently, a proteomic approach for the identification of new promoters for the recombinant expression in G*luconobacter* was proposed by Hu (Y. Hu et al., 2015). From a 2D-electrophoresis proteome analysis of *G. oxydans* ATCC 621H (DSM 2343) strain, the best expressed protein was identified, the DNA sequence upstream the relative ORF was characterized using BPROM software and a putative promoter sequence was identified (PB932_2000). GFP and D-sorbitol dehydrogenase (sldh) were utilized as reporter genes to assess the new promoter strength. Comparing the expression of reporter genes obtained using PB932_2000 promoter in G*luconobacter* with *E. coli* and *G. oxydans* expression of the same reporters with tufB promoter, authors defined PB932_2000 (complete with the −10 and −35 motif sequences) as a strong promoter.

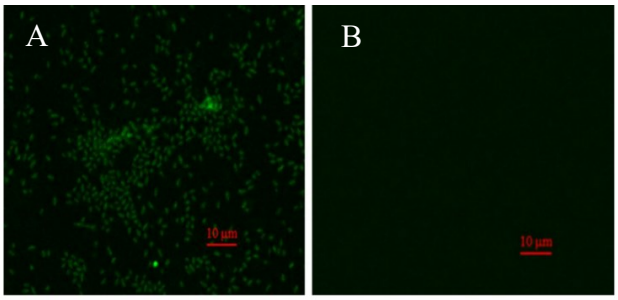

Figure 8 (A) *G. oxydans DSM 2003 transformed with pBBR1pgHp0169-gfp plasmid carrying GFP as reporter and* ***(B)*** *G. oxydans DSM 2003 without GFP.* (L. Shi et al., 2014)

The presence of well characterized promoters, common restriction sites and pBBR1 origin, which have been demonstrated to replicate in a huge list of Gram-negative bacteria (Elzer et al. 2002, Kovach et al. 1995) makes those preferable to other cryptic plasmid for heterologous expression in *G. oxydans* earlier reported in literature (Tonouchi, Sugiyama, and Yokozeki 2003, L. Zhang et al. 2010 and L. Zhang et al. 2010). The usefulness of those vectors is proved by the high number of subsequent publications that refer to those plasmids for expression in *AAB* of different enzymes.

Komagataeibacter genus

AABs of the *Komagataeibacter* genus were the most utilized as host organisms for the recombinant expression of homologous and heterologous genes for their peculiar ability to secrete bacterial cellulose (BC). This enzymatic ability has been observed in different AAB (*Gluconacetobacter xylinus, Gluconacetobacter hansenii* and *Komagataeibacter rhaeticus*) and non AAB strains, but among those microorganisms, *K. xylinus* shows the best production yield.

In the last decade industrial interest in BC exploded due to the numerous described possible applications in very diverse industrial fields. Despite the vast list of possible applications only few are sustainable due to the high costs of BC production at industrial level. Nowadays BC industrial production is mainly utilized for small pharmaceutical applications characterized by their

high added value. The bottleneck for a wide industrial utilization of BC is represented by the low production yields, the necessity of highly pure culture media and the necessity of purification steps that drastically raise the price of this material.

To overcome the limitations related to the production costs, researchers tried to increase BC production with different strategies. The possibility of utilize industrial wastes as a substrate for BC biosynthesis was deeply investigated. Even if different defined culture media have been utilized to maximize BC production at laboratory scale, the utilization of agro-industrial wastes seems to be a necessary step for a sustainable industrial production of this material (Hussain et al., 2019). Agrifood residues, brewery, sugar and textile industry wastes have already been already described as suitable feedstocks for this kind of production. For instance good yields have been obtained from citrus peels (Andritsou et al. 2018, Güzel and Akpınar 2019) hydrolysate of wheat straw from agrifood industry (Al-Abdallah & Dahman, 2013), distillery effluents and wastes from fermentation broth of breweries (Ha et al., 2008), grape skins and crude waste glycerol (Carreira et al., 2011).

With culture media composition, the control of fermentation parameters is essential for efficient BC production. Bioprocess parameters usually utilized for BC production are 25-30°C, pH between 4.5 and 7.5 with an optimum at 6.5 and 10% saturation of dissolved oxygen (Watanabe and Yamanaka 1995 and Watanabe et al. 1998). Even if it must be pointed out that the utilization of oxygen-enriched air can increase BC production yields, it was demonstrated that the BC production yield is dependent on the oxygen percentage as to the type of cultivation, in fact in static culture the best yields were obtained with hypoxic conditions. Usually, BC biofilms are produced in static cultures in batch fermentations in simple low layer vessels filled with culture medium or with aerosol reactors (Lee et al., 2014). Stirred bioreactors are also utilized, most popular are membrane, rotary and continuous as horizontal lift bioreactors (Kim et al., 2007).

Together with process parameters and media composition, the intrinsic capability of microorganisms to secrete BC is the other limiting step for a sustainable production of this material. In this perspective, the deep knowledge of the molecular mechanism responsible of BC production as the possibility to boost enzymatic machinery with molecular biology tools is essential. Characterization of the genetic organization of the cellulose synthase operon (Wong et al., 1990) and genome sequencing of BC producer and non-producer Acetobacter strains (Iyer et al., 2010) helped to elucidate the molecular aspects related to BC production and regulation (Kubiak et al., 2014). In the last twenty years the interest in the material exponentially increased for its possible application in many novel industrial manufactures.

Evolutionary reasons that led AAB to optimize this peculiar phenotypic ability are still debated. BC may allow the bacterium to grow on a highly aerated surface, provide protection from UV light and maintain a minimal humidity necessary for microbial growth during the drying of natural substrates (Scott Williams and Cannon 1989 and Gomes, 2018). Iguchi also proposed that BC could serve as a natural niche, where nutrients can easily diffuse, that can protect the bacterium from heavy-metal ions and environmental dangers (M. Iguchi; et al., 2000).

The formation of BC is catalyzed from UDP-glucose by bc synthase, a membrane associated enzymatic complex composed by four subunits, BCsA, BCsB, BCsC and BCsD (Jacek, Ryngajłło and Bielecki 2019) modulated by the cyclic nucleotide activator bis-cyclic diguanylic acid (C-di-GMP) (Wong et al., 1990). The regulation of cellulose biosynthesis is complex and varies among different BC producers. BC production is regulated at different levels: several genetic elements (J. X. Gao et al. 2017 and Gerstel and Römling 2003) together with post-transcriptional regulations (Martínez & Vadyvaloo, 2014) were identified as crucial elements for BC synthesis. UDP-glucose is generated by three cytoplasmatic enzymatic reaction steps that consist of the phosphorylation of glucose to glucose-6-phosphate by glucokinase, the isomerization of glucose-6-phosphate to glucose-1-phosphate by

phosphoglucomutase and the generation of UDP-glucose by UDP-glucose pyrophosphorylase (Gullo, 2018). The of BC biosynthesis starts with the C-di-GMP binding to BcsA protein that acts as a regulatory subunit. Then, the synthesis proceeds with the polymerization of UDP-glucose substrate into a 1,4-β-glucan chain operated by membrane-anchored bcsB and the formation of glucose chains (Weinhouse et al. 1997 and Krystynowicz et al. 2005).

BcsC and bcsD are responsible for the extrusion of glucan chain respectively through the outer and periplasmic membranes (Taweecheep et al., 2019a). AcsC and AcsD genes are also recognized as responsible for crystallinity of the cellulose since several strains lacking those genes produced non crystal cellulose (Taweecheep et al. 2019, S. Q. Hu et al. 2010, Saxena et al. 1994). It has been proposed that the inhibition of cellulose biosynthesis is regulated with a feedback system by the presence of UDP but not by the accumulating cellulose polymer (Omadjela et al., 2013).

Recently Florea, after sequencing *Gluconacetobacter hansenii* ATCC 53582 genome, previously referred to as *Acetobacter*, identified several new genes associated with cellulose synthesis (Florea, Reeve, et al., 2016). Two additional strictly phylogenetically self-related BCs operons were identified such as the BCsY gene, hypotized to be responsible for the production of acetylated BC, (Umeda et al., 1999). Moreover, through optimized protocols for transformation and identification of plasmid backbones suitable for replication in the strain, it was developed an established gene expression system for *Komagataeibacter hansenii. Komagataeibacter* genus is now a model organism used for genetic, molecular and biochemical studies (Florea et al. 2016; Gilbert et al. 2021; Caro-Astorga et al. 2021 and Goosens et al. 2021).

Molecular approaches to increase BC production

Several molecular biology strategies have been utilized to improve AAB ability to produce BC. Genetic engineering attempts for increasing BC biosynthesis or for ameliorating intrinsic characteristics of the material are based on the

expression of homologous genes responsible for BC secretion, foreign gene or even on the disruption or downregulation of other genes connected with production of the polymer. Random approaches based on chemical and mechanical mutations also have been successfully tried (R. Q. Wu et al., 2010).

Random transposon mutagenesis was applied by Battad-Bernardo for the insertion of an *E. coli* LacZ gene in *K. xylinus* to gain BC production using milk whey as carbon source (Battad-Bernardo et al., 2004). In the report, a pLBT vector containing a transposase gene inside the insertion sequence, bounded by mosaic elements, presents a kanamycin resistance for mutant isolation and the LacZ gene. Biparental mating conjugation was used for *K. xylinus* transformation of pLBT plasmid using *E. coli* S17 as donor strain, furthermore, also simple electroporation was demonstrated to be effective for transformation and conjugation of those kinds of elements (Martínez-García et al., 2011). Similarly sucrose synthase was randomly inserted into the *Acetobacter xylinus* genome to allow BC production from a wider spectra of culture media (Nakai et al. 1999 and Battad-Bernardo et al. 2004).

Homologous recombination such as rational gene deletion was also applied to increase BC biosynthesis. Glucose dehydrogenase was knocked-out to decrease cytoplasmic oxidation of glucose to keto gluconic acid and a significant enhancement of BC (Kuo et al., 2015), a similar result was obtained using a Tn5 transposon insertion in non-cellulose-producing mutants of *Gluconacetobacter hansenii* ATCC 23769 (Deng et al., 2013). Random mutagenesis methods, already mentioned above for *Gluconobacter* random mutations, were effectively employed for BC producer strains. *Gluconacetobacter xylinus* was mutagenized using ultraviolet (UV) radiation, ethyl methanesulfonate (EMS) and sulfaguanidine treatments and after the treatment, a bacterial strain with higher cell growth and BC productivity was identified (Hungund and Gupta 2010, Ishikawa et al. 1995 and Li et al. 2016).

A more classic approach for enhancement of BC production was the transformation of replication plasmids carrying heterologous genes.

Komagataeibacter strains were successfully transformed by electroporation with Broad-host-range replicative (pBBR122 (Mostafa et al., 2002), pTI99 (Jacek et al., 2019), pSA19 (Onouchi et al., 2003) and pBAV1C (Mangayil et al., 2017) vectors.

K. xylinus homologous BCs operon was successfully overexpressed to study the piezoelectric activities of BC (Mangayil et al., 2017). Furthermore, also homologous genes were expressed *in K. xylinus* employing plasmid vectors, for instance a tailored plasmid derived from *K. xylinus* indigenous pFF6 plasmid carrying an endo-beta-1,4-glucanase (Kawano et al. 2002). The overexpression of bacterial hemoglobin led to a remarkable increase of BC secretion by *K. xylinus* thanks to an increase of dissolved oxygen inside the cell. (Liu et al., 2018)

Until the last few years only strong promoters in broad host range vectors or in tailored expression vectors derived from cryptic homologous plasmid, or some random transposon mediated recombination have been utilized in metabolic engineering and synthetic biology studies regarding BC producer strains. Tom Ellis and How Tan groups with their recent synthetic biology publications, in this sense established a setpoint in the genetic engineering of BC producer strains proponing and characterizing different genetic elements respectively inducible, constitutive promoters, reporter genes and sRNA system for rhaeticus were studied by Tom Ellis while terminators, RBS, degradatin tags, CRISPR system in xylinus, rhaeticus and acetobacter strains were investigates by Teh (Teh et al. 2019). BC producer strains employed by the above mentioned research groups are G*luconacetobacter xylinus* ATCC 700178, *Gluconacetobacter hansenii* ATCC 53582 and *Komagataeibacter rhaeticus* iGEM (Florea et al. 2016a, Florea et al. 2016b, Gilbert et al. 2021, Caro-Astorga et al. 2021, Goosens et al. 2021). Furthermore, for the first time CRISPRcas9 interference technology was applied for AAB genetic engineering

Despite the numerous efforts made by researchers to make BC production sustainable a from an industrial point of view, many limiting factors still limit

BC large scale production. However, interest in this material remain high since novel applications are constantly proposed by researchers and the demand for the material by industries is constantly increasing.

References

Al-Abdallah, W., & Dahman, Y. (2013). Production of green biocellulose nanofibers by Gluconacetobacter xylinus through utilizing the renewable resources of agriculture residues. *Bioprocess and Biosystems Engineering*, *36*(11), 1735–1743. https://doi.org/10.1007/s00449-013-0948-9

Alauzet, C., Teyssier, C., Jumas-Bilak, E., Gouby, A., Chiron, R., Rabaud, C., Counil, F., Lozniewski, A., & Marchandin, H. (2010). Gluconobacter as well as Asaia species, newly emerging opportunistic human pathogens among acetic acid bacteria. *Journal of Clinical Microbiology*, *48*(11), 3935–3942. https://doi.org/10.1128/JCM.00767-10

Alonso, S., Rendueles, M., & Díaz, M. (2013). Bio-production of lactobionic acid: Current status, applications and future prospects. *Biotechnology Advances*, *31*(8), 1275–1291. https://doi.org/10.1016/j.biotechadv.2013.04.010

Andritsou, V., De Melo, E. M., Tsouko, E., Ladakis, D., Maragkoudaki, S., Koutinas, A. A., & Matharu, A. S. (2018). Synthesis and Characterization of Bacterial Cellulose from Citrus-Based Sustainable Resources. *ACS Omega*, *3*(8), 10365–10373. https://doi.org/10.1021/acsomega.8b01315

Azuma, Y., Hosoyama, A., Matsutani, M., Furuya, N., Horikawa, H., Harada, T., Hirakawa, H., Kuhara, S., Matsushita, K., Fujita, N., & Shirai, M. (2009). Whole-genome analyses reveal genetic instability of Acetobacter pasteurianus. *Nucleic Acids Research*, *37*(17), 5768–5783. https://doi.org/10.1093/nar/gkp612

Bassetti, M., Pecori, D., Sartor, A., Londero, A., Villa, G., Cadeo, B., Brillo, F., Bongiorno, D., Campanile, F., & Stefani, S. (2013). First report of endocarditis by Gluconobacter spp. in a patient with a history of

intravenous-drug abuse. *Journal of Infection*, *66*(3), 285–287. https://doi.org/10.1016/j.jinf.2012.05.006

Battad-Bernardo, E., McCrindle, S. L., Couperwhite, I., & Neilan, B. A. (2004). Insertion of an E. coli lacZ gene in Acetobacter xylinus for the production of cellulose in whey. *FEMS Microbiology Letters*, *231*(2), 253–260. https://doi.org/10.1016/S0378-1097(04)00007-2

Bell, E. L., Finnigan, W., France, S. P., Hepworth, L. J., Lovelock, S. L., Hayes, M. A., Osuna, S., Romero, E., Ryan, K. S., Turner, N. J., & Flitsch, S. L. (2021). *Biocatalysis 1 1 2*. *0123456789*, 1–21. https://doi.org/10.1038/s43586-021-00044-z

Blank, M., & Schweiger, P. (2018). Surface display for metabolic engineering of industrially important acetic acid bacteria. *PeerJ*, *2018*(4), 1–19. https://doi.org/10.7717/peerj.4626

Bolger, A. M., Lohse, M., & Usadel, B. (2014). Trimmomatic: a flexible trimmer for Illumina sequence data. *Bioinformatics*, *30*(15), 2114–2120. https://doi.org/10.1093/bioinformatics/btu170

Bron, P. A., & Kleerebezem, M. (2018). Lactic acid bacteria for delivery of endogenous or engineered therapeutic molecules. *Frontiers in Microbiology*, *9*(AUG), 1–4. https://doi.org/10.3389/fmicb.2018.01821

Caro-Astorga, J., Walker, K. T., Herrera, N., Lee, K. Y., & Ellis, T. (2021). Bacterial cellulose spheroids as building blocks for 3D and patterned living materials and for regeneration. *Nature Communications*, *12*(1), 1–9. https://doi.org/10.1038/s41467-021-25350-8

Carreira, P., Mendes, J. A. S., Trovatti, E., Serafim, L. S., Freire, C. S. R., Silvestre, A. J. D., & Neto, C. P. (2011). Utilization of residues from agro-forest industries in the production of high value bacterial cellulose.

Bioresource Technology, *102*(15), 7354–7360. https://doi.org/10.1016/j.biortech.2011.04.081

Carvalho, R. D. D. O., do Carmo, F. L. R., Junior, A. de O., Langella, P., Chatel, J. M., Bermúdez-Humarán, L. G., Azevedo, V., & de Azevedo, M. S. (2017). Use of wild type or recombinant lactic acid bacteria as an alternative treatment for gastrointestinal inflammatory diseases: A focus on inflammatory bowel diseases and mucositis. *Frontiers in Microbiology*, *8*(MAY), 1–13. https://doi.org/10.3389/fmicb.2017.00800

Chavarrı, M., Silva-rocha, R., Martı, E., Heras, A. De, Pa, A. D., Arce-rodrı, A., Kim, J., Nikel, P. I., Durante-rodrı, G., & Lorenzo, D. (2013). *The Standard European Vector Architecture (SEVA): a coherent platform for the analysis and deployment of complex prokaryotic phenotypes*. *41*(November 2012), 666–675. https://doi.org/10.1093/nar/gks1119

Chhabra, S. R., & Keasling, J. D. (2019). Metabolic design and control for production in prokaryotes. *Comprehensive Biotechnology*, 217–230. https://doi.org/10.1016/B978-0-444-64046-8.00018-5

Collén, A., Saloheimo, M., Bailey, M., Penttilä, M., & Pakula, T. M. (2005). Protein production and induction of the unfolded protein response in Trichoderma reesei strain Rut-C30 and its transformant expressing endoglucanase I with a hydrophobic tag. *Biotechnology and Bioengineering*, *89*(3), 335–344. https://doi.org/10.1002/bit.20350

Deng, Y., Nagachar, N., Xiao, C., Tien, M., & Kao, T. H. (2013). Identification and characterization of non-cellulose-producing mutants of Gluconacetobacter hansenii generated by Tn5 transposon mutagenesis. *Journal of Bacteriology*, *195*(22), 5072–5083. https://doi.org/10.1128/JB.00767-13

Deppenmeier, U., Hoffmeister, M., & Prust, C. (2002). Biochemistry and

biotechnological applications of Gluconobacter strains. *Applied Microbiology and Biotechnology*, *60*(3), 233–242. https://doi.org/10.1007/s00253-002-1114-5

Devine, P. N., Howard, R. M., Kumar, R., Thompson, M. P., Truppo, M. D., & Turner, N. J. (2018). Extending the application of biocatalysis to meet the challenges of drug development. *Nature Reviews Chemistry*, *2*(12), 409–421. https://doi.org/10.1038/s41570-018-0055-1

Elzer, P. H., Roop, R. M., Kovach, M. E., Robertson, G. T., Peterson, K. M., Steven Hill, D., & Farris, M. A. (2002). Four new derivatives of the broad-host-range cloning vector pBBR1MCS, carrying different antibiotic-resistance cassettes. *Gene*, *166*(1), 175–176. https://doi.org/10.1016/0378-1119(95)00584-1

Faber, K. (2011). Biocatalytic Applications. In *Biotransformations in Organic Chemistry*. https://doi.org/10.1007/978-3-642-17393-6_2

Florea, M., Hagemann, H., Santosa, G., Abbott, J., Micklem, C. N., Spencer-Milnes, X., De Arroyo Garcia, L., Paschou, D., Lazenbatt, C., Kong, D., Chughtai, H., Jensen, K., Freemont, P. S., Kitney, R., Reeve, B., & Ellis, T. (2016). Engineering control of bacterial cellulose production using a genetic toolkit and a new celluloseproducing strain. *Proceedings of the National Academy of Sciences of the United States of America*, *113*(24), E3431–E3440. https://doi.org/10.1073/pnas.1522985113

Florea, M., Reeve, B., Abbott, J., Freemont, P. S., & Ellis, T. (2016). Genome sequence and plasmid transformation of the model high-yield bacterial cellulose producer Gluconacetobacter hansenii ATCC 53582. *Scientific Reports*, *6*(September 2015), 1–9. https://doi.org/10.1038/srep23635

FREESE, E. B. (1961). *TRANSITIONS AND TRANSVERSIONS INDUCED BY DEPURINATING AGENTS*. 540–545.

Fukaya, M., & Iwata, T. (1985). Improved transformation method for acetobacter with plasmid dna. *49*(5), 1349–1355.

Fukaya, M., Tayama, K., Okumura, H., Masai, H., & Beppu, T. (2014). *Improved Transformation Method for Acetobacter with Plasmid DNA*. *1369*. https://doi.org/10.1080/00021369.1985.10867039

Fukaya, M., Tayama, K., Okumura, H., Masai, H., Uozumi, T., & Beppu, T. (1985). Improved transformation method for acetobacter with plasmid dna. *Agricultural and Biological Chemistry*, *49*(7), 2091–2097. https://doi.org/10.1080/00021369.1985.10867039

Gao, F., & Zhang, C.-T. (2008). Ori-Finder: A web-based system for finding oriC s in unannotated bacterial genomes. *BMC Bioinformatics*, *9*(1), 79. https://doi.org/10.1186/1471-2105-9-79

Gao, J. X., Li, P., Du, X. J., Han, Z. H., Xue, R., Liang, B., & Wang, S. (2017). A negative regulator of cellulose biosynthesis, bcsR, affects biofilm formation, and adhesion/invasion ability of Cronobacter sakazakii. *Frontiers in Microbiology*, *8*(SEP), 1–11. https://doi.org/10.3389/fmicb.2017.01839

Gao, L., Wu, X., Zhu, C., Jin, Z., Wang, W., & Xia, X. (2020). Metabolic engineering to improve the biomanufacturing efficiency of acetic acid bacteria: advances and prospects. *Critical Reviews in Biotechnology*, *40*(4), 522–538. https://doi.org/10.1080/07388551.2020.1743231

Geng, Y., & Doberstein, B. (2010). *Developing the circular economy in China : Challenges and opportunities for achieving ' leapfrog development ' Developing the circular economy in China : Challenges and opportunities for achieving ' leapfrog development .' 4509*. https://doi.org/10.3843/SusDev.15.3

Gerstel, U., & Römling, U. (2003). The csgD promoter, a control unit for biofilm formation in Salmonella typhimurium. *Research in Microbiology*, *154*(10), 659–667. https://doi.org/10.1016/j.resmic.2003.08.005

Gilbert, C., Tang, T. C., Ott, W., Dorr, B. A., Shaw, W. M., Sun, G. L., Lu, T. K., & Ellis, T. (2021). Living materials with programmable functionalities grown from engineered microbial co-cultures. *Nature Materials*. https://doi.org/10.1038/s41563-020-00857-5

Gomes, R. J., Hernan, R. J., & Spinosa, A. (2018). *Acetic Acid Bacteria in the Food Industry : Systematics , Characteristics and Applications*. *0262*, 0–2. https://doi.org/10.17113/ftb.56.02.18.5593

Goosens, V. J., Walker, K. T., Aragon, S. M., Singh, A., Senthivel, V. R., Caro-astorga, J., Buat, M. L. A., Song, W., Lee, K., & Ellis, T. (2021). *Komagataeibacter tool kit (KTK): a modular cloning system for multigene constructs and programmed protein secretion from cellulose producing bacteria 3*. 1–21.

Guizelini, D., Raittz, R. T., Cruz, L. M., Souza, E. M., Steffens, M. B. R., & Pedrosa, F. O. (2016). GFinisher: a new strategy to refine and finish bacterial genome assemblies. *Scientific Reports*, *6*(1), 34963. https://doi.org/10.1038/srep34963

Gullo, M. (2018). *Biotechnological production of cellulose by acetic acid bacteria : current state and perspectives*. 6885–6898.

Güzel, M., & Akpınar, Ö. (2019). Production and Characterization of Bacterial Cellulose from Citrus Peels. *Waste and Biomass Valorization*, *10*(8), 2165–2175. https://doi.org/10.1007/s12649-018-0241-x

Ha, J. H., Shehzad, O., Khan, S., Lee, S. Y., Park, J. W., Khan, T., & Park, J. K. (2008). Production of bacterial cellulose by a static cultivation using

the waste from beer culture broth. *Korean Journal of Chemical Engineering*, *25*(4), 812–815. https://doi.org/10.1007/s11814-008-0134-y

Hanke, T., Nöh, K., Noack, S., Polen, T., Bringer, S., Sahm, H., Wiechert, W., & Bott, M. (2013). Combined fluxomics and transcriptomics analysis of glucose catabolism via a partially cyclic pentose phosphate pathway in Gluconobacter oxydans 621H. *Applied and Environmental Microbiology*, *79*(7), 2336–2348. https://doi.org/10.1128/AEM.03414-12

Hattori, H., Yakushi, T., Matsutani, M., Moonmangmee, D., Toyama, H., Adachi, O., & Matsushita, K. (2012). High-temperature sorbose fermentation with thermotolerant Gluconobacter frateurii CHM43 and its mutant strain adapted to higher temperature. *Applied Microbiology and Biotechnology*, *95*(6), 1531–1540. https://doi.org/10.1007/s00253-012-4005-4

Hayata, Y. (2002). NII-Electronic Library Service. *Chemical Pharmaceutical Bulletin*, *43*, 2091.

Hu, S. Q., Gao, Y. G., Tajima, K., Sunagawa, N., Zhou, Y., Kawano, S., Fujiwara, T., Yoda, T., Shimura, D., Satoh, Y., Munekata, M., Tanaka, I., & Yao, M. (2010). Structure of bacterial cellulose synthase subunit D octamer with four inner passageways. *Proceedings of the National Academy of Sciences of the United States of America*, *107*(42), 17957–17961. https://doi.org/10.1073/pnas.1000601107

Hu, Y., Wan, H., Li, J., & Zhou, J. (2015). Enhanced production of l-sorbose in an industrial Gluconobacter oxydans strain by identification of a strong promoter based on proteomics analysis. *Journal of Industrial Microbiology and Biotechnology*, *42*(7), 1039–1047. https://doi.org/10.1007/s10295-015-1624-7

Hungund, B. S., & Gupta, S. G. (2010). Strain improvement of Gluconacetobacter xylinus NCIM 2526 for bacterial cellulose production. *African Journal of Biotechnology*, *9*(32), 5170–5172. https://doi.org/10.5897/AJB09.1877

Hussain, Z., Sajjad, W., Khan, T., & Wahid, F. (2019). Production of bacterial cellulose from industrial wastes: a review. *Cellulose*, *26*(5), 2895–2911. https://doi.org/10.1007/s10570-019-02307-1

Inoue, T., Sunagawa, M., Mori, A., Imai, C., Fukuda, M., Takagi, M., & Yano, K. (1989). Cloning and sequencing of the gene encoding the 72-kilodalton dehydrogenase subunit of alcohol dehydrogenase from Acetobacter aceti. *Journal of Bacteriology*, *171*(6), 3115–3122. https://doi.org/10.1128/jb.171.6.3115-3122.1989

Ishikawa, A., Matsuoka, M., Tsuchida, T., & Yoshinaga, F. (1995). Increase in Cellulose Production by Sulfaguanidine-Resistant Mutants Derived from Acetobacter Xylinum Subsp. Sucrofermentans. *Bioscience, Biotechnology, and Biochemistry*, *59*(12), 2259–2262. https://doi.org/10.1271/bbb.59.2259

Iyer, P. R., Geib, S. M., Catchmark, J., Kao, T. H., & Tien, M. (2010). Genome sequence of a cellulose-producing bacterium, Gluconacetobacter hansenii ATCC 23769. *Journal of Bacteriology*, *192*(16), 4256–4257. https://doi.org/10.1128/JB.00588-10

Jacek, P., Ryngajłło, M., & Bielecki, S. (2019). Structural changes of bacterial nanocellulose pellicles induced by genetic modification of Komagataeibacter hansenii ATCC 23769. *Applied Microbiology and Biotechnology*, *103*(13), 5339–5353. https://doi.org/10.1007/s00253-019-09846-4

Jakob, F., Pfaff, A., Novoa-Carballal, R., Rübsam, H., Becker, T., & Vogel, R.

F. (2013). Structural analysis of fructans produced by acetic acid bacteria reveals a relation to hydrocolloid function. *Carbohydrate Polymers*, *92*(2), 1234–1242. https://doi.org/10.1016/j.carbpol.2012.10.054

Jun, H., Kieselbach, T., & Jönsson, L. J. (2011). Enzyme production by filamentous fungi: Analysis of the secretome of Trichoderma reesei grown on unconventional carbon source. *Microbial Cell Factories*, *10*, 1–10. https://doi.org/10.1186/1475-2859-10-68

Kallnik, V., Meyer, M., Deppenmeier, U., & Schweiger, P. (2010). Construction of expression vectors for protein production in Gluconobacter oxydans. *Journal of Biotechnology*, *150*(4), 460–465. https://doi.org/10.1016/j.jbiotec.2010.10.069

KAWANO, S., TAJIMA, K., KONO, H., ERATA, T., MUNEKATA, M., & TAKAI, M. (2002). Effects of Endogenous Endo-β-1,4-Glucanase on Cellulose Biosynthesis in Acetobacter xylinum ATCC23769. *Journal of Bioscience and Bioengineering*, *94*(3), 275–281. https://doi.org/10.1263/jbb.94.275

Kiefler, I., Bringer, S., & Bott, M. (2015). SdhE-dependent formation of a functional Acetobacter pasteurianus succinate dehydrogenase in Gluconobacter oxydans—a first step toward a complete tricarboxylic acid cycle. *Applied Microbiology and Biotechnology*, *99*(21), 9147–9160. https://doi.org/10.1007/s00253-015-6972-8

Kiefler, I., Bringer, S., & Bott, M. (2017). Metabolic engineering of Gluconobacter oxydans 621H for increased biomass yield. *Applied Microbiology and Biotechnology*, *101*(13), 5453–5467. https://doi.org/10.1007/s00253-017-8308-3

Kim, Y.-J., Kim, J.-N., Wee, Y.-J., Park, D.-H., & Ryu, H.-W. (2007). Bacterial Cellulose Production by Gluconacetobacter sp. RKY5 in a Rotary Biofilm Contactor. *Applied Biochemistry and Biotecnology*, *136*(4), 529–537.

https://doi.org/10.1007/978-1-60327-181-3_44

Kondo, K., & Horinouchi, S. (1997). A new insertion sequence IS1452 from Acetobacter pasteurianus. *Microbiology*, *143*(2), 539–546. https://doi.org/10.1099/00221287-143-2-539

Kosciow, K., Zahid, N., Schweiger, P., & Deppenmeier, U. (2014). Production of a periplasmic trehalase in gluconobacter oxydans and growth on trehalose. *Journal of Biotechnology*, *189*, 27–35. https://doi.org/10.1016/j.jbiotec.2014.08.029

Kovach, M. E., Elzer, P. H., Hill, D. S., Robertson, G. T., Farris, M. A., Roop, R. M., & Peterson, K. M. (1995). Four new derivatives of the broad-host-range cloning vector pBBR1MCS, carrying different antibiotic-resistance cassettes. *Gene*, *166*(1), 175–176. http://www-ab.informatik.uni-tuebingen.de/toolbox/index.php?view=domainpred

Krystynowicz, A., Koziołkiewicz, M., Wiktorowska-Jezierska, A., Bielecki, S., Klemenska, E., Masny, A., & Płucienniczak, A. (2005). Molecular basis of cellulose biosynthesis disappearance in submerged culture of Acetobacter xylinum. *Acta Biochimica Polonica*, *52*(3), 691–698. https://doi.org/10.18388/abp.2005_3432

Kubiak, K., Kurzawa, M., Jedrzejczak-Krzepkowska, M., Ludwicka, K., Krawczyk, M., Migdalski, A., Kacprzak, M. M., Loska, D., Krystynowicz, A., & Bielecki, S. (2014). Complete genome sequence of Gluconacetobacter xylinus E25 strain-Valuable and effective producer of bacterial nanocellulose. *Journal of Biotechnology*, *176*(1), 18–19. https://doi.org/10.1016/j.jbiotec.2014.02.006

Kuo, C. H., Teng, H. Y., & Lee, C. K. (2015). Knock-out of glucose dehydrogenase gene in Gluconacetobacter xylinus for bacterial cellulose production enhancement. *Biotechnology and Bioprocess Engineering*,

20(1), 18–25. https://doi.org/10.1007/s12257-014-0316-x

Le Loir, Y., Azevedo, V., Oliveira, S. C., Freitas, D. A., Miyoshi, A., Bermúdez-Humarán, L. G., Nouaille, S., Ribeiro, L. A., Leclercq, S., Gabriel, J. E., Guimaraes, V. D., Oliveira, M. N., Charlier, C., Gautier, M., & Langella, P. (2005). Protein secretion in Lactococcus lactis: An efficient way to increase the overall heterologous protein production. *Microbial Cell Factories*, *4*, 1–13. https://doi.org/10.1186/1475-2859-4-2

Lee, K. Y., Buldum, G., Mantalaris, A., & Bismarck, A. (2014). More than meets the eye in bacterial cellulose: Biosynthesis, bioprocessing, and applications in advanced fiber composites. *Macromolecular Bioscience*, *14*(1), 10–32. https://doi.org/10.1002/mabi.201300298

Legastelois, I., Buffin, S., Peubez, I., Mignon, C., Sodoyer, R., & Werle, B. (2017). Non-conventional expression systems for the production of vaccine proteins and immunotherapeutic molecules. *Human Vaccines and Immunotherapeutics*, *13*(4), 947–961. https://doi.org/10.1080/21645515.2016.1260795

Li, Y., Tian, J., Tian, H., Chen, X., Ping, W., Tian, C., & Lei, H. (2016). Mutation-based selection and analysis of Komagataeibacter hansenii HDM1-3 for improvement in bacterial cellulose production. *Journal of Applied Microbiology*, *121*(5), 1323–1334. https://doi.org/10.1111/jam.13244

Liu, M., Li, S., Xie, Y., Jia, S., Hou, Y., Zou, Y., & Zhong, C. (2018). Enhanced bacterial cellulose production by Gluconacetobacter xylinus via expression of Vitreoscilla hemoglobin and oxygen tension regulation. *Applied Microbiology and Biotechnology*, *102*(3), 1155–1165. https://doi.org/10.1007/s00253-017-8680-z

Lynch, K. M., Zannini, E., Wilkinson, S., Daenen, L., & Arendt, E. K. (2019).

Physiology of Acetic Acid Bacteria and Their Role in Vinegar and Fermented Beverages. *Comprehensive Reviews in Food Science and Food Safety*, *18*(3), 587–625. https://doi.org/10.1111/1541-4337.12440

M. Iguchi;, S. Yamanaka;, & A. Budhiono; (2000). Bacterial cellulose - a masterpiece of nature's arts. *Journal of Materials Science*, *35*(2), 261–270. https://doi.org/10.1023/A

TOWARDS THE CIRCULAR ECONOMY.

Macauley-Patrick, S., Fazenda, M. L., McNeil, B., & Harvey, L. M. (2005). Heterologous protein production using the Pichia pastoris expression system. *Yeast*, *22*(4), 249–270. https://doi.org/10.1002/yea.1208

Mangayil, R., Rajala, S., Pammo, A., Sarlin, E., Luo, J., Santala, V., Karp, M., & Tuukkanen, S. (2017). Engineering and Characterization of Bacterial Nanocellulose Films as Low Cost and Flexible Sensor Material. *ACS Applied Materials and Interfaces*, *9*(22), 19048–19056. https://doi.org/10.1021/acsami.7b04927

Marchler-Bauer, A., Derbyshire, M. K., Gonzales, N. R., Lu, S., Chitsaz, F., Geer, L. Y., Geer, R. C., He, J., Gwadz, M., Hurwitz, D. I., Lanczycki, C. J., Lu, F., Marchler, G. H., Song, J. S., Thanki, N., Wang, Z., Yamashita, R. A., Zhang, D., Zheng, C., & Bryant, S. H. (2015). CDD: NCBI's conserved domain database. *Nucleic Acids Research*, *43*(D1), D222–D226. https://doi.org/10.1093/nar/gku1221

Martínez-García, E., Calles, B., Arévalo-Rodríguez, M., & De Lorenzo, V. (2011). PBAM1: An all-synthetic genetic tool for analysis and construction of complex bacterial phenotypes. *BMC Microbiology*, *11*(1), 38. https://doi.org/10.1186/1471-2180-11-38

Martínez, L. C., & Vadyvaloo, V. (2014). Mechanisms of post-transcriptional

gene regulation in bacterial biofilms. *Frontiers in Cellular and Infection Microbiology*, *5*(MAR), 1–15. https://doi.org/10.3389/fcimb.2014.00038

Matsushita K., Toyama H., Tonouchi N., O.-K. A. (eds). (2016). Industrial Application of Acetic Acid Bacteria (Vitamin C and Others). In *Acetic Acid Bacteria.: Vol. 1호* (Issue May, pp. 31–48).

Matsutani, M., Nishikura, M., Saichana, N., Hatano, T., Masud-Tippayasak, U., Theergool, G., Yakushi, T., & Matsushita, K. (2013). Adaptive mutation of Acetobacter pasteurianus SKU1108 enhances acetic acid fermentation ability at high temperature. *Journal of Biotechnology*, *165*(2), 109–119. https://doi.org/10.1016/j.jbiotec.2013.03.006

Merfort, M., Herrmann, U., Bringer-Meyer, S., & Sahm, H. (2006). High-yield 5-keto-D-gluconic acid formation is mediated by soluble and membrane-bound gluconate-5-dehydrogenases of Gluconobacter oxydans. *Applied Microbiology and Biotechnology*, *73*(2), 443–451. https://doi.org/10.1007/s00253-006-0467-6

Merfort, M., Herrmann, U., Ha, S. W., Elfari, M., Bringer-Meyer, S., Görisch, H., & Sahm, H. (2006). Modification of the membrane-bound glucose oxidation system in Gluconobacter oxydans significantly increases gluconate and 5-keto-D-gluconic acid accumulation. *Biotechnology Journal*, *1*(5), 556–563. https://doi.org/10.1002/biot.200600032

Meyer, M., Schweiger, P., & Deppenmeier, U. (2013). Effects of membrane-bound glucose dehydrogenase overproduction on the respiratory chain of Gluconobacter oxydans. *Applied Microbiology and Biotechnology*, *97*(8), 3457–3466. https://doi.org/10.1007/s00253-012-4265-z

Mientus, M., Kostner, D., Peters, B., Liebl, W., & Ehrenreich, A. (2017). Characterization of membrane-bound dehydrogenases of Gluconobacter

oxydans 621H using a new system for their functional expression. *Applied Microbiology and Biotechnology*, *101*(8), 3189–3200. https://doi.org/10.1007/s00253-016-8069-4

Mostafa, H. E., Mostafa, H. E., Geis, A., & Geis, A. (2002). Cloning of. *Society*, *68*(5), 2619–2623. https://doi.org/10.1128/AEM.68.5.2619

Murooka, Y., Takizawa, N., & Harada, T. (1981). Introduction of bacteriophage mu into bacteria of various genera and intergeneric gene transfer by RP4::Mu. *Journal of Bacteriology*, *145*(1), 358–368. https://doi.org/10.1128/jb.145.1.358-368.1981

Nakai, T., Tonouchi, N., Konishi, T., Kojima, Y., Tsuchida, T., Yoshinaga, F., Sakai, F., & Hayashi, T. (1999). Enhancement of cellulose production by expression of sucrose synthase in Acetobacter xylinum. *Proceedings of the National Academy of Sciences of the United States of America*, *96*(1), 14–18. https://doi.org/10.1073/pnas.96.1.14

Ninla Elmawati Falabiba, Anggaran, W., Mayssara A. Abo Hassanin Supervised, A., Wiyono, B. ., Ninla Elmawati Falabiba, Zhang, Y. J., Li, Y., & Chen, X. (2014). Central Carbon Metabolism and Respiration in Gluconobacter oxydans. In *Acetic Acid Bacteria: Ecology and Physiology* (Vol. 5, Issue 2, pp. 40–51).

Ohmori, S., Uozumi, T., & Beppu, T. (1982). Loss of acetic acid resistance and ethanol oxidizing ability in an Acetobacter strain. *Agricultural and Biological Chemistry*, *46*(2), 381–389. https://doi.org/10.1080/00021369.1982.10865082

Okonechnikov, K., Golosova, O., & Fursov, M. (2012). Unipro UGENE: a unified bioinformatics toolkit. *Bioinformatics*, *28*(8), 1166–1167. https://doi.org/10.1093/bioinformatics/bts091

Okumura, H., Tagami, H., Fukaya, M., Masai, H., Kawamura, Y., Horinouchi, S., & Beppu, T. (1988). Cloning of the β-Isopropylmalate Dehydrogenase Gene from Acetobacter aceti and Its Use for Construction of a New Host-Vector System for Acetobacter. *Agricultural and Biological Chemistry*, *52*(12), 3125–3129. https://doi.org/10.1271/bbb1961.52.3125

Omadjela, O., Narahari, A., Strumillo, J., Mélida, H., Mazur, O., Bulone, V., & Zimmer, J. (2013). BcsA and BcsB form the catalytically active core of bacterial cellulose synthase sufficient for in vitro cellulose synthesis. *Proceedings of the National Academy of Sciences of the United States of America*, *110*(44), 17856–17861. https://doi.org/10.1073/pnas.1314063110

Onouchi, N. T., Ugiyama, M. S., & Okozeki, K. Y. (2003). *Construction of a Vector Plasmid for Use in Gluconobacter oxydans*. *67*(1), 211–213.

Park, S., Baker, J. O., Himmel, M. E., Parilla, P. A., & Johnson, D. K. (2010). Cellulose crystallinity index: measurement techniques and their impact on interpreting cellulase performance. *Biotechnology for Biofuels*, *3*(1), 10. https://doi.org/10.1186/1754-6834-3-10

Pasteur, L. P. (1864). *Mémoire sur la fermentation acétique Annales*. *1*.

Patel, R. N. (2016). Green biocatalysis. In *Hoboken, New Jersey : John Wiley & Sons*. https://doi.org/10.1201/9781482269802-30

Peterbauer, C., Maischberger, T., & Haltrich, D. (2011). Food-grade gene expression in lactic acid bacteria. *Biotechnology Journal*, *6*(9), 1147–1161. https://doi.org/10.1002/biot.201100034

Peters, B., Junker, A., Brauer, K., Mühlthaler, B., Kostner, D., Mientus, M., Liebl, W., & Ehrenreich, A. (2013). Deletion of pyruvate decarboxylase by a new method for efficient markerless gene deletions in

Gluconobacter oxydans. *Applied Microbiology and Biotechnology*, *97*(6), 2521–2530. https://doi.org/10.1007/s00253-012-4354-z

Peters, B., Mientus, M., Kostner, D., Junker, A., Liebl, W., & Ehrenreich, A. (2013). Characterization of membrane-bound dehydrogenases from Gluconobacter oxydans 621H via whole-cell activity assays using multideletion strains. *Applied Microbiology and Biotechnology*, *97*(14), 6397–6412. https://doi.org/10.1007/s00253-013-4824-y

Qi, Z., Wang, W., Yang, H., Xia, X., & Yu, X. (2014). Mutation of Acetobacter pasteurianus by UV irradiation under acidic stress for high-acidity vinegar fermentation. *International Journal of Food Science and Technology*, *49*(2), 468–476. https://doi.org/10.1111/ijfs.12324

Saichana, N., Matsushita, K., Adachi, O., Frébort, I., & Frebortova, J. (2015). Acetic acid bacteria: A group of bacteria with versatile biotechnological applications. *Biotechnology Advances*, *33*(6), 1260–1271. https://doi.org/10.1016/j.biotechadv.2014.12.001

Saito, Y., Ishii, Y., Hayashi, H., Imao, Y., Akashi, T., Yoshikawa, K., Noguchi, Y., Soeda, S., Yoshida, M., Niwa, M., Hosoda, J., & Shimomura, K. (1997). Cloning of genes coding for L-sorbose and L-sorbosone dehydrogenases from Gluconobacter oxydans and microbial production of 2-keto-L-gulonate, a precursor of L-ascorbic acid, in a recombinant G. oxydans strain. *Applied and Environmental Microbiology*, *63*(2), 454–460. https://doi.org/10.1128/aem.63.2.454-460.1997

Sauer, U., & Eikmanns, B. J. (2005). The PEP—pyruvate—oxaloacetate node as the switch point for carbon flux distribution in bacteria: We dedicate this paper to Rudolf K. Thauer, Director of the Max-Planck-Institute for Terrestrial Microbiology in Marburg, Germany, on the occasion of his 65th. *FEMS Microbiology Reviews*, *29*(4), 765–794. https://doi.org/10.1016/j.femsre.2004.11.002

Saxena, I. M., Kudlicka, K., Okuda, K., & Brown, R. M. (1994). Characterization of genes in the cellulose-synthesizing operon (acs operon) of Acetobacter xylinum: Implications for cellulose crystallization. *Journal of Bacteriology*, *176*(18), 5735–5752. https://doi.org/10.1128/jb.176.18.5735-5752.1994

Schleyer, U., Bringer-meyer, S., & Sahm, H. (2008). *An easy cloning and expression vector system for Gluconobacter oxydans*. *125*, 91–95. https://doi.org/10.1016/j.ijfoodmicro.2007.04.016

Schmidt, F. R. (2004). Recombinant expression systems in the pharmaceutical industry. *Applied Microbiology and Biotechnology*, *65*(4), 363–372. https://doi.org/10.1007/s00253-004-1656-9

Scott Williams, W. S., & Cannon, R. E. (1989). Alternative environmental roles for cellulose produced by Acetobacter xylinum. *Applied and Environmental Microbiology*, *55*(10), 2448–2452. https://doi.org/10.1128/aem.55.10.2448-2452.1989

Shi, L., Li, K., Zhang, H., Liu, X., Lin, J., & Wei, D. (2014). Identification of a novel promoter gHp0169 for gene expression in Gluconobacter oxydans. *Journal of Biotechnology*, *175*(1), 69–74. https://doi.org/10.1016/j.jbiotec.2014.01.035

Shi, Y. Y., Li, K. F., Lin, J. P., Yang, S. L., & Wei, D. Z. (2015). Engineered Expression Vectors Significantly Enhanced the Production of 2-Keto-D-gluconic Acid by Gluconobacter oxidans. *Journal of Agricultural and Food Chemistry*, *63*(22), 5492–5498. https://doi.org/10.1021/acs.jafc.5b01652

Siemen, A., Kosciow, K., Schweiger, P., & Deppenmeier, U. (2018). Production of 5-ketofructose from fructose or sucrose using genetically modified Gluconobacter oxydans strains. *Applied Microbiology and*

Biotechnology, *102*(4), 1699–1710. https://doi.org/10.1007/s00253-017-8699-1

Solieri Lisa, G. P. (2009). Vinegars of the World. In *Spiringer*.

Spohner, S. C., Müller, H., Quitmann, H., & Czermak, P. (2015). Expression of enzymes for the usage in food and feed industry with Pichia pastoris. *Journal of Biotechnology*, *202*, 118–134. https://doi.org/10.1016/j.jbiotec.2015.01.027

Stell, R., & Walker, T. K. (1957). A comparative study of cellulose-producing cultures and celluloseless mutants of certain Acetobacter spp. *Journal of General Microbiology*, *17*(2), 445–452. https://doi.org/10.1099/00221287-17-2-445

Steiner, P., & Sauer, U. (2003). Long-term continuous evolution of acetate resistant Acetobacter aceti. *Biotechnology and Bioengineering*, *84*(1), 40–44. https://doi.org/10.1002/bit.10741

Taweecheep, P., Naloka, K., Matsutani, M., Yakushi, T., Matsushita, K., & Theeragool, G. (2019a). Superfine bacterial nanocellulose produced by reverse mutations in the bcsC gene during adaptive breeding of Komagataeibacter oboediens. *Carbohydrate Polymers*, *226*(September), 115243. https://doi.org/10.1016/j.carbpol.2019.115243

Taweecheep, P., Naloka, K., Matsutani, M., Yakushi, T., Matsushita, K., & Theeragool, G. (2019b). Superfine bacterial nanocellulose produced by reverse mutations in the bcsC gene during adaptive breeding of Komagataeibacter oboediens. *Carbohydrate Polymers*, *226*(May), 115243. https://doi.org/10.1016/j.carbpol.2019.115243

Tayama, K., Fukaya, M., Okumura, H., Kawamura, Y., Horinouchi, S., & Beppu, T. (1994). Transformation of acetobacter polyoxogenes with

plasmid dna by electroporation. *Bioscience, Biotechnology and Biochemistry*, *58*(5), 974–975. https://doi.org/10.1080/bbb.58.974

Teh, M. Y., Ooi, K. H., Danny Teo, S. X., Bin Mansoor, M. E., Shaun Lim, W. Z., & Tan, M. H. (2019). An Expanded Synthetic Biology Toolkit for Gene Expression Control in Acetobacteraceae [Research-article]. *ACS Synthetic Biology*, *8*(4), 708–723. https://doi.org/10.1021/acssynbio.8b00168

Tonouchi, N., Sugiyama, M., & Yokozeki, K. (2003). Construction of a vector plasmid for use in gluconobacte. *Bioscience, Biotechnology and Biochemistry*, *67*(1), 211–213. https://doi.org/10.1271/bbb.67.211

Umeda, Y., Hirano, A., Ishibashi, M., Akiyama, H., Onizuka, T., Ikeuchi, M., & Inoue, Y. (1999). Cloning of cellulose synthase genes from Acetobacter xylinum JCM 7664: Implication of a novel set of cellulose synthase genes. *DNA Research*, *6*(2), 109–115. https://doi.org/10.1093/dnares/6.2.109

Uozumi, T., & Beppu, T. (1985). Construction of Plasmid Vectors and a Genetic Transformation System for Acetobacter aceti. *Agricultural and Biological Chemistry*, *49*(4), 1011–1017. https://doi.org/10.1271/bbb1961.49.1011

Verma, V., Qazi, G. N., & Parshad, R. (1992). Intergeneric protoplast fusion between Gluconobacter oxydans and Corynebacterium species. *Journal of Biotechnology*, *26*(2–3), 327–330. https://doi.org/10.1016/0168-1656(92)90016-3

Walsh, G. (2018). Biopharmaceutical benchmarks 2018. *Nature Biotechnology*, *36*(12), 1136–1145. https://doi.org/10.1038/nbt.4305

Wang, P., Zeng, W., Xu, S., Du, G., Zhou, J., & Chen, J. (2018). Current

challenges facing one-step production of L-ascorbic acid. *Biotechnology Advances*, *36*(7), 1882–1899. https://doi.org/10.1016/j.biotechadv.2018.07.006

Watanabe, K., Tabuchi, M., Morinaga, Y., & Yoshinaga, F. (1998). Structural features and properties of bacterial cellulose produced in agitated culture. *Cellulose*, *5*(3), 187–200. https://doi.org/10.1023/A:1009272904582

Watanabe, K., & Yamanaka, S. (1995). Effects of Oxygen Tension in the Gaseous Phase on Production and Physical Properties of Bacterial Cellulose Formed Under Static Culture Conditions. *Bioscience, Biotechnology, and Biochemistry*, *59*(1), 65–68. https://doi.org/10.1271/bbb.59.65

Weinhouse, H., Sapir, S., Amikam, D., Shilo, Y., Volman, G., Ohana, P., & Benziman, M. (1997). C-di-GMP-binding protein, a new factor regulating cellulose synthesis in Acetobacter xylinum. *FEBS Letters*, *416*(2), 207–211. https://doi.org/10.1016/S0014-5793(97)01202-7

Wilkins, M. R., Suryawati, L., Maness, N. O., & Chrz, D. (2007). Ethanol production by Saccharomyces cerevisiae and Kluyveromyces marxianus in the presence of orange-peel oil. *World Journal of Microbiology and Biotechnology*, *23*(8), 1161–1168. https://doi.org/10.1007/s11274-007-9346-2

Wong, H. C., Fear, A. L., Calhoon, R. D., Eichinger, G. H., Mayer, R., Amikam, D., Benziman, M., Gelfand, D. H., Meade, J. H., Emerick, A. W., Bruner, R., Ben-Bassat, A., & Tal, R. (1990). Genetic organization of the cellulose synthase operon in Acetobacter xylinum. *Proceedings of the National Academy of Sciences of the United States of America*, *87*(20), 8130–8134. https://doi.org/10.1073/pnas.87.20.8130

Woodley, J. M. (2020). New frontiers in biocatalysis for sustainable synthesis. *Current Opinion in Green and Sustainable Chemistry*, *21*, 22–26. https://doi.org/10.1016/j.cogsc.2019.08.006

Wu, R. Q., Li, Z. X., Yang, J. P., Xing, X. H., Shao, D. Y., & Xing, K. L. (2010). Mutagenesis induced by high hydrostatic pressure treatment: A useful method to improve the bacterial cellulose yield of a Gluconoacetobacter xylinus strain. *Cellulose*, *17*(2), 399–405. https://doi.org/10.1007/s10570-009-9388-8

Wu, S., Snajdrova, R., Moore, J. C., Baldenius, K., & Bornscheuer, U. T. (2021). Biocatalysis: Enzymatic Synthesis for Industrial Applications. *Angewandte Chemie - International Edition*, *60*(1), 88–119. https://doi.org/10.1002/anie.202006648

Zdobnov, E. M., & Apweiler, R. (2001). InterProScan - an integration platform for the signature-recognition methods in InterPro. *Bioinformatics*, *17*(9), 847–848. https://doi.org/10.1093/bioinformatics/17.9.847

Zhang, L., Lin, J., Ma, Y., Wei, D., & Sun, M. (2010). Construction of a novel shuttle vector for use in gluconobacter oxydans. *Molecular Biotechnology*, *46*(3), 227–233. https://doi.org/10.1007/s12033-010-9293-2

Zhang, Y. X., Perry, K., Vinci, V. A., Powell, K., Stemmer, W. P. C., & Del Cardayré, S. B. (2002). Genome shuffling leads to rapid phenotypic improvement in bacteria. *Nature*, *415*(6872), 644–646. https://doi.org/10.1038/415644a

Zheng, Y., Zhang, K., Su, G., Han, Q., Shen, Y., & Wang, M. (2015). The evolutionary response of alcohol dehydrogenase and aldehyde dehydrogenases of Acetobacter pasteurianus CGMCC 3089 to ethanol adaptation. *Food Science and Biotechnology*, *24*(1), 133–140.

https://doi.org/10.1007/s10068-015-0019-x

Zheng, Y., Zhang, K., Wang, C., Liu, H., Luo, J., & Wang, M. (2010). Improving acetic acid production of Acetobacter pasteurianus AC2005 in hawthorn vinegar fermentation by using beer for seed culture. *International Journal of Food Science and Technology*, *45*(11), 2394–2399. https://doi.org/10.1111/j.1365-2621.2010.02413.x

Zhong, C. (2020). Industrial-Scale Production and Applications of Bacterial Cellulose. In *Frontiers in Bioengineering and Biotechnology* (Vol. 8, p. 605374). Frontiers Media S.A. https://doi.org/10.3389/fbioe.2020.605374

Aim of the project

This PhD project was aimed to develop novel biocatalytic and fermentative approaches to produce molecules of industrial interest using agri-food wastes as feedstocks. In other words, inspired by the concepts of circularity and sustainability, our goal was to propose and develop innovative concepts for the valorization of agro and food industrial wastes.

Chapter 2

Whole recombinant cells of *E. coli* harboring cytochrome CYP153A as biocatalyst for regioselective hydroxylation of monoterpene derivatives

Abstract

Optimized recombinant whole cells of *E. coli* bearing CYP153A6 have been employed for catalyzing the hydroxylation of different monoterpene derivatives. In most of the cases, high selectivity was observed with exclusive hydroxylation of the allylic methyl group bound to the aliphatic ring. In the case of carvone, hydroxylation occurred also on the other allylic methyl group, although to a lesser extent. Biotransformation carried out in a fed-batch with (*S*)-limonene and a-terpineol mode showed that recombinant whole cells retained activity for at least 24 h allowing for the recovery of 3.25 mg mL^{-1} of perillyl alcohol and 5.45 mg mL^{-1} of 7-hydroxy-*α*-terpineol.

Introduction

Allylic hydroxylation can be accomplished by a variety of chemical methods (especially selenium and chromium reagents) with good chemo-, regio-, and stereoselectivity; however, catalytic reactions and the use of molecular oxygen as co-oxidant are strongly requested (Nakamura, 2013). Therefore, the use of transition metal catalysts able to use O_2 has been developed as alternative methods for allylic C-H oxidation (Campbell, 2012). On the other hand, biocatalytic allylic hydroxylation offers a number of advantages, such as mild reaction conditions and high selectivity, but they are often hampered by low productivity (Bogazkaya, 2014; Boeglin, 2012 and De Montellaro, 2010). The efficiency can be limited by different factors, such as low (bio)catalyst stability, multi-component nature of the enzymatic system, necessity for cofactors, and low substrate and O_2 solubility (Bernhardt, 2014; M.K. Julsing, 2008 and Y. Liang 2018).

Cytochrome P450 CYP153A6 from *Mycobacterium* sp. strain HXN-1500 is a soluble enzyme able to catalyze the selective hydroxylation of the terminal methyl group of different alkanes (Kubota, 2005).

Whole cells (*Pseudomonas putida* or *Escherichia coli*) expressing heterologous CYP153A6 and its electron (Park, 2020; Pennec, 2014 and Song, 2019). Transport partners (ferredoxin reductase and ferredoxin) have been used as biocatalysts. The enzyme showed no activity on methylene groups and very poor activity with simple cyclic alkanes (Pennec, 2014), but it was very active towards specific methyl groups, such as the one of linear C6-C11 alkanes (thus furnishing the corresponding 1-alkanols) and the C7 methyl of (*S*)-limonene (giving perillyl alcohol) in high chemical purity (Park, 2020; Pennec, 2014 and Song, 2019); directed evolution of CYP153A6 allowed for hydroxylation of n-butane into 1-butanol (Van Beilen, 2006) CYP153A6 in whole cells is limited by coupling efficiencies rather than cofactor supply (Olaofe, 2013). However, the most significant limitation in recombinant *E. coli* whole cells is hydrocarbon transport, with substrate import being the main determinant of hydroxylation rates, and product export playing a key role in system stability (Funhoff, 2006 and Gudiminchi, 2012). Whole cell systems bearing co-expression of alkane transporters or systems for cofactor regeneration have been employed, together with two-liquid phase systems and permeabilization of the whole cells (Funhoff, 2007).

All these studies revealed that activity of CYP153A6 is characterized by high selectivity, allowing specific oxyfunctionalization of structurally different substrates. In this work, based on the observation of the selective hydroxylation of (*S*)-limonene, we have revisited the potential of CYP153A6 as a preparative biocatalyst for smooth hydroxylation of allylic methyl groups of various terpene derivatives.

Experimental section

Chemicals

All reagents were purchased from Sigma-Aldrich (Milan, Italy) and/or from VWR International and were used without further purification. All the solvents were HPLC grade. Analytical Thin Layer Chromatography TLC was performed on silica gel 60 F254 or 60 RP-18 F254s precoated aluminum sheets (0.2 mm layer; Merck, Darmstadt, Germany); components were detected under an UV lamp (λ 254 nm), by spraying with a vanillin/H_2SO_4 solution in EtOH [6% (w/v) vanillin + 1% (v/v) H_2SO_4], followed by heating at about 150 °C.

Product purification was accomplished by flash chromatography (silica gel 60, 40–63 mm, Merck).

GC analyses was performed using a Dani® 86.10 HT gas chromatographer equipped with a flame ionization detector (200 °C, p(H_2) 0.8 atm, p(air) 1.5 atm). Chromatographic conditions were as follows: column, DeMePeβCDxPS086 Mega® (25 m x 0.25 mm); injection volume: 1 μL (split (1/50), 230°C); injection solvent: EtOAc; carrier: H_2 (0.6 mL/min).

Analyses were performed with the following programs: (A) i) gradient from 80 °C to 110 °C (10°C/min), ii) isocratic at 110 °C for 9 min, iii) gradient from 110 °C to 180 °C (10°C/min), iv) isocratic at 180 °C for 3 min; (B) i) gradient from 50 °C to 110 °C (10°C/min), ii) isocratic at 110 °C for 9 min, iii) gradient from 110 °C to 180 °C (10 °C/min), iv) isocratic at 180 °C for 3 min; (C) i) isocratic at 50°C, ii) gradient from 50°C to 110 °C (10 °C/min), iii) isocratic at 110 °C for 9 min, iv) gradient from 110 °C to 180° C (10° C/min), v) isocratic at 180° C for 3 min.

Data were processed with the EZChrom Elite software. Retention times were reported in minutes.

1H NMR spectra were recorded on a Varian Oxford 300 MHz NMR spectrometer equipped with a VnmrJ software package (Varian Medical Systems, Palo Alto, California, USA) at 300 K, unless stated otherwise. 1H

chemical shifts (δ) are given in parts per million and were referenced to the solvent signals (δ_H 7.26 ppm from tetramethylsilane (TMS) for $CDCl_3$).

CYP153A6 cloning

The synthetic gene encoding CYP153A6 operon was designed and amplified using the following primer:

Forward: 5'-CACCATATGACCGAAATGACCGTGGC-3'

Reverse: 5'-ATTGCTCGAGTCAATGCTGCGCGGC-3'

The amplified gene was then cloned into the pET100/D-TOPO® vector (Invitrogen) and the correct construct sequence was confirmed by DNA sequencing (Eurofins Biolab Srl).

Expression of recombinant CYP153A

Expression of the recombinant CYP153A6 operon was performed using BL21(DE3)Star *E. coli* strain harbouring pET100-CYP53A6 expression vectors. Seed cultures were prepared by inoculating 0.2 mL of glycerol stock of the recombinant strain in 20 mL of broth with 100 mg mL^{-1} ampicillin and incubating at 37 °C in Erlenmeyer flasks for 16 h. The seed cultures were used as inoculum in 1 L baffled flasks containing 200 mL of the selected medium supplemented with ampicillin (25 µg/mL) to get an initial cells density of 0.1 OD_{600}/mL. The resulting suspensions were incubated at 37 °C and 120 rpm until 0.6-0.8 OD_{600}/mL (2-4 h), brought to 15 °C for 5 min and induced for 4 h with isopropyl-*β*-D-thiogalactopyranoside (IPTG, 0.5 mM). The following liquid media were used: Luria–Bertani (LB: 10 g L^{-1} bacto-tryptone, 5 g L^{-1} yeast extract, 10 g L^{-1} NaCl), Super Broth (SB: 32 g L^{-1} bacto-tryptone, 20 g L^{-1} yeast extract and 5 g L^{-1} NaCl), Terrific Broth (TB: 12 g L^{-1} bacto-tryptone, 24 g L^{-1} east extract, 8 g L^{-1} glycerol, 9.4 g L^{-1} KH_2PO_4 and 2.2 g L^{-1} K_2HPO_4).

Chemical synthesis of substrates

Synthesis of **1e** and **1f**: $LiAlH_4$ (1.0 M in THF, 4.0 mL, 4.00 mmol, 1.20 equiv) was added dropwise at -78° C to a solution of **1c** or **1d** (0.52 mL, 3.32 mmol, 1.00 equiv) in dry THF (10 mL) under inert atmosphere. The mixture was

stirred while warming to room temperature for 3 h. H_2O (1 mL), 1 M NaOH (2 mL) and H_2O (3 mL) were added at 0° C and the suspension was extracted with Et_2O (3 x 20 mL). The reunited organic phases were then washed with brine (2 x 10 mL), dried over Na_2SO_4 and evaporated. The resulting crude was purified by flash column chromatography (cyclohexane-EtOAC, 85:15). **1e** was obtained as a colorless oil in quantitative yield (504 mg, 3.31 mmol): 1H NMR (300 MHz, $CDCl_3$): *δ* 5.51 (ddt, *J* = 5.3, 2.7, 1.4 Hz, 1H), 4.75-4.73 (m, 2H), 4.20 (dddd, *J* = 6.0, 4.4, 2.5, 1.2 Hz, 1H), 2.33-2.22 (m, 1H), 2.21-202 (m, 1H), 2.02-1.88 (m, 1H), 1.76 (dt, *J* = 4.0, 1.5 Hz, 3H), 1.75 (t, *J* = 1.1 Hz, 3H), 1.57-1.45 (m, 2H). **1f** was obtained as a colorless oil in 99% yield (502 mg, 3.30 mmol): 1H NMR (300 MHz, CDCl3): *δ* 5.50 (ddt, *J* = 5.2, 2.7, 1.4 Hz, 1H), 4.75-4.73 (m, 2H), 4.20 (dddd, *J* = 8.3, 6.1, 2.5, 1.2 Hz, 1H), 2.33-2.22 (m, 1H), 2.21-201 (m, 2H), 2.01-1.88 (m, 1H), 1.76 (dt, *J* = 2.5, 1.4 Hz, 3H), 1.74 (t, *J* = 1.1 Hz, 3H), 1.57-1.44 (m, 2H).

Synthesis of **1g** and **1h**: pyridine (151 µL, 1.87 mmol, 1.89 equiv) and acetyl chloride (1.50 equiv) were added at 0 °C to a solution of **1e** or **1f** (150 mg, 0.99 mmol, 1.00 equiv) in dry CH_2Cl_2 (2.0 mL) under N_2. The mixture was stirred at room temperature for 5 h. The resulting yellow suspension was diluted with CH_2Cl_2 (30 mL) and washed with sat. NH_4Cl (2 x 30 mL), sat. $NaHCO_3$ (2 x 30 mL). The organic phase was dried over Na_2SO_4 and evaporated. The resulting crude was purified by flash column chromatography (*n*-hexane-EtOAc, 7:3). **1g** was obtained as a colorless oil in 43% yield (82 mg, 0.42 mmol); **1h** was obtained as a colorless oil in 42% yield (86 mg, 0.41 mmol): 1H NMR (300 MHz, $CDCl_3$): *δ* 5.61 (dq, *J* = 5.3, 1.8 Hz, 1H), 5.50-5.40 (m, 1H), 4.74-4.69 (m, 2H), 2.31 (tdd, *J* = 11.3, 5.0, 2.4 Hz, 1H), 2.20 (ddt, *J* = 12.0, 6.2, 2.2 Hz, 1H), 2.09 (s, 3H), 1.99 (ddt, *J* = 11.2, 3.6, 2.5 Hz, 1H), 1.95-1.88 (m, 1H), 1.72 (br t, *J* = 1.1 Hz, 3H), 1.64 (dq, *J* = 2.5, 1.4 Hz, 3H), 1.52-1.46 (m, 1H).

Synthesis of **1i** and **1j**: pyridine (302 µL, 3.74 mmol, 3.78 equiv) and benzoic anhydride (335 mg, 1.48 mmol, 1.50 equiv) were added to a solution of **1e** or **1f** (150 mg, 0.99 mmol, 1.00 equiv) in EtOAc (2.0 mL) under N_2. The mixture

was refluxed overnight. The light orange solution was washed with sat. NH_4Cl (2 x 30 mL) and sat. $NaHCO_3$ (2 x 30 mL), dried over Na_2SO_4 and evaporated. The resulting crude was purified by flash column chromatography (*n*-hexane-EtOAc, 8:2) to get **1i** and **1j** as colorless oils (**1i**: 33 mg, 0.13 mmol, 13%; **1j**: 38 mg. 0.15 mmol, 15%): 1H NMR (300 MHz, CDCl3): *δ* 8.09-8.05 (m, 2H), 7.60-7.53 (m, 1H), 7.48-7.41 (m, 2H), 5.76-5.64 (m, 2H), 4.75-4.73 (m, 2H), 2.46-2.37 (m, 1H); 2.37-2.29 (m, 1H), 2.21-2.09 (m, 1H), 2.09-1.95 (m, 1H), 1.74 (br t, *J* = 1.1 Hz, 3H), 1.71 (dq, *J* = 2.6, 1.4 Hz, 3H), 1.67-1.61 (m, 1H).

Biotransformations

Cell pellets were recovered by centrifugation at 5000 rpm for 10 min at 4 °C and washed once with 100 mM potassium phosphate buffer; cell pellets were suspended in potassium phosphate buffer (100 mM, pH 7.0) to get the desired cells density and transferred in a flat bottom flask without exceeding 10-15% of the total volume. The substrates at different concentrations were added to the suspension and the flasks tightly sealed; the reaction was incubated at 28° C for 16 h at 150 rpm. Preparative biotransformations were carried out with a total volume of 50 mL. For GC analysis, proper amounts of the mixture (500 µL) were withdrawn at fixed times, extracted with EtOAc (1:1 volume ratio), dried under nitrogen stream at 4° C, diluted in EtOAc and directly injected. For product purification, the mixture was extracted with EtOAc (3 x reaction volume). The reunited organic phases were dried over Na_2SO_4 and evaporated under vacuum at 4°C. The resulting crude was purified by flash chromatography (n-hexane/EtOAc, from 5 to 25% EtOAc in n-hexane) to get either a mixture of constitutional isomers (**2c**+**3c** and **2d**+**3d**) or pure products (**2e**, **2f**, **2k** and **2l**). The ratio between isomers was determined by 1H NMR analysis.

7-Hydroxy-(*R*)-carvone (**2c**+**3c**). The product was obtained as an off-white solid in 67% yield. ^{1}H NMR (300 MHz, $CDCl_3$): *major isomer*: *δ* 6.94 (ddt, *J* = 5.9, 2.5, 1.1 Hz, 1H), 4.81 (br pd, *J* = 1.5, 0.6 Hz, 1H), 4.75 (br tq, *J* = 1.5, 0.8 Hz, 1H), 4.24 (br s, 2H), 2.77-2.25 (m, 5H), 1.74 (s, 3H); *minor isomer*: 6.96-

6.91 (m, 1H, covered by *major isomer*), 5.10 (br q, *J* = 1.3 Hz, 1H), 4.92 (br p, *J* = 0.9 Hz, 1H), 4.11 (br s, 2H), 2.77-2.25 (m, 5H, covered by *major isomer*), 1.01 (d, *J* = 6.5 Hz, 3H).

7-Hydroxy-(*S*)-carvone (**2d**+**3d**). The product was obtained as an off-white solid in 70% yield. ^{1}H NMR (300 MHz, $CDCl_3$): *major isomer*: *δ* 6.94 (ddd, *J* = 5.8, 2.6, 1.3 Hz, 1H), 4.83 (br pent, *J* = 1.5 Hz, 1H), 4.79-4.76 (m, 1H), 4.27 (br d, *J* = 4.8 Hz, 2H), 2.85-2.26 (m, 5H), 1.76 (s, 3H); *minor isomer*: 6.97-6.92 (m, 1H, covered by *major isomer*), 5.13-5.11 (m, 1H), 4.96-4.94 (m, 1H), 4.12-4.09 (m, 2H), 2.85-2.26 (m, 5H, covered by *major isomer*), 1.09 (br dd, *J* = 6.9, 1.2 Hz, 3H).

(1*R*,5*R*)-7-Hydroxycarveol (**2e**). The product was obtained as an off-white solid in 68% yield. ^{1}H NMR (300 MHz, $CDCl_3$): *δ* 5.80-5.74 (m, 1H), 4.75 (s, 2H), 4.57-4.48 (m, 1H), 4.23 (s, 2H), 2.57 (br s, 2H), 2.29 (br td, *J* = 12.7, 4.0 Hz, 1H), 2.22-2.09 (m, 2H), 2.09-1.93 (m, 1H), 1.75 (s, 3H), 1.56 (td, *J* = 12.2, 9.7 Hz, 1H).

(1*S*,5*S*)-7-Hydroxycarveol (**2f**). The product was obtained as an off-white solid in 64% yield. ^{1}H NMR (300 MHz, $CDCl_3$): *δ* 5.78-5.73 (m, 1H), 4.76-4.72 (s, 2H), 4.56-4.46 (m, 1H), 4.21 (s, 2H), 2.99-2.58 (m, 2H), 2.27 (br td, *J* = 12.9, 3.7 Hz, 1H), 2.21-2.08 (m, 2H), 2.08-1.92 (m, 1H), 1.73 (s, 3H), 1.56 (td, *J* = 12.2, 9.8 Hz, 1H).

3-Caren-10-ol (**2k**), The product was obtained as an oil in 39% yield. ^{1}H NMR (300 MHz, $CDCl_3$): 5.72-5.49 (m, 1H), 3.92 (s, 2H), 2.55–2.32 (m, 2H), 2.08-1.95 (m, 2H), 1.63 (s, 1H), 1.11 (s, 3H), 0.82 (s, 3H), 0.74-0.81 (m, 1H), 0.69 (br t, *J* = 8.4 Hz, 1H).

7-Hydroxy-*α*-terpineol (**2l**). The product was obtained as an off-white solid in 65% yield. ^{1}H NMR (300 MHz, $CDCl_3$): *δ* 5.71 (br s, 1H), 4.08-3.96 (m, 2H), 2.23-2.02 (m, 5H), 1.98 (ddt, *J* = 9.4, 4.9, 2.0 Hz, 1H), 1.88 (dddt, *J* = 17.4, 13.4, 4.1, 2.1, 1H), 1.56 (tdd, *J* = 11.5, 5.1, 2.4 Hz, 1H), 1.34-1.25 (m, 1H), 1.22 (s, 3H), 1.21 (s, 3H).

Results and Discussion

Optimization of microbial growth and activity

The chemically competent strain of *Escherichia coli* BL21 Star™ (DE3) was transformed by expression of the redox synthetic gene operon (CYP153A6) which encodes a cytochrome P450, a ferredoxin, and a ferredoxin reductase from *Mycobacterium* sp. strain HXN-1500 by using the broad-host-range vector pET100. Growth of *E. coli* and expression of CYP153A6 were optimized by using three culture media (LB, SB and TB broth) and different times of growth and induction (0.5 mM IPTG). The observed specific growth rates were higher in SB (0.45 h^{-1}) than in LB and TB (0.38 h^{-1} and 0.31 h^{-1}, respectively); SB media allowed higher production of biomass (2.9 g L^{-1}) in comparison to LB (0.6 g L^{-1}) and TB (1.8 g L^{-1}). Besides higher biomass production, SB medium also gave higher CYP153A6 expression, determined both as volumetric activity (U L^{-1}) and specific activity (U $g_{dry\ cells}^{-1}$) towards (*S*)-limonene (**1a**). Up to 4-fold increases were observed in SB medium (Figure 1).

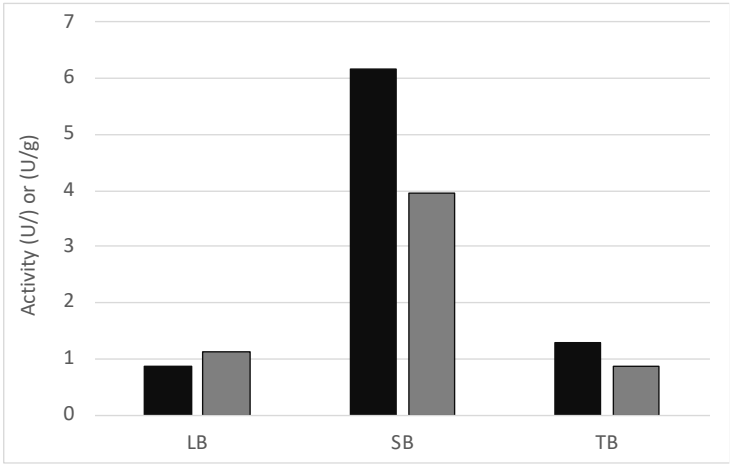

Figure 1. *Activity of CYP153A6 towards (S)-limonene (2 mM) in E. coli using different media, expressed as U/L (grey bars) and U/$g_{dry\ weight}$ (black bars) after induction with 0.5 mM IPTG at mid-exponential phase (cells collected after 16 h at 28° C).*

Optimization of biotransformation with whole recombinant cells

Resting cells of *E. coli* BL21 Star™ (DE3) bearing the redox synthetic gene operon (CYP153A6) and grown in a SB medium were employed for the hydroxylation of (*S*)-limonene (**1a**) in different phosphate buffers; optimization was firstly performed by keeping constant the concentration of substrate (7.5 mM) and by simultaneously evaluating different parameters of the biotransformation (pH, temperature, and biomass concentration) using a Multisimplex experimental design. Immiscibility and high volatility of **1a** made it difficult to achieve an accurate measurement of the actual molar conversion, since formation of perillyl alcohol **2a** ended after 4-5 h, albeit no other side-products were observed. Therefore, space time yield (expressed as amount of product obtained after 4 h per gram of dry cell used) was chosen as response parameter. Optimized conditions were found at relatively high cell density (50 $mg_{dry\ cells}$/mL) used in phosphate buffer at pH = 8.0 and 30 °C, with formation of 0.60 mg/mL of (*S*)-perillyl alcohol detected after 4 h, corresponding to 22.0 $mmol_{product}/g_{cells}$ h. The effect of substrate concentration was investigated using these optimized conditions.

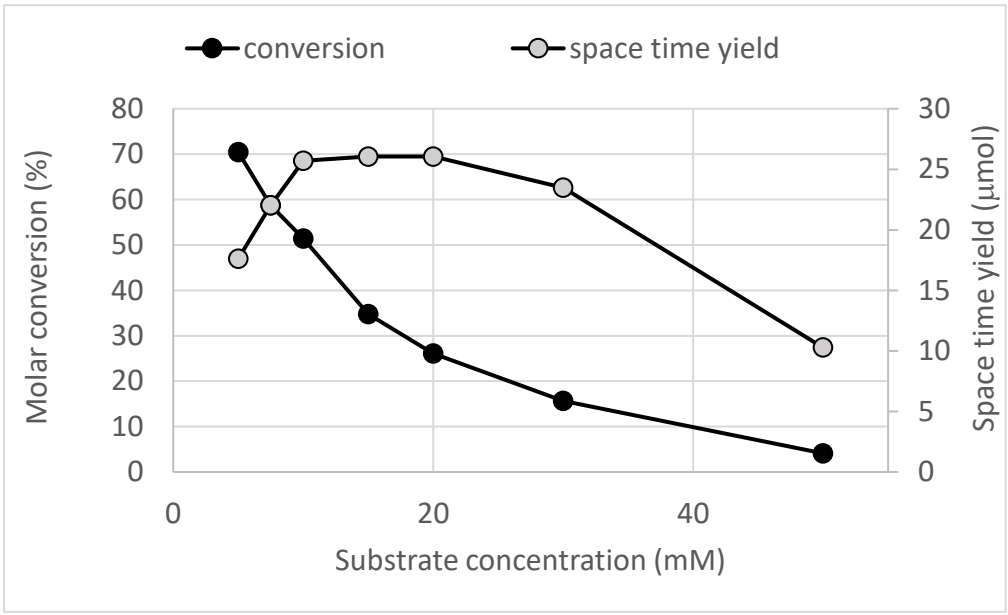

Figure 2. *Effect of substrate concentration on the biotransformation of (S)-limonene with recombinant E. coli. Molar conversion (grey circles) and space time yields (black circles) after 4 h.*

The best compromise between conversion and space time yields was found at an initial substrate concentration of 10 mM (Figure 2). The use of water-miscible organic solvents (ethanol, DMSO, DMF, acetone) for enhancing the solubility of **1a** did not give noticeable improvement of the space time yield. Interestingly, only traces (< 5%) of perilla aldehyde were detected also at prolonged times, implying negligible activity of unspecific oxidative enzymes of the whole cells system towards **2a**.

Very similar space time yield and conversion were observed when (*R*)-limonene **1b** was used as substrate, showing that the stereocenter at C6 position does not affect the activity of the enzyme.

Biotransformation of other monoterpene derivatives

Recombinant whole cells of *E. coli*, grown under optimized conditions, were used as resting cells for the biotransformation of the series of monoterpene derivatives **1c**-**1n** (Figure 3).

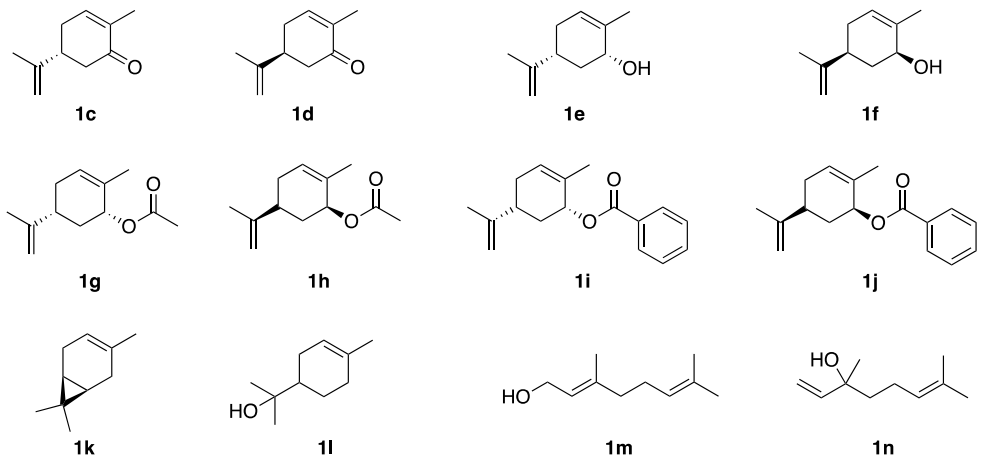

Figure 3. *Panel of terpene derivatives tested as substrates for CYP153A6.*

Hydroxylation of 10 mM of (*R*)-carvone (**1c**) occurred with total conversion of the substrate and formation of the two regioisomers resulting from hydroxylation at C7 (**2c**) and C10 (**3c**) position (Scheme 1). In this case, recovered yields were higher than what found with limonene, most likely because **1c** and its products of hydroxylation are less volatile. It was investigated if substrate concentration could have an effect on the regioselectivity of the enzyme (Table 1).

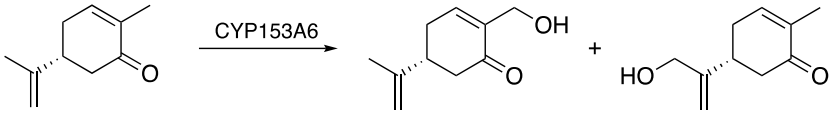

1c **2c** **3c**

Substrate concentration (mM)	Conversion (%)[a]	**2c**/**3c** [b]
2.5	78	87/13
5.0	75	77/23
7.5	74	66/34
10.0	72	57/43

***Table 1**. Effect of substrate concentration in the hydroxylation of (R)-carvone **1b** using whole recombinant cells of E. coli harboring CYP153A6. Molar conversion after 5 h. [a] Calculated as amounts of total products recovered per amount of substrate. [b] As determined by GC and 1H NMR.*

With low substrate concentration (2.5 mM), predominant formation of **2c** (87/13 ratio of **2c**/**3c**) was observed; when substrate concentration was increased, the conversion remained in the range of 72-75%, but with higher production of the regioisomer **3c**, indicating a substantial competition between the two possible allylic hydroxylations. The reaction occurred on (*R*)-carvone (**1 d**) with selectivity and conversions like those observed for the *S*-enantiomer, showing again that activity was not affected by the stereochemistry of the substrate.

Hydroxylation of other terpene derivatives catalyzed by CYP153A6 is reported in Table 2.

Entry	Substrate	Product	Recovered yield (%)
1	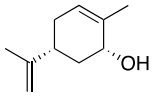 **1e**	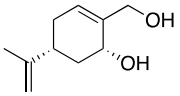 **2e**	68
2	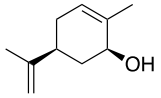 **1f**	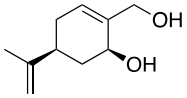 **2f**	64
3	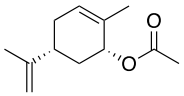 **1g**	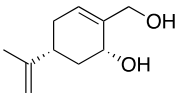 **2e**	65
4	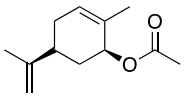 **1h**	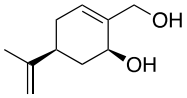 **2f**	69
5	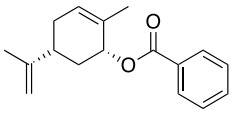 **1i**	no reaction	-
6	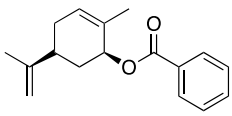 **1j**	no reaction	-
7	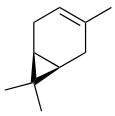 **1k**	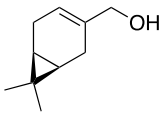 **2k**	39
8	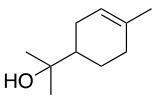 **1l**	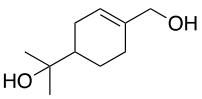 **2l**	65

9	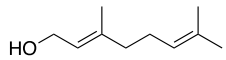 **1m**	no reaction	-
10	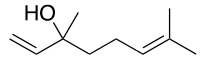 **1n**	no reaction	-

Table 2. *Hydroxylation of terpene derivatives using recombinant cells of E. coli harboring CYP153A6. Biotransformation conditions: substrates (10.0 mM) were added to suspension of whole cells of recombinant E. coli (50 mg mL^{-1}) in phosphate buffer (100 mM, pH 7.0) at 30° C; products were recovered after 5 h of biotransformation.*

Regioselectivity of CYP153A6 was further investigated using the two *syn*-stereoisomers of carveol (**1e**: *R,R*-stereoisomer; **1f**: *S,S*-stereoisomer) as substrates; **1e** and **1f** were transformed with total regioselectivity (hydroxylation in 7 position), furnishing diols **2e** and **2f**, respectively (entry 5 and 6, Table 1). Biotransformation of the enantiomers of carveol acetate (**1g** and **1 h**) resulted in the formation of diols **2e** and **2f**, revealing that hydroxylation proceeded together with acetate hydrolysis, most likely catalyzed by unspecific endogenous esterase(s) present in the whole cells (no hydrolysis was observed in the absence of the biocatalyst). Benzoyl esters of carveol **1i** and **1j** were not converted at all, showing that hydroxylation cannot occur on these bulkier substrates and endogenous esterase(s) of *E. coli* cannot hydrolyze the benzoyl ester.

In our screening for establishing the substrate scope of CYP153A6, we included D^3-carene **1k** and a-terpineol **1l**. Selective hydroxylation of the allylic methyl group was found as the only apparent reaction in both the cases, albeit with different yields; products **2k** and **2l** were recovered in lower yields, albeit no other by-products were observed by GC or during the isolation of the product, indicating that (as in the case of limonene) volatility of the substrate limited the real conversion. Finally, no activity was observed on acyclic monoterpenes encompassing allylic methyl groups, such as geraniol **1l** and linalool **1m**.

Fed-batch biotransformation

Fed-batch biotransformation of (*S*)-limonene **1a** was carried out for improving the amounts of product accumulated during the bioprocess. Fresh substrate **1a** (10 mM) was added after 4 h of biotransformation, when no residual substrate was present.

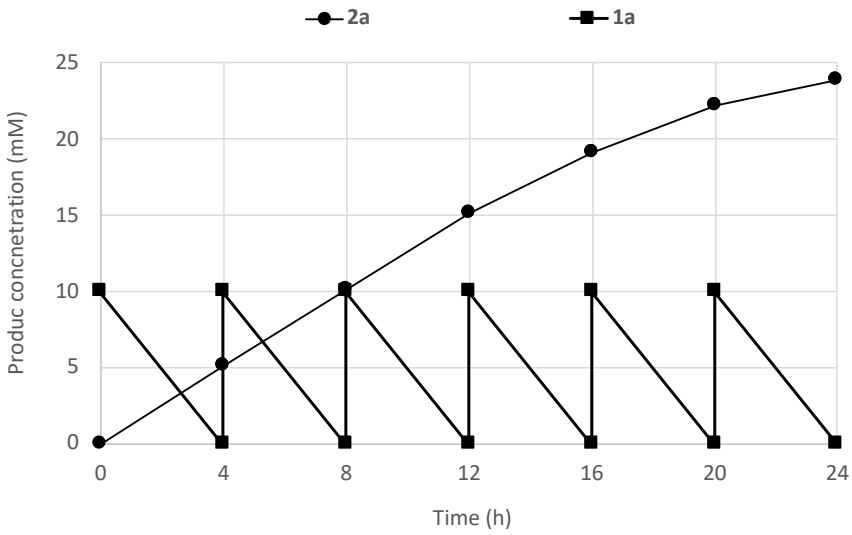

Figure 4. *Fed-batch biotransformation of (S)-limonene with recombinant cells of E. coli harboring CYP153A6.*

Whole cells progressively lost hydroxylating activity and, after 24 h of fed-batch operation, 30-35% of the original activity was maintained; the reaction occurred with minor accumulation of aldehyde (< 0.1 mg/mL). After 24 hours of operation, 23.9 mM (3.25 mg mL^{-1}) of **2a** were accumulated in the biotransformation medium (Figure 4)..

A similar procedure was also applied, as proof of concept, to the hydroxylation of a-terpineol furnishing 32.0 mM (5.45 mg mL^{-1}) of the corresponding hydroxylated product **2k**.

Discussion

Cytochrome P450 (CYP450) is an enzyme family widely used for the biocatalytic hydroxylation of different types of molecules (Julsing, 2008). Among them, functionalization of methyl groups under mild conditions is an attractive biotransformation since it is difficult to be obtained with green methodology and high selectivity using conventional synthetic methods (Nakamura 2013 and Campell 2012). Cytochrome P450 (CYP153A6) from *Mycobacterium* sp. strain HXN-1500 was previously found as a selective system for the hydroxylation of methyl groups occurring in linear and cyclic hydrocarbons, such as *n*-octane, (*S*)-limonene, and *p*-cymene. The entire operon of CYP153A6 consists of the monooxygenase and its electron partners (ferredoxin reductase and ferredoxin) and their recombinant expression was achieved in different bacterial hosts (*P. putida*, *E. coli*); a noteworthy improvement of the biocatalyst activity was obtained by expressing the operon with a pET vector *in E. coli* (Song, 2019). In this work, we used a similar vector and the activity towards (*S*)-limonene was optimized by studying different growth media, noticing that Super Broth liquid medium was particularly suited for promoting the desired activity.

The selectivity displayed towards (*S*)-limonene is remarkable, since CYP153A6 distinguishes between the two methyl groups (both in allylic position) and hydroxylates only the one directly attached to the aliphatic ring. We here investigated if this selectivity could be exploited for the hydroxylation of a series of monoterpene derivatives carrying allylic methyl groups. Complete selectivity for the hydroxylation of the methyl group directly attached to the ring (C7 for menthane structure and C10 for carane structure) was observed in most of the cases, with the exception of carvone which was also hydroxylated at the allylic methyl group at C10 position. The presence of a substituent at C6 position seems relevant for the recognition of the substrate. The two enantiomers of carveol (with OH at C6 position) were regioselectively hydroxylated at C7 methyl, with no trace of other products and the same

situation was observed when no substituents were present at C6; on the other hand, the two enantiomers of carvone (with a C=O at C6 position) were hydroxylated at both allylic positions, indicating that the occurrence of the carbonyl group partially hampered reactivity at C7 position.

Preparative biotransformations (50 mL-scale) were accomplished starting from 10 mM of susbtartes and furnishing variable yields (in the range of 0.6-1.1 mg mL^{-1}), strongly depending on the volatility of the compounds involved in the reactions; an improvement of product accumulation was achieved with a simple fed-batch procedure. The fed-batch process was applied to the hydroxylation of (S)-limonene and a-terpineol (chosen for their different volatility and as general concept validation), allowing for the recovery of 3.25 mg mL-1 of (S)-perillyl alcohol **2a** and 5.45 mg mL^{-1} of 7-hydroxy-a-terpineol **2k**. In both cases, the biocatalyst maintained good activity for 16 h and lost around 65-70% of the initial activity after 24 h.

In conclusion, these results pointed out that optimized whole cells of *E. coli* harboring the operon of monooxygenase CYP153A6 can be used for highly regioselective hydroxylation of different monoterpene derivatives.

References

A. Nakamura, M. Nakada. Allylic Oxidations in Natural Product Synthesis. Synthesis 2013, 45, 1421–1451

A.N. Campbell, S.S. Stahl, Overcoming the “Oxidant Problem”: Strategies to Use O_2 as the Oxidant in Organometallic C–H Oxidation Reactions Catalyzed by Pd (and Cu), Accounts Chem Res. 45 (2012) 851–863. https://doi.org/10.1021/ar2002045.

A.M. Bogazkaya, C.J. von Bühler, S. Kriening, A. Busch, A. Seifert, J. Pleiss, S. Laschat, V.B. Urlacher, Selective allylic hydroxylation of acyclic terpenoids by CYP154E1 from *Thermobifida fusca* YX, Beilstein J Org Chem. 10 (2014) 1347–1353. https://doi.org/10.3762/bjoc.10.137.

W.E. Boeglin, A.R. Brash, Cytochrome P450-type Hydroxylation and Epoxidation in a Tyrosine-liganded Hemoprotein, Catalase-related Allene Oxide Synthase, J Biol Chem. 287 (2012) 24139–24147. https://doi.org/10.1074/jbc.m112.364216.

P.R.O. de Montellano, Hydrocarbon Hydroxylation by Cytochrome P450 Enzymes, Chem Rev. 110 (2010) 932–948. https://doi.org/10.1021/cr9002193.

R. Bernhardt, V.B. Urlacher, Cytochromes P450 as promising catalysts for biotechnological application: chances and limitations, Appl Microbiol Biot. 98 (2014) 6185–6203. https://doi.org/10.1007/s00253-014-5767-7.

M.K. Julsing, S. Cornelissen, B. Bühler, A. Schmid, Heme-iron oxygenases: powerful industrial biocatalysts? Curr Opin Chem Biol. 12 (2008) 177–186. https://doi.org/10.1016/j.cbpa.2008.01.029.

Y. Liang, J. Wei, X. Qiu, N. Jiao, Homogeneous Oxygenase Catalysis, Chem Rev. 118 (2018) 4912–4945. https://doi.org/10.1021/acs.chemrev.7b00193.

B J.B. van Beilen, E.G. Funhoff, A. van Loon, A. Just, L. Kaysser, M. Bouza, R. Holtackers, M. Röthlisberger, Z. Li, B. Witholt, Cytochrome P450 Alkane Hydroxylases of the CYP153 Family Are Common in Alkane-

Degrading Eubacteria Lacking Integral Membrane Alkane Hydroxylases, Appl Environ Microb. 72 (2006) 59–65. https://doi.org/10.1128/aem.72.1.59-65.2006.

O.A. Olaofe, C.J. Fenner, R. Gudiminchi, M.S. Smit, S.T. Harrison, The influence of microbial physiology on biocatalyst activity and efficiency in the terminal hydroxylation of n-octane using *Escherichia coli* expressing the alkane hydroxylase, CYP153A6, Microb Cell Fact. 12 (2013) 8. https://doi.org/10.1186/1475-2859-12-8.

E. G. Funhoff, U. Bauer, I. Garcıa-Rubio, B. Witholt, J. B. van Beilen. CYP153A6, a soluble P450 oxygenase catalyzing terminal-alkane hydroxylation. *J. Bacteriol.* **2006**, *188*, 5220-5227.

E.G. Funhoff, J. Salzmann, U. Bauer, B. Witholt, J.B. van Beilen, Hydroxylation and epoxidation reactions catalyzed by CYP153 enzymes, Enzyme Microb Tech. 40 (2007) 806–812. https://doi.org/10.1016/j.enzmictec.2006.06.014.

R.K. Gudiminchi, C. Randall, D.J. Opperman, O.A. Olaofe, S.T.L. Harrison, J. Albertyn, M.S. Smit, Whole-cell hydroxylation of n-octane by Escherichia coli strains expressing the CYP153A6 operon, Appl Microbiol Biot. 96 (2012) 1507–1516. https://doi.org/10.1007/s00253-012-3984-5.

D.J. Koch, M.M. Chen, J.B. van Beilen, F.H. Arnold, In Vivo Evolution of Butane Oxidation by Terminal Alkane Hydroxylases AlkB and CYP153A6, Appl Environ Microb. 75 (2008) 337–344. https://doi.org/10.1128/aem.01758-08.

A. Pennec, C.L. Jacobs, D.J. Opperman, M.S. Smit, Revisiting Cytochrome P450-Mediated Oxyfunctionalization of Linear and Cyclic Alkanes, Adv Synth Catal. 357 2015) 118–130. https://doi.org/10.1002/adsc.201400410.

S. Cornelissen, M.K. Julsing, J. Volmer, O. Riechert, A. Schmid, B. Bühler, Whole-cell-based CYP153A6-catalyzed (S)-limonene hydroxylation efficiency depends on host background and profits from monoterpene

uptake via AlkL, Biotechnol Bioeng. 110 (2013) 1282–1292. https://doi.org/10.1002/bit.24801.

Chapter 3

Expression of cytochrome CYP153A6 in acetic acid bacteria: preparation of new biocatalysts for converting hydrocarbons into aldehydes and carboxylic acids

Abstract

In this work we cloned and functionally expressed CYP153A6 from *Mycobacterium* sp., an enzyme able to hydroxylate in a regioselective manner a wide range of organic molecules, in two acetic acid bacteria (AAB) strains: *Komogataeibacter xylinus* DSM 2325 and *Acetobacter malorum* MIM 2000/28 DSM 112354. CYP153A6 was transformed employing three tailor-made plasmids carrying respectively an strong constitutive Anderson promoter (J23104) and two inducible promoters (ptet01 and pLux01). The designed biocatalyst showed high regioselective hydroxylation yields towards limonene and octane and the newly formed alcohols (perillyl alcohol and octanol) were easily converted into the corresponding carboxylic acid by all the engineered recombinant strains. Furthermore, a microbial biosensor to detect the biotransformation of limonene to perillic acid was developed, employing a *K. xylinus* whole-cell bacterial GFP biosensor.

Introduction

Acetic acid bacteria (AAB) are aerobic microorganisms widely used in biotechnological applications for their peculiar ability to carry out incomplete oxidation of primary and secondary alcohols (including mono- and disaccharides) thus producing aldehydes, ketones, and carboxylic acids (Raspor & Goranovič, 2008). These oxidative reactions are generally catalyzed by membrane-bound alcohol dehydrogenase (ADH) and aldehyde dehydrogenase (ALDH), situated on the periplasmic side of the bacterial membrane (Saichana et al., 2015); these reactions are a good alternative to conventional chemical oxidations since they are often highly selective and can be carried out under mild and ecologically compatible conditions avoiding the use of toxic reagents and solvents (Dong et al., 2018). Moreover, AAB are highly acidophilic, being able to accumulate high amounts of carboxylic acids

(Molinari et al., 1997 and Zhang et al., 2016) and show good tolerance towards hydrophobic organic solvents (Villa et al., 2002).

Engineering AAB with heterologous genes can expand their potential as biocatalysts (Gao et al., 2020). The incorporation of monooxygenases into AAB would allow the transformation of non-functionalized molecules into alcohols which could be subsequently easily oxidized by AAB (Romano et al., 2012). In this way, the introduction of a terminal monooxygenase (*e.g.,* Cytochrome P450 CYP153A6) (Funhoff et al., 2006) with the ability to form primary alcohols from hydrocarbons should pave the way to convert alkenes into aldehydes and/or carboxylic acids by endogenous ALDHs and ADHs (Scheme 1).

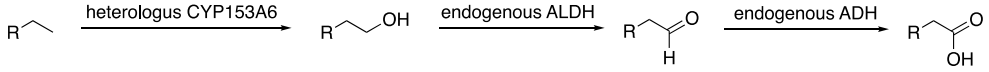

Scheme 1. *Sequential oxidation of methyl groups of hydrocarbons using AAB engineered with terminal monooxygenases.*

Cytochrome P450 CYP153A6 from *Mycobacterium* sp. strain HXN-1500 catalyzes the hydroxylation of the methyl group of different hydrocarbons (Romano et al., 2012). Recombinant strains of *Pseudomonas putida* and *Escherichia coli* carrying CYP153A6 together with its electron transport partners have been used as biocatalysts for the preparation of alcohols and carboxylic acids, by regioselective hydroxylation of unfunctionalized molecules, such as limonene and *n*-octane (Gudiminchi et al., 2012 and Cornelissen et al., 2013).

Among the natural hydrocarbons found in nature, limonene is a cheap and highly available terpene, one of the major components of the oily fraction of orange peels and the citrus pulps that are the main by-products of the citrus processing industry. Molecules deriving from the oxy-functionalization of limonene, such as perillyl alcohol and perillic acid formed respectively by its enzymatic allyl methyl hydroxylation and further oxidation, have been reported

to have anti-cancer and anti-metastatic potential (Kuttan et al., 2011). Perillartine, produced from perillyl aldehyde condensation with hydroxylamine, is a food additive 2000 times sweeter than sucrose, while methylperillate, a precursor of terephthalic acid which is the main precursor polyethylene terephthalate (PET) plastic, can be produced by enzymatic methylation of perillic acid by O-methyltransferase. (Jongedijk et al., 2020 and Jongedijk et al., 2018). Recent studies have reported the usage of perillyl alcohol and perillic acid as promising antiviral and antimetastatic drugs (Mello et al., 2020 and Ravera et al., 2021). Regioselective hydroxylation can be performed by cytochrome monooxygenases CYP450, a class of enzymes able to hydroxylate a wide range of organic molecules; CYP153A6 from Mycobacterium sp. strain HXN-1500 is a soluble enzyme able to catalyze the regioselective hydroxylation of limonene at C-7, furnishing perillyl alcohol (Scheme 1) (Fujita et al., 2009).

Among the wide range of alcohols that can be oxidized by AAB, perillyl alcohol is known to be oxidized by different AAB strains into perillyl aldehyde and perillic acid (scheme 1) (Zambelli et al., 2012). *Komagataeibacter xylinus* (DSM 2325) was chosen because of its peculiar ability to produce bacterial cellulose from different carbon sources. Furthermore, recently a characterization of different molecular tools of a phylogenetically related strain was reported (Florea, Hagemann, Santosa, Abbott, & Micklem, 2016 and Teh et al., 2019). A second AAB strain, isolated in our laboratory (*Acetobacter malorum*) was employed in this study.

Material and methods

Microorgnisms and grown media

Acetobacter malorum DSM 112354 was isolated in our laboratory from "mother of vinegar". For isolation, the mother was homogenized with a dispersion tool (Ika, Germany) until a suspension was obtained, the cell suspension was centrifuged (2000g, 10 minutes at 4°C), and washed twice with PBS buffer (pH 7.00). The suspension was plated on a solid medium (GYC) and incubated at 28°C for three days. The colonies which produced a large $CaCO_3$ solubilization halo were singularly picked up and streaked again on GYC medium four times. The purity of the strain was routinely inspected under microscope. The isolated strain was maintained on GYC agar slants and stored as glycerol stocks at −80◦C.

Komagataeibacter xylinus DSM 2325 was purchased by Leibniz Institute DSMZ-German Collection of Microorganisms and Cell Cultures (Braunschweig Germany) and maintained on GYC medium.

The two acetic acid bacteria were grown on different liquid media reported in Table 1. *E.coli* DH5α (Invitrogen) or *E. coli* XL1-Blue (Stratagene, USA) were used as a host strain for cloning and plasmid propagation. Both the *E. coli* strains were cultivated on LB medium.

Medium	Composition
GYC	Glucose 50 g L^{-1}, yeast extract 10 g L^{-1}, $CaCO_3$ 30 g L^{-1}, pH 6.5
Hestrin and Schramm glucose (HS-GLU)	Glucose, 20 g $L^{-1,}$ peptone, 5 g $L^{-1,}$ yeast extract, 5 g $L^{-1,}$ Na_2HPO_4, 2.7 g $L^{-1,}$ citric acid, 1.15 g/L; pH 6.0
Hestrin and Schramm sucrose (HS-SAC)	Sucrose, 20 g L^{-1}, peptone, 5 g $L^{-1,}$ yeast extract, 5 g L^{-1}, Na_2HPO_4, 2.7 g $L^{-1,}$ citric acid, 1.15 g $L^{-1,}$ pH 6.0
GLY	Glycerol 25 g L^{-1}, yeast extract, 10 g L^{-1}, pH 6.0
SBY	Sorbitol 50 g L^{-1}, peptone, 5 g L^{-1}, yeast extract, 5 g L^{-1}, pH 6.0

Table 1. *List of culture media employed in this study for AAB cultivation.*

Molecular identification by 16S rRNA

For DNA extraction and 16s DNA identification of *Acetobacter malorum* DSM 112354, genomic DNA was extracted from an overnight culture grown at 28°C in a 100 mL baffled flask containing 20 mL of GLY medium using the DNeasy UltraClean Microbial Kit (Qiagen); 1.8 mL of cell suspension was used for DNA extraction. Genomic DNA quality was then checked by agarose gel electrophoresis. The 16S ribosomal DNA (rDNA) gene was amplified by PCR, using primers P0 and P6 (Table S1). PCR reactions were performed in a 25 µL reaction mixture containing 100 ng bacterial DNA, 2.5 µL 10×reaction buffer Dream TaqTM (Fermentas, Vilnius, Lithuania), 200 µmol L^{-1} of each dNTP 0.5 mmol.L−1 MgCl2, 0.5 µmol L^{-1} each primer, and 0.5 U Dream TaqTM DNA polymerase.

PCR thermal cycling conditions were: 2 min at 94 °C, 35 cycles of 45 s at 94 °C, 45 s at 55 °C, 1 min at 72 °C, followed by a 7-min final extension at 72 °C. PCR amplification product was checked by agarose gel electrophoresed in 0.8% and purified using PCR Isolate II PCR and Gel Kit (Bioline) according to manufacturer's instructions. Then PCR amplification was checked by Sanger sequencing (Eurofins genomics, Ebersberg, Germany) using pA primer (Edwards et al. 1989). BLAST algorithm was used to determine the most related 16S rRNA gene sequences among acetobacter taxid in the NCBI nucleotide sequence database.

The isolate was deposited on DSMZ colture collection under the name DSM 112354 name, 16S rRNA gene sequence of *Acetobacter malorum* 112354 has been deposited NCBI GenBank database with the accession number MW365538.

AAB Electrocompetent cells preparation and transformation

K. xylinus DSM 2325 electrocompetent cells were prepared as described by (Florea et al. 2016). *Acetobacter malorum* electrocompetent cells were prepared as follows: a single colony of *Acetobacter malorum* was grown at

28°C for two days in a 100mL baffled flask, filled with 20 mL of GLY medium. The culture was diluted 1:100 into 20 mL of GLY medium and incubated overnight as above. The following day right amount of seed culture was inoculated in a 1000mL baffled flask with 100mL of GLY medium to achieve an $O.D.600_{nm}$ of 0.01. Cells were incubated until they reached the early log phase $O.D.600_{nm}$ 0.5-0.7 (about 12 hours). Whole culture was aseptically transferred into 50mL sterile centrifuge tubes and incubated on ice for 15 min. The cells were centrifuged at 5000 g for 20 min at 4°C, cells were pooled in a single tube and resuspended 10 mL ice-cold 1mM HEPES buffer pH 7.00. Then resuspension was centrifuged again for 20 minutes at 5000 g and resuspended in 10 mL of HEPES buffer. Finally, cells were centrifuged at 5000 rpm for 20 minutes at 4°C, the supernatant was discarded and the obtained cell pellet was resuspended in 2 mL ice-cold 15% glycerol - water solution. Aliquots of 100 µL were transferred in 1.5mL sterile Eppendorf tubes and frozeen at -80 °C.

DSM 2325 and DSM112354 strains were transformed by electroporation with electropulser (Gene Pulser® II Electroporation System, BioRad, CA, USA) at 1.8 kV, 5-6 ms, 200 Ohm resistance, 25 µF capacitance. Pulse was applied to 100 µL aliquots of electrocompetent cells adding at least 100 ng of plasmid DNA in 1 mm with electroporation cuvettes. After electroporation, DSM2325 cells were recovered with HS (1%v/v cellulases), MIM 2000/28 were recovered with GLY medium. After 16h of incubation at 28°C – 220 rpm, transformed cells were plated on HS-GLU (20 g/L) Petri dishes (chloramphenicol 320mg/L, 1%v/v cellulases) and grown at 28°C for 2-4 days.

Characterization of Constitutive and Inducible promoters strength in AAB, optimization of the culture conditions using mRFP1 fluorescence as reporter.

PLux01 and pTet01 mRFP constructs were obtained from Addgene (www.addgene.com) respectively catalog #78281 and #78283. We

investigated the strength of the selected promoters transformed in A. *malorum* and in DSM2325. Promoter strength was accessed by quantifying the mRFP1 fluorescence intensity normalized per OD unit. DSM 2325 was cultivated in the presence of cellulase to avoid cellulose formation. For constitutive promoter analysis single colonies of DSM 2325 and *A. malorum* were cultivated overnight in 5mL of the selected culture medium, the following day the seed cultures were subcultured to a fresh medium to OD600 0.1 and grown overnight, then 200 µL of culture were transferred in 96-well plates. Measurement of mRFP1 fluorescence (excitation 580 nm, emission 610 nm) were performed with Spark multimode microplate reader (Tecan, Switzerland). All the measurements were performed in triplicates. PLux01 and pTet01 inducible promoters were characterized employing resting cells treated as described for constitutive promoter characterization. We transformed the plasmids constructed by Florea for the characterization of *K. xylinus* with anhydrotetracycline (ATc) or N-acyl homoserine lactone (AHL) inducible promoters (Florea, Hagemann, Santosa, Abbott, Micklem, et al., 2016). For inducible promoter strength analysis, the precultures of the recombinant strains were cultivated as described above for constitutive promoter strength characterization. Seed cultures were subcultured in 5mL of fresh medium to 0.1 OD_{nm} and grown to mid-exponential phase (0.4-0.6 600_{nm}), the inducers were added to the cultures at different concentrations. Fluorescence measurement was performed with Spark multimode microplate reader (Tecan, Switzerland) with wavelengths 485 nm (excitation) and 510 nm (emission) and the signal was proportioned to that of the noninduced cells and normalized on the OD value of each sample. All the measurements were performed in triplicates. We analyze mRFP1 fluorescence as a reporter employing different antibiotic concentrations and media to optimize the best culture conditions. We cultivated the strains employing 320 mg/L and 32 mg/L of chloramphenicol to investigate the possibility to keep plasmid replication even using lower antibiotic concentration (for plasmid transformations we employed HS-GLU plates with 320 mg/L of chloramphenicol). MIM2000/28

mRFP strain was cultured in GLY and HS-GLU media while DSM2325 was cultivated in SBY and HS-GLU medium.

Recombinant DNA and Engineering of constitutive and inducible constructs

Restriction enzymes, Phusion High-Fidelity DNA Polymerase, Taq Polymerase, dNTPs were purchased from ThermoFisher, Q5 Site-directed mutagenesis kit from Neb (E0554, Neb). NucleoSpin®Plasmid and PCR clean-up kits were purchased by Macherey–Nagel. All the plasmids and primers used in this study are listed in table S1 and in table S2, respectively. The sequence (2.9Kbp) coding for *Mycobacterium sp.* Limonene monooxygenase operon was synthesized, codon-optimized for expression in Acetobacteriacee and inserted in pUC57b vector by BaseClear (Leiden, The Netherlands). J23104-mRFP1-331Bb, pLux01 and pTet1 plasmids (containing Chloramphenicol acetyltransferase resistance, ORI pBBR1 oriV, the sequence coding for pBBR1 replication protein) were purchased from Addgene. The plasmids were chosen to investigate in both strains the expression of Red fluorescent protein (mRFP1) driven by the constitutive J23104 promoter or pLux and Ptet inducible promoters. J23104-mRFP1-331Bb (AddGene #78274) carries mRFP1 protein downstream the constitutive Anderson promoter J23104, pLux01 plasmid (AddGene #78281) expresses mRFP1 behind an N-acyl homoserine lactone (AHL) inducible construct while pTet1 (AddGene #78283) plasmid expresses mRFP1 behind an ATc-inducible promoter. The inducible and constitutive promoters utilized in this study were already characterized by (Florea, Hagemann, Santosa, Abbott, Micklem, et al., 2016 and Teh et al., 2019) for different Acetobacteriacee *G. xylinus* 700178*, G. hansenii* 53582*, and K. rhaeticus* iGEM. We aimed to find the optimal induction and cultivation conditions for our isolate strain MIM DSM 112354 strain keeeping K. *xylinus* as a positive control, using mRFP1 as a reporter gene.

For the construction of CYP450 expression vector called J23104 CYP450, J23104-mRFP1-331Bb plasmid was amplified with “NDEI_20_10” and “Stop_codon_XHOI” primers with Phusion polymerase from the edges of mRFP1 gene and the obtained PCR product was checked by 1% agarose gel electrophoresis. Then, one microliter of the purified PCR product, containing template plasmid and PCR product, was treated with NEB Q5 Site-Directed Mutagenesis kit to cleave template plasmid and circularize PCR product, obtaining “J23104 mut” plasmid that was used in further experiments as a negative control. The reaction mixture was transformed in *E.coli* DH5a competent cells, plated on LB AGAR plates with 30 mg/L chloramphenicol and grown overnight at 37°C. Right circularization was checked by colony PCR with check1 and check2 primers and by plasmid extraction and sequencing.
Lim. Monooxygenase Operon full sequence was amplified from pUC57 vector by polymerase chain reaction with Phusion polymerase with OP. LIM NDEI_CM and LIM XHOI_CM primers and cloned in J23104 mut vector obtaining “J23104 CYP450” plasmid. Positive colonies were selected by colony PCR with check1 and check2 primers, inoculated in 20 mL of LB medium supplemented with 30 mg/L of Chloramphenicol. After plasmid extraction, the sequence of the obtained vector was checked by Sanger sequencing. Similarly, plasmids carrying CYP450150A3 operon under the inducible pLux1 and pTet1 promoters were constructed amplifying pLux01_mRFP1 (#78281) pTet1_mRFP1 (#78283) AddGene plasmids respectively with primers: pLux!_NDEI - pLuX_XhoI and pTet_BamHI - ptet_XhoI to eliminate mRFP1 gene and insert suitable restriction sites. Then, PCR products were ligated with Lim. Monooxygenase Operon sequence amplified from pUC57b vector with primers OP-LYMIC-NDEI-CM - OP-LYMIC-XHOI-CM and OP-LYMIC-BAMHI - OP-LYMIC-XHOI-CM and vector constructs were transformed into *K. xylinus* and *MIM 2000/28* as described in “AAB Electrocompetent cells Preparation and transformation”. The transformants were checked by colony PCR using check1 and check2 primers

located on the plasmid. SnapGene Software (GSL Biotech, Chicago, IL, USA) was used to check sequences and to generate plasmid maps.

Limonene and octane biotransformation with DSM 2325 and *A. malorum*

Before testing the hydroxylation ability of recombinant strains we tested the oxydation capabilities of wild type strains toward peryllil alcohol and octanol. We grew the strains in different culture media to evaluate the activity of membrane-bound dehydrogenases. The strains were cultured in HS-GLU and GLY media as follows without the employment of antibiotic. Single colonies of recombinant *K. xylinus* transformed with J23104 CYP450 were inoculated in 20mL of HS -GLU with 0.5% v/v of cellulases from *Trichoderma Reseei* to avoid bacterial cellulose fibrils formation and *Acetobacter malorum* CYP450 strain was cultured in GLY medium supplemented with 32mg/L chloramphenicol and incubated for three days at 28°C. Then, 500mL baffled flasks with 50 mL of HS cellulase liquid medium [0.5% (v/v)] containing 32 mg/L chloramphenicol were inoculated from precultures starting from an O.D. 600_{nm} of 0.1 and incubated overnight at 28 °C at 160 rpm. The following day the cells were harvested, washed and resuspended in phosphate buffer (0.1 M, pH 7.0) and neat substrates were directly added to the cultures. Peryllil alcohol and octanol were employed as the substrate for biotransformations employing wild type strains. Limonene and octane were employed as substrates for biotransformations employing recombinant strains. Biotransformations were carried out employing 1 g/L of substrates. Furthermore, employing *K. xylinus* CYP450 recombinant strains different limonene concentrations were tested keeping the same above mentioned biotransformation conditions. (32 mg/L chloramphenicol, 2% cellulase from *Trichoderma reesei*). Alternatively, the monooxygenase enzymatic activity of DSM2325 CYP450 was tested employing growing cells with limonene as substrate added to overnight cultures grown on SBY medium (50mL of SBY medium in 500mL baffled flasks).

Limonene biotransformation employing DSM 2325 bacterial cellulose and pellicle weight determination

Enzymatic activity of BC pellicle produced by recombinant DSM2325 J23104 CYP450 was tested. As a negative control, cellulose from DSM2325 wild type was utilized. For BC production glycerol stocks, obtained from precultures of biotransformation experiments with recombinant *K. xylinus* J23104 CYP450, were inoculated in 20 mL of HS-GLU medium in presence of chloramphenicol 32mg/L and grown at 28°C overnight in 100mL baffled flasks in aerobic conditions in an orbital shaker at 160 rpm. Then, 100mL of fresh HS-GLU medium (32mg/l chloramphenicol) was inoculated in 150mm diameter Petri dishes adding 20mL of preculture and grown under static conditions at 28°C for two days. For biotransformation cellulose pellicle was extensively rinsed with HQ-water until cells release from pellicle was stopped. Enzymatic activity of CYP450 was tested under static and agitated conditions. Biotransformations under agitated conditions were carried out with BC biofilm inserted in 250mL flask with 25mL of 100 mM phosphate buffer pH 7.0 (160rpm), biotransformations under static conditions were performed in 150mm diameter plate with 150mL of KP buffer, incubated at 28°C. Limonene (0,5 g/L) was used as a substrate for both the conditions and the biotransformations were carried out for three days and the formation of perillic acid was analyzed by GC-MS. After biotransformation we checked BC production yields of the recombinant strain comparing BC production of bacterial cellulose pellicles were boiled for 30 min in 0.5 M NaOH solution, washed until neutral pH was reached, dried at 60°C and measurements of dry weight were taken at room temperature. Similarly, we tested BC production yield of *K. xylinus* J23104 mut and *K. xylinus* J23104 mRFP recombinants strains employing the same culture conditions described above for *K. xylinus* J23104 CYP450.

Analytical methods

Enzymatic activity of recombinant AAB carrying CYP450 was quantified by gas mass chromatography (GC-MS), analyzing substrate hydroxylation and further oxidation products. For instance, was monitored limonene hydroxilation to perillyl alcohol and his further oxidation caused by AAB DHs to perillyl aldehyde and perillic acid. With the same rationale, octane hydroxylation was accessed by analyzing octanol formation. Then the further alcohol oxydation products were followed analyzing octanaldehyde and octanoic acid. We performed for the quantitative determination of bioreaction yields. At different times 0.1 or 0.5 mL of biotransformation were centrifugated at 11.000 rpm for 2 min. Conversion products were extracted with ethyl acetate after acidification to pH 1.00 with hydrochloric acid. Gas chromatography analyses were carried out using An Agilent Gas Chromatograph (series 6890) using HP-5MS capillary column (30 m, 0.25 mm ID, 0.25 μm film thickness). For the analysis helium was utilized as carrier gas (flow rate: 1 mL min – 1, inlet temp.: 250 °C, split 1:50). The temperature ramp program was set from 80°C to 250°C with a gradient of 1°C/min. Oxidation products corresponding to chromatographic peaks were identified by comparison with internal standards and by comparison with a mass spectral library fragmentation patterns library.

Construction and development of a sfGFP fluorescence microbial biosensor for limonene oxidation and perillic acid detection

Recently a synthetic p-isopropyl benzoate (cumate) inducible promoter has been reported for *E.coli*, *Bacillus subtilis* and *Bacillus megaterium* (Seo & Schmidt-Dannert, 2019). The authors described the synthetic induction system (pCT5-bac2.0, adddgene #119872) as a tight regulated and concentration-dependent expression system, in which sfGFP expression is driven by the presence of cumate, a cheap and non-metabolizable molecule. Inspired by p-isopropyl benzoate (cumate) structural similarity to perillic acid

we investigated the possibility to exploit the cumate induction system (Seo & Schmidt-Dannert, 2019) for the detection of limonene oxidation products using our developed AAB recombinant strains to transform limonene into POH, PAL and PA. For the experiment, DSM2325 J23104 CYP450 strain was chosen due to its hydroxylation capabilities and for his ability to produce BC. In a first place we cloned the synthetic cumate induction cassette from pCT5-bac2.0 into pSEVA331 vector and, after having transformed DSM2325, we studied the possibility to utilize limonene, peryllil alcohol, peryll aldehyde and perillic acid as inducers of the induction system . The cumate sfGFP inducible construct for *K. xylinus* was constructed by cloning the cumate induction cassette from pCT5-bac2.0 (Addegene catalog #119872) into pSEVA331Bb vector backbone. The cumate induction cassette was amplified from pCT5-bac2.0 with “ecoRI_cumate” and “xbaI_cumate” primers and cloned into pSEVA331 vector digested with EcoRI and XbaI restriction enzymes obtaining “pSEVA331cumate sfGFP” plasmid.

To evaluate the sfGFP expression level induced by limonene and his hydroxylation products single colonies of *K. xylinus transformed with* pSEVA331cumate sfGFP were inoculated in five milliliters of HS-GLU medium (chloramphenicol 32mg/L - 5% v/v cellulases) and grown at 30°C at 300rpm to stationary phase. Then the culture was inoculated in five millilitres of HS-GLU medium fresh medium to an OD_{600} value =0.1 and growth until the mid-exponential phase of growth was reached (0,4 – 0,8 OD_{600}). The cells were centrifuged (12000g x 5 min), washed with PBS buffer and the inducers (dissolved in DMSO) were added to the cells using different concentrations (from 5nm to 1000nm). Aliquots of 200 µL were moved to 96-well plates and incubated at 28°C with a TECAN microplate reader. Two shakings of three minutes for an hour were performed and the fluorescence and optical density values were analyzed after 16 hours.

Furthermore, we grew *K. xylinus* “pSEVA331cumate sfGFP” recombinant in static conditions in presence of limonene, PA, POH and PAC to evaluate if the strain could be used as a solid bacterial cellulose-microbial biosensor for the

detection of the above mentioned molecules. Bacterial cellulose sheets were obtained from 6 days of static cultivation at 28°C in 10mL of HS-GLU at 30°C (chloramphenicol 32mg/L) inoculated from glycerol stocks. In this case, the inducers were added directly to the culture media together with the cell inoculum.

To evaluate the possibility to engineer a strain able to transform limonene into perillic acid and to detect limonene degradation we assembled a plasmid vector with a suitable antibiotic resistance and origin of replication. We constructed a plasmid vector carrying CYP153A6 operon under the J23104 strong constitutive promoter together with the cumate induction system and evaluated how limonene hydroxylation and overoxidation affected the sfGFP induction of the novel CYP- cumate induction plasmid.

For the plasmid construction, we cloned the cumate induction cassette into J23104 CYP450 plasmid by restriction cloning. The cassette was amplified using ecoRI_cumate" and "xbaI_cumate primers and subcloned into J23104 CYP450.

To evaluate the effectiveness of the system we growth a single recombinant *K. xylinus* in 10 ml of HS-GLU (chloramphenicol 32mg/L) at 28°C in 10mL flask in presence of cellulases for 48 hours. The cells were centrifuged and washed with PBS buffer and resuspended in two ml of 100mM KPHO buffer pH 7.00 to get a final concentration of 10 OD/mL in screw caps vial tubes; limonene was added to the cell resuspension (100nm) and incubated overnight with magnetic stirring at 28°C. As negative control the same culture without the addition of limonene was utilized. The following day sfGFP fluorescence of the "limonene induced" and "limonene not-induced "culture was evaluated and the formation of perillic acid was checked by GC-MS analysis as described above in "Analytical methods".

Results and discussion

Selection of the strains

Komagataeibacter xylinus DSM 2325 was included in our study since in the last decade it has been utilized for different genetic engineering studies, mostly due to its well characterized ability to produce bacterial cellulose on different carbon sources, together with closely related organisms, such as *Gluconacetobacter xylinus*, *Gluconacetobacter hansenii* and *Komagataeibacter rhaeticus* (Battad-Bernardo et al., 2004, Florea, Hagemann, Santosa, Abbott, & Micklem, 2016, Teh et al., 2019, Liu et al., 2020, Goosens et al., 2021, Gilbert et al., 2021). *Acetobacter malorum* was isolated from a mother of vinegar and was selected for its ability to grow on glucose and glycerol with good biomass production.

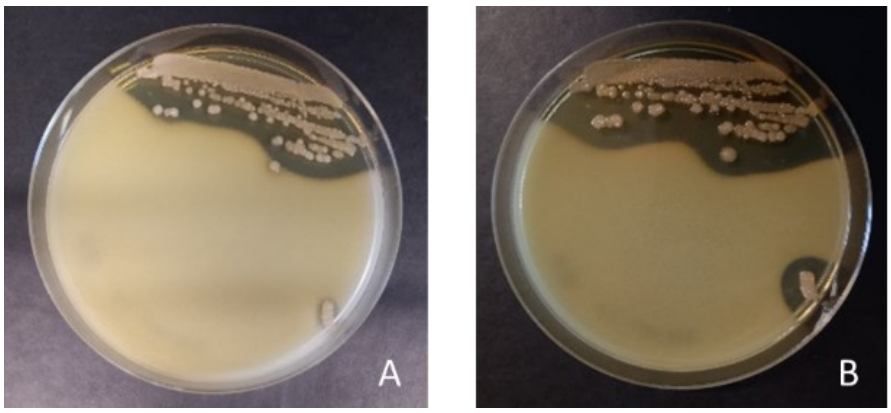

Figure 1. *Pure culture of Acetobacter malorum isolated from a mother of vinegar. The strain, cultivated on GYC plates, during the first two days of growth formed white colored and soft colonies (A), after five days of incubation the colonies turned into brown color and firm consistence morphology (B). An increase of calcium carbonate acidification halo was visible during strain growth on GYC plates*.

Komagataeibacter xylinus DSM 2325 and *Acetobacter malorum* were firstly tested for their activity as resting cells towards limonene and perillyl alcohol; the two strains were grown on different carbon sources (glucose and glycerol) since it is known that glycerol generally stimulates a higher membrane-bound

dehydrogenase activity than glucose. The two wild-type strains were not active on the hydrocarbons, whereas they were able to oxidize the primary alcohols with endogenous dehydrogenases, albeit at different extents, depending on the C-source used for their growth (Figure 2, 3).

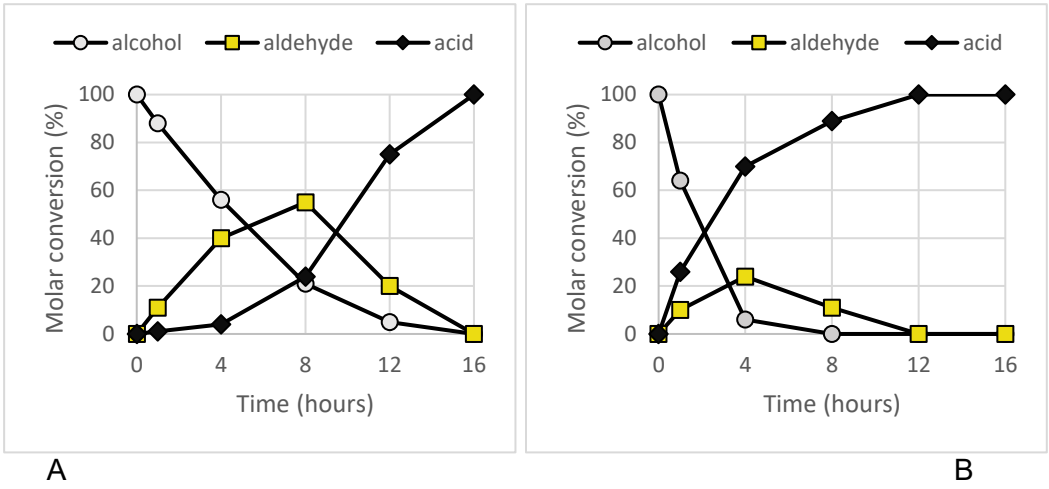

***Figure 2**. Oxidation of perillyl alcohol with Komagataeibacter xylinus DSM 2325. A) cells grown on glucose; B) cells grown on glycerol.*

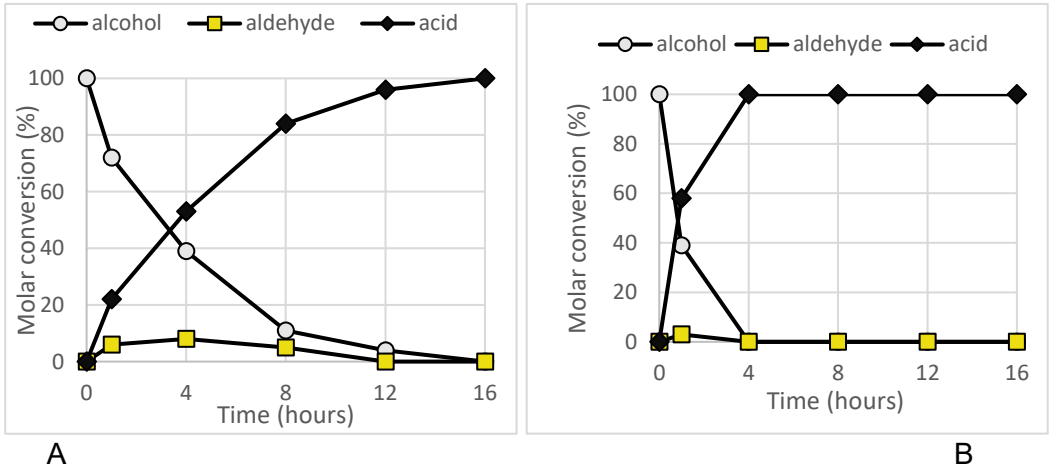

***Figure 3.** Oxidation of perillyl alcohol with Acetobater malorum A) cells grown on glucose; B) cells grown on glycerol.*

Oxidation was generally faster when cells were grown on glycerol; with *Acetobater malorum,* poor formation of the transient aldehyde was observed

and complete conversion of perillyl alcohol into acid was achieved within 4 hours with glycerol-grown cells. On the other side, a significant accumulation of perillaldehyde (55% after 8 hours) was detected with *Komagataeibacter xylinus* DSM 2325 grown on glucose. However, in all cases, the total conversion of the substrate to acid was achieved.

Preparation of the recombinant strains

We achieved in the transformation of the novel isolate *A. malorum and K. xylinus* strain with high efficiency and after five days of incubation, no colonies were detected on the negative control transformed without plasmid DNA. Then, after having accessed the transformability, we aimed to find out the best conditions to grow the recombinant strains to maximize protein expression of the gene carried into the transformed plasmids. A comparison of the two AAB recombinants transformed with the J23104 strong inducible and inducible plux1 and ptet1 inducible promoters was carried out analyzing mRFP1 measurement as reporter gene. RFP1 fluorescence derived from J23104 constitutive promoter cultures, resulted to be higher for both *K. xylinus* and *A. malorum* compared with fluorescence measurement of inducible promoter cultures (figure 5) (Lux mRFP1 *K. xylinus* - pLux mRFP1 *A. malorum* - pTet mRFP1 *K. xylinus* - pTet mRFP1 *A. malorum).* Having accessed J23104 constitutive promoter as optimal expression driver for the two selected AAB strains, we investigated the utilization of variable culture conditions to get a maximal mRFP1 expression employing different culture media and antibiotic concentrations. Analyzing fluorescence data normalized on OD values of different conditions we identified HS-GLU 32mg/L chloramphenicol as the optimal condition for *K. xylinus* growth and GLY 32mg/L for *A. malorum* cultivation (figure 5A).

Similarly to some recent descriptions of the *K. raethicus* Igem strain (Florea et al. 2016 and Teh et al., 2019), Ptet promoter was found to be leaky in *K. xylinus* and for *A. malorum* we noticed similar behaviour. We observed that,

inducing *A. malorum* Ptet01 mRFP1 transformant with increasing concentrations of ATc, mRFP1 fluorescence resulted to be slightly incremented in presence of 0,25 nM of ATc, while in *K. xylinus* Ptet01 mRFP1 strain, the mRFP1 expression was not controlled by ATc addition (figure 5B). The induction of Plux promoter transformed cultures resulted to give decent control on expression for *K. xylinus*, whereas the addiction AHLs on *A. malorum* Plux mRFP1 transformants resulted to not give any control on the fluorescence signal (figure 5D).

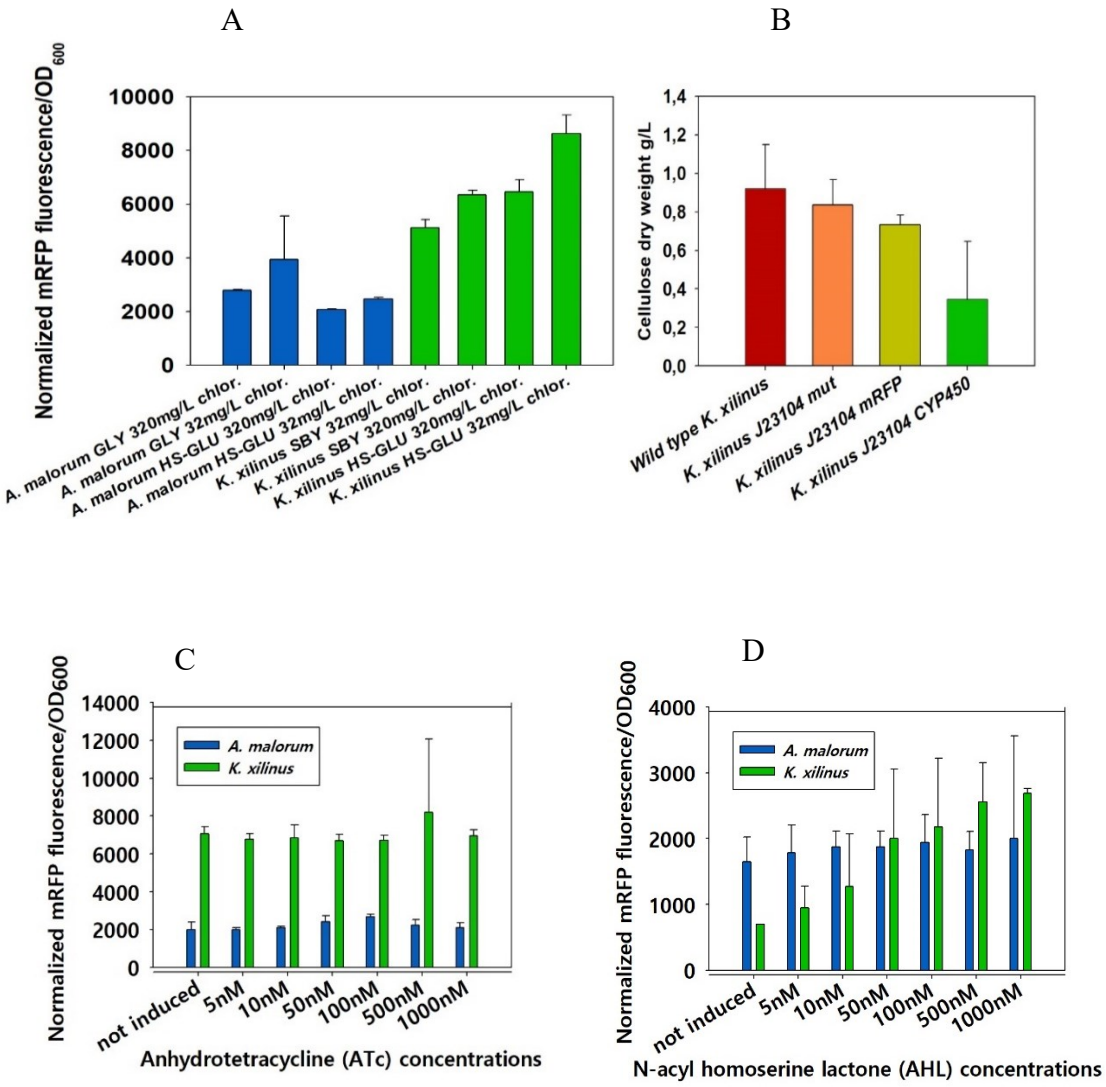

Figure 5. A: *Normalized mRFP fluorescence of K. xylinus (green bars) and A. malorum (blue bars) transformed J23104-mRFP1-331Bb grown with variable culture conditions. A higher red fluorescence was observed with K. xylinus compared with A. malorum in all the conditions tested. K. xylinus was cultivated on HS-GLU (20 g/L, 1% v/v cellulases), A. malorum was cultivated in GLY medium. Data are represented as mean ± Standard deviation D (3 biologial replicates).* ***B:*** *Effect of different protein expression on bacterial cellulose yield. The expression of CYP153A6 caused a significant decrease in BC production yield. The BC yield of J23104-mRFP1-331Bb and J23104mut transformed was slightly affected. Data are represented as mean ± Standard deviation D (3 biologial replicates). K. xylinus was cultivated on HS-GLU (20 g/L, 1% v/v cellulases).* ***C:*** *Characterization of ptet inducible promoter in K. xylinus (green bars)*

and A. malorum (blue bars). The expression of mRFP was induced adding increasing concentrations of anhydrotetracycline (ATc). Data are represented as mean ± Standard deviation D (3 biologial replicates). K. xylinus was cultivated on HS-GLU (20 g/L, 1% v/v cellulases), A. malorum was cultivated in GLY medium. ***D:*** *Characterization of pLux inducible promoter in K. xylinus (green bars) and A. malorum (blue bars). The expression of mRFP was induced adding increasing concentrations of anhydrotetracycline (ATc) or N-acyl homoserine lactone (AHL). Data are represented as mean ± Standard deviation D (3 biological replicates). K. xylinus was cultivated on HS-GLU (20 g/L, 1% v/v cellulases), A. malorum was cultivated in GLY medium.*

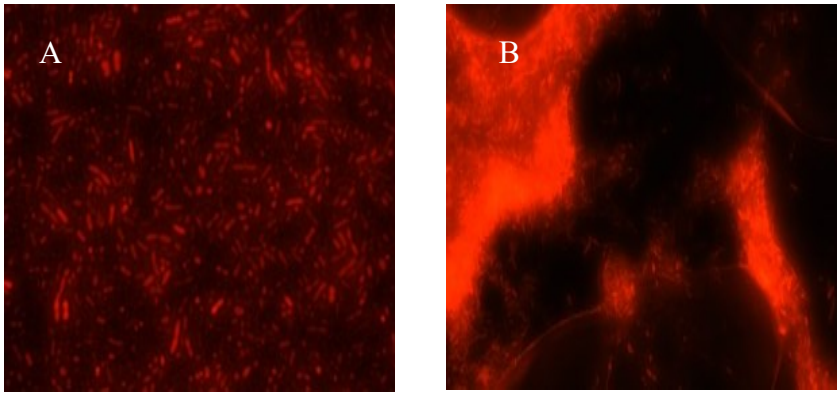

Figure 4: *mRFP1fluorescence analysis by fluorescence microscopy of A. malorum (A) and K. xylinus (B) transformed with J23104-mRFP1-331Bb plasmid. Both strains showed a high red fluorescence.*

Biotransformation with recombinant strains

We initially tested the activity of *K. xylinus* J23104 CYP450 (or *Komagataeibacter xylinus* DSM 2325_CYP153A6) grown on glucose towards (*S*)-limonene, one of the preferred substrates for CYP153A6 (Funhoff et al., 2006). Biotransformation of (*S*)-limonene (0.5 % vol/vol) with growing cells of *K. xylinus* DSM 2325_CYP153A6 showed the complete disappearance of the substrate within 4 hours with the formation of perillic acid as the only detectable product. Immiscibility and high volatility of limonene cause important loss of the substrate; therefore, to limit limonene evaporation, we tested the biotransformation with resting cells in screw-capped vials. The initial reaction mixture was a two-liquid phase system composed of water and limonene with different values of phase ratio (from 9.5/0.5 to 8.0/2.0). No

significant inhibition of the enzymatic activities due to the presence of limonene was observed and a maximum concentration of perillic acid was observed in all the cases of 6.6-6.9 mM. The observation that the maximum final yield of perillic acid was virtually the same in the presence of different amounts of initial limonene can be due to its poor availability in the aqueous phase and its high volatility which caused a marked loss of the substrate even in sealed reactors. Nevertheless, these experiments showed that *K. xylinus* J23104 CYP450 was able to hydroxylate limonene with the heterologous CYP153A6 and then oxidize the intermediate perillyl alcohol with endogenous dehydrogenase to perillic acid. The time course of the biotransformation is shown in Figure 6 (A).

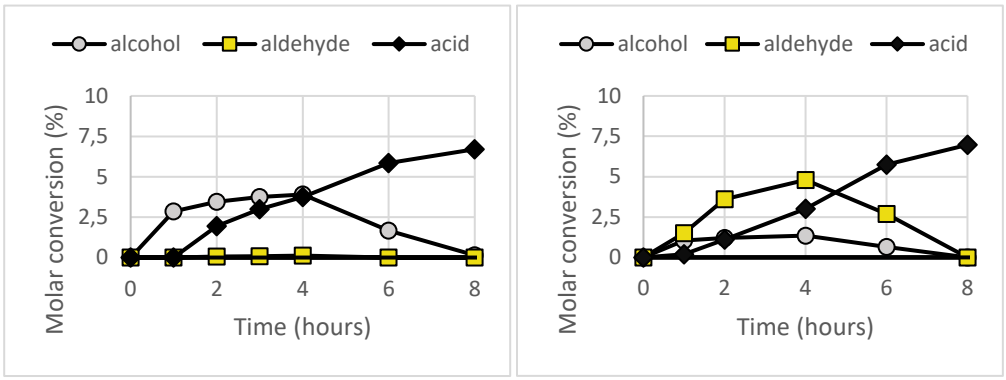

Figure 6. *Oxidation of (S)-limonene with Komagataeibacter xylinus DSM 2325_CYP153A6 (A) and Acetobacter malorum _CYP153A6 (B). The applied cell concentration was 20 $mg_{dry\ cells}$/mL with a phase ratio water/limonene of 95/5. The aqueous phase was a phosphate buffer pH 7.0 (100 mM).*

A biotransformation was carried out under the same conditions using recombinant *Acetobater malorum* DSM figure 6 (B), showing that the reaction occurred with a similar final outcome. As expected from the experiment on gene expression with mRFP as reporter (Figure 5A), the rate of hydroxylation was higher with *Komagataeibacter xylinus* DSM 2325_CYP153A6 but with more transient accumulation of perilla aldehyde than perillyl alcohol. Also in these cases, hydroxylation of limonene gave perillyl alcohol as the main product in the first part of the reaction, whereas at prolonged times endogenous dehydrogenases catalyzed further oxidation to perillic acid, which was the only product detectable in the biotransformation mixture at the end of the reaction.

(*S*)-Limonene was used as substrate to test the activity of the recombinant strains obtained with different molecular approaches. *K. xylinus* and *A. malorum* transformants, carrying CYP153A6 operon downstream the inducible promoters pLux and pTet, were grown and treated as described in the experimental section. As observed from fluorescence measurements with plux mRFP1 and pTet mRFP1 experiments (figure 5), where the maximal fluorescence obtained from inducible promoters was significatively lower

compared to the ones observed for J23104 strong constitutive promoter, CYP153A6 activity driven by the inducible promoters was lower compared to the hydroxylation yields observed for the transformants with the strong inducible promoter J23104. Despite a lower hydroxylation activity, a complete oxidation of limonene occurred in 24 hours of biotransformation employing both the plasmid with the two recombinants employed in this study (Table 2, 3). Complete oxidation of limonene occurred also employing bacteria cellulose sheet as biocatalyst, the reaction was checked by GC after 24 hours of biotransformation (Table 4).

(A)

Strain	Plasmid	Yield after 0,5h (%)		Yield after 5h (%)		Yield after 24h (%)	
K. xylinus	pLux 450	limonene	91,7	limonene	94,7	limonene	0
		alcohol	8,2	alcohol	0	alcohol	0
		aldehyde	0	aldehyde	5,2	aldehyde	0
		acid	0	acid	0	acid	100

(B)

strain	plasmid	Yield after 1 h (%)		Yield after 5 h (%)		Yield after 24 h (%)	
A. malorum	pLux 450	limonene	75,5	limonene	67,7	limonene	0
		alcohol	24,4	alcohol	0,5	alcohol	0
		aldehyde	0	aldehyde	31,6	aldehyde	0
		acid	0	acid	0	acid	100

Table 2. *Oxidation of (S)-limonene with Komagataeibacter xylinus DSM 2325_pLux CYP153A6 (A) and Acetobacter malorum _pLux CYP153A6 (B). The applied cell concentration was 20 $mg_{dry\ cells}$/mL with a phase ratio water/limonene of 95/5. The aqueous phase was a phosphate buffer pH 7.0 (100 mM).*

(A)

Strain	Plasmid	Yield after 1 h (%)		Yield after 5 h (%)		Yield after 24 h (%)	
K. xylinus	pTet 450	limonene	94,9	limonene	71,1	limonene	0
		alcohol	4,2	alcohol	0,9	alcohol	0
		aldehyde	0,8	aldehyde	27,9	aldehyde	0
		acid	0	acid	0	acid	100

(B)

Strain	Plasmid	Yield after 1 h (%)		Yield after 5 h (%)		Yield after 24 h (%)	
A. malorum	pTet 450	limonene	95,9	limonene	90,3	limonene	0
		alcohol	4,1	alcohol	9,5	alcohol	0
		aldehyde	0	aldehyde	0,1	aldehyde	0
		acid	0	acid	0	acid	100

Table 3. *Oxidation of (S)-limonene with Komagataeibacter xylinus DSM 2325_pTet CYP153A6 (A) and Acetobacter malorum _pTet CYP153A6 (B). The applied cell concentration was 20 $mg_{dry\ cells}$/mL with a phase ratio water/limonene of 95/5. The aqueous phase was a phosphate buffer pH 7.0 (100 mM).*

Strain	Biotransformation conditions	Plasmid	Yield after 24 h (%)	
K. xylinus - (Bacterial cellulose sheet)	Agitated (160rpm) 28°C 0.5 g/L limonene	J23104 450	limonene	0
			alcohol	0
			aldehyde	0
			acid	100
K. xylinus - (Bacterial cellulose sheet)	Static 28°C 0.5 g/L limonene	J23104 450	limonene	0
			alcohol	0
			aldehyde	0
			acid	100

Table 4. *Oxidation of (S)-limonene with bacterial cellulose sheet produced by Komagataeibacter xylinus DSM 2325 J23104 CYP153A6 in agitated and static conditions.*

The possibility to functionalize hydrocarbons using recombinant AAB was also checked using *n*-octane as substrate. Equally, in this case, the initial reaction mixture was a two-liquid phase system composed of water and *n*-octane (phase ratio 95/5) and the reaction was carried out with 20 $mg_{dry\ cells}$/mL of cells suspended in phosphate buffer at pH 7.0. Oxidation of *n*-octane occurred, similarly to what was observed with limonene, with the final formation of the correspondent carboxylic acid. Hydroxylation occurred at higher rates with both strains.

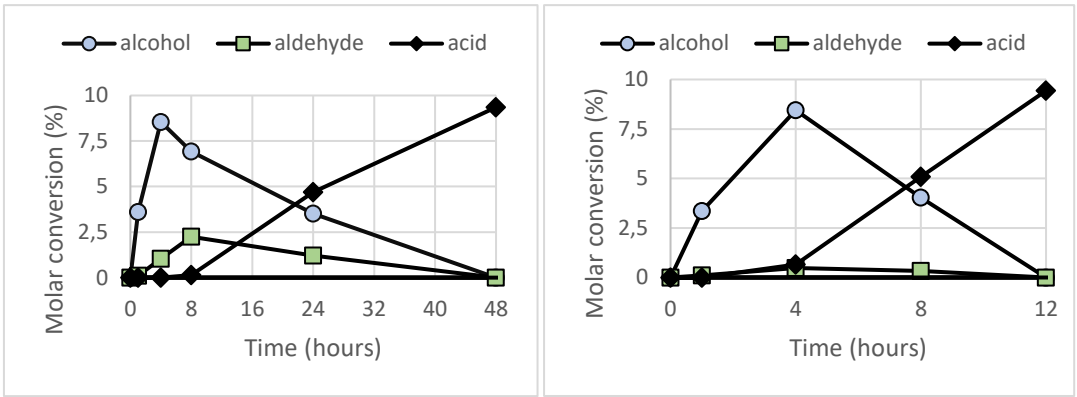

A B

Figure 7. *Oxidation of n-octane with Komagataeibacter xylinus DSM 2325_CYP153A6 (A) and Acetobacter malorum _CYP153A6 (B). The applied cell concentration was 20 $mg_{dry\ cells}$/mL with a phase ratio water/n-octane of 95/5. The aqueous phase was a phosphate buffer pH 7.0 (100 mM).*

Furthermore, employing *K. xylinus* J23104 CYP450 recombinant strains we performed limonene biotransformation testing increased substrate concentrations. We grew the strain as described above and we added limonene at 1, 2, 10 g/L and performed biotransformation in screw cap vials. Limonene was completely consumed at concentration of 2 g/L, while around the 60% of substrate was found after biotransformation (24 hours) employing 10g/L of limonene (Figure S2).

sfGFP fluorescence microbial biosensor for the detection of limonene oxidation and perillic acid formation

We aimed to construct a microbial biosensor to detect limonene degradation and perillic acid (PA) formation, exploiting a microbial cumate induction system recently described for *Bacillus* and *E. coli*. We constructed a plasmid to evaluate the response of the cumate induction system *in K. xylinus* by cloning the induction system in pSEVA331 (minimal plasmid backbone, empty backbone). The plasmid was constructed by restriction cloning to change the origin of replication and antibiotic resistance of the original plasmid vector (pCT5-bac2.0 as template Addegene catalog #119872) to ones suitable for *K. xylinus*. pSEVA331 vector was cloned by restriction cloning with the cumate induction cassette amplified with ecoRI_cumate" and "xbaI_cumate" primers and "pSEVA331cumate sfGFP" was obtained (Figure S1). The plasmid was transformed in *K. xylinus* and the response of the induction system, measured as sfGFP fluorescence, was evaluated using limonene and peryllil alcohol (POH), peryllil aldehyde (PAL) and PA as inducers in the presence (Figure 8A) and in absence of cellulases (figure 8B). Employing growing cells in presence of cellulases we observed only a slight difference in the sfGFP fluorescence in presence of a low concentration of inducer (5nM). Instead at high concentration (0.1 mM) the difference in fluorescence in the presence with PA, POH and PAC was appreciable. A low fluorescence, comparable to the not induced culture, was detected using limonene as inducer, and the fluorescence in presence of PA, PAL and PA was ten times higher than the ones induced with limonene. (Figure 8A)

To evaluate the possibility to use BC sheet produced by "pSEVA331cumate sfGFP" transformant to detect the above mentioned

molecules, we incubated the strain from glycerol stock in presence of 0.1 mM of the inducers and we grow BC statically for six days. We visually evaluated sfGFP of BC sheets after six days exposing BC pellicles under a blue-light transilluminator. Similarly to what was observed in presence of 0.1 mM of substrate employing planktonic cells, a higher GFP fluorescence, compared to not induced cultures, was evaluated in presence of PA, PAL and PA. Also in this case, the fluorescence of the BC sheets obtained with limonene induction was similar to the one obtained with not induced cultures. (Figure 8B)

Then, once the features of the induction system were accessed with limonene and his derivates, we assembled a construct flanking CYP450 operon with the induction cassette from “pSEVA331cumate sfGFP” plasmid. The cumate induction cassette was inserted into J23104 CYP450 plasmid vector by restriction cloning. The cassette was amplified as described above with ecoRI_cumate” and “xbaI_cumate” and cloned into the multiple cloning site of J23104 CYP450, digested with ecoRI and xbaI restriction enzymes (Figure S1). With this latter *K. xylinus* recombinant strain called “pSEVA cumate – J23104 CYP450”, we performed limonene biotransformation to perillic employing 0.1mM of substrate. After 16 hours of biotransformation, when limonene and his hydroxylation products were completely converted to perillic acid, we evaluated the sfGFP fluorescence. Biotransformation conditions were kept as described above in “Limonene and octane biotransformation with DSM 2325 and *A. malorum*” and the formation of PA was evaluated by GC-MS as reported in “analytical methods”. Once the reaction was completed we observed a difference in the fluorescence from the control strain (without limonene) even if an increased promoter leacking was observed compared to the induction

experiments performed with “pSEVA331cumate sfGFP” using limonene, PA, POH and PAC as inducers (figure 8C).

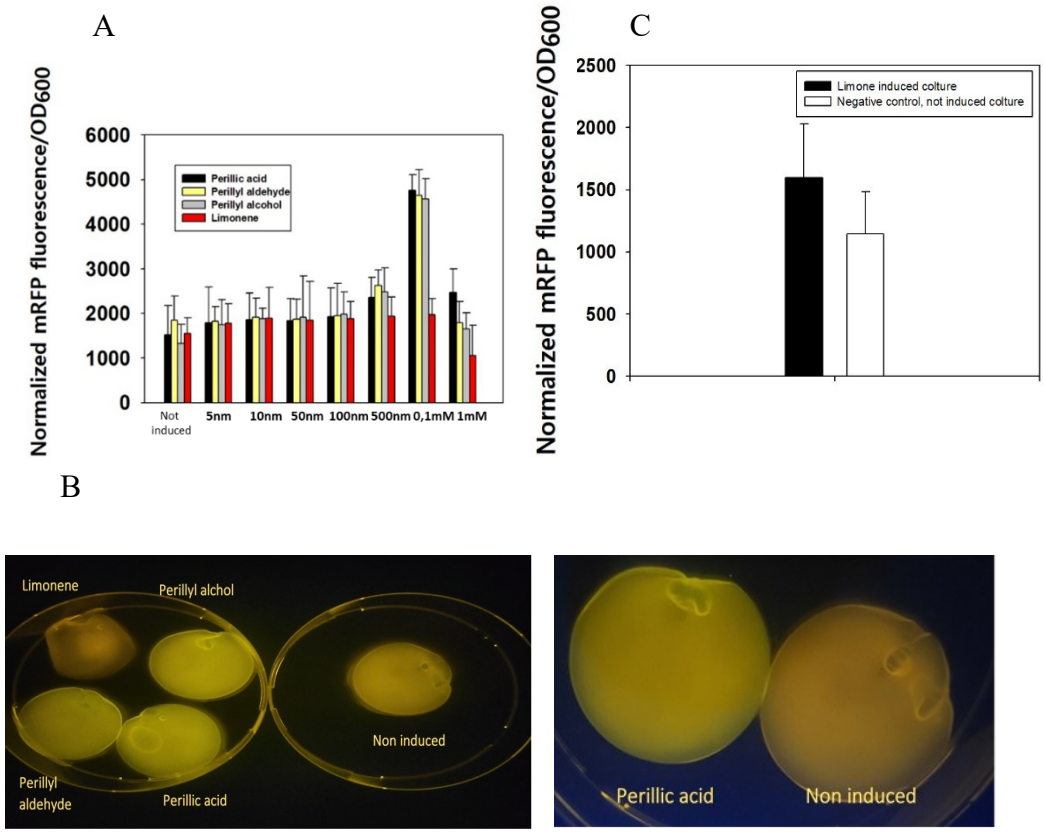

Figure 8. A: *Green sfGFP fluorescence of K. xylinus transformed with pSEVA331cumate sfGFP” plasmid, induced by limonene and POH, PAL and PA at increasing concentrations. The recombinant strain was grown in presence of cellulases and inducers were added directly into the cultures at exponential phase. Data are represented as mean ± Standard deviation D (3 biologial replicates).* ***B:*** *Green sfGFP fluorescence of K. xylinus transformed with pSEVA331cumate sfGFP” plasmid, induced by 1mM of limonene, POH, PAL and PA. The recombinant strain was grown in absence of cellulases in 6 well plates 10mL HS-GLU and inducers were added directly into the cultures at the moment of the inoculum.* ***C:*** *Analysis of green sfGFP fluorescence of K. xylinus transformed with “pSEVA cumate – J23104 CYP450” plasmid” after the complete biotransformation of limonene into perillic acid.*

Supplementary

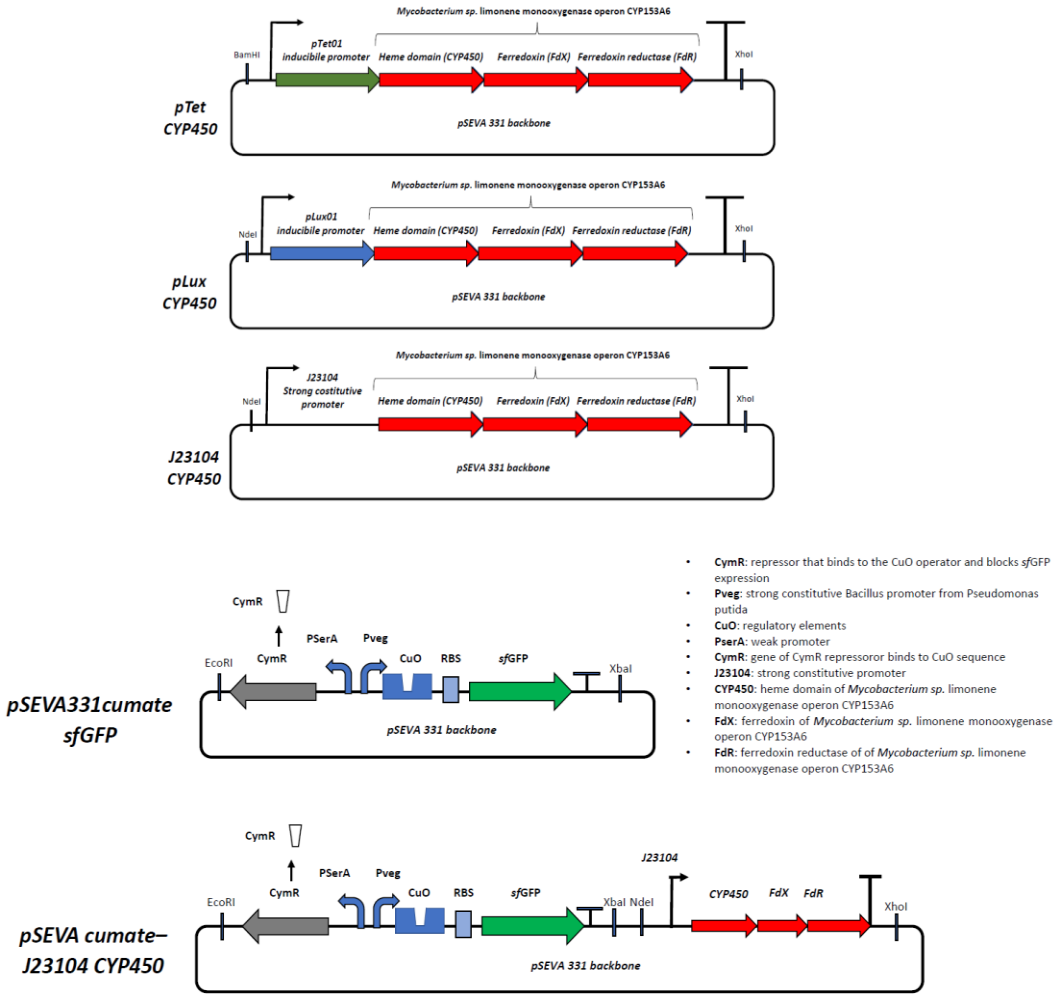

- **CymR**: repressor that binds to the CuO operator and blocks *sf*GFP expression
- **Pveg**: strong constitutive Bacillus promoter from Pseudomonas putida
- **CuO**: regulatory elements
- **PserA**: weak promoter
- **CymR**: gene of CymR repressoror binds to CuO sequence
- **J23104**: strong constitutive promoter
- **CYP450**: heme domain of *Mycobacterium sp.* limonene monooxygenase operon CYP153A6
- **FdX**: ferredoxin of *Mycobacterium sp.* limonene monooxygenase operon CYP153A6
- **FdR**: ferredoxin reductase of of *Mycobacterium sp.* limonene monooxygenase operon CYP153A6

Figure S1: *Schematic representation of plasmids constructed for this study*

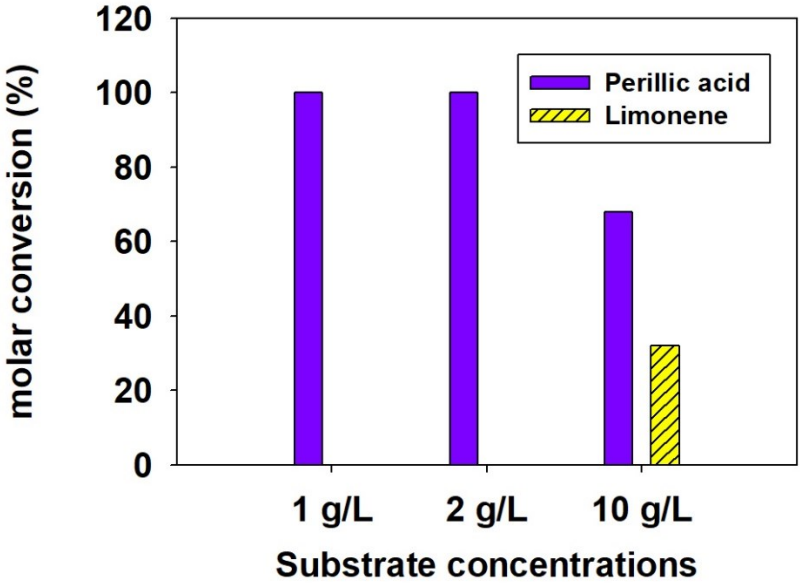

***Figure S2**: Conversion of different limonene concentrations to perillic acid employing K. xylinus J23104 CYP450*

Table S1 *List of primers utilized in this study*

Name	Sequence	Restriction enzyme	Template
OP-LYMIC-NDEI-CM	CACCATATGACCGAAATGACCGTGGC	NdeI	pUC57/ pET101OP.Lim
OP-LYMIC-XHOI-CM	ATTGCTCGAGTCAATGCTGCGCGG	XhoI	pUC57/ pET101OP.Lim
OP-LYMIC-BAMHI-CM	CTCGGGATCCCCGAAATGACCGTGGC	BamHI	pUC57/ pET101OP.Lim
NDEI_20_10	CATATGGTATTTCTCCTCTTTCACTAGTAG	NdeI	J23104-mRFP1-331Bb
Stop_codon_XHOI	CATATGGTATTTCTCCTCTTTCACTAGTAG	XhoI	J23104-mRFP1-331Bb
pLux!_NDEI	CATGCATATGGTATTTCTCCTCTTTCACTAGTATTTATTCGAC	NdeI	pLux01
pLuX_XhoI	CATGCTCGAGTAACGCTGATAGTGCTAGTGTAGATCGCT	XhoI	pLux01
pTet_BamHI	CTAGGGATCCTTTCTCCTCTTTCTAGTAGTGCTCAG	BamHI	pTet01
ptet_XhoI	CTAGCTCGAGTAACGCTGATAGTGCTAGTGTAGATCG	XhoI	pTet01
P0	GAAGAGTTTGATCCTGGCTC	none	MIM2000/28 gDNA
P6	CTACGGCTACCTTGTTACGA	none	MIM2000/28 gDNA
pA	AGAGTTTGATCCTGGCTCAG	none	MIM2000/28 gDNA
check_1_oriV	GCTCGCGGCCATCGT	none	J23104 OP.Lim/J23104mut
check_2_t0_terminator	CAACAGGAGTCCAAGCTGCAG	none	J23104 OP.Lim/J23104mut

Table S2 *List of plasmids utilized in this study*

Name	**Description**	**Source**
pUC57 OP-LYMIC	Template vector purchased from Baseclear	This study
J23104-mRFP1-331Bb	Vector for expression in AAB of mRFP1	Addgene plasmid # 78274
J23104mut	Empty vector utilized as negative control for biotransformation	This study
J23104 CYP450	Vector for expression in AAB of CYP450	This study
pSEVA 331	Minimal plasmid backbone employed for *K. xylinus*	Addgene plasmid #78269
pLux01	mRFP1 expressed behind an AHL-inducible construct	Addgene plasmid #78281
pTet01	mRFP1 expressed behind an ATc-inducible construct	Addgene plasmid #78283
pLux CYP450	Express the CYP450A6 operon under the pLux01 inducible promoter	This study
pTet CYP450	Express the CYP450A6 operon under the pTet01 inducible promoter	This study
pCT5-bac2.0	Plasmid vector for *E. coli* an *Bacillus* carrying cumate induction cassette	Addegene catalog #119872
pSEVA331cumate sfGFP	pSEVA331 vector cloned with cumate induction cassete from pCT5-bac2.0	This study
pSEVA cumate–J23104 CYP450	pSEVA331 vector cloned with cumate induction cassete from pCT5-bac2.0 and expressing CYP 450 operon downstream the J23104 strong constitutive promoter	This study

Cycling step	Temperature	Time	Number of Cycles	Reagents
Initial Denaturation	98°C	10 minutes	1	PCR Buffer HF [5X]
Denaturation	98°C	50 seconds	X 30	dNTPs (2.5 mM)
Annealing	62°C	50 seconds		OP-LYMIC-NDEI-CM (100 pmol/µL)
Extension	72°C	3 minutes		OP-LYMIC-XHOI-CM (100 pmol/µL)
				pUC57OP.LIM (1 ng/µL)
Final Extension	72°C	10 minutes	1	Phusion DNA Polymerase
Hold	20°C	∞	1	Sterile H_20

Table S3 *PCR conditions and mastermix composition used for the amplification CYP153A6 operon from pUC57OP.LIM plasmid* employed for J23104 CYP450 construction

Cycling step	Temperature	Time	Number of Cycles	Reagents
Initial Denaturation	98°C	2 minutes	1	PCR Buffer HF [5X]
Denaturation	98°C	30 seconds		dNTPs (2.5 mM)
Annealing	72°C	30 seconds	X 30	NDEI_20_10 (100 pmol/µL)
Extension	72°C	3 minutes		Stop_codon_XHOI (100 pmol/µL)
				J23104-mRFP1-331Bb (1 ng/µL)
Final Extension	72°C	10 minutes	1	Phusion DNA Polymerase
Hold	20°C	∞	1	Sterile H_20

Table S4*. PCR conditions and mastermix composition for J23104-mRFP1-331Bb plasmid backbone amplification*

Cycling step	Temperature	Time	Number of Cycles
Initial Denaturation	98°C	10 minutes	1
Denaturation	98°C	50 seconds	X 30
Annealing	62°C	50 seconds	
Extension	72°C	3 minutes	
Final Extension	72°C	10 minutes	1
Hold	20°C	∞	1

Reagents
PCR Buffer HF [5X]
dNTPs (2.5 mM)
OP-LYMIC-NDEI-CM (100 pmol/µL)
OP-LYMIC-XHOI-CM (100 pmol/µL)
pUC57OP.LIM (1 ng/µL)
Phusion DNA Polymerase
Sterile H_20

Table S5. *PCR conditions and mastermix composition used for the amplification CYP153A6 operon from pUC57OP.LIM plasmid* employed for pLux CYP450 construction

Cycling step	Temperature	Time	Number of Cycles
Initial Denaturation	98°C	2 minutes	1
Denaturation	98°C	30 seconds	X 30
Annealing	72°C	30 seconds	
Extension	72°C	3 minutes	
Final Extension	72°C	10 minutes	1
Hold	20°C	∞	1

Reagents
PCR Buffer HF [5X]
dNTPs (2.5 mM)
pLux!_NDEI (100 pmol/µL)
pLuX_XhoI (100 pmol/µL)
pLux-mRFP1-331Bb (1 ng/µL)
Phusion DNA Polymerase
Sterile H_20

Table S6. *PCR conditions and mastermix composition for pLux-mRFP1-331Bb plasmid backbone amplification*

Cycling step	Temperature	Time	Number of Cycles	Reagents
Initial Denaturation	98°C	10 minutes	1	PCR Buffer HF [5X]
Denaturation	98°C	50 seconds	X 30	dNTPs (2.5 mM)
Annealing	62°C	50 seconds		OP-LYMIC-BAMHI-CM (100 pmol/µL)
Extension	72°C	3 minutes		OP-LYMIC-XhoI-CM (100 pmol/µL)
				pUC57OP.LIM (1 ng/µL)
Final Extension	72°C	10 minutes	1	Phusion DNA Polymerase
Hold	20°C	∞	1	Sterile H_20

***Table S7**. PCR conditions and mastermix composition for the amplification CYP153A6 operon from pUC57OP.LIM employed for pTet CYP450 construction*

Cycling step	Temperature	Time	Number of Cycles	Reagents
Initial Denaturation	98°C	10 minutes	1	PCR Buffer HF [5X]
Denaturation	98°C	30 seconds		dNTPs (2.5 mM)
Annealing	72°C	30 seconds	X 30	pTet_BamHI (100 pmol/µL)
Extension	72°C	3 minutes		ptet_XhoI (100 pmol/µL)
				for pTet-mRFP1-331Bb (1 ng/µL)
Final Extension	72°C	10 minutes	1	Phusion DNA Polymerase
Hold	20°C	∞	1	Sterile H_20

***Table S8.** PCR conditions and mastermix composition for pTet-mRFP1-331Bb plasmid backbone amplification*

Cycling step	Temperature	Time	Number of Cycles
Initial Denaturation	98°C	1 minute	1
Denaturation	98°C	30 seconds	X 30
Annealing	72°C	3 seconds	
Extension	72°C	1,5 minutes	
Final Extension	72°C	10 minutes	1
Hold	20°C	∞	1

Reagents
PCR Buffer HF [5X]
dNTPs (2.5 mM)
ecoRI_cumate (100 pmol/µL)
xbaI_cumate (100 pmol/µL)
pCT5-bac2.0 (1 ng/µL)
Phusion DNA Polymerase
Sterile H_20

Table S9. *PCR conditions and mastermix composition for amplification of cumate induction cassette from pCT5-bac2.0 (Addegene catalog #119872) employed for "pSEVA331cumate sfGFP" construction*

Cycling step	Temperature	Time	Number of Cycles
Initial Denaturation	98°C	1 minute	1
Denaturation	98°C	30 seconds	X 30
Annealing	62°C	30 seconds	
Extension	72°C	2 minutes	
Final Extension	72°C	10 minutes	1
Hold	20°C	∞	1

Reagents
PCR Buffer HF [5X]
dNTPs (2.5 mM)
CHECK 1 (100 pmol/µL)
CHECK 2 (100 pmol/µL)
OP-L-pUC100 (6 ng/µL)
Phusion DNA Polymerase
Sterile H_20

Table S10. *PCR conditions and mastermix composition for colony PCR for transformants screenings*

References

Battad-Bernardo, E., McCrindle, S. L., Couperwhite, I., & Neilan, B. A. (2004). Insertion of an E. coli lacZ gene in Acetobacter xylinus for the production of cellulose in whey. *FEMS Microbiology Letters*, *231*(2), 253–260. https://doi.org/10.1016/S0378-1097(04)00007-2

Cornelissen, S., Julsing, M. K., Volmer, J., Riechert, O., Schmid, A., & Bühler, B. (2013). Whole-cell-based CYP153A6-catalyzed (S)-limonene hydroxylation efficiency depends on host background and profits from monoterpene uptake via AlkL. *Biotechnology and Bioengineering*, *110*(5), 1282–1292. https://doi.org/10.1002/bit.24801

Dong, J. J., Fernández-Fueyo, E., Hollmann, F., Paul, C. E., Pesic, M., Schmidt, S., Wang, Y., Younes, S., & Zhang, W. (2018). Biocatalytic Oxidation Reactions: A Chemist's Perspective. *Angewandte Chemie - International Edition*, *57*(30), 9238–9261. https://doi.org/10.1002/anie.201800343

Florea, M., Hagemann, H., Santosa, G., Abbott, J., & Micklem, C. N. (2016). Engineering control of bacterial cellulose production using a genetic toolkit and a new cellulose- producing strain. *Proc. Natl. Acad. Sci. U. S. A.*, 3431–3440. https://doi.org/10.1073/pnas.1522985113

Florea, M., Hagemann, H., Santosa, G., Abbott, J., Micklem, C. N., Spencer-Milnes, X., De Arroyo Garcia, L., Paschou, D., Lazenbatt, C., Kong, D., Chughtai, H., Jensen, K., Freemont, P. S., Kitney, R., Reeve, B., & Ellis, T. (2016). Engineering control of bacterial cellulose production using a genetic toolkit and a new celluloseproducing strain. *Proceedings of the National Academy of Sciences of the United States of America*, *113*(24), E3431–E3440. https://doi.org/10.1073/pnas.1522985113

Fujita, N., Sumisa, F., Shindo, K., Kabumoto, H., Arisawa, A., Ikenaga, H., & Misawa, N. (2009). Comparison of two vectors for functional expression

of a bacterial cytochrome P450 gene in escherichia coli using CYP153 genes. *Bioscience, Biotechnology and Biochemistry*, *73*(8), 1825–1830. https://doi.org/10.1271/bbb.90199

Funhoff, E. G., Bauer, U., García-Rubio, I., Witholt, B., & Van Beilen, J. B. (2006). CYP153A6, a soluble P450 oxygenase catalyzing terminal-alkane hydroxylation. *Journal of Bacteriology*, *188*(14), 5220–5227. https://doi.org/10.1128/JB.00286-06

Gao, L., Wu, X., Zhu, C., Jin, Z., Wang, W., & Xia, X. (2020). Metabolic engineering to improve the biomanufacturing efficiency of acetic acid bacteria: advances and prospects. *Critical Reviews in Biotechnology*, *40*(4), 522–538. https://doi.org/10.1080/07388551.2020.1743231

Gilbert, C., Tang, T. C., Ott, W., Dorr, B. A., Shaw, W. M., Sun, G. L., Lu, T. K., & Ellis, T. (2021). Living materials with programmable functionalities grown from engineered microbial co-cultures. *Nature Materials*. https://doi.org/10.1038/s41563-020-00857-5

Goosens, V. J., Walker, K. T., Aragon, S. M., Singh, A., Senthivel, V. R., Caro-astorga, J., Buat, M. L. A., Song, W., Lee, K., & Ellis, T. (2021). *Komagataeibacter tool kit (KTK): a modular cloning system for multigene constructs and programmed protein secretion from cellulose producing bacteria 3*. 1–21.

Gudiminchi, R. K., Randall, C., Opperman, D. J., Olaofe, O. A., Harrison, S. T. L., Albertyn, J., & Smit, M. S. (2012). Whole-cell hydroxylation of n-octane by Escherichia coli strains expressing the CYP153A6 operon. *Applied Microbiology and Biotechnology*, *96*(6), 1507–1516. https://doi.org/10.1007/s00253-012-3984-5

Jongedijk, E., Müller, S., Van Dijk, A. D. J., Schijlen, E., Champagne, A., Boutry, M., Levisson, M., Van Der Krol, S., Bouwmeester, H., Beekwilder, J., & Takahashi, H. (2020). Novel routes towards bioplastics from plants:

Elucidation of the methylperillate biosynthesis pathway from Salvia dorisiana trichomes. *Journal of Experimental Botany*, *71*(10), 3052–3065. https://doi.org/10.1093/jxb/eraa086

Jongedijk, E., van der Klis, F., de Zwart, R., van Es, D. S., & Beekwilder, J. (2018). Methyl Perillate as a Highly Functionalized Natural Starting Material for Terephthalic Acid. *ChemistryOpen*, *7*(2), 201–203. https://doi.org/10.1002/open.201700178

Kuttan, G., Pratheeshkumar, P., Manu, K. A., Kuttan, G., Pratheeshkumar, P., Manu, K. A., & Kuttan, R. (2011). Inhibition of tumor progression by naturally occurring terpenoids Inhibition of tumor progression by naturally occurring terpenoids. *Pharmaceutical Biology*, *0209*. https://doi.org/10.3109/13880209.2011.559476

Liu, L. P., Yang, X., Zhao, X. J., Zhang, K. Y., Li, W. C., Xie, Y. Y., Jia, S. R., & Zhong, C. (2020). A lambda red and FLP/FRT-mediated site-specific recombination system in komagataeibacter xylinus and its application to enhance the productivity of bacterial cellulose. *ACS Synthetic Biology*, *9*(11), 3171–3180. https://doi.org/10.1021/acssynbio.0c00450

Molinari, F., Villa, R., Aragozzini, F., Cabella, P., Barbeni, M., & Squarcia, F. (1997). Multigram-scale production of aliphatic carboxylic acids by oxidation of alcohols with Acetobacter pasteurianus NCIMB 11664. *Journal of Chemical Technology and Biotechnology*, *70*(3), 294–298. https://doi.org/10.1002/(SICI)1097-4660(199711)70:3<294::AID-JCTB755>3.0.CO;2-S

Raspor, P., & Goranovič, D. (2008). Biotechnological applications of acetic acid bacteria. *Critical Reviews in Biotechnology*, *28*(2), 101–124. https://doi.org/10.1080/07388550802046749

Romano, D., Villa, R., & Molinari, F. (2012). Preparative Biotransformations: Oxidation of Alcohols. *ChemCatChem*, *4*(6), 739–749.

https://doi.org/10.1002/cctc.201200042

Saichana, N., Matsushita, K., Adachi, O., Frébort, I., & Frebortova, J. (2015). Acetic acid bacteria: A group of bacteria with versatile biotechnological applications. *Biotechnology Advances*, *33*(6), 1260–1271. https://doi.org/10.1016/j.biotechadv.2014.12.001

Seo, S. O., & Schmidt-Dannert, C. (2019). Development of a synthetic cumate-inducible gene expression system for Bacillus. *Applied Microbiology and Biotechnology*, *103*(1), 303–313. https://doi.org/10.1007/s00253-018-9485-4

Teh, M. Y., Ooi, K. H., Danny Teo, S. X., Bin Mansoor, M. E., Shaun Lim, W. Z., & Tan, M. H. (2019). An Expanded Synthetic Biology Toolkit for Gene Expression Control in Acetobacteraceae [Research-article]. *ACS Synthetic Biology*, *8*(4), 708–723. https://doi.org/10.1021/acssynbio.8b00168

Villa, R., Romano, A., Gandolfi, R., Sinisterra Gago, J. V., & Molinari, F. (2002). Chemoselective oxidation of primary alcohols to aldehydes with Gluconobacter oxydans. *Tetrahedron Letters*, *43*(34), 6059–6061. https://doi.org/10.1016/S0040-4039(02)01221-2

Zambelli, P., Pinto, A., Romano, D., Crotti, E., Conti, P., Tamborini, L., Villa, R., & Molinari, F. (2012). One-pot chemoenzymatic synthesis of aldoximes from primary alcohols in water. *Green Chemistry*, *14*(8), 2158–2161. https://doi.org/10.1039/c2gc35764j

Zhang, H., Liu, G., Zhang, J., & Bao, J. (2016). Fermentative production of high titer gluconic and xylonic acids from corn stover feedstock by Gluconobacter oxydans and techno-economic analysis. *Bioresource Technology*, *219*, 123–131. https://doi.org/10.1016/j.biortech.2016.07.068

Chapter 4

Optimization of molecular and fermentative approaches for the valorization of limonene from orange peel wastes employing *Komagataeibacter xylinus*

Abstract

In this study, we investigated the possibility to utilize orange peel wastes (OPW) as a valuable feedstock for the extraction of a sugar-rich fermentation medium called orange peel juice (OPJ). OPJ was utilized as a culture medium for *K. xylinus* growth and as a limonene source for perillyl alcohol and perillic acid production via limonene hydroxylation in C-7 position by heterologous CYP153A6 from *Mycobacterium* sp. strain HXN-1500 operon and further oxidation of perillyl alcohol to perillic acid by endogenous dehydrogenases. We optimized the fermentation process and the conditions of biotransformation to convert *R*-(+)-Limonene, contained into the OPJ, to perillyl alcohol and perillic acid testing two inducible and a constitutive promoter.

Introduction

The emerging interest in circular economy faced the society with the problem of limiting and valorizing food wastes and pushed to find sustainable alternatives to fossil non-renewable resources (Dahiya, 2017 and Branduardi, 2021). According to the Food and Agriculture Organization of the United Nations (FAO), food waste is defined as the loss of part of the edible products throughout the supply chain that specifically leads to edible food for human consumption (Dahiya, 2018). Roughly one-third of the food globally produced every year, which corresponds to 1.3 billion tons of edible goods, is lost or wasted (Blakeney, 2019).

Among the Italian food production, citrus processing factories, represent 56% per cent of the national fruit production (ISTAT, 2014). Oranges are the citrus fruit mostly cultivated in Italy (61.7% of total citrus production). Every year around 1.8 million tons of oranges are produced into the national territory and consequently it is calculated that more than 0.6 million tons of orange peel

waste are generated in Italy every year and most of the cultivation is concentrated in southern regions (ISTAT, 2014 and Valenti, 2017).

Currently, the main part of oranges harvested in Italy (70%) is employed as raw material for derivative products such as orange juice and industrial preparations such as jams, marmalade, or food flavoring agents (Sharma, 2017). On the total weight of the orange, only around 50% of the fruit is utilized by industrial processes; consequently, a large number of organic residues, characterized by a high water content (80%) (Garcia-Castello, 2011 and Chavan, 2018) and is produced along with the industrial processing of citrus fruits (Valenti, 2012). The orange peel wastes (OPW) derived from food processing industries are composed of a liquid and a semisolid fraction. The semisolid part of OPW is composed of peels, albedo and seeds discarded from the juice extraction process; this insoluble fraction is rich in cellulose (9.21 g/100 g), pectins (42.5 g/100 g), and hemicellulases (10.5 g/100 g), while the soluble molecules are mainly simple sugars (16.9 g/100 g), organic acids, amino acids, essential oils, and proteins (Sharma, 2017 and Chavan, 2018).

The orange peel wastes (OPW) derived from food processing industries, which in Italy are named as *pastazzo*, are generally utilized for incineration due to their high calorific power (4545 kcal kg^{-1} dry matter) or employed in anaerobic digestion processes (Valenti, 2012).

Small and medium-sized companies, which represent the majority of the Italian industrial factories (Bresciani, 2013), due to the lack of resources and insufficient amount of processed row material, prefer to utilize OPW as cattle feed for its high digestibility (85-90%) and energy availability (2.76-2.9 Mcal ME/kg DM and 1.66−1.76 Mcal NE/kg DM) for lactating dairy cows (Wadhwa, 2013), or sometimes, tent to scatter the biomasses into the environment. OPW wastes derived from small orange processing industries, due to the above-mentioned reasons, are frequently dispersed into the landfill or, with more environmental issues, discarded into lakes, ponding and wells (Sharma, 2017). The unregulated dispersion of OPW might cause danger for the

environment, such as the contamination of groundwater with consequent damage to aquatic species from polluted water basins and defoliation of trees in the surrounding areas (Sharma, 2016 and Chavan, 2018).

Due to these reasons, the utilization OPW as a feedstock to produce added-value products was deeply investigated in the last years (Chavan, 2018). OPW was proposed as a valuable feedstock for biofuel production for its high content of cellulose, hemicellulose, lignin, and fermentable sugars contained in the biomass (119.7 million tons) (Chavan, 2018). Large scale bioprocesses for biogas and bioethanol have been already implemented at industrial scale (Mizuki, 1990) and even an anaerobic digestion process of orange wastes coupled with a leaching pretreatment to recover limonene from the highly volatile oily fraction of peel, was reported, using hexane as solvent (Wikandari, 2015).

Citrus peels are the main source, together with apple pomace, of pectins on the market (Wikandar, 2015). Pectins are polymers mainly formed by D-galacturonic acid units linked by an alpha-(1-4) bond, whose carboxylic groups are esterified by methoxy groups (Thakur, 1997). Pectins, due to their gelling and thickening properties are largely employed in the food industry as stabilizers and gelling agents in jams, fruit juices and sweets (Moneim, 2013). The classical extraction process of pectins from orange peels involves heating and simultaneous acidification of the feedstocks. Because of the extraction process, many toxic residues are produced during the extraction and degradation caused by the high acidity of the chemical structure of the polymer (Mesbahi, 2005). Due to the different applications of pectins and due to the high availability of citrus wastes as raw material, the interest to find new applications and novel processes to extract the polymer by companies and academic research is extremely high. Novel, less expensive and environmentally sustainable extraction processes from orange peels have been proposed and moreover, novel pectin-based food packaging biofilms have been proposed as a sustainable alternative to the non-renewable

polymers currently employed for food packaging applications (Cavallaro, 2013 and Makaremi, 2017).

Other appealing applications made by OPW for the food packaging industry have been proposed by Kasai (2017) who developed a paper incorporated with citrus peel residues as a valuable material for food packaging applications due to the enhanced barrier properties to water and oxygen as for the antioxidant peculiarity of the material.

The synthesis of novel biodegradable packaging materials was recently reported from the whole dried citrus peel (Shan, 2016) and peel oil (Bähr, 2012). In the latter application, the orange peel oil was treated to oxidize his major component limonene into limonene oxide and employ it together with carbon dioxide as a building block for the synthesis of the novel citrus-based biomaterial (Parrino, 2018, Arrieta, 2014 and Chavan, 2018).

The oily fraction of citrus peels, composed mainly of terpenes (D-limonene, α-terpinolene, α-pinene) is well known for its antioxidant antiviral, anticancerogenic and antifungal activities (Mahato, 2018) and furthermore, citrus oils were found to inhibit yeast and bacteria growth (Fisher, 2006). Moreover, it was recently reported that OPW extracts might be an attractive candidate for topical application on the human skin as an effective treatment of human skin disorders due to their anti-inflammatory properties (Kim, 2008 and Zayed, 2021).

The economic interest in the extraction of essential oil can be justified by its high value in the wider pharmaceutical industry, as a flavouring agent in the food and beverage industry and cleaning products. Many efforts have been done by researchers to develop novel methods of extraction (e.g., ultrasound, microwaves (Londoño, 2012) and supercritical fluids) (Kim, 2009) to overcome the classical cost-effective steam distillation process utilized nowadays for essential oil extraction from citrus peel residues (Chavan, 2018).

D-limonene is the major component of the oily fraction of orange peels and finds application in many industrial applications since it is utilized as a flavoring agent in food and beverages as in pharmaceutical products such as in hand

sanitizing alcohol-based gels, whose utilization radically increased after the COVID-19 pandemic (Chavan, 2018).

The interest of pharmaceutical and food industries in limonene C-7 hydroxylation products namely alcohol and on the corresponding perilla aldehyde and perillic acid, increased in the last years due to the last findings on their activities as food preservatives, antioxidant and antiviral activities (Mello, 2020; De Lima, 2020; Ravera, 2021 and Muktar, 2018).

Furthermore, recent studies investigated the effect of perillyl alcohol and perillic acid on brain cancer through intranasal administration in rats concluding that those terpenes might have potential significance in brain cancer treatment (De Silva, 2021 and Nehra, 2021).

Hydroxylation of limonene can be performed at different positions by Cytochrome monooxygenases CYP450, a class of enzymes able to hydroxylate a wide range of organic molecules often in a regioselective manner (Tai, 2016 and Groeneveld, 2016); CYP153A6 from Mycobacterium sp. strain HXN-1500 is a soluble enzyme able to catalyze the regioselective hydroxylation of limonene at C-7 furnishing perillyl alcohol (Fujita et al., 2014).

The study aims to optimize an efficient fermentative process employing *K. xylinus* recombinant strain carrying CYP153A6 operon utilizing orange peel juice as a culture medium to maximize the production of perillic acid from limonene naturally contained in citrus peels. We investigated the employment of different inducible and constitutive promoters, whose behaviour was recently tested in different BC producer strains such as *Gluconacetobacter xylinus* ATCC 700178, *Gluconacetobacter hansenii* ATCC 53582 and *Komagataeibacter rhaeticus* iGEM (Florea, 2015; The, 2019 and Florea, 2016), upstream the CYP153A6 operon, to maximize the yield of perillic acid produced from the fermentation of an orange peel juice obtained from orange peel wastes. OPJ inhibition on enzymatic expression during microbial growth was investigated employing mRFP1 as a reporter gene carried by the same plasmid backbones employed for CYP450 expression.

Material and methods

Citrus peel wastes (CPW) biomass origin and treatment

Orange peel wastes were collected from a supermarket (K-market Herkkuduo, Kauppias Kari saimipuro) in Hervanta, Tampere, Finland. Orange peels are derived from the waste of an automatic orange squeezer (Juice bottles / Solotop) for the service of a fresh orange juice distributor.

Orange peels were collected in May 2021 and stored at -20°C before pretreatment. 240g of peels derived from seven oranges, were ground with a mixer grinder until uniform particles (2-5mm size) were obtained. The equal of the 25%V/W OPW weight of sterile deionized water (60mL) was added to particles and mixed to increase the water content and facilitate the enzymatic hydrolysis. Enzymatic pretreatment was started by adding 3mL of cellulases from *T. reseei* to the peels (1% V/W) and carried out in a 1-litre Round-bottom flask incubated at 28°C for 16h at 300rpm. After the treatment, the hydrolyzed CPW was manually compressed with a gauze to extract the liquid orange peel juice (OPJ). The obtained OPJ was stored at -20°C before further use. Before the fermentation, the OPJ were thawed and diluted with different amounts of sterile deionized water. The less diluted samples (1:2) were centrifuged in 50mL falcon tubes (8000rpm, 30 min) to get rid of solid insoluble residues that interfered with optical density measurements. Before inoculum OPJ samples were brought to pH 7.00 with NaOH to avoid CYP450 inhibition due to acidic conditions.

Bacterial strains and plasmid vectors

Growth curve, fluorescence data and limonene oxidation were obtained from the cultivation of recombinant *K. xylinus* inoculated from glycerol stocks. Glycerol stocks were prepared by culturing single colonies of newly transformed *K. xylinus* transformants (following Florea (2016) protocol for competent transformation and plasmid electroporation). Single colonies were cultivated in 20mL of HS-GLU medium (32mg/L chloramphenicol, 1% cellulases) for three days, then cells were centrifuged (1200g – 10min)

washed twice with and resuspended in one milliliter of sterile phosphate-buffered saline (PBS) pH 7.0 and stored at -80°C. The fermentation experiments were carried out in 100mL flask containing a 10mL of HS-GLU medium or OPJ.

PSEVA vectors carrying mRFP as reporter gene were purchased from Addgene (J23104-mRFP1-331Bb catalog number: 78274, pLux01 mRFP1catalog number: 78281, pTet01 mRFP1 catalog number: 78283).

CYP153A6 from Mycobacterium sp. strain HXN-1500 expression in *K. xylinus* was achieved by transforming J23104 CYP450, pLux CYP450 and pTet CYP450 vectors constructed as described above in chapter 3 from above mentioned addgene vectors replacing mRFP1 with CYP153A6 operon keeping the same promoter, terminator and ribosome binding sites unchained.

Fluorescence analysis

Initially, we investigated the possible inhibition effect caused by OPJ medium on the induction, driven by the three tested promoters, employing mRFP1 as reporter gene. We employed recombinant *K. xylinus* transformed with pSEVA plasmids carrying the promoters J23104, pLux01 and pTet01 (Florea, 2015; The, 2019 and Florea, 2016) upstream the mRFP1 gene. The strains carrying mRFP fluorescent protein were cultivated in four different OPJ dilutions. The dilutions employed for K. cultivation were 1:2, 1:10, 1:50, 1:100. Cultivations were carried out in 10mL of OPJ (cellulase 2% (v/v), 34 µg/mL of chloramphenicol at 30 °C with 220 rpm shaking), inoculating 50 µL of glycerol stocks of *K. xylinus* transformants prepared as described above.

We performed a quantitative analysis of mRFP1 fluorescence of *K. xylinus* grown on different dilutions of OPJ and utilized HS-GLU liquid medium as a positive control. To detect the actual expression of mRFP1 driven by the J23104 strong constitutive promoter and AHL (pLux01) and ATc (pTet01,) inducible promoters we analyzed cells fluorescence and normalized the values on OD_{600} values. Fluorescence analysis was started after 12 hours

from the moment of the inoculum, right after the addition of the inducers for inducible constructs AHL (pLux01) and ATc (pTet01) cultivations. The expression of mRFP1 was initiated by adding 10 μM N-acyl homoserine lactone (AHL) for pLux01 cultures while pTet01 recombinant strains were induced with 10 μM anhydrotetracycline (ATc). The cultivations were carried out in 10mL of OPJ or HS-GLU medium. The incubations were carried out for five days. Culture fluorescence was analyzed during cell growth, washing the cells with PBS buffer and then moving 200μL of the cell resuspension into flat bottom transparent microplates, mRFP1 fluorescence (excitation 580 nm, emission 610 nm) and OD_{600} measurement were taken in a Spark multimode microplate reader (Tecan, Switzerland).

Shake Flask fermentation for the enzymatic transformation of limonene to perillic acid

OPJ was used as the sole medium for bacterial strain growth and source of D-limonene: we cultivated *K. xylinus* recombinants testing different fermentation conditions employing serial dilutions (in sterilized deionized water) of the OPJ brought to pH 7.00. The dilutions employed for cultivation were 1:2, 1:10, 1:50, 1:100 as done for mRFP expression analysis. We tested *K. xylinus* growth in OPJ employing J23104 CYP450, pLux CYP450 and pTet CYP450 transformants. OPJ inocula were performed with 50 μL of glycerol stocks, bacterial strains were grown in presence of cellulase [2% (v/v)] to avoid cellulose production in 100mL flasks filled with 20mL of OPJ adding 34 μg/mL of chloramphenicol at 30 °C with 220 rpm shaking, the fermentations were carried out for five days.

Then to find the optimal fermentation we screened two different fermentation conditions. We tested the employment of OPJ (sample dilution 1_2) without any pH adjustment to investigate if OPJ pH adjustment step could be avoided in a large scale fermentation process. In this case we employed *K. xylinus* J23104 CYP450 recombinant strain. Then, to limit limonene evaporation we

employed sealed flasks to limit limonene evaporation and to maximize perillic acid recovered yield. In this case, we tested all three recombinant strains.

In all fermentation trials of this study, the fermentation of *K. xylinus* recombinants transformed with inducible promoters was carried out until the OD_{600} reached a value of 0.4-0.6, then CYP450 expression was initiated by adding inducers in the fermentation medium. *K. xylinus* carrying pLux CYP450 construct was induced by 10 µM N-acyl homoserine lactone (AHL) while pTet CYP450 recombinants by 10 µM anhydrotetracycline (ATc).

Bacterial growth and medium acidification were followed during the fermentation. Samples were collected and stored at -80°C before GC-MS and HPLC analysis, while cell density and pH were analyzed before sample freezing. Optical density was measured by spectrophotometer (Ultrospec 500 pro, Amersham Biosciences, UK) and pH values were determined by a pH meter (S470, Mettler Toledo).

Analytical methods

HPLC

The consumption of glucose, sucrose and sorbitol in the OPJ was followed during the fermentation of OPJ (dilution 1_2) with *K. xylinus* J23104 CYP450 by HPLC. The amount of sugars in OPJ was quantified along the bacterial growth by comparing the area of the peaks with an internal calibration curve. The range of the standard curves utilized for sugar consumption were ranging from 0.3125 to 100mM. Samples were taken during the fermentation and stored at -80°C. OPJ samples were analyzed and the calibration curves were constructed utilizing an HPLC coupled with a Rezex RFQ-Fast Acid H+ (8%) (Phenomenex, Torrance, CA, USA) column an autosampler (SIL-20AC HT, Shimadzu) and a refractive index detector (RID-10A, Shimadzu). The analysis was carried out at 80°C, 0.005 N H_2SO_4 was utilized as eluent with a flow rate of 0.5 mL/min. Samples were collected along with the fermentation and stored

-80°C. Before the analysis, the samples were thawed, centrifuged at 3000rpm for 3 minutes and filtered with a 0.22-µm filter.

GC-MS

The presence in the OPJ of limonene, peryllic alcohol (PAL) and perillic acid (PA) was evaluated before and during the fermentation using chromatography-mass spectrometry (GC– MS). Samples were prepared sampling 500uL from OPJ fermentation, the samples were stored at -20°C before analysis.

Samples were brought to pH 1.00 with 5M Hydrochloric acid, extracted with an equal amount of ethyl acetate. The organic phase was filtered with a 0.22-µm filter and analyzed by GC-MS. An Agilent Gas Chromatograph (Agilent series 6890 N GC system) coupled with flame ionization detector FID and an Agilent 5975 Series Gas Chromatograph/Mass detection system was used. A ramp program was set from 80°C to 250°C with a rate of 1°C/min. Helium was utilized as the gas carrier with a flow rate of 1 mL min^{-1}, the inlet temperature was 250 ◦C, and the split ratio was set at 1:20). The column was a capillary HP- 5MS (30 m, 0.25 mm ID, 0.25 µm film thickness). Limonene hydroxylation and oxidation products were identified and quantified with a calibration curve made with internal standards (Sigma). The amount of limonene, PAC and PA in the OPJ before and during fermentation were evaluated with a 5-point with internal standards, performed in triplicates. The range of the standard curve was calculated from 0,0625g/L to 1 g/L. The area of each concentration point was plotted against the corresponding concentration. OPJ composition before and after the fermentation was constructed with a fragmentation pattern Mass Spectral Library.

Results and discussion

Citrus peels pretreatments

OPJ was obtained from orange peel waste (OPW) derived from an automatic vending machine of orange juice. OPW were milled and enzymatically treated to obtain a soft paste which was manually pressed obtaining a dense juice that was utilized as a medium culture for cell growth and as a limonene source. Orange peel wastes from an automatic orange juice distributor were added up with sterile deionized water (25%V/W of total OPW weight) and milled with a kitchen mixer until small particles (around 2-5mm) were obtained (figure 1, A). Orange pieces were then treated with cellulases by *T. reseei* for 16 hours at 28°C to improve the extraction of fermentable sugars (Figure 1, B) in the soluble fraction extracted through a manual pressing of the biomass. On the total weight treated OPW (figure 1, B), after manual extraction, was obtained the 54% of the total weight as a liquid fraction called orange peel juice (OPJ) (figure 1, D). The leftover insoluble residue, which represented 46% of the total OPW, was discarded (figure 1, C). Before utilization as a fermentation medium, the OPJ was diluted with variable amounts of deionized water and brought to pH 7.00. We hypothesize that autoclaving the OPJ could cause an important Limonene loss. To investigate the possibility to utilize as substrate non-sterile OPJ we incubated the OPJ without inoculum in the same conditions and for the same time as the fermentation samples. Any visible contamination was observed from the negative control with OPJ substrate without inoculum, despite any sterilizing procedures of the OPW and OPJ being performed.

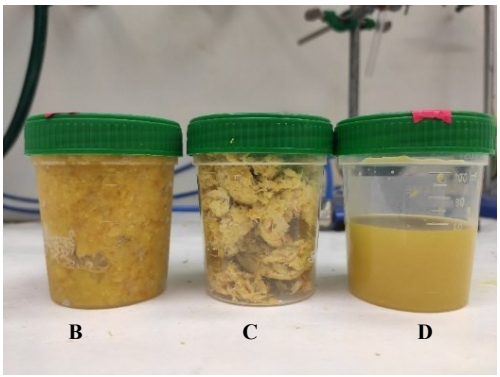

***Figure 1**: **A:** orange peel waste (OPW). (The image reports the orange peels treated to extract the orange peel juice); **B:** 2-5mm size particles obtained after orange peels milling and after enzymatic hydrolysis with cellulases by T. reseei; **C:** Leftover solid residues obtained by orange peels particles (B) squeezing; **D:** Orange peel juice (OPJ) obtained by orange peels particles (B) squeezing.*

name	**description**	**source**
J23104-mRFP1-331Bb	Vector for expression in AAB of mRFP1	Addgene plasmid # 78274
J23104 CYP450	Vector for expression in AAB of CYP450	Chapter 3
pLux01 mRFP1	mRFP1 expressed behind an AHL-inducible construct	Addgene plasmid # 78281
pTet01 mRFP1	mRFP1 expressed behind an ATc-inducible construct	Addgene plasmid #78283
pLux CYP450	Express the CYP450A6 operon under the pLux01 inducible promoter	Chapter 3
pTet CYP450	Express the CYP450A6 operon under the pTet01 inducible promoter	Chapter 3

***Table 1.** Lists of plasmids employed in this study*

A

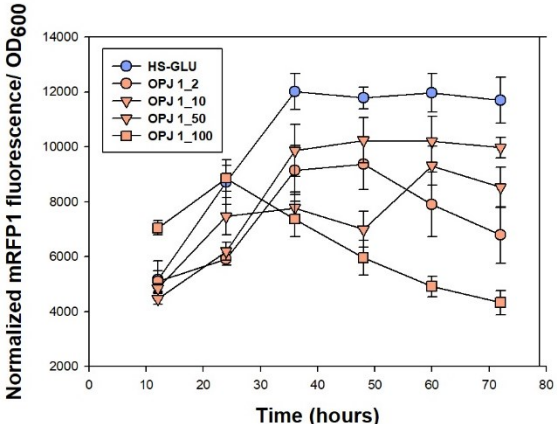

B

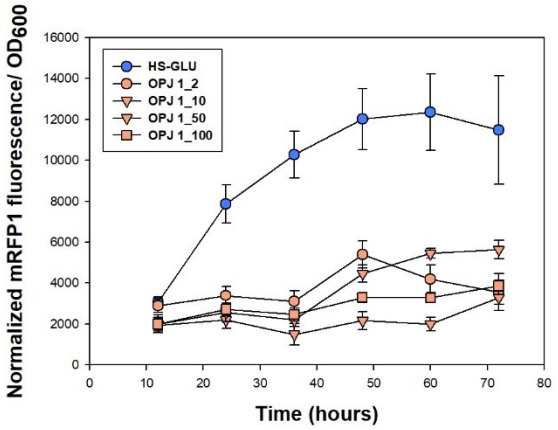

C

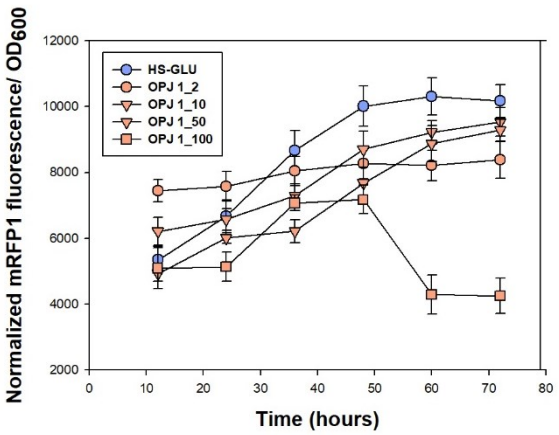

Figure 2 *Fluorescence data obtained from K. xylinus transformants (**A:** J23104-mRFP1-331Bb, **B**: pLux01 mRFP1, **C** pTet mRFP1) cultivated in OPJ fermentation (dilution 1_2, pH 7.00), data represent the average values obtained from triplicate cultivations.*

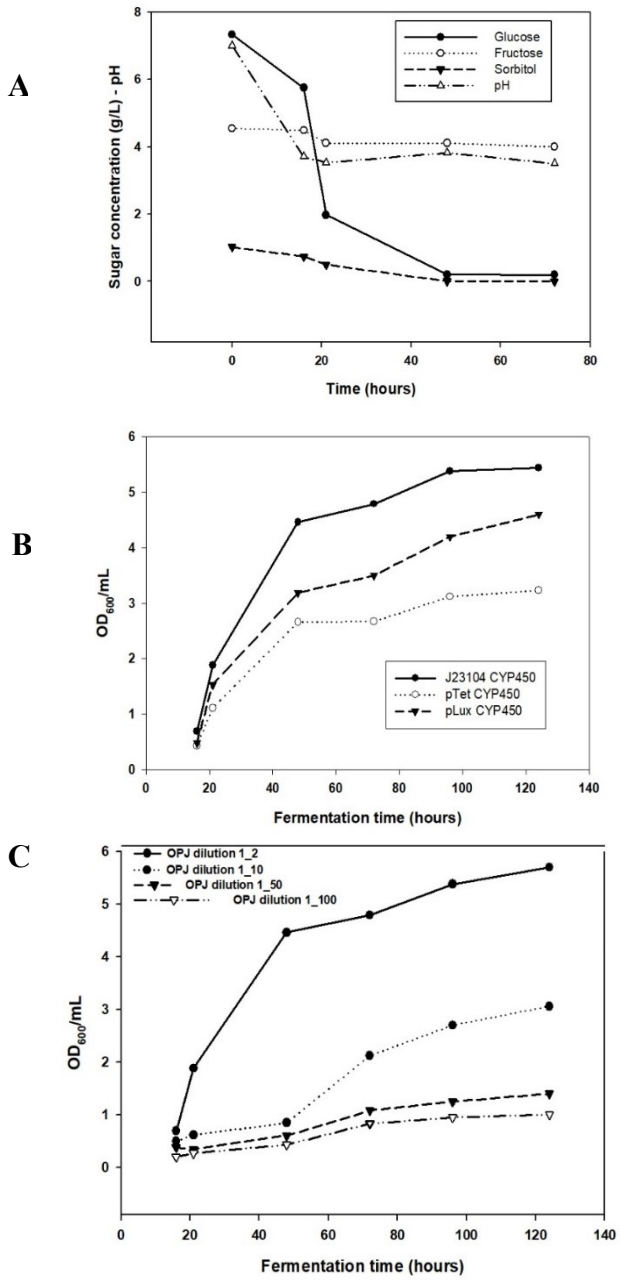

***Figure 3 A**: Sugar consumption and pH drop along with OPJ fermentation, sugar utilization was fallowed during OPJ (dilution 1_2) fermentation employing K. xylinus J23104 CYP450 by HPLC. **B**: Microbial growth of K. xylinus J23104 CYP450, K. xylinus pLux CYP450, K. xylinus pTet CYP450 in OPJ (dilution 1_2). **C**: Microbial growth of K. xylinus J23104 CYP450 on different OPJ dilutions (1_2, 1_10, 1_50, 1_100)*

RFP1 Fluorescence analysis

Fluorescence measurements were performed washing cells with PBS buffer to avoid OPJ interference with fluorescence analysis and to exclude the autofluorescence of HS-GLU or OPJ medium from the fluorescence quantification.

Expression analysis experiments, carried out employing mRFP1 as a reporter gene, showed a general mRFP inhibition caused by OPJ. Control experiments carried out cultivating the three strains in HS-GLU resulted to give a higher fluorescence compared to the same strains cultivated in OPJ.

Interestingly, the Inhibition of mRFP expression was not correlated to OPJ dilution, since for all the constructs the more diluted OPJ medium (OPJ 1_100) furnished the lowest mRFP fluorescence during the strain growth while the more concentrated OPJ sample (OPJ 1_2) generally gave, among the OPJ dilutions samples, high fluorescence values.

The strong constitutive Anderson promoter namely J23104 gave a higher mRFP1 expression compared to the inducible promoters pTet and pLux. The fluorescence of pLux strains inducted with AHL seemed to be highly inhibited by OPJ, while grown in HS-GLU medium*, K. xylinus* plux strain seemed to be well controlled by AHL induction as already reported by numerous reports. (Zheng, Florea, 2016 and Gooseng, 2021) for different Komagataeibacter strains (Figure 2). PTet promoter, as recently reported (Zheng, Florea, 2016 and Gooseng, 2021), showed a general lack of inducibility by anhydrotetracycline (ATc) when cultivated in HS-GLU and in OPJ medium.

Microbial growth employing OPJ as culture medium, limonene hydroxylation and perillic acid production yields

We tested microbial growth of *K. xylinus* in increasing OPJ dilutions employing J23104 CYP450 recombinant. As expected, we observed a higher microbial growth in the less diluted OPJ samples due to the higher sugar content. The analysis microbial growth of *K. xylinus* pLux CYP450 and *K. xylinus* pTet CYP450 revealed also, in this case, J23104 CYP450 as the fastest growing

strain. From HPLC analysis a rapid glucose consumption was observed during *K. xylinus* J23104 CYP450 growth on OPJ (dilution 1_2) (Figure 3A).
Consistently with the RFP fluorescence results obtained with OPJ employing pLux mRFP transformants, where a high inhibition by OPJ of the RFP expression was observed a very low expression of CYP153A6 was probably obtained in OPJ cultures employing pLux CYP450 transformants. In the end, as a consequence of high limonene volatility (figure S2) and the high expression inhibition by OPJ, no trace of perillic acid was detected during the fermentation. Accordingly with this supposition, when we employed the transformants carrying the strong constitutive promoter J23104 we observed the highest RFP fluorescence and the highest recovered perillic acid concentrations. As a result of the complete leakage of pTet promoter, CYP153A6 enzymatic activity was enough to hydroxylate a minimal amount of limonene into the more water-soluble perillyl alcohol getting after three days of fermentation only 2,78 mg/L of PA (OPJ dilution 1_2) (Table 1).
It seems clear that the limiting factors to implement the final perillic acid recovered yields are the high limonene volatility (figure S2) and the high request of aeration for CYP450 enzymatic reaction. In the fermentation of OPJ (dilution 1_2) with a sealed cap flask (Table 1) any trace of perillic acid was detected in the end of the fermentation, this fact could be attributed to the insufficient oxygen supply to the CYP153A6 catalytic domain and to Ferredoxin and Ferredoxin Reductase carried by *Mycobacterium* sp. operon. We assumed that the absence of perillic acid after the fermentation in sealed cap flasks is caused by insufficient oxygen supply to CYP153A6 since that the optical density reached in five days of fermentation was equal to the one obtained in normal flasks (5 OD/mL) (Figure 3C).

OPJ dilution	Initial OPJ pH / fermentation flask	Initial limonene conc. (mg/L)	Perillic acid concentration after three days of fermentation (mg/L)		
			J23104 CYP450	pLux CYP450	pTet CYP450
1_100	7.00	1,02	0	0	0
1_50	7.00	2,04	0	0	0
1_10	7.00	10,2	5,43	0	0
1_2	7.00	102	51,00	0	2,78
1_2	7.00 – sealed cap	102	0	0	0
1_2	4.30	102	19,67	-	-

Table 1 *Initial limonene and recovered perillic acid concentration after three days fermentation of K. xylinus J23104 CYP450, pLux CYP450 and pTet CYP450 employing OPJ in different dilutions and at different pHs.*

Conclusions

Orange peel wastes represent highly available, green and removable biomass which, for the interesting chemical composition, can be exploited as a fermentation medium for the microbial growth for different purposes. In this work, we tested the implementation of different microbial recombinants for the valorization of OPW. A high fermentable liquid rich of sugars and limonene, called orange peel juice (OPJ), was obtained from orange peel wastes derived from an automatic orange squeezer. Here we demonstrated that OPJ could be utilized as a valuable feedstock for the production of perillic acid from the enzymatic transformation of limonene naturally contained into orange peels. Employing different cultivation conditions and genetic elements we analyzed microbial growth, sugar consumption and perillic acid recovered yields from OPJ fermentation trials. From our experiments, we selected J23104 CYP450 as the best plasmid to perform OPJ fermentation with *K. xylinus* for limonene hydroxylation and perillic acid recovery. Further implementation in scale fermenters should be carried out to test the economic feasibility of the proposed fermentation process.

Supplementary material

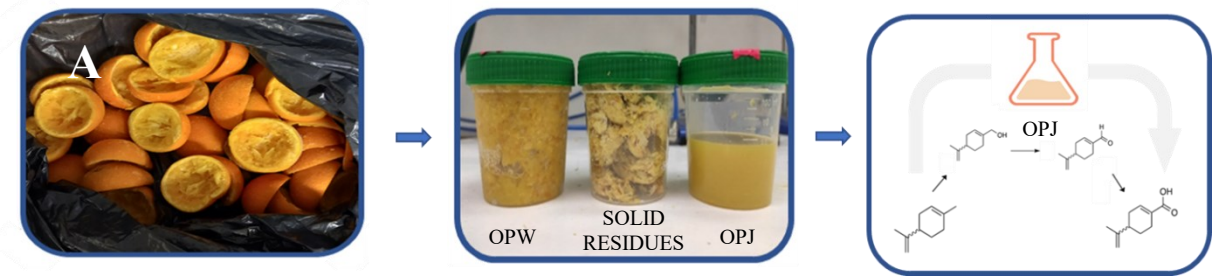

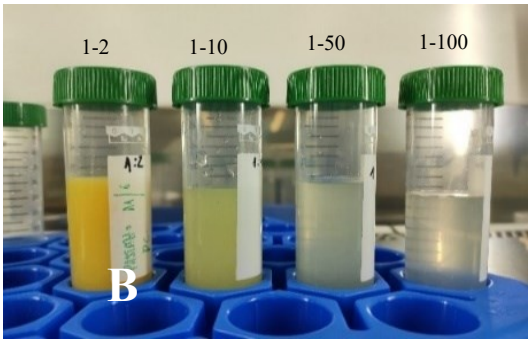

Figure S1. A: *Graphical abstract,* ***B:*** *Orange peel juice (OPJ) dilutions employed in the study. Different dilutions were obtained diluting OPJ from extraction with different amounts of sterile deionized water.*

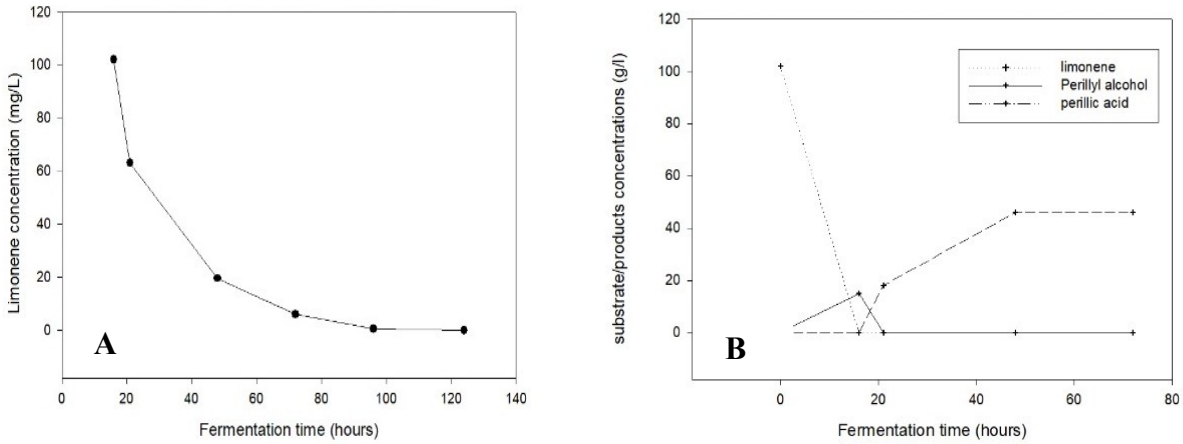

Figure S2. A: *Evaporation of limonene during OPJ incubation in the same conditions employed for OPJ fermentation (28°C, 300rpm).* ***B:*** *Limonene, perillyl alcohol and perillic acid trends during OPJ fermentation (dilution 1_2, pH 7.00) with K. xylinus J23104 CYP450.*

	compound	Peak percentage	Retention time (min)	Predicted chemical formula	Match factor (MF)	Reverse match factor (RMF)
2	Propanal, 2,3-dihydroxy-, (S)-	0,964	4.849	C3H6O3	649	649;
3	(1R)-2,6,6-Trimethylbicyclo[3.1.1]hept-2-ene	10%	8.227	C10H16	633	633
4	β-Myrcene	1	9.616	C10H16	687;	767
5	D-Limonene	81	10.358	C10H16;	942	942
6	Linalool	4	11.719	C10H18O;	883	885
7	Cyclobutane-1,1-dicarboxamide, N,N'-di-benzoyloxy-	3	12.840	C20H18N2O6;	864	886
8	Cyclohexene, 3-methyl-6-(1-methylethylidene)-	0,054	13.298	C10H16;	570	690
9	Cyclohexanol, 4-ethenyl-4-methyl-3-(1-methylethenyl)-, (1α,3α,4β)-	0,029	13.821	C12H20O;	516	662
10	4-Acetoxy-3-methoxystyrene	0,657	15.116	C11H12O3;	810;:	827
11	2,7-Octadiene-1,6-diol, 2,6-dimethyl-, (Z)-	0,517	15.460	C10H18O2;	558	705
12	Ether, 3-butenyl pentyl	0,733	17.425	C9H18O;	450	500
13	Selenourea	1	20.953	CH4N2Se;	553	630

14	trans-Ferulic acid	4	21.680		805	810
15	Xylose	0,678	22.580	C5H10O5;	606	606
16	Cyclohexane, 1-methyl-4-(1-methylethenyl)-, trans-	1	24.230	C10H18;	693	753

1

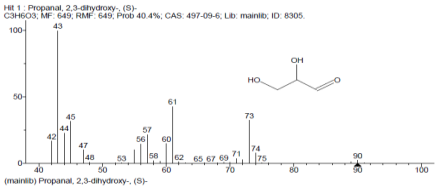

2

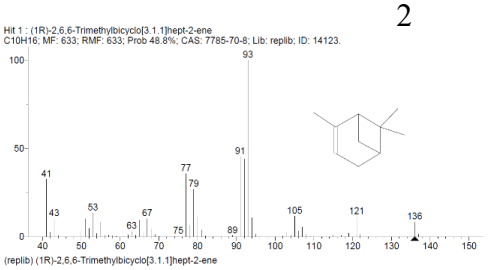

3

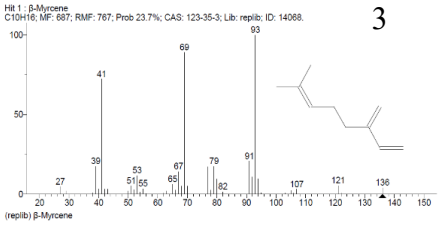

4

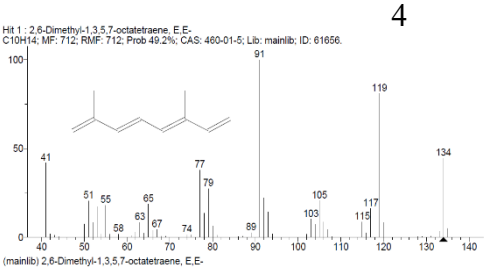

5

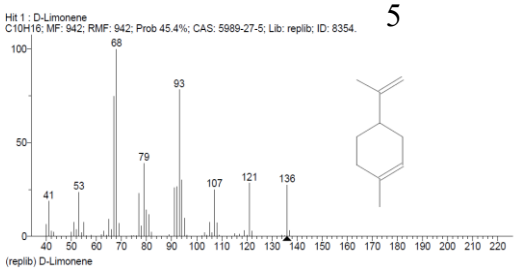

6

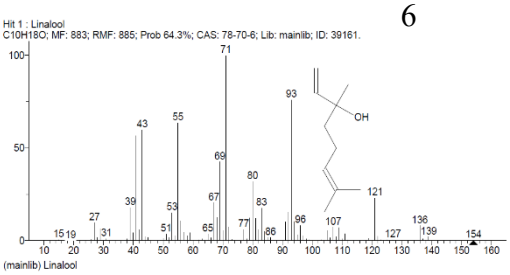

7

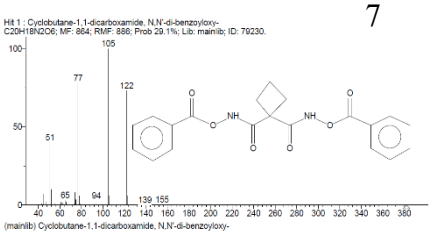

8

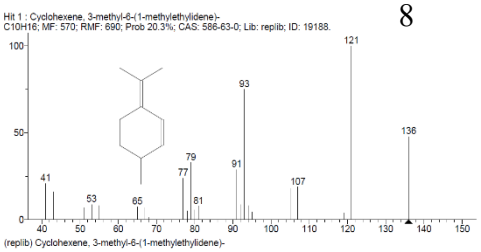

9

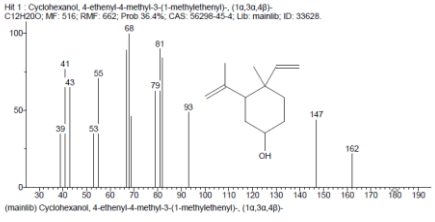

10

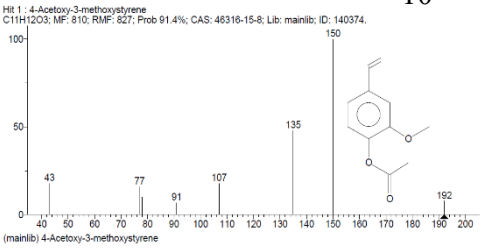

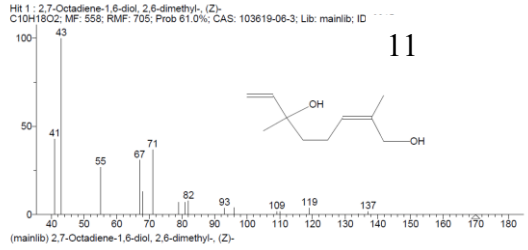

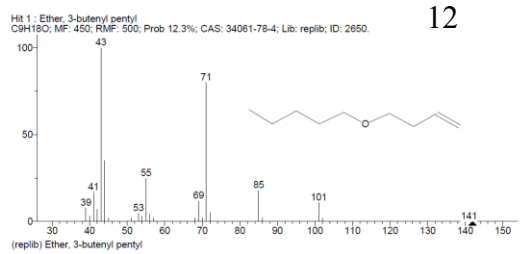

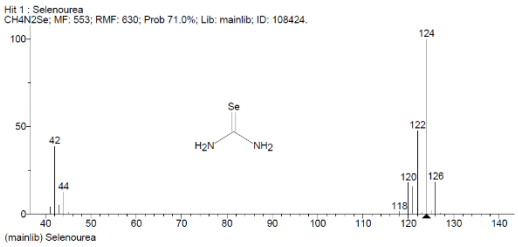

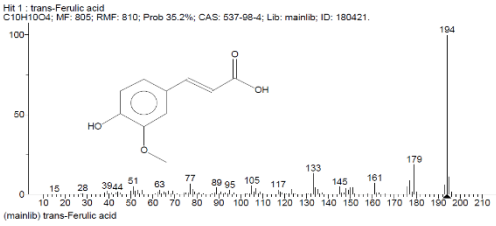

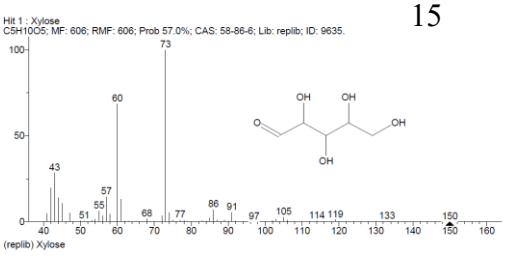

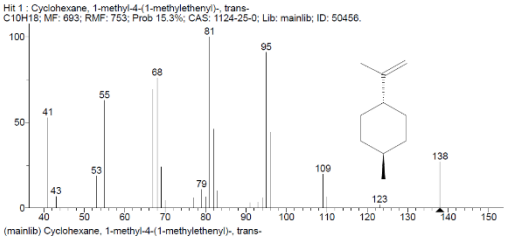

Table S1. *Composition of OPJ (dilution 1_2) before fermentation detected by GC-MS predicted chemical structures*

	compound	Peack percentage (%)	Retention time (min)	Predicted chemical formula	Match factor (MF)	Reverse match factor (RMF)
1	Propanal, 2,3-dihydroxy-, (S)-	9,799	4.849	C3H6O3	649;	649;
2	Dihydroxyacetone	31,545	7.240	C3H6O3	689	689
3	Ethaneperoxoic acid, 1-cyano-1,4-diphenylpentyl ester	1.924	9.608	C20H21NO3		781
4	Sorbic Acid	26,213	11.318	C6H8O2;	770	770
5	1-Cyclohexene-1-carboxylic acid, 4-(1-methylethenyl)-	4,215	16,712	C10H14O2;	666	674
6		6.279%	28.086			
7	Chloramphenicol	20,024	30.604	C11H12Cl2N2O5;	597	693

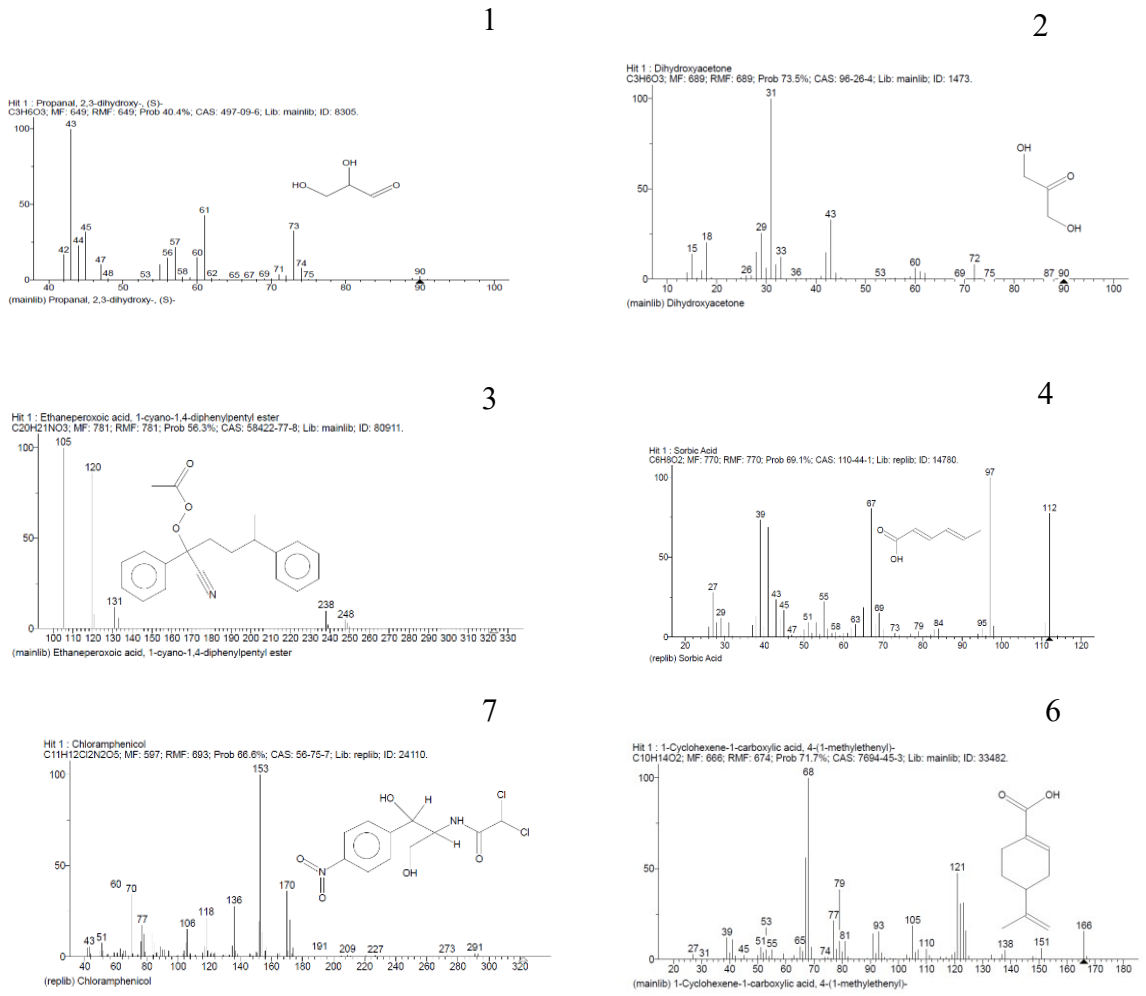

Table S1. *Composition of OPJ after fermentation (dilution 1_2, pH 7.00) with K. xylinus J23104 CYP450 detected by GC-MS and predicted chemical structures*.

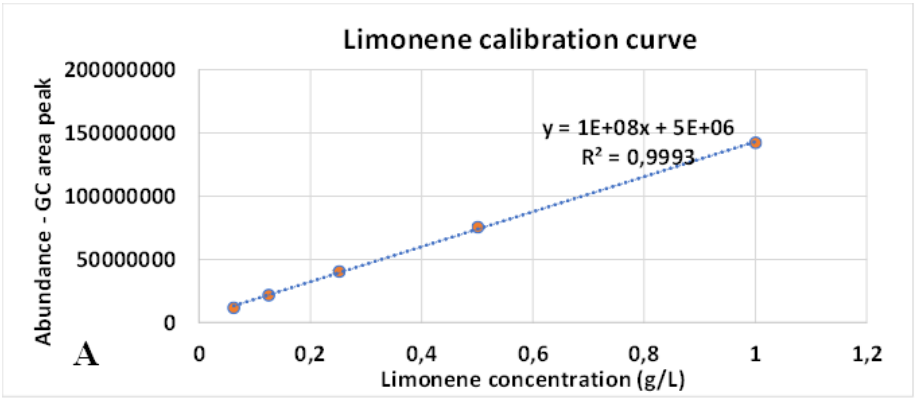

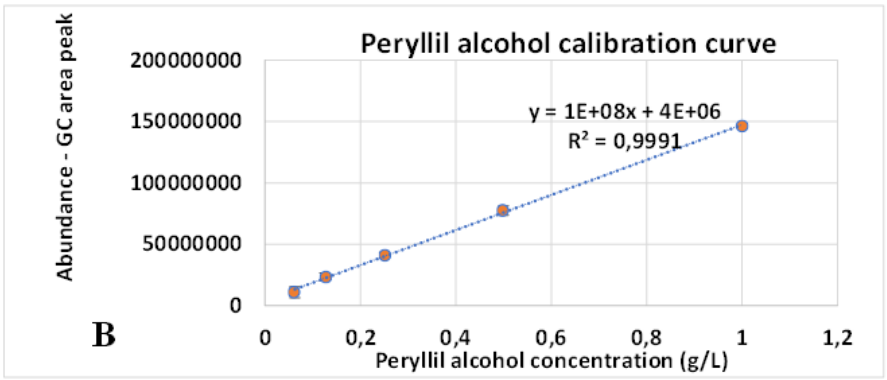

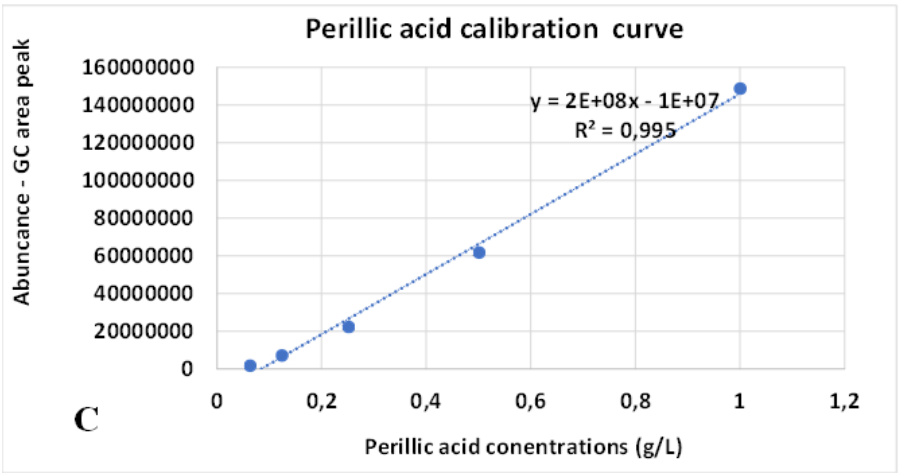

Figure S3 Calibration curves employed for limonene (A), perillyl alcohol (B) and perillic acid (C)quantification in OPJ. The data points represent the means of three injections, the error bars are smaller than the sphere symbol.

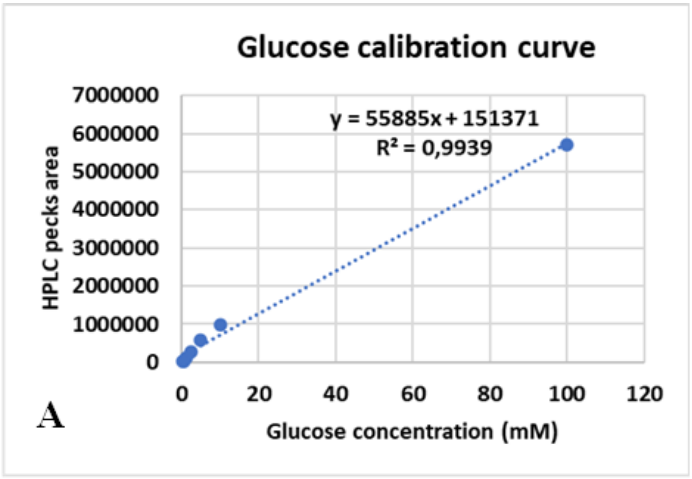

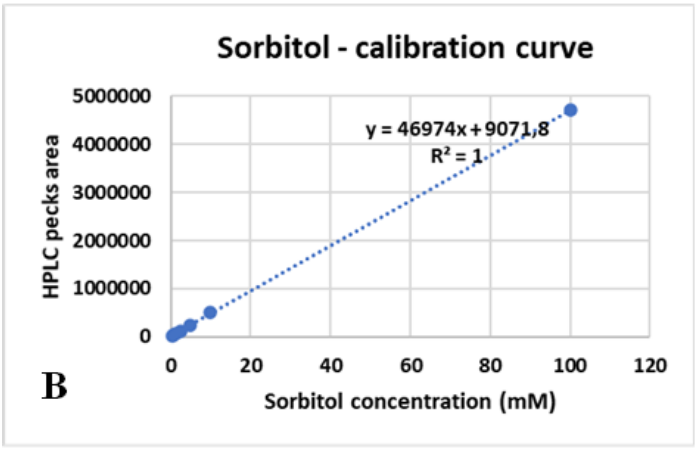

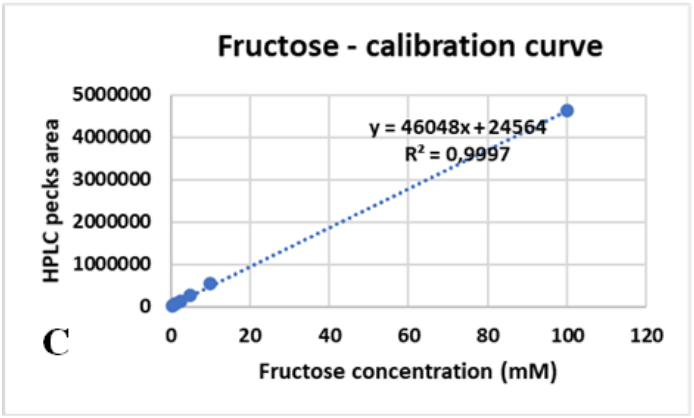

Figure S4: HPLC calibration curves employed for glucose (A), sorbitol (B), fructose (C) in OPJ. The data points represent the means of three injections, in some cases the error bars are smaller than the sphere symbol.

References

Dahiya S, Kumar AN, Shanthi Sravan J, Chatterjee S, Sarkar O, Mohan SV. Food waste biorefinery: Sustainable strategy for circular bioeconomy. *Bioresource Technology*. 2018;248(July 2017):2-12. doi:10.1016/j.biortech.2017.07.176

Branduardi P. Closing the loop: the power of microbial biotransformations from traditional bioprocesses to biorefineries, and beyond. *Microbial Biotechnology*. 2021;14(1):68-73. doi:10.1111/1751-7915.13713

Blakeney M. *Food Loss and Food Waste: Causes and Solutions*.; 2019. doi:10.4337/9781788975391

Valenti F, Porto SMC, Chinnici G, et al. Use of citrus pulp for biogas production: A GIS analysis of citrus-growing areas and processing industries in South Italy. *Land Use Policy*. 2017;66(March):151-161. doi:10.1016/j.landusepol.2017.04.041

Sharma K, Mahato N, Cho MH, Lee YR. Converting citrus wastes into value-added products: Economic and environmently friendly approaches. *Nutrition*. 2017;34:29-46. doi:10.1016/j.nut.2016.09.006

Chavan P, Singh AK, Kaur G. Recent progress in the utilization of industrial waste and by-products of citrus fruits: A review. *Journal of Food Process Engineering*. 2018;41(8):1-10. doi:10.1111/jfpe.12895

Garcia-Castello EM, Mayor L, Chorques S, Argüelles A, Vidal-Brotóns D, Gras ML. Reverse osmosis concentration of press liquid from orange juice solid wastes: Flux decline mechanisms. *Journal of Food Engineering*. 2011;106(3):199-205. doi:10.1016/j.jfoodeng.2011.05.005

Francesca Valenti, Simona MC Porto, Gaetano Chinnici, Giovanni Cascone CA. A GIS-based model to estimate citrus pulp availability for biogas production: an application to a region of the Mediterranean Basin. *Biofuels, Bioproducts and Biorefining*. 2012;6(3):246-256. doi:10.1002/bbb

Crowe M, Nolan K, Collins C, et al. Biodegradable Municipal Waste Management in Europe: Part 3 - Technology and Market Issues. 2002;(15):32.

Bresciani S, Thrassou A, Vrontis D. Change through innovation in family businesses: Evidence from an Italian sample. *World Review of Entrepreneurship, Management and Sustainable Development*. 2013;9(2):195-215. doi:10.1504/WREMSD.2013.052359

Wadhwa M, Bakshi SPM. *Utilization of Fruit and Vegetable Wastes as Livestock Feed and as Substrates for Generation of Other Value-Added Products*.; 2013.

Sharma K, Mahato N, Cho MH, Lee YR. Converting citrus wastes into value-added products: Economic and environmently friendly approaches. *Nutrition*. 2017;34:29-46. doi:10.1016/j.nut.2016.09.006

Mizuki E, Akao T, Saruwatari T. Inhibitory effect of Citrus unshu peel on anaerobic digestion. *Biological Wastes*. 1990;33(3):161-168. doi:10.1016/0269-7483(90)90002-A

Wikandari R, Nguyen H, Millati R, Niklasson C, Taherzadeh MJ. Improvement of biogas production from orange peel waste by leaching of limonene. *BioMed Research International*. 2015;2015. doi:10.1155/2015/494182

Thakur BR, Singh RK, Handa AK. Chemistry and Uses of Pectin - A Review. *Critical Reviews in Food Science and Nutrition*. 1997;37(1):47-73. doi:10.1080/10408399709527767

Moneim A, Sulieman E, Khodari KMY, Salih ZA. Extraction of Pectin from Lemon and Orange Fruits Peels and Its Utilization in Jam Making. *International Journal of Food Science and Nutrition Engineering*. 2013;2013(5):81-84. doi:10.5923/j.food.20130305.01

Mesbahi G, Jamalian J, Farahnaky A. A comparative study on functional properties of beet and citrus pectins in food systems. *Food Hydrocolloids*. 2005;19(4):731-738. doi:10.1016/j.foodhyd.2004.08.002

Cavallaro G, Lazzara G, Milioto S. Sustainable nanocomposites based on halloysite nanotubes and pectin/polyethylene glycol blend. *Polymer Degradation and Stability*. 2013;98(12):2529-2536. doi:10.1016/j.polymdegradstab.2013.09.012

Makaremi M, Pasbakhsh P, Cavallaro G, et al. Effect of Morphology and Size of Halloysite Nanotubes on Functional Pectin Bionanocomposites for Food Packaging Applications. *ACS Applied Materials and Interfaces*. 2017;9(20):17476-17488. doi:10.1021/acsami.7b04297

Kasaai MR, Moosavi A. Treatment of Kraft paper with citrus wastes for food packaging applications: Water and oxygen barrier properties improvement. *Food Packaging and Shelf Life*. 2017;12:59-65. doi:10.1016/j.fpsl.2017.02.006

Shan Y. Production of Biodegradable Packages Using Citrus Peel. *Comprehensive Utilization of Citrus By-Products*. Published online 2016:91-92. doi:10.1016/b978-0-12-809785-4.00008-3

Bähr M, Bitto A, Mülhaupt R. Cyclic limonene dicarbonate as a new monomer for non-isocyanate oligo- and polyurethanes (NIPU) based upon terpenes. *Green Chemistry*. 2012;14(5):1447-1454. doi:10.1039/c2gc35099h

Parrino F, Fidalgo A, Palmisano L, Ilharco LM, Pagliaro M, Ciriminna R. Polymers of Limonene Oxide and Carbon Dioxide: Polycarbonates of the Solar Economy. *ACS Omega*. 2018;3(5):4884-4890. doi:10.1021/acsomega.8b00644

Arrieta MP, López J, Hernández A, Rayón E. Ternary PLA-PHB-Limonene blends intended for biodegradable food packaging applications. *European Polymer Journal*. 2014;50(1):255-270. doi:10.1016/j.eurpolymj.2013.11.009

Mahato N, Sharma K, Sinha M, Cho MH. Citrus waste derived nutra-/pharmaceuticals for health benefits: Current trends and future perspectives. *Journal of Functional Foods*. 2018;40(August 2017):307-316. doi:10.1016/j.jff.2017.11.015

Fisher K, Phillips CA. The effect of lemon, orange and bergamot essential oils and their components on the survival of Campylobacter jejuni, Escherichia coli O157, Listeria monocytogenes, Bacillus cereus and Staphylococcus aureus in vitro and in food systems. *Journal of Applied Microbiology*. 2006;101(6):1232-1240. doi:10.1111/j.1365-2672.2006.03035.x

Kim SS, Lee JA, Kim JY, Lee NH, Hyun CG. Citrus peel wastes as functional materials for cosmeceuticals. *Journal of Applied Biological Chemistry*. 2008;51(1):7-12. doi:10.3839/jabc.2008.002

Zayed A, Badawy MT, Farag MA. Valorization and extraction optimization of Citrus seeds for food and functional food applications. *Food Chemistry*. 2021;355(February):129609. doi:10.1016/j.foodchem.2021.129609

Londoño-Londoño J, Lima VR de, Lara O, et al. Clean recovery of antioxidant flavonoids from citrus peel: Optimizing an aqueous ultrasound-assisted extraction method. *Food Chemistry*. 2010;119(1):81-87. doi:10.1016/j.foodchem.2009.05.075

Kim JW, Nagaoka T, Ishida Y, Hasegawa T, Kitagawa K, Lee SC. Subcritical water extraction of nutraceutical compounds from citrus pomaces. *Separation Science and Technology*. 2009;44(11):2598-2608. doi:10.1080/01496390903014375

Mello CP, Quirico-Santos T, Amorim LF, et al. Perillyl alcohol and perillic acid exert efficient action upon HSV-1 maturation and release of infective virus. *Antiviral Therapy*. 2020;25(1):1-11. doi:10.3851/IMP3315

De Lima DC, Rodrigues SV, Boaventura GT, et al. Simultaneous measurement of perillyl alcohol and its metabolite perillic acid in plasma and lung after inhalational administration in Wistar rats. *Drug Testing and Analysis*. 2020;12(2):268-279. doi:10.1002/dta.2722

Ravera M, Gabano E, Zanellato I, et al. Cis,cis,trans-[PtIVCl2(NH3)2(perillato)2], a dual-action prodrug with excellent cytotoxic and antimetastatic activity. *Dalton Transactions*. 2021;50(9):3161-3177. doi:10.1039/d0dt04051g

Mukhtar YM, Adu-Frimpong M, Xu X, Yu J. Biochemical significance of limonene and its metabolites: Future prospects for designing and developing highly potent anticancer drugs. *Bioscience Reports*. 2018;38(6):1-12. doi:10.1042/BSR20181253

Da Silva Santos J, Diedrich C, Machado CS, da Fonseca CO, Khalil NM, Mainardes RM. Intranasal administration of perillyl alcohol–loaded nanoemulsion and pharmacokinetic study of its metabolite perillic acid in plasma and brain of rats using ultra-performance liquid chromatography/tandem mass spectrometry. *Biomedical Chromatography*. 2021;35(4):1-9. doi:10.1002/bmc.5037

Nehra G, Andrews S, Rettig J, et al. Intranasal administration of the chemotherapeutic perillyl alcohol results in selective delivery to the cerebrospinal fluid in rats. *Scientific Reports*. 2021;11(1):1-11. doi:10.1038/s41598-021-85293-4

Tai YN, Xu M, Ren JN, et al. Optimisation of α-terpineol production by limonene biotransformation using Penicillium digitatum DSM 62840. *Journal of the Science of Food and Agriculture*. 2016;96(3):954-961. doi:10.1002/jsfa.7171

Groeneveld M, van Beek HL, Duetz WA, Fraaije MW. Identification of a novel oxygenase capable of regiospecific hydroxylation of D-limonene into (+)-trans-carveol. *Tetrahedron*. 2016;72(46):7263-7267. doi:10.1016/j.tet.2015.12.061

Teh MY, Ooi KH, Danny Teo SX, Bin Mansoor ME, Shaun Lim WZ, Tan MH. An Expanded Synthetic Biology Toolkit for Gene Expression Control in Acetobacteraceae. *ACS Synthetic Biology*. 2019;8(4):708-723. doi:10.1021/acssynbio.8b00168

Florea M, Reeve B, Abbott J, Freemont PS, Ellis T. Genome sequence and plasmid transformation of the model high-yield bacterial cellulose producer Gluconacetobacter hansenii ATCC 53582. *Scientific Reports*. 2016;6(September 2015):1-9. doi:10.1038/srep23635

Florea M, Hagemann H, Santosa G, Abbott J, Micklem CN. Engineering control of bacterial cellulose production using a genetic toolkit and a new cellulose- producing strain. *Proc Natl Acad Sci U S A*. Published online 2016:3431-3440. doi:10.1073/pnas.1522985113

Zheng W, Lim S, Tan MH. Supplementary Information An expanded synthetic biology toolkit for gene expression control in Acetobacteraceae. :1-29.

Goosens VJ, Walker KT, Aragon SM, et al. Komagataeibacter rhaeticus, Published online 2021:1-21.

Chapter 5

Characterization of *Komagataeibacter* isolate reveals new prospects on waste stream valorization for bacterial cellulose production

Abstract

Komagataeibacter spp. have been used for the bioconversion of industrial wastes and lignocellulosic biomasses to bacterial cellulose (BC). Interestingly, recent studies have demonstrated the capacity of *Komagataeibacter* spp. in the biotransformation of aromatic lignin-derived monomers (LDMs) and acetate. In general, detoxification and BC synthesis from lignocellulosic inhibitors requires a carbon flow from acetyl-coA towards tricarboxylic acid and gluconeogenesis, respectively. However, the molecular aspects related to such capacities have not been identified yet. In this study, we aimed to isolate a cellulose producing bacteria capable of synthesizing BC in a minimal medium containing crude glycerol, a by-product from biodiesel production process. The isolate, affiliated to *Komagataeibacter* genus, synthesized cellulose in MA/9 minimal medium containing glucose (3.3±0.3 g/L), pure glycerol (2.2±0.1 g/L) and crude glycerol (2.1±0.1 g/L). Genome assembly and annotation identified four copies of bacterial cellulose synthase operon and genes for redirecting the carbon from central metabolic pathway to gluconeogenesis. According to the genome annotations, a BC production route from acetyl-CoA, a central metabolic intermediate, was hypothesized and was validated using acetate. We identified that when *K. rhaeticus* ENS9b was grown in minimal medium supplemented with acetate, BC production was not observed. However, in presence of readily utilizable substrates, such as spent yeast hydrolysate, acetate contributed towards BC synthesis.

Introduction

Bacterial cellulose (BC), the nanofibrillar form of cellulose, is synthesized by bacteria of diverse genera, among which the most efficient cellulose producers are found in the genus *Komagataeibacter* (formerly *Acetobacter* and *Gluconacetobacter*). In general, BC biogenesis starts with the synthesis

of UDP-glucose (the actual building block) from the glycolytic pathway (via the catalytic activities of glucokinase, phosphoglucomutase and UDP-glucose pyrophosphorylase). BcsA, BcsB, BcsD, and BcsC proteins [encoded by the bacterial cellulose synthase (bcs) operon] catalyse the polymerization of UDP-glucose to β-1,4-glucan units, transport of the synthesized glucan chain through the periplasmic space, formation of crystalline regions and extracellular export of the synthesized polysaccharide, respectively (Römling, 2015).

BC is a versatile biopolymer with unique characteristics such as biodegradability, purity (not complexed with lignin, hemicellulose, or pectin) and superior material properties. Owing to these interesting material properties, BC is extensively studied for its use in various fields of applications (Wang, 2019; Mangayil, 2017 and Vuorinen, 2018). Despite of the versatile characteristics, studies to improve the production metrics and alternative carbons sources for BC production have been investigated (Vuorinen, 2018 and Thorat, 2018). To surpass the low production metrics, rational strategies to engineer the cellulose production machinery and optimize the carbon flow through the cellulose synthesis pathway have been conducted in *Komagataeibacter* spp. (Florea, 2016 and Kuo, 2015). By employing residual carbon sources from agriculture and industries, researchers have coupled BC production with strategic waste disposal. (Wu, 2019; Cavka,2013; Guo, 2013; Keshk, 2006 and Tsouko, 2015). For instance, Wu et al. (2019) reported a BC titre of ~1.5 g/L from *A. xylinum* using crude glycerol, a by-product of biodiesel production from kitchen waste (Wu, 2019). In a study from Leif Jönsson's group, BC production by *K. xylinus* ATCC 23770 was investigated in a medium containing 3-fold diluted detoxified spruce hydrolysate. The researchers identified that the BC production was absent in cultivation medium with non-detoxified hydrolysate. Detoxification with activated charcoal removed ~94% of furan aldehydes (hydroxymethyl furfural (HMF) and furfural) and ~60 – 70% of aliphatic acids (acetic acid and formic acid) from the spruce hydrolysate,

enabling *K. xylinus* ATCC 23770 to produce 8.2 g/L BC (Guo, 2013). However, in these mentioned studies the waste compounds were supplemented to rich growth medium containing other sources of carbon, restricting an exact elucidation of the substrate's contribution towards BC synthesis (Holwerda, 2012). Chemically defined media have been used to circumvent the requirement and influence of other carbon containing compounds in growth and BC production by *Komagataeibacter* spp (Yuste, 2000). I*n our recent study* a BC titer of 2.9±0.3 g/L was obtained from a *Komagataeibacter* isolate statically grown in MA/9 minimal medium containing crude glycerol (Mangayl, 2021).

In the present study, we report isolation, biochemical characterization, and phylogenetic analysis of a *Komagataeibacter* strain, isolated from Kombucha SCOBY (symbiotic colony of bacteria and yeast). The study progresses by comparing the strain's BC production metrics from glucose, pure glycerol and crude glycerol supplemented to both complex and minimal media. The genome of the strain was sequenced and assembled, and the genetic insights related to carbohydrate uptake mechanisms, BC biogenesis and gluconeogenesis are reported. Taking the genome insights, carbon redirection from pyruvate metabolism towards BC production, via acetate supplementation to complex medium and minimal medium, together with baker's yeast hydrolysate was investigated.

Materials and methods

Kombucha SCOBY (symbiotic colony of bacterial and yeast) was obtained from Sri Dhanvanthiri Probiotics Ltd, Kodaikanal, India (True Brew Kombucha tea). Sodium chloride, sodium molybdate, potassium chloride, di sodium hydrogen phosphate, dipotassium hydrogen phosphate, potassium dihydrogen phosphate, calcium carbonate, calcium chloride, magnesium sulphate, disodium hydrogen phosphate, citric acid, bromothymol blue and oxidase test disks (Product no: 70439) were purchased from Merck (Germany). Acetic acid and agar were purchased from Fisher Scientific (UK).

Glucose and casein amino acids were purchased from VWR International (Belgium). Tryptone, peptone and yeast extract were from Lab M Limited (UK). Ethanol was from Altia Oyj (Finland). Cycloheximide (Product no: C7698), and cellulase from *Trichoderma reesei* ATCC 26921 (Product no: C2730) was purchased from Sigma-Aldrich (USA). GeneJET Genomic DNA Purification Kit was purchased from Thermo Scientific (USA). Crude glycerol was generously provided by Perstrop AB (Sweden).

Isolation, culturing, and characterization of BC-producing isolates

Cellulose producing bacteria were isolated from Kombucha SCOBY of Indian origin (True Brew Kombucha, Sri Dhanvanthiri Probiotics Ltd, Kodaikanal, India). The SCOBY material was cut into small pieces using sterile scalpel and lysed in 50 ml 1X Phosphate Buffered Saline (PBS; g/L, 8 NaCl, 0.2 KCl, 1.44 Na_2HPO_4, and 0.24 KH_2PO_4; pH 7.4) containing 1% cellulase and incubated overnight (O/N) at 30°C and 180 rpm. Cycloheximide (100 g/L), a fungicide, was included in the isolation experiments in order to prevent the growth of yeast cells in the SCOBY material. The cells released from SCOBY were centrifuged at 1000g for 10 minutes at 4°C, washed thrice with sterile PBS, resuspended and serially diluted in the buffer. Presence of acetic acid bacteria was verified by plating aliquots on to Glucose-Yeast Extract-Calcium carbonate agar (GYC; g/L, 40 glucose, 10 yeast extract, 30 $CaCO_3$ and 15 agar) containing 100 g/L cycloheximide. Colonies around the $CaCO_3$ solubilization zones were individually picked, streaked on Hestrin–Schramm agar (HS-glucose agar; g/L, 5 peptone, 5 yeast extract, 2.7 Na_2HPO_4, 1.15 citric acid and 15 agar) containing glucose (20 g/L) and cycloheximide (100 g/L) and incubated at 30°C for 3-5 days. Single colonies from HS agar were inoculated to sterile 6-well culture plates (Argos Technologies, Cole-Parmer, US) containing HS medium and incubated at 30°C statically for 5 days. The cellulose pellicles synthesized at the air/liquid interface were subjected to lysis in 5 ml HS-glucose medium containing 0.5% cellulase and 100 g/L cycloheximide. The cell suspensions were washed in PBS and restreaked on

HS-glucose agar. Single colonies were further picked, and the enrichment was iterated for two more rounds. BC production in HS-glucose medium, colony and cell morphologies were routinely inspected in between each enrichment steps. The isolated colonies were preserved by resuspending the cells in 25% glycerol stocks and storing in -80°C freezer.

For biochemical characterization tests, the cells released from the BC pellicle, synthesized from static cultivation of the glycerol stock in HS-glucose medium, were used as the pre-inoculum. The characterization tests were conducted in MA/9 minimal medium (Santala, 2011) and peptone-yeast extract medium (PY; g/L, 3 peptone and 2 yeast extract) (Asai, 1958). Growth only in the presence of 30% glucose, 0.35% acetic acid, 3% ethanol, or 3% ethanol with 4% acetic acid, as well as acetate and lactate oxidation tests, and catalase test were conducted as described in Asai (1958). Presence of oxidase was tested using oxidase test disks as per manufacturer's instructions.

For strain identification by 16S rRNA gene sequencing, the genomic DNA (gDNA) was prepared, from the cells released from the BC pellicle, using GeneJET Genomic DNA Purification Kit as per manufacturer's instructions. Using the identification service offered by Macrogen (Netherlands), the 16S rRNA gene was amplified from the gDNA using primers 27F (AGAGTTTGATCMTGGCTCAG) and 1492R (TACGGYTACCTTGTTACGACTT) and sequenced with primer pairs 785F (GGATTAGATACCCTGGTA) and 907R (CCGTCAATTCMTTTRAGTTT). The 16S rRNA gene sequence can be found in the NCBI GenBank database under the accession number MT093993. Homology comparisons of the 16S rRNA gene were conducted using the nucleotide BLAST tool (Altschul, 1958) against the NCBI GenBank 16S rRNA gene sequence repository for *Komagataeibacter* (taxid:1434011). Multiple sequence alignment and evolutionary analysis against the 16S rRNA gene sequences of *Komagataeibacter* type strains were conducted using ClustalW (Thompson, 1994) and MEGA X using the Neighbor-Joining method with Kimura 2-parameter model (Kumar, 2018), respectively.

BC production

The BC production tests were conducted in HS and MA/9 minimal medium in 6-well culture plates containing 10ml of respective growth medium individually supplemented with 2% glucose, pure glycerol and crude glycerol statically incubated at 30°C for 10 days. The tests were conducted in duplicates. A substrate blank (i.e., cultivation without the studied carbon sources) was included to detect the effect of yeast extract and tryptone (in HS medium) and casein amino acids (in MA/9 medium) on BC production. Additionally, non-inoculated growth medium was included as the contamination control.

BC synthesis from acetate was studied by cultivating the cells in 50 ml tubes (Star Lab, Germany) containing 10 ml of either HS, MA/9 and M9 (MA/9 medium devoid of casein amino acids) medium and 10-mM and 50-mM acetate. Influence of other carbon sources on BC synthesis from acetate was tested by supplementing 2% sodium gluconate or 50% of baker's yeast hydrolysate (dry yeast purchased from local market) to MA/9 medium containing acetate. The pre-treatment of baker's yeast was performed using the method described in Luo (2020). The tests were conducted in duplicates in 6-well culture plates containing 10ml of culture medium. Growth medium devoid of acetate and cells were used as controls to monitor background BC production and contamination, respectively.

Purification of BC pellicles and dry weight measurements

The BC pellicles produced at the air/liquid interface were collected from the cultivation vessel. To eliminate the loosely bound cellulose fibrils, the BC pellicles were rinsed thoroughly with ultrapure water (Milli-Q, EMD Millipore, Germany). To remove the medium components and bacterial cells entrapped within the pellicle, BC was incubated in 0.5 M NaOH solution and ultrapure water at 60°C O/N. Following the treatments, the cellulose pellicles were washed thoroughly with ultrapure water until neutral pH was attained and oven dried O/N on pre-weighed 46 x 46 x 8 mm weighing boats (Heathrow

Scientific, USA) at 60°C. For acetate production tests in HS medium, BC pellicles were subjected to drying after collecting from the cultivation medium.

Amino acid utilization test

For amino acid utilization test, *K. rhaeticus* ENS9b pre-inoculum were prepared from static cultivation of cells in MA/9 medium containing 2% glucose. The pre-inoculum was inoculated to 96-well microtiter plate wells (initial OD_{600nm}, 0.1) individually containing 22 L-amino acids (alanine, arginine, asparagine, aspartic acid, cysteine, cystine, glutamic acid, glutamine, glycine, histidine, hydroxyproline, isoleucine, leucine, lysine, methionine, phenyl alanine, proline, serine, threonine, tryptophan, tyrosine and valine) as sole carbon source, with a final concentration of 20 mM (except for cystine and tyrosine for which the concentration was 10 mM due to low solubility) in M9 medium (total volume, 200µl/well). The tests included triplicates for each amino acid. M9 medium devoid of amino acid supplementation and *K. rhaeticus* ENS9b cells were included as experimental controls to monitor the background growth and contamination, respectively. The microtiter plates were incubated at 30°C for 8 days and the optical density measurements at 600nm (OD_{600nm}) were taken once every 24 hours.

Analytical techniques

Biomass was determined as optical density measurements at 600nm wavelength (OD_{600nm}) using a spectrophotometer (Ultraspec 500pro, Amersham Biosciences, UK). Substrate utilization, and liquid end metabolites were analysed using HPLC equipped with 300 mm × 8 mm Shodex SUGAR column (Phenomenex), SIL-20AC HT autosampler (Shimadzu), RID-10A refractive index detector (Shimadzu), and 0.01 M H_2SO_4 as the mobile phase. The HPLC samples were prepared as described in Salmela (2018) and the concentrations of carbon substrates and liquid fermentation metabolites were analysed using respective external standards. The BC dry weights were measured using analytical balance (ES 220A, Precisa, Switzerland). The

carbohydrate content in the baker's yeast hydrolysate was analysed using the phenol–sulfuric acid method described in Masuko (2005) and glucose standards (0.1 – 1mM).

Material characterization

BC films (oven-dried prepared from MA/9 medium) synthesized from each carbon source are designated as BC-glucose, BC-glycerol, BC-crude glycerol, BC-sHS and BC-YhMA/9. BC surfaces and cross-sectional images were analyzed using a scanning electron microscope (SEM; Zeiss ULTRAPlus, Germany).

The X-ray diffraction patterns of the dried BC films were analysed using a X-ray diffractometer (XRD; Empyrean multipurpose diffractometer, PANalytical B.V, US) as described previously (Mangayil et al. 2017). The degree of crystallinity was defined as the ratio between the sum of the [101], [10-1], and [002] peaks and the sum of the aforementioned and the amorphous peak. The values were obtained from a peak deconvolution study.

The thermal behavior of the BC films was determined using Thermogravimetric analyzer (TG 209 F3 Tarsus, Netzsch-Gerätebau GmbH, Germany). The weight loss from duplicate samples (size, 3.5–6.0 mg) were studied under N_2 atmosphere in 30 °C to 600 °C range at heating rate of 10 °C/min.

Genome sequencing, assembly and bioinformatics

K. rhaeticus ENS9b gDNA was extracted as mentioned previously (section Isolation, culturing and characterization of BC-producing isolates) and sequenced at Novogene Europe (Cambridge, UK) using Illumina Novaseq 6000. The raw reads were trimmed using Trimmomatic (Bolger et al., 2014) and *de novo* assembled into contigs by SPAdes (Bankevich, 2012) The contig scaffolding was conducted by SOPRA scaffold assembly tool at Galaxy Europe web platform (usegalaxy.eu; Galaxy Version 0.1) using the SPAdes contig assembly and the paired end Illumina sequencing data (Dayarian,

2010). The minimum contig length used in scaffold assembly was assigned as 200 bp. Misassemblies were identified using QUAST (5.0.2) (Gurevich, 2013). Contig reordering, missassembly correction and gap filling were conducted using GFinisher with *K. rhaeticus* iGEM genome (GenBank accession number, LT575493.1) as the reference sequence (Guizelini et al., 2016) and the genome quality was assessed again using QUAST. The genome was annotated using Prokka (Seeman, 2014). The genome completeness was analyzed using the CheckM plugin in the KBase web platform (Parks, 2015 and Arkin, 2018). Functional annotation was conducted through the KEGG Automatic Annotation Server (https://www.genome.jp/kaas-bin/kaas_main, accessed on 10.09.2020) (Moriya, 2007). Proteins associated with cellulose synthesis, substrate catabolism, and gluconeogenesis were identified either through manual search within the Prokka annotated GenBank file using Unipro UGENE software (v. 33.0) (Okonechnikov et al., 2012). For functional analysis of the annotated proteins and domain predictions, the query amino acid sequences were searched against NCBI's conserved domain database (CDD) and InterProScan signatures (Marchler-Bauer et al., 2015; Zdobnov & Apweiler, 2001). Plasmids in the raw sequencing reads and the assembled contigs were identified using plasmidSPAdes (Antipov, 2016) and Recycler, respectively (Rozov, 2016). Genome coverage was estimated using Bowtie2 (Langmead, 2012). The origin of replication (oriC) was predicted using Ori-finder tool (http://tubic.org/Ori-Finder/; accessed on 05.08.2020) (F. Gao & Zhang, 2008). For rRNAs and tRNA prediction, a homology search was conducted using RNAmmer (Lagese, 2007) and tRNAscan-SE (Lowe, 2016) tools at the RNAspace (v1.2.1, rnaspace.org, accessed on 28.08.2020) web environment (Cros, 2011).

The chromosome sequence of *K. rhaeticus* ENS9b can be found in the NCBI GenBank under the accession number CP061369 and the plasmids at CP061370 (p9b_1), CP061371 (p9b_2), CP061372 (p9b_3), CP061373 (p9b_4) and CP061374 (p9b_5).

Results

Characterization and classification of the cellulose producing isolate

Colony isolation from $CaCO_3$ solubilized zones and iterated streaking of cells from BC pellicles on HS-glucose agar resulted in the enrichment of small, irregularly edged, white coloured smooth colonies (Fig. S1A). Prolonged incubation resulted in the appearance of a white mass on the colony tip changing the morphology to pulvinated colonies which were difficult to pick using an inoculation loop. The isolate, hereafter designated at ENS9b, appeared as rod-shaped cells either singularly, in pairs or in chains with a cell size of 2.6–4.5 µm * 0.6–0.7 µm (Fig. S1B).

Phylogenetic analysis using the ENS9b 16S rRNA gene against the *Komagataeibacter* type strains positioned the isolate among *K. rhaeticus* with a 99% similarity towards *K. rhaeticus* DST GL02^T (Fig. 1).

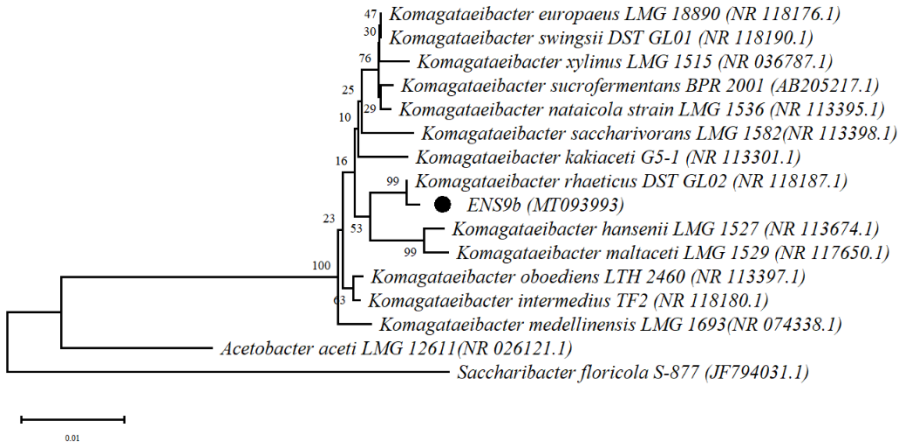

***Figure 1**: Phylogenetic relationship of ENS9b and Komagataeibacter type strains. The 16S rRNA gene tree was rooted using Saccharibacter floricola S-877^T and Acetobacter aceti LMG 12611^T. The position of ENS9b in the phylogenetic tree is highlighted with a dot. NCBI accession numbers are provided in parenthesis.*

To restrict the influence of peptone and yeast extract on the isolate's growth, the biochemical characterization tests were initially conducted in MA/9 minimal medium. However, the isolate grew well with 30% glucose but poorly with 0.35% acetic acid, 3% ethanol and 3% ethanol and 4% acetic acid as sole carbon sources in MA/9 medium, similarly to what observed from a related species (Mangayil, 2021). Thus, the characterization tests were conducted in PY medium (Asai, 1958). For cultivations in 3% ethanol and 4% acetic acid, the medium pH remained stable until day 11 with a slight drop thereafter (Fig. S2). Growth in the presence of 0.35% acetic acid did not reveal any major changes in the medium pH trend (Fig. S2). However, the capacity of ENS9b to metabolize acetic acid was confirmed by the formation of BC pellicles and its absence in the control cultivation (PY medium without 0.35% acetic acid or 3% ethanol, Fig. S3). Similar to other *Komagataeibacter* spp., *K. rhaeticus* ENS9b showed positive and negative results for catalase and oxidase tests, respectively, did not require acetic acid for growth, oxidized acetate and lactate in PY medium and demonstrated acetic acid overoxidation (Fig. S4) (Marič,2020 and Senjonovs, 2017).

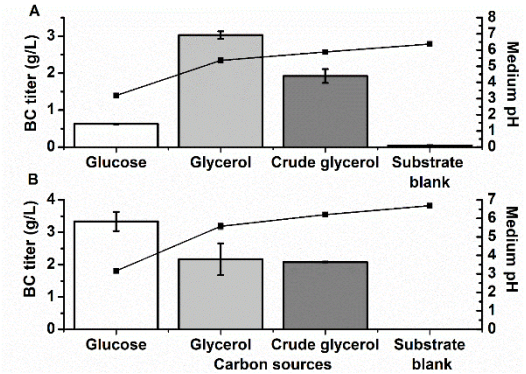

Figure 2: *BC production (bars), and pH (line) plots from static cultivations in (A) HS and (B) MA/9 growth medium supplemented with 2% glucose, pure glycerol and crude glycerol (MA/9). Substrate blank was included to identify the contribution of medium components (yeast extract and peptone and casein amino acids in HS medium and MA/9 medium, respectively) towards BC production. The data points represent mean experimental results and standard deviations from duplicate cultivations. In some cases, the error bars are smaller than the symbol.*

Bacterial cellulose production in rich and minimal growth medium

The BC production and pH profiles from cultivations in HS medium with respective carbon sources are presented in Figure 2A. When grown in HS medium, *K. rhaeticus* ENS9b produced the highest BC titer (and yield) in the medium containing pure glycerol [3.0±0.1 g/L and 1.5 mg/$g_{substrate}$], utilizing 55±0.5% of the substrate. With crude glycerol as the substrate, the strain utilized 48% of the carbon source, producing 1.9±0.2 g/L BC (0.9 mg/$g_{substrate}$). After the 10-day cultivation period, *K. rhaeticus* ENS9b completely utilized the supplemented glucose albeit producing only 0.6±0.0 g/L BC and gluconic acid as the main liquid end-metabolite (14.5±0.3 g/L, corresponding to 74% of the initial glucose concentration). Nevertheless, HS medium containing other carbon containing compounds, such as yeast extract and tryptone, can contribute towards biomass and background BC production. In substrate blank cultivation, *K. rhaeticus* ENS9b produced 0.05±0.0 g/L BC. In contrast to HS medium, BC production was not observed from cultivations in MA/9 medium devoid of studied carbon sources (substrate blank). Growth in MA/9-glucose medium improved BC synthesis (3.3±0.3 g/L and 1.7 mg/$g_{substrate}$) and reduced gluconate generation (7.2±0.2 g/L, corresponding to 35% of initial substrate concentration). With pure and crude glycerol as the sole carbon sources, *K. rhaeticus* ENS9b utilized 72% of the supplemented substrate synthesizing 2.2±0.1 and 2.1±0.1 g/L of BC (~1.0 mg BC/$g_{substrate}$), respectively.

BC film characterization

The surface and cross-sections as well as the results of XRD and thermogravimetric analyses (TGA) of BC films synthesized by *K. rhaeticus* ENS9b grown in MA/9 medium with 2% glucose, pure glycerol and crude glycerol are shown in Figure 3. The surface and cross-sections of BC synthesized from different carbon sources (Fig. 3A) demonstrated the cellulose fibrils to contain the general crisscross network with ordered interconnected layers of BC pellicles.

The XRD analysis of BC films synthesized by *K. rhaeticus* ENS9b grown in MA/9 medium with 2% glucose, pure glycerol and crude glycerol are shown in Figure 3B. Consistent with a previous reports (Lu, 2020), the diffractograms revealed two dominant peaks between 14.6° to 17.0°, and between 22.8° to 25.1° representing the cellulose I allomorphs Iα and Iβ, respectively. Though with low intensities and asymmetric shapes, amorphous regions in BC-glucose, BC-pure glycerol and BC-crude glycerol were identified at peaks 21.6°, 21.1° and 20.3°, respectively. Peak height method (or Segal method) is the widely accepted method to calculate BC crystallinity indices (Vasquez, 2013). However, for uniformity with our previous study (Mangayil, 2017 and 2021) and comprehensive assessment using both amorphous and crystalline regions, the CI values in this study were calculated using a peak deconvolution method (Park et al., 2010). The CI values of BC films produced from glucose, pure and crude glycerol were 87±13%, 89±10% and 96±2%, respectively.

The results from thermogravimetric analysis (TGA) of BC films are presented in Figure 3C. The mass losses were observed in three stages. At the first stage (30°C to 120°C), a primary mass loss due to moisture removal was observed as 5%, 5% and 3.6% for BC-glucose, BC-pure glycerol and BC-crude glycerol, respectively. The second phase, i.e. destruction of crystalline regions and decomposition of the cellulose into glucopyranose monomers, leading to a sharp weight loss was observed at temperatures between 250°C - 360°C. During this phase, BC-glucose, BC-pure glycerol and BC-crude glycerol demonstrated a major mass loss of 59%, 64% and 69%, respectively, at onset temperature ranging from 280°C – 299°C. Though the mass loss values varied

slightly, the residual mass (%) of the tested BC films remained in the ranges of 27% – 29%.

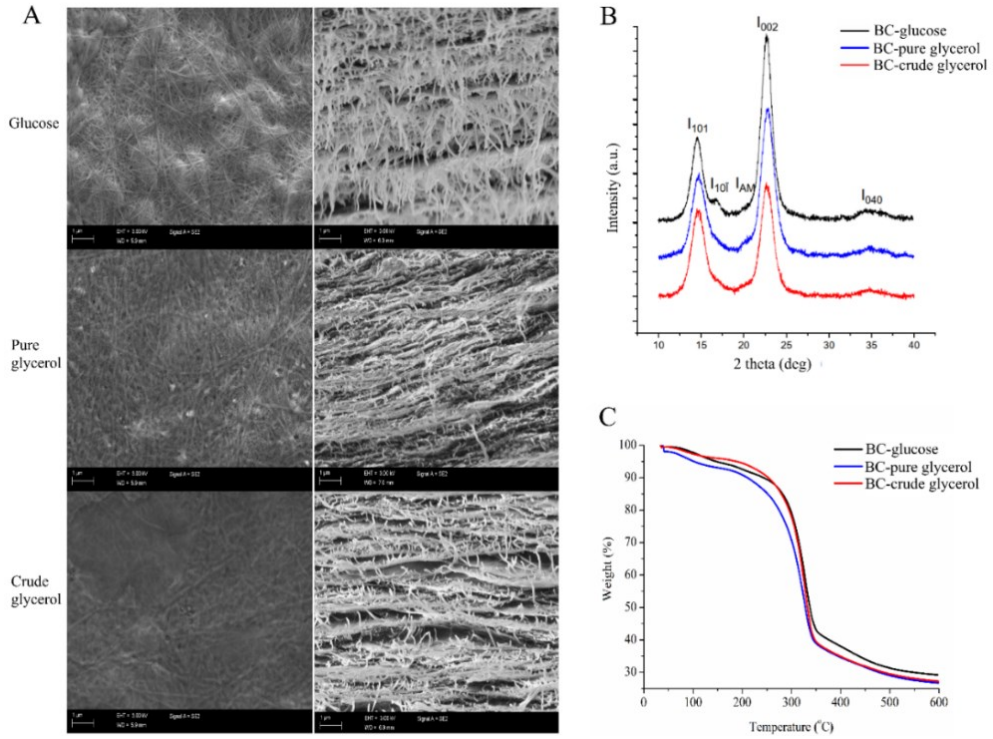

***Figure 3**: BC film characterization. (A) SEM surface and cross-sectional images, (B) XRD diffractograms and (C) thermogravimetric analysis (TGA) of BC films synthesized from MA/9 medium containing 2% glucose (BC-glucose), pure glycerol (BC-pure glycerol) and crude glycerol (BC-crude glycerol). The diffraction peaks (subfigure B) at I101 and I10ī, I002 and I040, and IAM represents the crystalline Iα, Iβ and amorphous regions.*

The assembly statistics and general features of *K. rhaeticus* ENS9b genome is presented in Table S1. The genome map and functional categorization of the gene annotations to KEGG orthology are presented in Figure 4. According to the functional analysis (KEGG classifications and InterProScan), manual search and amino acid alignments (BlastP), and domain predictions (CDD), genes encoding for proteins involved in carbohydrate uptake and metabolism, bacterial cellulose synthesis, and gluconeogenesis from central metabolic pathway were identified from the genome. The genomic positions of genes encoding for the mentioned enzymes and the respective amino acid sequences are presented, in the order, in the Supplementary material.

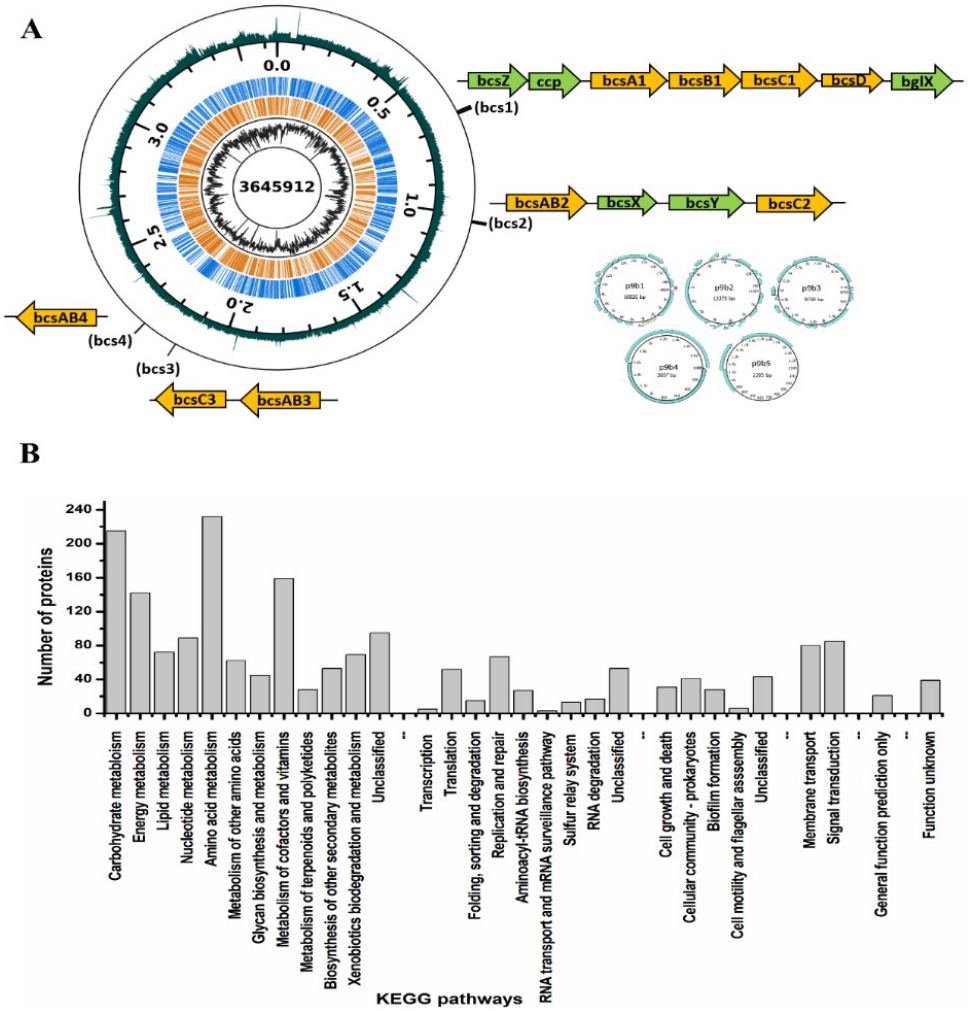

***Figure 4**: Overview of K. rhaeticus ENS9b genome. (A) Genome map. The K. rhaeticus ENS9b genome totals 3.69Mbp (GC% of 63.05%), containing 3360 protein-coding gene predictions, 3 rRNAs, 1 tmRNA, 46 tRNAs and 3 non coding RNAs. A genome completeness of 100% was identified from CheckM. The genome consists of a chromosome of 3.65 Mbp (3302 predicted protein-coding regions) and at least 5 plasmids; p9b1 (18.8 Kbp), p9b2 (13.4 Kbp), p9b3 (9.8 Kbp), p9b4 (3 Kbp) and p9b5 (2.3 Kbp) (A inset). Seven contigs (totalling 90Kbp) could not be confidently placed in the genome. The displayed data from centre to perimeter are: chromosome size (bp), GC-percentage, CDSs on the reverse strand (in the middle, orange), CDSs on the forward strand (in the middle, blue), chromosome position (major ticks 500 kbp, minor ticks 100 kbp), and coverage (outermost). Both GC-percentage and coverage were calculated with 1 kbp window size. GC-percentage ranged from 33.6 % to 75.5 % and coverage (number of reads mapping to the locus) from 380 to 49600. Coverage is displayed with logarithmic scaling. The bcs operon (orange filled arrows) and the flanking accessory genes (green filled arrows) indicated in the manually curated figures directs to its position in the genome. (B) KEGG classification and functional categorization.*

BC biogenesis machineries: *K. rhaeticus* ENS9b genome contained four copies of bcs operon. The complete bcs operon (bcs1, 9100 bp) comprising of individual physically adjacent bcsA1, bcsB1, bcsC1 and bcsD genes, in the order, was identified at genomic position 666919:676019 bp. The gene cluster was flanked by accessory genes, bcsZ (genomic position 664722:665759 bp), ccpAx (genomic position 665756:666736 bp) and bglX (genomic position 676251:678452 bp) encoding for β-1,4-glucanase, cellulose complementing factor protein, and β-glucosidase, respectively. An additional copy of bglX gene (bglX2) was identified at genomic position 522700:524739 bp. A second bcs operon (bcs2) comprising of a gene fusion encoding for the catalytic and regulatory subunits, bcsAB2, and bcsC2 genes was identified at genomic position 1020008:1030553 bp. The third (at genomic position 2136184:2144443 bp) and fourth (at genomic position 2248494:2253065 bp) bcs clusters were arranged in complement in the genome and comprised of bcsAB3 and bcsC3, and bcsAB4 genes, respectively, and were not flanked with accessory genes associated with BC assembly/production

Predicted genes involved in carbohydrate uptake and metabolism: In the *K. rhaeticus* ENS9b genome annotations, 7 genes that encodes for putative carbohydrate-selective porins of porin B (OprB) family were identified. Additionally, three copies of aquaporin Z, a major bacterial protein involved in water and glycerol diffusion across the cell membrane was identified from the genome. Similar to other *Komagataeibacter* spp., an incomplete glycolytic pathway, due to the lack of phosphofructokinase, was observed from *K. rhaeticus* ENS9b genome (Liu, 2018 and Zhang, 2017). Thus, glucose oxidation occurs through pentose phosphate pathway (PPP) and Entner – Duodoroff pathway (EDP) via gluconate as the intermediate (catalysed by quinoprotein glucose dehydrogenases, genes found at 1924182 :1926572 and 2594170:2596791 bp). For glycerol metabolism, genes encoding for glycerol uptake facilitator protein (at positions 1285133:1285972 bp), glycerol kinases (1286008:1287507 bp and 1389048:1390547 bp), glycerol

dehydrogenases (1201435:1203437 and 1673449:1676036 bp), dihydroxyacetone kinase (1848749:1850380 bp) and triosephosphate isomerase (2116868:2117611 bp) entering into the gluconeogenetic, and central metabolic pathways were identified from the genome.

Putative genes encoding for enzymes involved in redirecting the carbon from Krebs cycle: Indications of BC biogenesis from acetate and putative genes responsible in redirecting the carbon from Krebs cycle towards gluconeogenesis in *K. rhaeticus* isolate was identified in our previous study (Mangayil, 2021). Similar to our finding, *K. rhaeticus* ENS9b genome lacked the genes encoding for pyruvate synthase (acetyl-CoA to pyruvate) and phosphoenolpyruvate carboxykinase (oxaloaceticacid to phosphoenolpyruvate). However, the genome contained annotations for genes encoding NAD-dependent malic enzyme (catalysing reversible malate to pyruvate reaction) and pyruvate phosphate dikinase (pyruvate to phosphoenol pyruvate).

BC production from acetate

To validate the catalytic activities of *in silico* predicted enzymes involved in gluconeogenesis and corroborate growth and BC production from acetyl-CoA, central compound linking the Krebs and gluconeogenetic pathways, *K. rhaeticus* ENS9b was grown in presence of acetate.

Acetate utilization and BC production was tested in PY, HS, MA/9 and M9 medium containing 10-mM and 50-mM acetate (Table 1). In PY medium, BC, observed as cellulose fibrils, were produced in both control (devoid of acetate) and sample cultivations. However, due to the absence of an intact pellicle, the fibrils could not be effectively separated from the culture medium for quantification (Fig. S5). At the end of the cultivation in PY-10-mM medium, the strain utilized 78±5% acetate. However, growth in PY-50-mM medium resulted in an increase in acetate concentration (61±7-mM). In the control cultivation without acetate, the strain produced 3.5-mM acetate.

Table 1. Biomass, BC production and acetate utilization from static growth in PY, HS, MA/9 and M9 medium containing 10-mM and 50-mM acetate				
Growth medium	Carbon containing compounds	BC production	OD_{600nm}	Endpoint acetate concentration (mM) and percentage utilized (%)
PY	2 g/L YE	Very loose pellicles. Could not be quantified.	1.4	3.5-mM
	2 g/L YE+10-mM acetate	Loose pellicles. Could not be quantified.	1.5±0.2	1.9±0.7 (78±5.4%)
	2 g/L YE+50-mM acetate	Loose pellicles. Could not be quantified.	1.8±0.4	61.2±7.8 (Higher than initially supplemented)
HS[1]	5 g/L YE	7 mg	Cells within the pellicle. Did not quantify.	ND
	5 g/L YE+10-mM acetate	17±4.5 mg	Cells within the pellicle. Did not quantify.	2.5±2.0 (74±29.4%)
	5 g/L YE+50-mM acetate	20±0.9 mg	Cells within the pellicle. Did not quantify.	34.6±4.9 (33±9.4%)
MA/9	-	ND	0.8	ND
	10-mM acetate	ND	1.4±0.2	0.9±0.0 (91.5±1.5%)
	50-mM acetate	ND	1.5±0.1	7.5±3.5 (79±7.8%)
M9	-	ND	0.1	ND
	10-mM acetate	ND	0.5±0.1	0.4±0.0 (95.3±0.2%)
	50-mM acetate	ND	0.9±0.1	2.2±1.5 (98.2±3.6%)

[1] Due to the fragile nature of the BC pellicles produced from the control cultivation, the pellicles were not subjected to alkali and MQ wash. The pellicles from the cultivation vessel were collected and oven-dried at 60°C. For comparison, the pellicles synthesized from HS containing 10-mM and 50-mM acetate were treated similarly. These pellicles can contain medium components that may alter the titers. Thus, the dried weights of untreated pellicles are presented.

After 14 days of static incubation in HS medium without acetate supplementation, *K. rhaeticus* ENS9b produced 7 mg of fragile BC pellicles (Fig. S6). As the pellicles were fragile, they were not subjected to alkali and MQ washes, rather oven-dried soon after collecting from the cultivation vessel. Supplementation of 10-mM and 50-mM acetate to HS medium resulted in intact pellicles. In HS medium containing 10-mM and 50-mM acetate, the *K. rhaeticus* cells synthesized 17±4.5 mg and 20±0.9 mg BC, respectively (Table 1). The BC pellicle weights from each replicate cultivations are presented in Fig. S6C. In M9 medium containing 10-mM and 50-mM acetate, cell growth was observed without BC synthesis (Table 1). Similar to M9 medium, BC synthesis was not observed in MA/9 cultivations. Nevertheless, supplementation of casein amino acids in MA/9 medium resulted in ~2-9-fold increase in OD_{600nm} values. Amino acid utilization test was conducted to study the influence of individual L-amino acids on *K. rhaeticus* growth in M9 medium. The cells could utilize L-alanine, L-arginine, L-asparagine, L-aspartic acid, L-glutamine, L-glutamic acid and L-proline as sole carbon sources for biomass formation (Fig. 5).

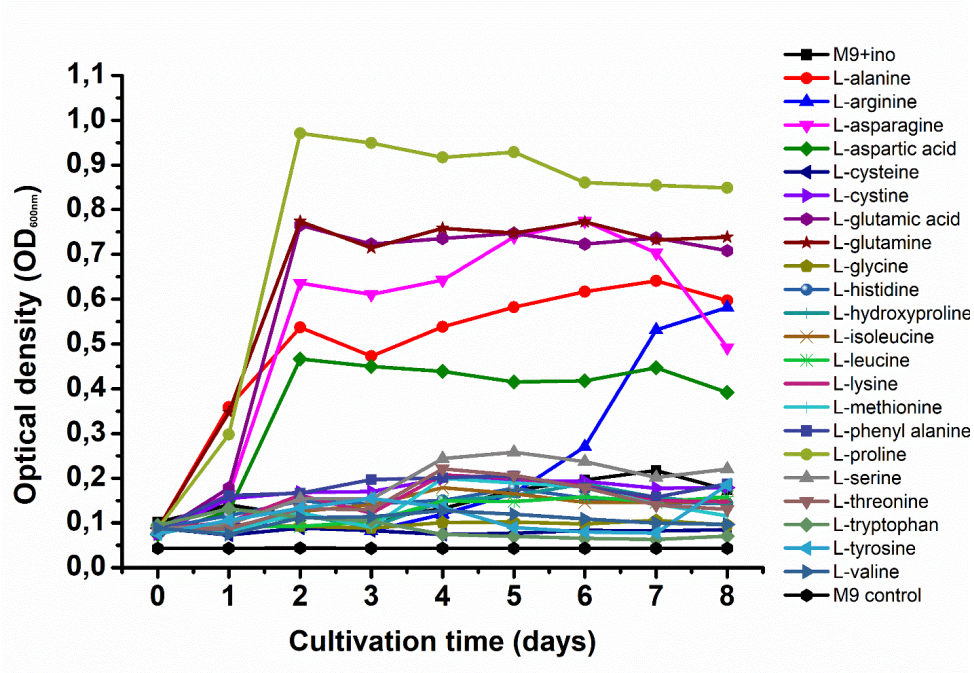

Figure 5*. Amino acid utilization profile of K. rhaeticus ENS9b cells grown in M9 medium individually containing 22 L-amino acids. The test was conducted in 96-well microtiter plate wells containing a total volume of 200µl/well. The experimental controls included M9 medium containing cells but devoid of amino acid supplementation (M9+ino control) and M9 medium devoid of cells and amino acids (M9 control). The microtiter plates were incubated at 30°C for 8 days and the OD_{600nm} measurements were taken once every 24 hours. The presented data is the averaged value obtained from triplicate cultivations. The error bars are not included for clarity.*

In comparison to the control cultivation, an improvement in BC production was observed from K. rhaeticus ENS9b cells grown in HS medium containing acetate. However, in a medium devoid of readily metabolizable substrates the carbon in acetate was directed towards biomass formation (Table 1). Taking these cues, we studied the effect of baker's yeast hydrolysate supplementation in MA/9 medium (YhMA/9) on BC production from acetate. HS and simulated HS media (sHS), i.e. HS medium with 50% of baker's yeast hydrolysate and 0.2% casein amino acids to replace the yeast extract and casein amino acids, respectively, were used as the experimental control (Fig. S7 A). Figure 7 presents the BC titers from acetate supplementation to HS, sHS and YhMA/9 media. In the cultivation media devoid of acetate, K. rhaeticus ENS9b cells synthesized BC from the control cultivations. In comparison to HS medium, the BC production was higher in sHS and YhMA/9 media attributing it towards the inclusion of 50% baker's yeast hydrolysate. The phenol-sulfuric acid test indicated a total carbohydrate content in HS (contributed by yeast extract) and sHS (from 50% of baker's yeast hydrolysate) medium as 7.7-mM and 76-mM, respectively. The results presented in Fig. 6 clearly distinguishes the improvement in BC production

from acetate supplemented media. However, only the cultivations YhMA/9 – acetate media demonstrated statistically significant ($p < 0.05$, Two-sample t-test) titers. Deducting the contribution of yeast extract and baker's yeast hydrolysate in respective medium, BC titers of 15 – 25 mg/L, 75 – 227 mg/L and 197 – 327 mg/L were obtained from acetate supplemented HS, sHS and YhMA/9 media.

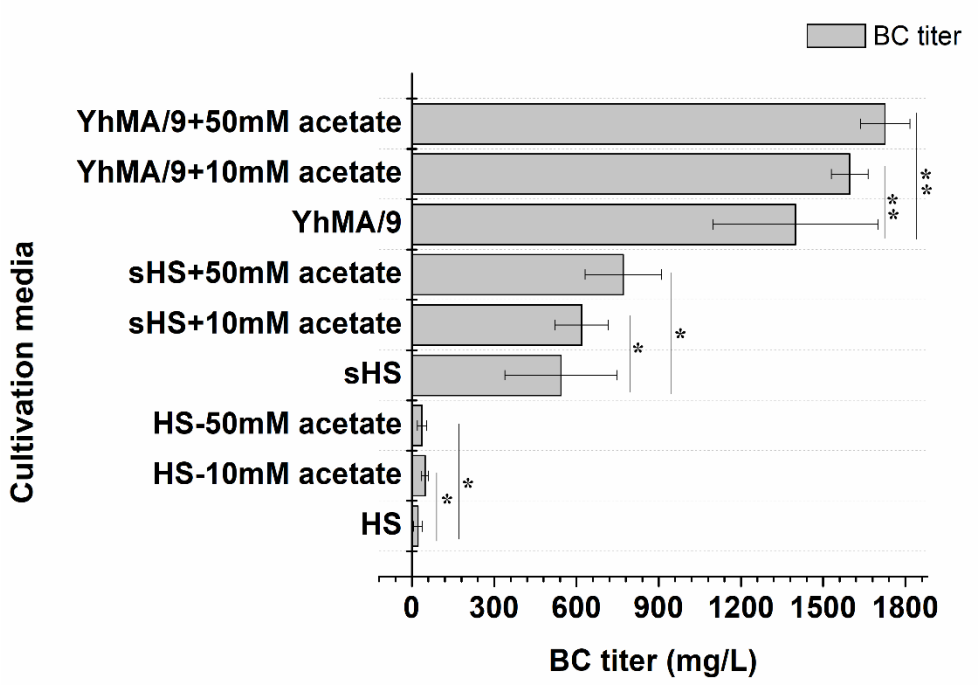

Figure 6. *BC production of K. rhaeticus ENS9b cells in control and sample cultivations containing 10-mM and 50-mM acetate in HS, sHS and YhMA/9 media. The presented results are the averaged values (duplicates for control cultivations and triplicates for media with acetate) and the error bars represent the standard deviations. Two sample t-test with equal variances using the log10 transformed values were implemented for the comparisons between the control and sample cultivations. Samples with $p > 0.05$ and $p < 0.05$ are represented by * and **, respectively.*

SEM, XRD and TGA characterization of BC films produced from acetate supplemented sHS and YhMA/9 medium are shown in Fig. S8. Consistent with the prior results (section BC film characterization), peaks representing cellulose I allomorphs (Iα and Iβ) and amorphous regions were identified at 14.7°, 16.9° and 22.2°, respectively. The peak deconvolution study identified the CI values from BC-sHS and BC-YhMA/9 as 94% and 92%, respectively. TGA analysis indicates a similar mass loss trend among the BC films, with a residual mass of ~28%.

Discussion

BC is a versatile biopolymer synthesized by bacteria that require mild conditions, simple growth medium and can utilize wide ranges of substrates for growth. *Komagataeibacter* strains have been investigated for its growth and BC production capacities from conventional sugars, industrial wastes and detoxified lignocellulosic biomass. Glucose is an excellent carbon source for BC production, as it is easily transported into the cell and is efficiently incorporated into the cellulose biosynthetic pathway. *Komagataeibacter* spp. lacks phosphofructokinase incompleting the glycolytic pathway. Glucose oxidation in *Komagataeibacter* spp. occurs in two routes, via glucose-6-phosphate (entering into PPP) and through gluconate generation which is exported extracellularly (or directly oxidized into the medium by surface exposed gdh). In addition to drop in the medium pH, gluconate synthesis reduces the glucose availability for BC biosynthesis (Mangayil, 2017, Kuo, 2015, Mangayil, 2021). The improved production titer (3.3±0.3 g/L BC) and reduced gluconic acid generation (7.2±0.2 g/L) from MA/9 cultivations can be attributed to the buffering capacity in the growth medium (Kuo, 2014). Additionally, the presence of essential macro and micronutrients in the original MA/9 medium composition, may positively contribute in bacterial growth and cellular metabolism (De Souza, 2019). The obtained BC titers from MA/9 medium are comparable to the previously published results from minimal media. For instance, Forng et al. (1989) reported a modest BC titer of 0.1 g/L from *A. xylinum* static cultivations (Forng, 1989). In another study, de Souza et al. (2019) reported a titer of 0.22 g BC from *K. hansenii* ATCC 23769 grown in 10 ml of minimal medium containing glucose (De Souza, 2019). Recently, using a *Komagataeibacter* isolate cultivated in similar conditions and 20 g/L glucose as the carbon source we reported a titer of 2.2 ± 0.1 g/L BC (Mangayil, 2021). In contrast to glucose cultivations in this study, glycerol as the growth substrate demonstrated an improved substrate utilization (HS medium, 55±0.5% and MA/9 medium, 72±4%), albeit with a slight drop in BC production titer (HS medium, 3.0±0.1 g/L; MA/9 medium, 2.2±0.1 g/L BC). BC synthesis

is regulated by the enzymatic activities of diguanylate cyclase, phosphodiesterase, UDP-glucose pyrophosphorylase, and bcs operon, that are in-turn regulated by the physiological conditions in which the bacterium is cultivated. When *Komagataeibacter* spp. are grown in minimal medium, the rate-limiting step for BC biogenesis is partly determined by the carbon source of choice. In case of glycerol, reduced carbon flux towards gluconeogenesis route could be attributed towards the production metrics (Ross, 1991).

In industrial point of view, it is reported that a BC titer of 15 g/L in 50 hours (productivity, 0.3 g/L/h) is required to match to the production efficiency of plant cellulose (Zhong, 2020). Thus far, the highest volumetric yield (15 g/L BC in 7 days) has been reported from a *Komagataeibacter* isolate cultivated in HS medium containing 4% glucose and 1.4% ethanol as the inducer (Son, 2001). However, utilization of conventional sugars and inducing compounds hinders the production costs and scale-up. Integrating waste valorization with cellulose production is one way to upscale the production processes. Agricultural and industrial waste residues, to name a few, citrus pulp waste, distillery wastewater, crude glycerol, fermentation by-products and detoxified lignocellulosic hydrolysates have been employed as alternative carbon and nitrogen sources for BC production, with titers ranging from 1 – 13 g/L in 2 – 15 cultivation days (Velásquez-Riaño, 2017, Cao, 2018 and Kongruang 2008). A recent study reported the production of 12 – 16 g/L BC from lignocellulosic biomass hydrolysates using *K. xylinus* ATCC 53524 statically grown in a medium containing 50 g/L glucose and 20 g/L corn steep liquor. Identification of respective enzymes involved in LDM biotransformation could pave way to exciting biotechnological prospects. Nevertheless, for BC synthesis from LDM catabolism, the carbon needs to be redirected from acetyl-coA towards gluconeogenesis. Initial observations of BC formation from acetate was observed from the biochemical characterization tests. In *Komagataeibacter* spp., acetyl-coA synthetase converts acetate to acetyl-coA, thereby entering into the TCA cycle. Hypothesizing that *Komagataeibacter* spp. can route the carbon from TCA cycle to gluconeogenesis as described previously for

Escherichia coli, acetate was used for the proof-of-concept study (Sauer & Eikmanns, 2005). Acetate is generally used as an inducer compound to augment BC production (Kuo, 2016). Wang et al., (2018) observed that *Komagataeibacter* sp. W1 strain could synthesize fragile BC pellicles (~70 mg) from HS medium containing 20 g/L of acetate. Our tests identified that availability of other carbon compounds was crucial to generate thick BC pellicles. In the absence of readily utilizable carbon, acetate was utilized for biomass formation (Table 1; MA/9 and M9). Employing baker's yeast hydrolysate as the alternative carbon source in MA/9 medium improved the BC titer from acetate. Future work will investigate the applicability of spent yeast hydrolysates on BC synthesis, bioprocess optimization using statistical design models and adapted laboratory evolution of the *K. rhaeticus* strain on LDMs.

Supplementary Materials

Supplementary figures

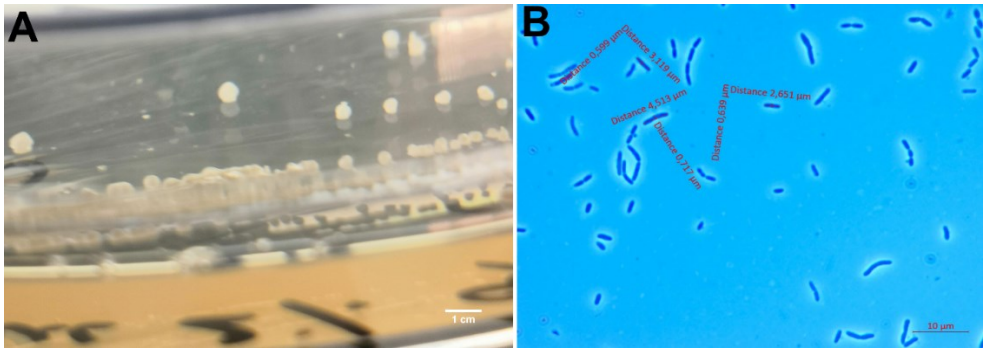

***Figure S1**: (A) Colony and (B) cell morphologies of ENS9b. The images were cropped and brightness and contrast were adjusted to improve clarity*

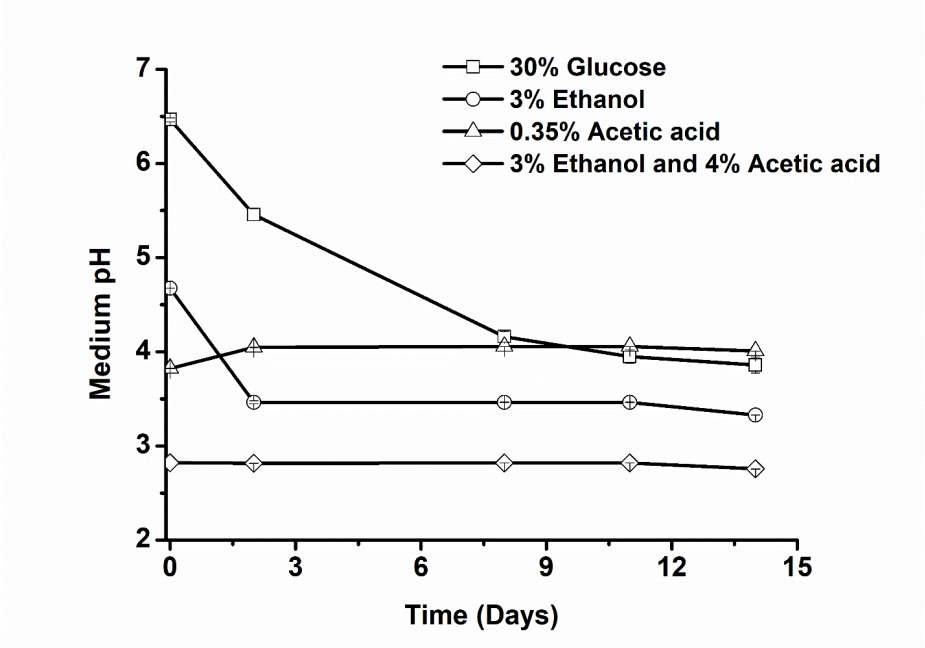

***Figure S2**: pH changes during cultivations in MA/9 containing 30% glucose and PY medium containing 3% ethanol, 0.35% acetic acid, 3% ethanol and 4% acetic acid. The cultivations were conducted at 30°C and 230 rpm for 14 days. Averaged values and standard deviations from duplicate cultivations are presented. In some cases, the error bars are smaller than the symbol*

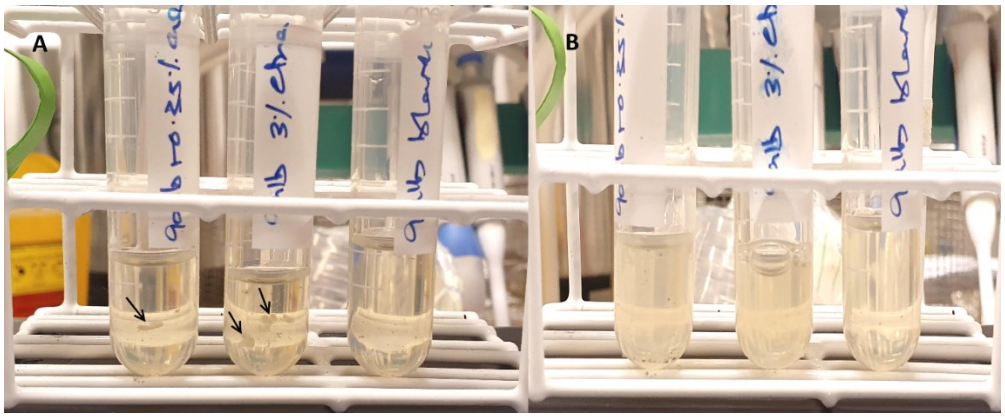

***Figure S3**. BC pellicle formation in PY medium containing 0.35% acetic acid, 3% ethanol and 4% acetic acid (A). Verification of BC pellicle, produced after 14-day cultivation in PY medium individually containing the above-mentioned carbons sources, were conducted using 1% cellulase. Lysis of BC pellicle and release of cells after the cellulase treatment is shown in B. The images were cropped and brightness and contrast were adjusted to improve clarity.*

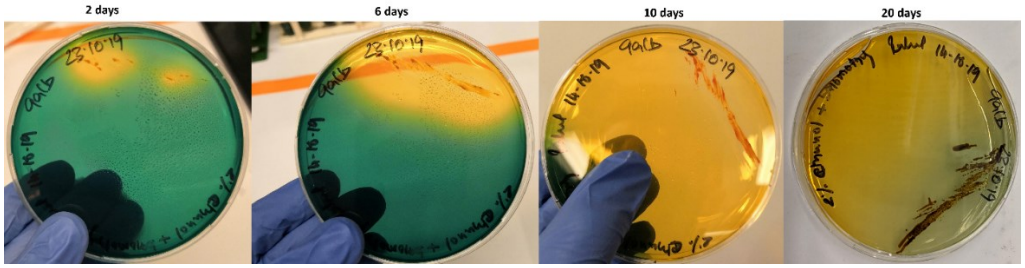

***Figure S4:** Overoxidation of acetic acid by ENS9B. Single colonies were streaked onto PY medium containing 2% ethanol and 0.0002% bromothymol blue as the pH indicator. Figures (from left to right) shows the acidification (blue to yellow coloration) and neutralization (yellow to blue) of PY agar during 2, 6, 10 and 20 days of incubation at 30°C. The images were cropped and brightness and contrast were adjusted to improve clarity.*

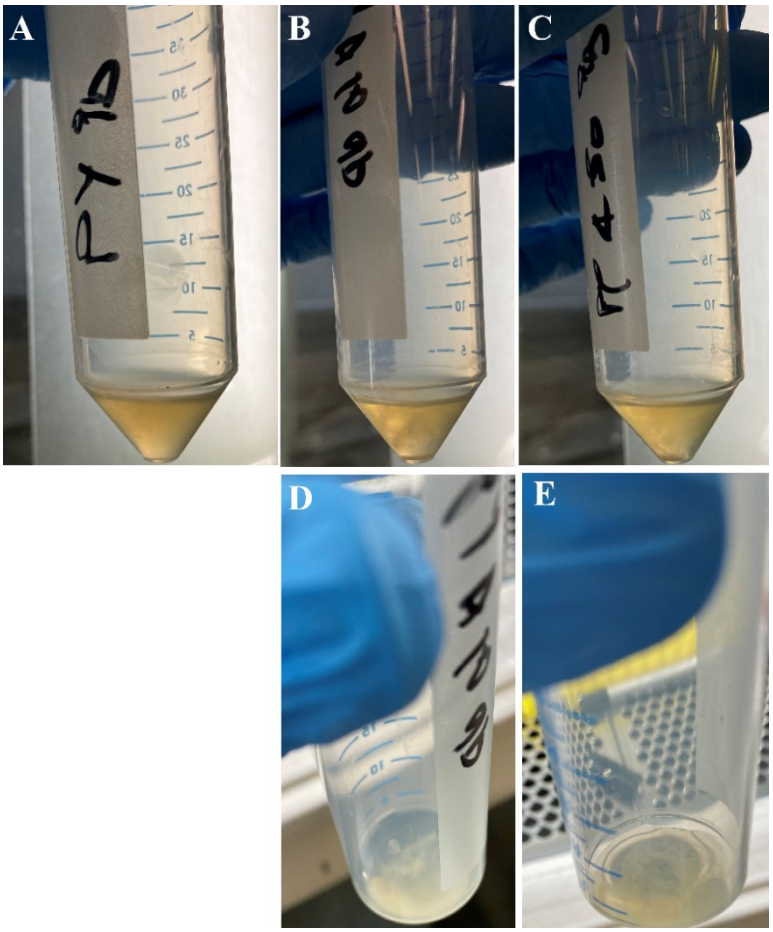

***Figure S5**: BC pellicle production by K. rhaeticus ENS9b cells statically grown in 50-ml tubes containing 10 ml (A) PY substrate control (i.e. devoid of acetate), (B) PY medium supplemented with 10-mM acetate and (C) PY medium supplemented with 50-mM acetate for 14 days at 30°C. The images were cropped and brightness and contrast were adjusted to improve clarity.*

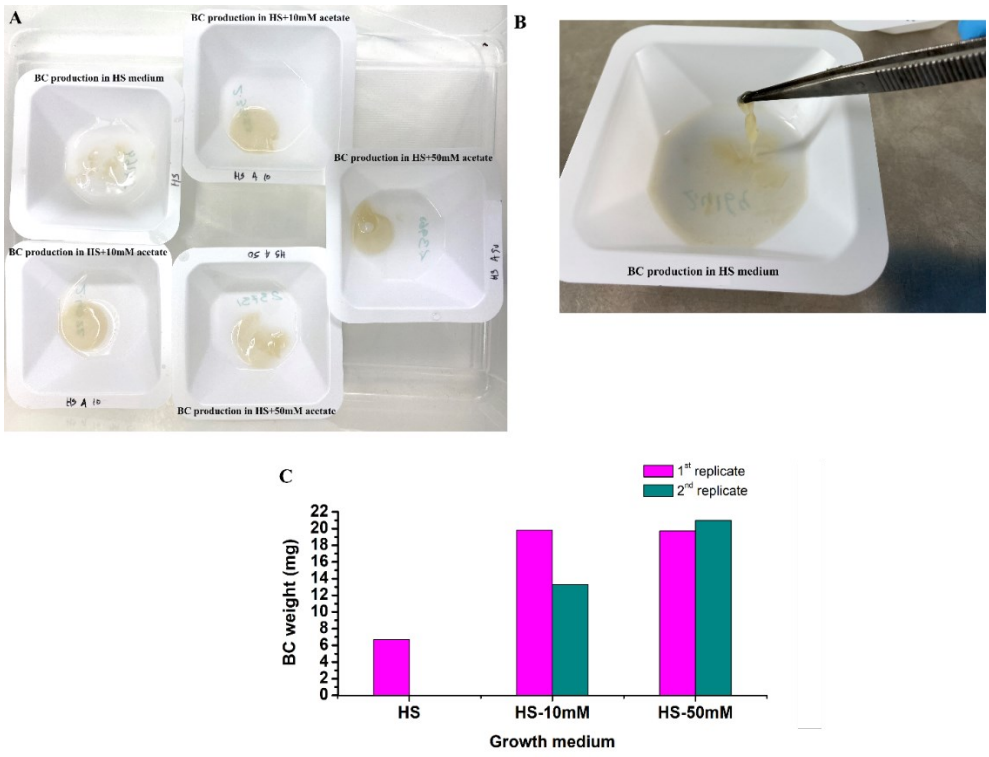

Fig. S6. *BC production by K. rhaeticus ENS9b cells grown statically in HS control (HS, without acetate) and sample (A10 and A50, medium containing 10-mM and 50-mM acetate) cultivation medium. (A) and (B) presents the pristine BC pellicles and the fragile pellicles produced from the control cultivation, respectively, placed on 46 x 46 x 8 mm pre-weighed weighing boats. The images were cropped and brightness and contrast were adjusted to improve clarity. (C) BC pellicle weights produced from HS medium with and without acetate supplementation. The BC pellicles produced from respective cultivations were collected and dried O/N at 60°C. The graph presents the BC weights (in milligrams) obtained from each replicate. The pellicles were not treated with alkali and MQ. Thus, the medium components present in the pellicles may alter the titers and thus, the BC weights are presented.*

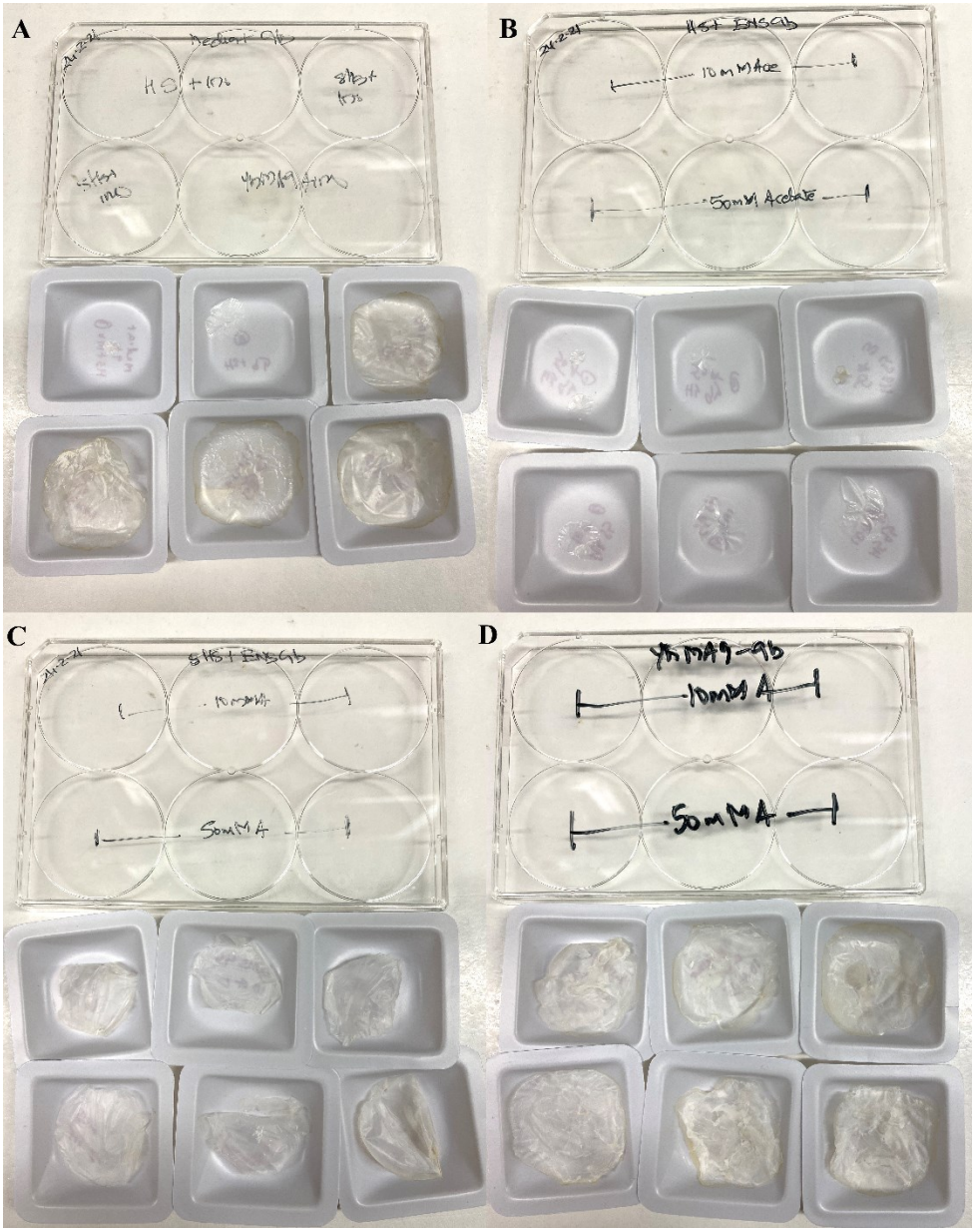

Fig. S7. *Dried BC sheets. BC pellicles produced by K. rhaeticus ENS9b grown statistically in (A) control cultivations devoid of acetate, (B) HS medium, (C) sHS medium and (D) YhMA/9 containing 10-mM and 50-mM acetate. The BC pellicles washed with alkali and ultra-pure water were placed on 46 x 46 x 8 mm pre-weighed weighing boats and dried O/N at 60°C. The images were cropped and brightness and contrast were adjusted to improve clarity.*

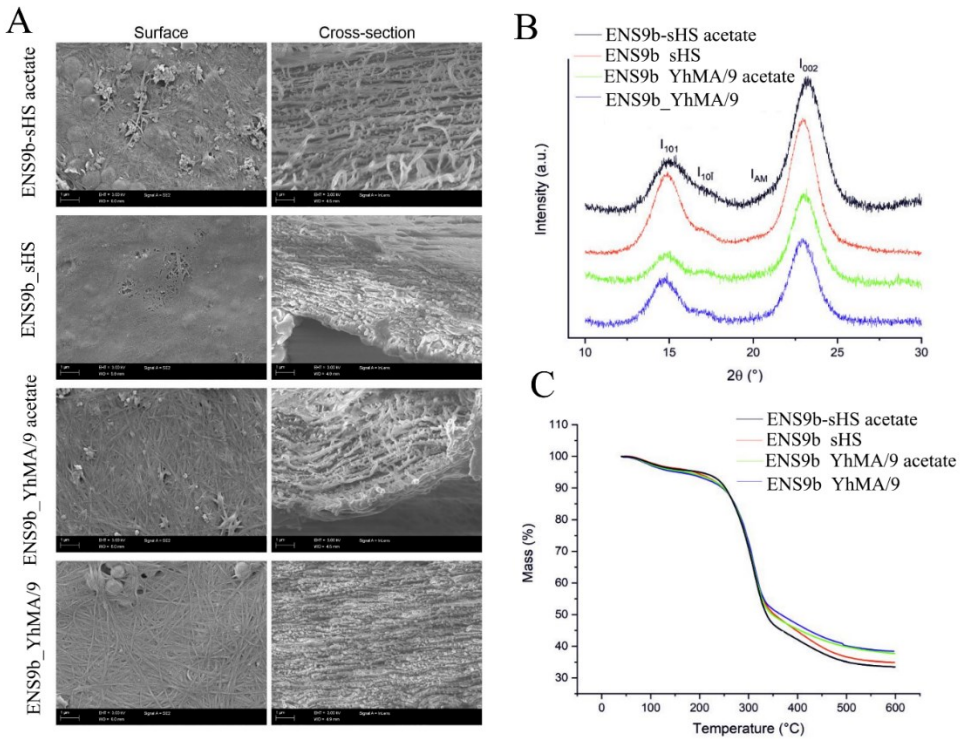

Figure S8: *BC film characterization. (A) TGA (B) XRD diffractograms and (C) SEM analysis of BC films synthesized from acetate supplemented sHS and medium and controls devoid of acetate (ENS9b_YhMA/9 and ENS9b_sHS).*

Supplementary Table

Table S1 General genome and assembly statistics of *K. rhaeticus* ENS9b genome	
Attribute	Value
N50 (shortest sequence length at 50% of the genome)	200461 bp
L50 (smallest number of contigs comprising of 50% of the genome)	6
Contigs unplaced in the genome	7 (90 kbp)
Bowtie2 mapping	94%
Chromosome	3645912 bp (GC content, 63.1%)
Origin of replication	At genomic position 1099952:1100308 bp
Number of protein-coding genes	3302
Number of repeat DNA	120
Number of rRNA	3
Number of tRNA	46
Number of gene annotations to KEGG orthology	1646
Predicted plasmids	5 [p9b_1 (18826 bp, GC 59%), p9b_2 (13375 bp, GC 60%), p9b_3 (9758 bp, GC 60%), p9b_4 (3007 bp, GC 66%) and p9b_5 (2295 bp, GC 67%)]

Amino acid sequences

Enzymes involved in carbohydrate uptake and metabolism

>Carbohydrate-selective porin 1, OprB family (encoding gene at position 1261539:1263020 bp)

MCVVVSFYCNLSWARKPVPDHAARTQSGLLVSQPHAEVRETPAAPHASV
STRLNSIFRTEGLSILLTNREDALRVRDLSAGYYASSEAPGHILPQIGALRSR
LQNRGVTFAFTYKGEAMADVGGGISRGMDYVHELTLQTQFDLGRLFGFTG
WTVHTLLMERVGREVSHDRVGDYNISLMEVYSLSGHSVAHLTDMYAQKSF
LHNTVDLAFGRMALTHVFATSPLLCSFMMTCSAPVAIKLDAGFSVYPKATW
GGRVRLRPTRDTLVQIGAYSVSPLNEDISGWAWAGEKSTGLMIPVEFAWQ
PFFGPRKLPGHYVLGFAHDTTRYADNIGDVPAGSAIRPHGGEARDTFYLEA
DQMLYRKGGASQMAGGYVLAGYIHNTPDVSVISDEFYVGSSLLGIIPHRPH
DRFGVMYSYYRMSPRTELGQQLRMDAGMALGVHVNGPQTHAAVLEAYY
GVPVYPGILVQPEFQYMMRPGETAHIPNAEVVGLKVIGTL

>Carbohydrate-selective porin 2, OprB family (encoding gene at position 1287655:1289154 bp)

MCVIKTCANNENKSAIKWNFIPVRIRLLAVAVGMLFIGCTLTSEVLAQTETAK
TAFTTHYDPAAFPMTEMGQVAIGPLVPMLTASPHLFGDWGGIQPWLTNRG
IFLNVTVNEEYMGNVTGGRQRANVAAGQVAGALDIDWQRLAGVPSFWTH
MLVVNGHGSSLSNAIGDSITNPEEIYGARGNVVAHLVDMYADKGFLRDRIIL
SVGVIPTGSFFNQDYLACSFMNVSVCGNPAPSKYVPGGRDWPSGNLGAV
LRVRPTLRTYIMGGIFAVSPHAYNGGISGWALGQDGLGKLSSQVEIGWSPS
FGRHHLLGHYKIGYWYDNSRYPNLYADINGNSFQATGLPRRYESGMNAA
WFLFNQMIHRSGDGLANGLIVIGGADYTQGSQVAMRDHEWIGLLQSGTPW
GRPLDQVGAMFQYMEMGHTVTLQQESSLALGLPYLSNQWGAVYGIQSHE
NVWEAFYSIHVARGTAFQPDFQYLQRPGATTTFHDAAVIGFQFTTNL

>Carbohydrate-selective porin 3, OprB family (encoding gene at position 1433875:1435551 bp)

MTHSILTKRILAGPSRFVPPFHTPHGSMCRQGLCAASCALGMGLIFSTSGM
AQTQIEEDRARLGNSTPLIQQIDPANVRDSERAQADVEEKAAGDGDKLDTS
GNLLGNMWGARPWLYKHGITFDIQEVDEVWGNGTGGSASGNDGAGGSG

TGPAYDGVTMPTLTIDTEKLFGLKGGLFNVSALQTRGRSISQDHLANFNPV
SGFEADRSTRLFELWYQQSFLKGTLDVKIGQQDLDTEFLISDYASLYLNAN
FGWPMAPSVNLYGGGPSWPLASPAIRIRYRPSEKFTFMFAAADDNPPGNR
YNSTPIQQATGSVSGYNSDPTSQTYDGANGTNFNMGTGALLITELQYALN
PQPADMSNVTKNPGLPGVYKLGGYYDTAKFADYRYNRNGGSLGAASVNP
DSTESDLTPRWDRGNWMVYGIIDQMIWRPSIRSARSVGIFARATGNSGDR
NMISFAVDAGINLKAPFRGRDNDTLGLGWGIGRASSGQRQFDRDSGSYVQ
GNENHLELTYQAQVTPWMVMQPDFQYIWHPSGGVADWTGLRRVGNEAV
FGLHSSITF

>Carbohydrate-selective porin 4, OprB family (encoding gene at position 2853448:2854926 bp)

MKYAIDTRMTRPFPRLFVSLPLFFLALFALCESASAQAIPGEGQGVVGAQP
SLNVNSRRNVSVNDPGSFFSAPYGNQHFFGDWAGLQPFLLKHGVHIEADV
HEELAGNFRGGAKQGVTDAGQVGVEIDIDWHKLAGAPKNFWTHTMIVNG
HGRNASTDYIHDSLAGVQQIYGARGNVVAHLVYMYAEQSLFHNRLDISAG
WIPVGSFFAASPLFCDFMNVSICGNPAPGKYVPGGRDWPSGNLGVVMRV
MPTVDTYIMASMFAVSPHSYNGGISGWSWAQSGLGKFSTPVEIGWLPEFG
RNHLAGHYKAGYGYDNSQYNDLYSDINGNSAVLTGQPFRKQSGVSTAWF
QADQMIMRNGAGPTNGLILLAGYMYTSGKVSAMKDHTWAGIVETGAKWG
RPLDTVGAMFHYYEMSRASILQQESSVLAGTPFLNNQWGKVWGIQTHEN
VYEVFYNIHTARGMSFQPDFQYINRPGGTTTYHDAAVMGLQFNCIL

>Carbohydrate-selective porin 5, OprB family (encoding gene at position 3040876:3042462 bp)

MKIPDPPPPRWTALSRLLFLSCMLIGPCGATTAHAQVPRTQIADDRARLGN
STPLIQQIDPATVRDSERAQADAQAPPSADALDTSGSLLGNMGGARPWLY
RHGISFDLQDVNELWGNATGGSASASDGAGGAGTGPAYDGVTMPTLTIDT
EKLFGLKGGLFNVSALQTRGRSISQDHLADFNPVSGFEADRSTRLFELWY
QHSFLGGKLDVKIGQQDLDTEFLISDYGALYLNANFGWPMGPSLNLYAGG
PSWPLASPAVRVRYRPDETFTFMFAAADDNPPGNSSNSFVIQNGGNRAD
PTSQTTNDGSGTQFNMGTGALLITELQYALNPQPADMGSATRNPGLPGVY
KLGGYYDTARFPDYRYNMQGRPLGTYGGMPRQDRGNWLLYGIIDQMIWR

PSLASPRSLGVFARATGNSGDRNMISFAIDAGLNLKAPFRGRNNDTIGLGW
GIGRASSGLREYDRTSGALLQGSENHLELTYQAQVTPWMVMQPDFQYVW
HPSGRVADWSGLRRVGNEVVCGLHASLTF

>Carbohydrate-selective porin 6, OprB family (encoding gene at position 3439017:3440453 bp)

MSVPGHAQTIPVAARDVWQADEIPASESQDTPSAAGGSLLGDMGGLRPW
LARYGMTLGIQDVNELWGNATGGIASTSGDGRGAGTGASYIGVTMPDLTA
DLEKLMGLVGGTFNVSALQIRGRAITQDHLADFNPISGFEADRSTRLFELW
YQQSFLKDTLDIKIGQQDLDTEFLISDYASQYLNASFGWPMGPSANLYAGG
PSWPLAAPAIRLRYRPGGNYTVMFAASDDNPSGNRDSNVFGVTSNPADP
TSQTMNDGSGTQFNMGTGALLITEIQYALNPRSGDRPGAVRHAGLPGVYK
LGGYYDTARFPDYRYNMQGQSLGAYGGTPRWDRGNWLIYGIVDQLIWRP
SPEGARALGVFVRATGNSGDRNIISFAIDAGLNLKAPFAGRTNDTLGLGWG
IGRATSGVRAYDRARGALVQGNENHFELTYQAQVTPWMVLQPDFQYVLD
PSGGLGNPSRPMRRIGNEAVFGLHTNVNF

>Carbohydrate-selective porin 7, OprB family (encoding gene at position 3440518:3441825 bp)

MVVFLAVLSPAYAQTVPVSVPSAGVTPRQSVPDHIDPRTRLSGDWGGMR
NWLLAQGIDIRISDTDELWANPVGGAQASENYIGSTAVEMVTDLHALTGLA
LGTFDISAMEIRGRPFSNAPLYVFNQTSNIEADDNGRLYELWYSQKFLRER
LALRIGKLDLGHDFMVSSVGLTFLNASFSWPIMPDNDLYDQGPVSPVTTPA
IRLRYTLSPRWNFLFAAADDNPVGGPFINVRDPWNQNRDPGGTRFSFSTG
ALFFGEVQYRRDISGRQGTYKLGGYFDTGRFPDQSDFAKSHKTNWAVYGI
VDQTLRHFGRITTLDAFIRGNWTADTDRNQIVYAVDGGIALSAPFHRRGDV
LGLGAGLGAASPCLAAADRRSGLPAQGNEYHLELTYQAQVTPWFMLQPDI
QGIVSPSGGVLDDRGRRVHDEAIFGLHGSVTF

>Aquaporin Z_1 (encoding gene at position 1386137:1387120 bp)

MKYIEIHGKRRSAYPTCRSTLFPHPPCSFKNIRGLEKGQKAHSPFPSNDNK
RIKWANMLKNRQFLGELIAECIAVAIIVMIGDSVAAMYALYDPSPYKLAYWG
VCIVWGLSVTIAIYITGSVSGTHANPAVSVALALYRGFPWRKVPAYCAAQIL
GGVIGAALVYTLYQPVIDHYNQLHALTRADGGAAGVFFTHPGEFITPFHAFV

DETILTGLLVFGIFAVTCEYNTVAPQANSGALIIGLLVASIGACSGYLEAWAIN
PARDFGPRLFCFLAGWGDSALPGPDHFWWVPVAGPVLGGVLGAGCYQF
LIRPFIPRQASPAVPPVS

>Aquaporin Z_2 (encoding gene at position 1847677:1848606 bp)

MRLPHLHLPYLHVHVHDRPLAGDPHPHNPFHWKLYFCETVATAILMVLGLS
GVILLTAPGSPLSPPLLHHPYVQTALCGLVFGLSGTAAAMTPFGKVSGAHIN
PSVTLAFSLAKRIGGVDALNYMIAQVIGAFLGTAVVYGLGRLVTWWGSMAV
AVRYGATVPYGRISIWWAMWSEMFVTAALIAMLYWLAAHPRWKFITPWSG
GLFFLIMNPFTAWLSGNSVNFARTLAPALFSGQWTGLWVYVVGPFAGASL
AVMAIRMNLMGRLHLLEARLVNFGHHGRVPGLDDPHRKLNHPDDPDHVP
PGTGPA

>Aquaporin Z_3 (encoding gene at position 3161790:3162686 bp)

MTATRPPGGSAITDRPLAGAPHPDHPLHWKLYGCEMVATMVLMLCGIVSV
TLLTTPQTPVGRMLAPHPVIQTMLCGLFFGLAGTVAAYTPFGRVSGAHVSP
SVSLAFSLARRLGWVDLCGYVAAQMLGACLAAVLLAGVGHVLPVWGKMA
QDATFAATVPFSGVAVVWPLVTEMVLTCLLVIMLCALAAHPVLKWFTPWA
GGVFFCLCNPVSAWLSGNSSNLARSFGPAVVTGQWDSFWIYALGPFTGA
AMAIWLLRSRLLGRIEVEEARLVNFGHHGRIPSLLHPGRRMEGGPAKYD

>Quinoprotein glucose dehydrogenase_1 (encoding gene at position 1924182:1926572 bp)

MNTPLRSAPLLAAAIGVCALAGLYLLGGGLWLCAIGGSFYYVVAGALLLVTA
FLLFRRQAVALTVYAALLLGTMAWAVNEAGLDFWALAPRGDILVPIGIVLLL
PWVTRHLQPATPGARLPLLGAIGAAVVVIGAALMGDPQDIAGSLPPVAQNA
PEPGDAHQMPDEDWQAYGRTQFGDRFSPLRQINTGNVSRLKVAWTFRT
GDMRGPNDPGEITDEVTPIKVRDTLYLCTPHQILFALDARTGKQRWKFDPQ
LQYNPTFQHLTCRGVSYHEDRVEAQADGAPAPAPAECARRIFLPTNDGQL
FALDAESGARCASFGNNGVVDLRDGMPVRTLGFYEPTSPPVVTDTTVIVS
GAVTDNYSTHEPSGVTRGFDVHTGALRWAFDPGNPDPNEMPSEHHTFVP
NSPNSWITSSYDAKLDLIYIPMGVQTPDIWGGNRGADAERYASAIVALNATT
GRLVWSYQTVHHDLWDMDIPAQPSLVDIRNEHGEVIPTLYAPAKTGNIFVL
DRRNGQLVVPAPEQPVPQGAAPGDHLSPTQPFSRLTFRPSQKLTDADMW

GGTMFDQLVCRIMFHRLRYEGTFTPPSLQGTLVFPGNLGMFEWGGLAVD
PERQIAIANPIAIPFVSKLIPRGPNNPATPDRSLPSGSESGVQPQFGVPYGV
DLHPFLSPLGLPCKQPAWGYMSGIDLRTNKIVWKHRNGTIRDSAPLPLPIW
MGVPSLGGPLTTAGGVAFLTSTLDYYIRAYDVTTGRVLWQDRLPAGGQST
PMTYAVDGRQYIVTADGGHGSFGTKLGDYIVAYTLADQN

>Quinoprotein glucose dehydrogenase_2 (encoding gene at position 2594170:2596791 bp)

MRQDLPFESHAREIPRNPSGAACLHHAVQTRWPHTGIESIMFPRPIENFRK
NAGMREGKQKLFSIITSALLALVGLFLFFGGAQLMVLGGSWFYVLAGCLLL
AVAVTGVKAPQLAMRVYAAFLVVATIWALTETGFNIWGLEVRLLAPIGFGA
WMLLPWVVWRSGGNWLADKRDMLGAIGLAVVVLVISCFTSYSIDGTVPDDR
MAAQGQADPAADGVADADWQAYGRTMGGDRYSPLAQITRGNVSHLKRA
WVTRTGDVEQDGEGTVAGPDQGHEFNLEVTPLKVGDTLYMCTPHSWVM
ALDATTGKVKWKFDPHPDTADLAKNVYLACRGVSYYRIPDEIQTSCRTRIY
SPVADVRIVALDAETGKPCDDFGDHGFISMRAYLGHVPHGFHFITSPPLVA
KNRLITGGWIFDNQANFEPSGAIRAFDATTGEIAWAWDAGHSPETWKPGP
TDVLTRDTPNAWGVYTADPALGMVYIPTGNAPPDNWGGSRRPFDDATSS
ATIALDIVTGERRWTYQTVHHDLWDMDIPSGPSMVELPGPNGESIPALVQS
TKRGEFFVLDRRTGAPVPGYPVEERPVPTAGAAPDDRVSPTQPYPAAMP
SLTPPNLKESDMWGATLLDQMICRIQYRQSAYEGQFTPPHVGRTTIVYPAF
YGVVDWQGITIDPQRKIMLANASYLPFRIKLEKRQGLEGKGVLPRWNGQG
EEPAAKGDALSVSPDYGTPYIALTNPWLNPLQIPCKGPVWGTITAIDLVTKKI
VWQHPVGTTRDTGPFRTHNNLPLPTGMYNIGGSIVTRGGLVFMGATADDY
LRAFDLATGKVIWTDRLPAGGQATPMSYEIGGKQYVLIAAGGHGGLGTRS
GDYIIAYTLDGEKGAASAQ

>Glycerol uptake facilitator protein (encoding gene at position 1285133:1285972 bp)

MNRVFLGELISEALAVFIIIAFGDSVAAMYLLYDPSPYLHAYWGVCIVWGLG
VTVAIYATGSVSGTHANPAVTLALATYRAFPWKKVIPYWFAQIVGGFLGAAL
VYALYYPVIDHFNDMHQLARMSGGGAGVFFTAPAPGITLWHAFSDEIILTAI
LVFGIFAITEQYNEMAPGANFGALIIGFLVAAIGASMGYLEAWAINPARDLGP

RLFAYVAGWHEAALPAAGHYWLVPVAGPLIGGLLGATAYEYLIYPFLPAQL
RARQALQGKIAEETIIIGE

>Glycerol kinase_1 (encoding gene at position 1286008:1287507 bp)

MTDYVGAIDQGTTSSRFMIFDRKGTIVSVAQKEHRQIYPRPGWVEHDPIEIL
ENTNEMIGAAMARANLGAASLVSVGITNQRETAVLWDRTTGLPLHNAIVW
QDTRVDQLVSEYGRDGGQDRFRAITGLPLASYFAGLKLRWLLDNVEGARQ
KAESGQALFGTVDSWLSWNLTGGTRGGIHITDVTNASRTQLMNLKTCAWD
EDMLAAFSIPAACLPRIVPSSQVYGTITIPSLQGTKLAGILGDQQAALVGQTC
FSPGEAKNTYGTGSFLLMNTGTDPVQSKAGLLTTVAYQFGTEEPRYALEG
SIAITGALVQWLRDNLKLFDLATQIEPLARSVADNGGVYIVPAFSGLYAPYW
KENARGVIVGLTRYVTRAHFARATLEATAYQVRDVVAAMEEDSGIVLRSLK
TDGGMVANELLMQFQADILNVPVVRPKVVETTALGAAYAAGLAVGYWKNI
DDLRANWEVDRTWQPTMPPEQRARYLAWWKKAVQKSFDWAE

>Glycerol kinase_2 (encoding gene at position 1389048:13890547 bp)

MNKKNRILAIDQGTTSTRSIVFDRDIAALSVARVEFAQHYPNQGWVEHDAE
EIWSNVLSTAREAIAKVGGPATIAGIGITNQRETIVVWDRKTGSPVHRAIVW
QDRRTTPVCMRMHEQGYEPLVRERTGLLLDPYFSATKIAWILDNVEGARA
RAERGELACGTIDSFLLWRLTGGRVHATDTTNASRTLLFNIHTCAWDDELL
ALFNVPRAILPEVRTNSEIFGETEADLFGEPLKVAGMAGDQNAAMVGQACF
KPGTAKATYGTGCFALLNTGTTPVNSENRMLTTIAYRIGDETVYALEGSIFV
AGAAIRWLRDGLGLITHASQTDDMATRVPHSHGVYMVPGFVGLGAPHWD
PDARGLICGMTLGSTAAHIARAALESVAYQTLDLMEAMREDGGGKLNALR
VDGGMSVNDWFCQFLADMLQTPVERPRQVETTALGAAFLAGLATGVWSS
IPELEGTWTRGHLFRPTMDKAQRDSMVAGWHLAVRRTLSSTVAA

>Glycerol dehydrogenase_1 (encoding gene at position 1201435:1203437 bp)

MRRYRFLAMGMAAAWLCLPVSSHAQFAAAGSGGPPGASIPGPGRADEPA
EQTPADPGYFAGPSPYAPQAPGVNAANLPDIGSVAADSLPAMLPQAGAAP
APGDWATYGRDDAQTRYSPLAQITPENVSHLQVAFTYHTGSYPRPGQTN
KWAAETTPIKVGDGLYMCSAQNDIMKLDPATGKEIWRRNLGEKYEAIPYTA
ACKGVTYFTSSQVPQGQPCHNRILEGTLDMRLVAVDAATGEFCPGFGHG

GQVNLMQGMGESVPGFVAMTVPPTVVNGVVVVNHQVLDGQRRWAPSGV
VRGYDAESGRFVWAWDVKHPDDHDQPTGNRHYSRGTPNSWAAMTGDD
ALGLVYVPTGNAAGDYFSGYRSAAENAVSTSIVALDVRTGSPRWVFQTVH
KDVWDYDMGSQVTMMDMPGTDGQTVPAIIVPTKRGQTFVLDRRTGQSILP
VEERPAPAGDVAGDTRAPTQPWSVGMPSLHMPDLREQDMWGMSPIDQL
YCRIKFRRAHYVGEFTPPSLDRPWIMYPGNNGGSDWGSMAYDPQTGILM
MLREYGGKPLVEWLVLLLGVVIFLVGLVFVAGGAELALLGGSLYYLLCGLVL
LASGTAMLMGRTLGALLYLAALAYTWAWSVWEVGFSPVDLLPRAFGPTLL
GLPVLFSIPVLRRMATRRAIGGIC

> Glycerol dehydrogenase_2 (encoding gene at position 1673449:1676036 bp)

MSRTPMPRGLLLGATIITGLSCATALAQVPPADQPPGTGNATVPPAQPTPP
ADAFSAPSPNGPQAPGVNAANIPDGPPAEPSEATPMVEQVVANPAHDDW
PGYARDDRATRYSPLDQITPANISHLKRAFIYHTGSKPGPGQVNKWAAETT
PIKVGDGMYMCSALNDMMRIDPATGKEVWHFHANEKYESIPYTAACKAVV
YYTSSTVPEGEHCHHRILEATLDERLIEVDSEDGKVCEGFGWHGMVNLMK
GMGESVPGFVAETAPPPIVNGAIITNQEILDGQRRWAPSGVIRGYDAETGR
FLWAWDVNRPHEHGEPKEGEHYSRGTPNSWAAMIGDNALGLVYVPTGN
SAADYYSAMRSPEENKVSSAVVAIDVKTGEPRWVFQTVHKDVWDYDIGS
QPTLMDFTKPDGSSVPALIMPTKRGQTFVLDRRTGEPVLPVEERPAPSPG
MVPGDPRAPTQPWSVGMPRLGFAPLKEADMWGMSPIDQLYCRLKYRRA
HYVGEFTPPSIDKPWLEYPGYNGGSDWGSVAYDEKTGILIANWNNTPMYD
QLVSRKKADQLGLMPVDDPNYKPGGGGAEGAGAMAETPYGIVVSPFWDE
YTGMMCNRPPYGMITAIDMHTQKVLWQHPLGSARANGPFGLPTHLPLTIG
TPNNGGPVITAGGLIFVAATTDNMIHAFDIHTGREVWNDVLPGGGQATPMT
YEYKGKQYVAIMAGGHHFMMTPVTDDLVVYALDNVNMSAFVTPQTPAGW
ATLGLAVIIILLGLPLLYMGAELAFIGGSWYYVIVGLAVTVAGLLMAMGRVAG
GLLYLAAVAFTWLWALWEVGLDGWGLLPRVFGPTLLALGVLACLPVLKRA
EAARSTLVREVA

>Dihydroxyacetone kinase (encoding gene at position 1848749:1850380 bp)

MKRFFNTRETIVTEALDGFLRSAAGQHLCRLDGYPDTCVIMQREPERGLVS
VISGGGSGHEPAHAGFVGRGMLTAAVCGALFASPCVDAIVAAILATTGEAG
CLLVVKNYTGDRLNFGLAAERARALGKQVEMVIVGDDIALPDSATPRGVAG
TVLAHKLAGYGAAQGWPLTRVAQFVRDGAGRMRTIGMALEDCNPYEPGR
ASRLAADEAELGLGIHGEPGAQRIALASASDLMRRVTETLEASLPATVRNT
RFAVVLNNLGCVPEVEMALLLEAFSHTRLARRVSHVIGPAPLMTALDMNGF
SLTLIELDESITHALQAPAQPPAWPGMVPLGSPAVAPMPVMPDAFPYPAST
DPTVRAMLEHGAKVLIANEAPLNELDGKIGDGDAGSTFAGAAREITAALDR
LPMADPHQLMTTVSNILTQHAGGSSGVLFAIMFSAAGRSRAPWREALREG
LEHMMACGGAKPGDRTMIDALYPALEALARTGSLTDAALAARKGADATTT
METARAGRAAYVPSAHVRNVPDPGAEAVARLLEGLARG

>Triosephosphate isomerase (encoding gene at position 2116868:2117611 bp)

MKQIIVGNWKMNGLSADADALVDALATGLAALPARADVVVCPPFTQLARLA
PKLKAAGMALGAQDCHKDRSGAHTGDISAPMLVDLGVEYVILGHSERRAE
HGELDETVREKAVAAMAAGLTPIVCVGENADQRDSGDSQEKVGWQIQGS
LPQGFTGIVAYEPVWAIGTGQAASQQDIADMSAFIRAELVRQFGEAGKTIRI
LYGGSVNERNVTDILPVENVDGALVGNASLKADAFVPLVRAARAS

Enzymes involved in BC biogenesis

>bcsA1 (encoding gene at position 666919:669156 bp)

MSEVQSSAPAESWFDRLSNKILSLRGASYIVGAIGLCALLAATTVTLSVNEQ
LIVALVCVVVFFIVGRRKSRRTQIFLEVLSALVSLRYLTWRLTETLDFDTWLQ
GTLGVTLLLAELYALYMLFLSYFQTISPLHRAPLPLSPNPEDWPTVDIFIPTY
DESLGIVRLTVLGALGIDWPPDKVNVYILDDGKREEFARFAEECGARYIARP
DNAHAKAGNLNYAIQHTSGEYILILDCDHIPTRAFLQISMGWMVEDKKIALM
QTPHHFYSPDPFQRNLAVGYRTPPEGNLFYGVIQDGNDFWDATFFCGSC
AILRRKAIEEINGFATETVTEDAHTALRMQRRGWSTAYLRIPLASGLATERL
VTHIGQRMRWARGMFQIFRVDNPMLGPGLKLGQRLCYLSAMTSFFFAIPR
VIFLASPLAFLFFSQNIIAASPLAVLAYAIPHMFHSVATAAKVNKGWRYSFW
SEVYETVMALFLVRVTIVTMMFPSKGKFNVTEKGGVLENEEFDLGATYPNII

FAVIMAIGLMRGLFALAFQHLDIISERAYALNCVWSVISLIILLAAIAVGRETKQ
IRHSHRVDARIPVTVYDYEGNSSHGITQDVSMGGVAIHMPWRNVTPDQPV
QTVVHAVLDGEVVNLPATMIRCANGKAVFTWNITSLPIEASVVRFVFGRAD
VWLQWNDYEHDRPLRSLWSLILSIKALFRKKGRMMIHSRPQNKPIALPVER
REPTSSQGGQKQEGKISRAAS

>bcsB1 (encoding gene at position 669157:671572 bp)

MRPRDMKMVSLIALLVFATGAQAAPVASKAPAPQPAGDNLPPLPAAAPAA
AAAPAGQQPAGAASAAPAVDPAAASAADAMVDNAENATGVGSDVATVHT
YSLRELGAENALTMRGAAPLQGLQFGIPGDQLVTSARLVVSGAMSPNLQP
DNSAVTITLNEQYIGTLRPDPSHPAFGPLSFDINPIFFVSGNRLNFNFSAGS
KGCTDPSNGLQWASVSEHSELQITTIPLPPRRQLSRLPQPFFDKNVRQKTV
IPFVLAQTFDAEVLKASGILASWFGQQTDFRGVNFPVFSTIPQTGNAVVVG
VADELPSALGRPAISGPTLMEVANPSDPNGTILLVTGRDRDEVITASKGIGF
SSSTLPVAARMDVAPIDVAPRAPNDAPSFIPTSRPVRLGELVPVSALQGEG
YTPGVLSVAFRTAPDLYTWRDRPYKLNVRFRAPDGPIVDLARSHLDVGINN
TYLQSYSLHEKDSVVDQLVQRFGGRGQTSGVQQHTLTIPPWMVFGQDQL
QFYFDAAPLTQPGCRPGPSLIHMSVDPDSTIDLSNAYHITRMPNLAYMASA
GYPFTTYADLSHSAVVLPDHPNGTVVSAYLDLMGFMGATTWYPVSGLDIV
SADHVNDVADRNLIVLSTLANSGEVSSLLSNSSYQIADGRLHMGMRSTLSG
VWNIFQDPMAAINNTHPTEVETTLSGGVGAMVEAESPLASGRTVLALLSAD
GQGLDNLVQILGQRKNQAKIQGDLVLAHGDDLTSYRSSPLYTVGTLPMWF
MPDWYMHNHPVRVIVVGLFGCLLVVAVLVRALLRHALFRRRQLQEERQKS

>bcsC1 (encoding gene at position 671575:675549 bp)

MNRRYVFSLSAGLLASSCMTVLVAVPLARAQQASTAMTGTQASGGSAAP
RQILLQQARFWLQQQQYDNARQALQNAQRVAPDAPDVLEVQGEYQTAIG
NREAAADTLRHLQQVAPGSTAANSLSDLLHERSISTSDLSQVRSLAASGHN
AQAVQGYQKLFNGGKPPHSLAVEYYQTMAGVPAEWDQARAGLAGIVASN
PQDYHAQLAFAQALTYNTATRMEGLARLKDLQGFRSQAPVEAAAASQSYR
QTLSWLPVTPTTQPLMQQWLDSHPNDTELREHMVHPPGGPPDKAGLARQ
AGYQQLNAGRIAAAEQSFQSALQINSHDADSLGGMGLVSMRQGDAAEAR
RYFQEAMAADPKTADRWRPALAGMEISGDYAAVRQLIAAHQYDAAKQRLS

ALARQSGQFTGATLMLADLQRTTGQMGAAEQEYQSVLARDPNSQLALMG
LARVEMAQGKTAEARQLLSRVGSQYATQVGEIEVTGLMAAASQTSDSARK
VSILREAMAQAPRDPWVRINLANALQQQGDMAEANRVMQPILSNPVTAQD
RQAGILFTYGSGNDAMTRRLLAGLSPEDYSPAIHAIATEMEIKQDLASRLSM
VANPVPLIREALSPPDPTGARGVAVADLFRQRGDMIHARMALRIASTRTLD
LSADQRLAYATEYMKISNPVAAARLLAPLGDGSGTGAGNALLPEQVQTLQ
QLRMGIAVAQSDLLNQRGDQAQAYDHLAPALQADPEATSPKLALARLYNG
QGKSGKALEIDLAVLRHNPQDLDARQAAVQAAVNSGRKSLATRLAMDGVQ
ESPMDARAWLAMAVADQADGHGHRTISDLRRAYDLRLQQVEGTRAVASG
TGEQESLEPPSSNPFRHHGYGRQTELGAPVTGGSYSMEATSPEASDQML
SSIAGQITTLRENLAPSIDGGLGFRSRSGEHGMGRLTEANIPIVGRLPLQAG
ESSLTFSITPTMIWSGQLNTGSVYDVPRFGTDMATQAYNQYVSYISQNNSS
STLHSELVKGGEAEAGFAPDVQFGNSWVRADLGASPIGFPITNVLGGVEF
SPRVGPVTFRVSAERRSITNSVLSYGGMRDPNYNTTLGRYARQLYGKELS
SQWSEEWGGVVTNHFHGQVEATLGNTIVYGGGGYAIQTGKHVQRNDERE
AGIGVNTLVWHNANMLVRIGVSLTYFGYANNQDFYTYGQGGYFSPQSYYA
ATVPIRYAGQHKRLDWDVTGSVGYQVFHEHSSPFFPTSSLLQSGAQYIAD
SYVQNATSSDYLSQETVNSAYYPGDSIASLTGGFNARVGYRFTHNLRLDLS
GRWQKAGNWTESGAMISAHYLIMDQ

>bcsD (encoding gene at position 675549:676019 bp)

MTTFNAKPDFSLFLQALSWEIDDQAGIEVRNDLLREVGHGMAGRLQPPLC
NTIHQLQIELNSLLAMINWGYVQLELLPEDHAMRIVHEDLPQVGSAGEPAG
TWLAPVLEGLYGRWITSQPGAFGDYVVTRDVDAEDLNSVPSQTIILYMRTR
SSSN

> bcsZ (encoding gene at position 664722:665759 bp)

MGRRSFLSVMAAAGSIPFLSTALAADDPAINAQWAIFRAKYFHPDGRIIDTG
NSGESHSEGQGYGMLFAATAGDQATFEAMWSWTRANLQHKTDALFSWR
YLDGHNPPVADKNNATDGDLLIALGLVRAGRLWKRADYIQDAIAIYGDVLKL
MTLQVGPYLVLLPGGVGFATKDSVTLNLSYYVMPSLMQAFALTGDARWQK
VMGDGLIIINQGRFGEWKLPPDWLSINRQNGHFSIANGWPPRFSYDAIRVP

LYLYWAHMLSPDLLADFTRFWNHFGASALPGWIDLTNGARSPYNAPPGYL
AVATCSGLSSAGGLPTLDKAPDYYSAALTLLVYIARGEGGGM

> ccpAx (encoding gene at position 665756:666736 bp)

MTTPNKESTEATPRPVVDMDNPQDVTRMLSSGYGLSGEGFHYHSFTRPV
MLDMTPELPHDSVDDTEHHLDDNVTEHESAPATAPVFVFDAAPEPAAPPV
VAEAAPPPPPPPPPEPAPPEPPPAPPPYTPVVTHVPPPPPVEETPVPEPVA
EAAAPARPRPVPPAQPAPDMASTGGRERRGLQPFAAPRAPSEPPVSSRA
AAPATPFVQADDWAPVPKAQQRRGQRPTGPGFFFAKGNDRVATARLFQP
VAVARPASKPDSKVTTMTKFDKTAQNAPTGRRPAPSDNSPTLTEVFMTLG
GRATDRLVPKPSLRDALLRKREEETGQS

> bglX (encoding gene at position 676251:672452 bp)

MKPSRKSFLLSAVAWGLVAALPAHARHAATAGDPADDQARQVLAHMSLQ
DKMALLFSVDGGGFNGSVAPPGGLGSAAYLRAPAGSGLPDLQISDAGLGV
RNPAHIRPNGAAVSLPSGLATASTWDVDMARQAGEMIGREAWLSGFNILL
GGGADLTRDPRGGRNFEYAGEDPLQTGRMVGSTIAGIQSQHVISTLKHYA
MNDLETSRMTMSADIDPVAMRESDLLGFEIAIETGHPGSVMCSYNRVNDL
YACENPYLLNTTLKQDWHYPGFVMSDWGATHSSARAALAGLDQESAGDH
ADARPYFTALLAADVKAGRVPVARIDDMAQRIVRSLFAAGLVAHPPQRGPL
DVVTDTLVAQRDEEEGAVLLRNEGGILPLSPTARIAVIGGHADAGVISGGGS
SQVDPIGGEAVKGPGKKEWPGDPVYFPSSPLKAMRAEAPNAHITYESGTN
IAAAVRAARAADVAVVYATQFTFEGMDAPSMHLDANADALITAVAAANPRT
VVVMETGDPVLMPWNSSVAGVLEAWFPGSGGGPAIARLLFGKVAPSGHL
TMTFPQAESQLAHPDIAGVTADNVFEMQFKTDQELVYDEGSDVGYRWFD
RNHLKPLYPFGYGLTYTTFSTDGLAVHRHHDAVTVTFTVHNTGNRPGVDV
PQVYVGLPDGGARRLAGWQRVSLAPGESRAVTVQLDPRLLAHFDGKKDR
WSIPSGTFRLWLGTSATDDSQQASLHLSGRTFAP

>bglX2 (encoding gene at position 522700:524739 bp)

MKYASLRYGLSALRCLIALCMGGLVLSALPVQARAAAGGSAGSAHAADMA
ARMQPAEQQAVLQARPIGGGEGATQAAADGLLAWPGVARLGLPALRMPD
FSSPARPADEGGHPMLPWLALAATWDPDLARRAGGARARAEWEQGRAV
VRVGGIDLLPSGRLQAGEDQVLAGTMAGMIGAGLLSGHVLPVFGSVAGDE

QARADGAVPGRTAPVPAAWLADGSLLGVAMALEVAHGGALLCGGLAVCQ
TVTGLGAMVHDAWHFPGMVMATPGGLGPARPDDASLLPGALGTGVDME
QVSSREGGHDMFGAPLRQAVRDGAVRPAQLQAMGMHVLASFYMAGSLD
HPPAFTPAHAAASPPVADTLVSDVEAEGAVLLQNENRVLPFDPALGPVLVL
VRAPMRHAADLLADELRHAGLGVSVVVAADGANAPGTLPPATAQAARTLV
LSGTDADNRMISTLADLGGHVVVVLTGDDPDRQMPWLDMVDSVVQAWA
WRDAHARPLAALLSGQQEFSGHLPVTLTGGFYPPGMVDADYRAFERAHV
APLFPFGYGLSARGHLTLSDLHVVREGTHLNASFSVTNPDGTAVRAIPQLY
VSPSSDQAAPRRLAAWRSIMVAPGHTLRLTLPVSLRLLAQWNAPAANWAV
AAGDYAFSLGFSSVMLVRHADVRLPAMHLPAALDMAAD

>bcsAB2 (encoding gene at position 1020008:1024567 bp)

MAQFVDKITRFMEQAATGRVPSWVPIVIGVVMMSFVGSVALLPDMQGLISI
GTVLLLLVLNRFKGRGITIFLMMLSLLVSMRYVVWRLTSTIEFHGWIQSALSI
LLLLAEVYALSTLCLSYFQMAWPLGRKEHPLPEDTSSWPHVDIYVPSYNEE
LSLVRSTVLGALKLDWPEDKLHVYILDDGRRVAFRDFALEAGAGYIIRSQNN
HAKAGNLNHALKITDGQFAVIFDCDHVPTRGFLKRTIGWMIADPKLALLQTP
HHFYAPDPFQRNLVAGAHVPPEGNMFYGLVQDGNDFWDATFFCGSCAVI
RRSAVLGIGGFATETVTEDAHTALKMQRRGWRTAYLREPLAGGLATERLIL
HIGQRVRWARGMLQIMRVDNPLLGRGLRWEQRLCYLSAMSHFLFAIPRVT
FLVSPLAYLFLGQNIIAASPLAISVYALPHIFHSILTLSRIESRWRYSFWSEIYE
TSLALFLVRITIVTLLQPHKGTFNVTDKGGLLEKSYFDVGAVYPNVILAVILFA
AFLRGIFGIVWQFHDRLALQSFALNTLWVVISLIIVLASIAVGRETRQTRAAP
RIAVALPVRITDMEGRSFAGHTRDISLGGLGVDLHWPADVARPDRVMMEY
VNERDGIHATVPATVLALDERSMRLQWERRDLEDESQIVDMVFGRNDAW
ANWADFEPDRPLRSIAMVLRSIGGLFKWQAREIPRHVADDEEAKAPVVEA
KLEKQSLVLKPVRRSARNGAAASAVLLVALAALSPVAMAQVQPAASASVP
DQTGVSAETPFGDSNTGTVPDMIPVIDQAAADRISDSEVTRTLSFRNLGAT
SGPLTLRGYSPLQGLDVIVPANRVVTHARLSISGALSPSLLPEASAVTVTLN
EQYIGTIKVDPEHPQFGPLTFDIDPLYFTGDNKLNFRFAGEYRRDCNDLFN
EILWARISDMSQITLTTVRIAPERKLSRLPAPFFDPNLRSTLRVPVVLPDTNS
KSSLKAAGLVASWFGKIADFRKLSFPVFTAIPASGNAVEVGENLPVDETGT

RPRGPMLAEIANPNDRWGTILVVTGRNAQEVEAAARSLVFSADTLGGVAA
KVVDDVSLEARQPYDAPAFVPTDRLVRFGELVGAADLQGGGFTPAGMTLP
FHLPPDLYTWRGRPFLMDMWIRAPGGPVVDLETSRVDVSLNNNYLQSYTL
SPPGLWQRWSQRLVNLHAGAVGHTTALPTWLLFGQNQLLFNFDARPIDR
GACRRTPGDIRMSVDSDSTLDFRRGYHFAELPNLSYFAEAAFPFSRMADL
SETTVVLPSHVDAGTAGAFLDLMGFFGASTWYPAAGVQIMTADQVGAAQP
GGDIVVLGTAEQLGSATSLLSRSPYVIRDGRIQVGEHMGLQGIWYLFQDRD
HAGLKNGVTARLNAPIVEAGLMLAAQSPYDHARSVVAFTGDTPERIHDLVL
SLRNKTDLPSLQGDLVIKNGNQFTSYRTAPTYTVGSLPLWVRADWYLSHH
PLALYLTGLAGAALTALGVWGWLRRLSRRRIENEELAGEQ

>bcsC2 (encoding gene at position 1026603:1030553 bp)

MTRQYCPARGRQPAVAWRKAPAAWVMRPAACRPSSAWLAGGGWKIICG
MVAGVIMAGEIAQAEPAWTAGPDSAASPAGGSTQITVTPDAGQNAANAHL
AHAAAVLELLLNQGYYWLGQHNLPKARETIQRALSIEPDNNEALFLLGRLQ
MAEGQTKLAAATLGRLIQNGNAPGLVADLRAQIHAGPIDPRGLAEARALAA
EGKMMPAMFKYRALFKNGDPPPDLAMEYYRVLGATTLGYQEAATRLAAW
VARNPRDLDAKLSLDRILTYHVTSRDEGLEGLRQLARSNASAAIRDGAIAA
WRDALLWEPVTGPTIALYNEWLDLHPGDAEIIDRRHKAQDAQNIIDGANYR
QQGFVLLSRRNIEGAADLFHRALAINAHDADSLGGMALVAQARQQPALAR
HYFQQAIQADPDSAAHWRAALKAMEAGGGGGMDPLVARIIQAINSGHYDA
AQSDLALLGRRGNTITLQALQGMLARRQGHMEEAERLYREILRRAPGNAD
ALFNLGGILIETGREAEAQDIIARLAHIRPDLARHLEVAGLSARSDRTRNNDE
KLSLLNRAMAMAPTDPWIRLKLARALDEAGNHAQAQAIMDGVTSGRAVTP
DDLQAAILYAMGRHDMARAEQLLARLPPGIESPGMARVAEQIELVRRIQEL
NRVPRAPNALLVALADRPDPTGERGMRIANALLDRHAPQDAQQVLATEER
LTQPPQPSQLLAYAGVYLRLHSAVDATRCLNAFDAMARARPTDITADQQEI
RNQIAIGLAIMTADGFNRYGQTARAYQVLAPVLQAHPDSAEAHLAMGRVY
QTRNMARRALEEDQIALRLKPHNIYALAAAARDAGGLHQMAEAKDYSTRL
AHEDPDGPMSWEVRSDIERIEGNTRAQLVDVEHARHAQCTLDGEGTCDG
QHESFLPDYRWPEIDSNYINLHGATLPATYHYIPEDDGPEAMDRQIVYLRD
SVSPQIDANSYVRSRTGTAGLGQLTEFAVPITGTLPFESWEHRLSFSIVPTL

LFTGNPLANPYSAHEFGTYAINGALPGSSHHYYTQGVGLSLNYVNHWFSA
DVGSSPLGFPITNVVGGVEFAPRLTRNLGLRISGGRRMVTDSELSYAGMR
DPGTGRLWGGVTRMFGHGALEWSEPTWNLYAGGGFAYLGGTHVVDNTE
VEAGAGGSATVWQSHDRQWLRVGLDLMYFGYKRDTYSFTWGQGGYFSP
QQYYGAMIPVEWSGHDRRWTWFLRGEAGFQHYHSNGAPYYPTDSALQA
LSVAHQPDYYGDEGESGLAGNIRGRVVYQFTHRLRLGMEGGYSRAGNWS
ETSGMWMAHYTFDGQ

>bcsAB3 (encoding gene at position 2139998:2144443 bp)

MIWRILKSPFVTGPLFALLMAVVSLTYLTPDHQFFVAVGGGVLFFLVRRHD
ERWSRCFLMVLSIVVSGRYLVWRFTSTLDLDGVLQGSLVLALAVGEIYTTIR
VGFTYFQLAWPLRRQIHPLPEDEGTWPVIDVYVPTYNEDISIVRTTVLGCLS
MDWPADRLNVYILDDGRRRAFRDFAGQVGAGYINRAENVHAKAGNLNHAI
GVTSGDIIAIFDCDHVPVRGFLKKTVGWMLADPNLALLQTPHHFYSPDPFR
RNMSRGMQVPPESNLFYGLLQDGNDFWNATFFCGSCALLRRRAIVSINGF
ATETVTEDAHTALRMQRKGWGTGYLREPLAAGLETETLLLQIGQRVRWAR
GMFQMLRIDNPMLGRGLRLTQRICYMAAATNYFFAIPRMMFLLAPLAYLFL
GVTMIAASPYELAVYALPHLFHTTMTMSRLQGRWRYSFWSEIYESMLAPFL
VRMTFVTMIAPHKGSFNVTDKGGLLDRERFDWRASYPGVIVAVVLAVGLV
SGIWAAIVHYHETLVFRAMAVNSIWVLFSLIIVLGGVAAARETRQRRHSHRV
AASLPFELVDAQGQVHACRSVDVSMGGCQLDAATVPGAAGGRVMLRWS
LPSGPATMGATIIARCGGRLHLQWVIAGLASERQVVALVFGRDDAWARWS
DFPPDRPLRSLYLLVASICALFRPPPRVRDETPHAVARKTAAQDETLPRQQ
LVIPPDRTVVLRDIGTALVLAAMLLLPAMDARAQAAPAMADAGPAVVADGS
VDAIDNAHMTSADVDEVSHQPVTRTRTLADMGRTEDMVLRANAPLHGLSA
GVGRDIIITAARLGISGTARGAAGRVAVAVSINNQDAGVICPTADGAFGPVD
LPLSPMFLDTRNRINFRLFLRAPQPADPSAPACGPDARGRDGSAAQVSDP
GVQVVISPRSTLTLTTVGLVPHRLLSALPYPVLDPDAARTAAVTFVLPGGRD
PAQLEAAGMVASWLGLQSRESGIHFNVAAIPPDQGSAVAIAPGQPGPWGR
APAGPALAVMPNPHDRFGTVLVVTGRTPAEVRTAAQALVLGAEHDAPGAF
AAAPVVHPPARQPYDAPGVVRTDRPVTLRELVSTAALRTRGLTSGTLDIAL
SLPPDLRSWRSRPFMARLQISAPEGGVLDRAKSRVSITLNGTYLHSYPLVP

LSLNPFRTPGAPVEHDLELPVWKMARHNELRLYFDVHPRHMTDAAAAASD
AVVELDPSSTIDFSKSRHFAVLPDVALFAASAFPFSRMADLSETTVLLPPHP
ADGTVGAFVDMMGFAGAISRYPATGVTVRATDMPVDASVTGDILLLSTLD
GLGNGRAALARAGCVRAPSLLARLRARVTQGRDVPACDFTQGALVAAQS
PFAAQRSVVAVLGGTPDALSAMVRDLRDPADTPRFQGDMVIRHGARLDSY
RTGGLYTVGNMPAWMLPDWYLGGHPLLLCGLGGLAALCGTSCAMRVLGA
RSRRRILNDDLTGDL

>bcsC3 (encoding gene at position 2136184:2139981 bp)

MPDGFAMPCRAFMPVGRPVRARMWGGVVLAGALCLYMPRAEAQTPLRY
AETILDGQIEEGAFWIHHGDDMHALHALQRALRIEPDNLEAGLMLGAVQVH
QNDMAGARATLQALQAQPGAQAQVAALRGWIGQAPIDPAALANARSAAD
TGKKLQATLLYRAVFQGAHPLPDMELEYDRVLSGSLSGYTEATQRLRALG
ALLPHDLEIRMALAQALSYRPATRPDAIEDMRQLATAATTPDFIRGEVMQS
WRRTLEWMGADPQAEPYYQEWLALHPDDTEIASRLKAEQAARAQAARLA
LVGAGYHALAHGELEQAERDFSSSMGTDPPRPEALEGLGLVAQRRGDIPA
ARRWLEQARALAPDDAGIRNALAGLDAPGGDPQLARLWALVARHQYDEA
QAMLPAVEKDHGRIADTLRVRAIIAHARHELPRAEAAWRAVLRLVPGDLPA
AAALSDVLIEEGRITEAEGWVARLRAAHYPGVTGLEAGVLGAMAENEPDQ
ARRALLLEQALRDAPHNGWLRLHLAQLWLARGQATRARALMAPLCNLPPK
TDEDTQVCFAFALQDQDMPRADALLARLPRADITAQMADGVAQVRLWHQI
SHLPPDDAQAVPMLEHMPVVPDPEGTQARLVVNALLTRHAPVTAAAGVLH
RALADSAGHVSVNQSLSYAGLFMQIDDPVAAQQVLDGLPAVARGRRLTPT
QARDLRDMTRSLAIAQADRDDIGGHPDAARRLLDPLLAQGPDDADLLLAR
GRVEAALRQPAQAVVYDQKALAIRPDDTMAQAALARDSLASGHEQAARA
MARTLQATHPQWGDTWEIQAEIAGLDGRDRRRLADVQRARALDCTPRDD
GDDSTGYGTRIDAGCAPYRAHAGDEWPDIGTNFVPGMGAGMPEVYHYDP
SLTPVQALDRQADYLQRALVPQADGNLEIRDRSGQPGLGHMTVVNIPMTAI
VPFSSTQHQLALSVMPSVLMSGDPLASGATAQQYGSVAAGGVRPGFHVP
AAVAGVALSAHYQWRWVAADVGSTPLGFTTTNVLGGIELAPHLTHSLTLRL
TGERRAVTDSLLAYSGARDPATGRVWGGVTRNRGHGQLEWAQPGYNLY
AGGGYAVMQGTHTVANHEAEAGAGGSGLLWHRQDAQHLRLGLDLVYFG

YRRNTYFFTWGQGGYFSPHAFMAALVPLTYDGHAGRWTWLFRGEAGYQ
HYTEHATAMFPLGEGGAMAGQRYAGQSTGGLAGNVLARAVYQLTPALRL
GVEGGYSRSGSWDEVHGMLMLHYAPG

>bcsAB4 (encoding gene at position 2248494:2253065 bp)

MLRELWLKWGGEALLTTPRRQAWLIALLMVVGAVLCVSVGDITLAPAEQA
YISIGTITLFFILNRRPGRHITCILMMLSLFVSFRYLIWRLGSTVEFHGPLQVA
MSLALLGAEGYALSTLCLSYFQMSWPLGRKPHRLPDDPADWPMVDVYVP
SYNEDLELVRSTVLGAMDLHWPADKLNVYILDDGRRKAFRDFAVESGAGYI
IRAENNHAKAGNLNHAMQITKGEFVVIFDCDHVPTRSFLLKTIGWLWADPK
LALLQTPHHFYSPDPFQRNLAAGYDVPPEGNMFYGLIQDGNDFWDATFFC
GSCAAIRRSALLSVGGFATETVTEDAHTALKMQRKGWGTAYLCQPLAAGL
ATERLILHIGQRVRWARGMLQIMRRDNPMLGGGLRWEQRLCYLSAMSHFL
FAIPRVTFLVSPLGFLFFGQNIIAASPFAIMVYALPHIFHSIMTLSRIEGRWRY
SFWSEIYETSLALFLIRITIVTLLQPHKGKFNVTDKGGLLARGYFDFSAVYPN
AIMAIILFGGMVRGIWGMIFQYHQKLAFQSFALNTLWITVSLIVVLASIAVGR
ETRQIRHKPRVRVKLPVEVCFADGRVFQAHTTDISLGGAGVTMHLPEQIET
PVDITLRYSKPDDGIDIAVPARILGQQRGSWLHLQWKLDTLEEEREVVSLVF
GRSDAWHNWADFKDDRPLNSIYQVIKSIGGLLAPPYLWSLPSKGQEESSE
SVHKEETLEKKSLVIPPVPHRLGTGIIMLLVGAMLAAIPARAQMPPGYSHTG
VSHLTPLGDTNSGDIPPATDTLDQKLADRVADAEITRTIAFRDLSRFPGPLT
LRGFSPLQGVDVVVPANRVVTHATLHLSGAISPSLLPEATAITVTLNEQYVG
TIRIDPAHPTFGPIEFSIDPLYFTGDSKLNFRFAGEYRRDCNDLYNDVLWAQ
ISDQSTITLTTARIEPVRSLSRLPTPFFDSNLKVAMRVPMVLPGSAMAPEVL
RAGGLVASWFGRLADTRQLTFPVARTLPDTGNAIEIGPRIAIDDRGTPPSG
PTLFEIANPNDKWGTILVVTGRTPAEVEVAARTLVFSPDTLGDLPGAVVED
VTLRPRVAYDAPSFIPTDRPVRFGELVTAGDLQAGGFAPDTLHVPFHLPPD
LYTWHRLPFLMDLWVRAPGNPVVDIAASRLDVSVNNTYIQSYSLLNNNLW
RIWSERMVTEHAGAVGHVTAIPPWLLFGQNDLQFQFDTRPVERGACRRTP
DSPHLEIDSDSVLDFRRGVHFTELPNLSYFAEIGFPFSRMADLGETTVVLPP
APDTDTIGAYFDLMGFFGSVTWYPVSGIHLATTEDIAHTPPEGDVILLAPVG
QMGAAATLLSRSAYRIDGDHIRVGQQTGLQGIWYIFQDRDGSGLRNGVTA

NLDMPVRNAALMIGSESPYASHRSVLALVGDNGIRIHELVASLHDPKVLPTI
QGDLVIKNGEHFTTYRTSPTYTVGHLPWWMWVDWFLSRHPMLMYLCGVT
GAVMLGTGAWLWLRARARRRVKAQEKLDEETARGEHH

>NAD-dependent malic enzyme (encoding gene at position 1377838:1379562 bp)

MSDTAHFPGQVPLHTALSGRELLDCPVLNKGNAFDRRERDLFGLHGLLPA
RIATLAEQVDLACMRLAALPDNFARHIALREIQDRNETLFYAIIDQAPESWLP
IIYTPAIGRACQQFSQIWTRPRGLFLNYTDRGRIAEILASPQWDGVRVIVAS
DGGSILGIGDQGANGMAIPIGKLSLYTACGGLDPACALPVLLDVGTDNAALL
ADPDYIGWRHARVRGAEYDAFIAEFVTAVAARWPDIALHWEDLSGADALRI
LRRYRGSLCTYNDDIQGTAGVTAGALLAAIRAGAAPLADQRIVIFGAGGAG
CGIADLLAQMMVRAGMAAHEARSRFFMVDINGLVRHGMEGVTEGQMPFA
QPADVAADWQVADPAHVTLAEVMAHVCPTTLIGTSGQGGAFTRQIVAPMA
RQAARPVVFALSNPTANIEALPADLLEWTDGRAIIGTGGPFAPVTHAGRTR
PVDQINNSYVFPGVGLAVMAGGITRMTDGMFLAAADALAGLSPAVGAGGG
HDAALLPPVSALRPVAMAVARAVIRQGGQAEGVAPAMPETGIGAMLAAAMW
SPRYRPYEKTPPARP

>Pyruvate phosphate dikinase (encoding gene at position 2567253:2569928 bp)

MTKWVYSFGDGLNEGRADMRNLLGGKGANLAEMAANGLPVPPGFTITTE
VCSAFYENGRKYPDELKAQVDAALQRVEQSMGLRFGDPEAPLLVSVRSG
ARVSMPGMMDTVLNLGLNDQTVEGLARSSGDARFAWDSYRRFIQMYGSV
VMGVPHHHFEDVLEQFKRANNVEDDTAITAGQWRAIVVDYTHIITTHTGTD
FPTNPQDQLWGAIGAVFGSWMNPRANTYRKLHEIPASWGTAVNVQSMVF
GNMGDDCATGVCFTRDPSTGENIFYGEYLINAQGEDVVAGIRTPQPMACA
RAEAGQHPMETTLPQAYAELLRVRSILETHYKDMQDIEFTVQRNVLYILQT
RNGKRTAAAALKIAIDMAREGLITQEEAIQRVPAASLDQLLHPTLDPRAERV
QLTRGLPASPGAAAGAVVFTAEECEARAAKGEDVILVRIETSPEDVHGMHA
ARGVLTTRGGMTSHAAVVARGMGRVCVAGAGGIHVDYAAGSLSVGSHTV
KEGEWITLDGGTGAVYLGRVPTIEPVLSDDFNTLMGWADGVRRLGVRANA
ETPDDARTARRFGAEGIGLARTEHMFFGPDRIGFVRQMIIADEESVRQKAIA

ALLPFQREDFASLFRIMAGLPVTVRLLDPPLHEFLPHEAAEMAEVAQALGR
SVEDVRARCAALAETNPMLGHRGCRLGLTSPEIYAMQVRALIQAAVLVEKE
LGRPIHPEIMIPLVATKAELATTRRAAEDEIARVLKEEGTNLSYSIGTMIELPR
AAIQADQIAEYADFFSFGTNDLTQTTFGLSRDDAGSFLPYYVDQGLLPRDP
FVSIDRDGVGALVRLGVERGRQTSADLKLGICGEHGGDPDSIAFFDEVGLD
YVSCSPFRVPVARLAAAQAALATRQKAASPA

References

Al-Abdallah, W., & Dahman, Y. (2013). Production of green biocellulose nanofibers by Gluconacetobacter xylinus through utilizing the renewable resources of agriculture residues. *Bioprocess and Biosystems Engineering*, *36*(11), 1735–1743. https://doi.org/10.1007/s00449-013-0948-9

Alauzet, C., Teyssier, C., Jumas-Bilak, E., Gouby, A., Chiron, R., Rabaud, C., Counil, F., Lozniewski, A., & Marchandin, H. (2010). Gluconobacter as well as Asaia species, newly emerging opportunistic human pathogens among acetic acid bacteria. *Journal of Clinical Microbiology*, *48*(11), 3935–3942. https://doi.org/10.1128/JCM.00767-10

Alonso, S., Rendueles, M., & Díaz, M. (2013). Bio-production of lactobionic acid: Current status, applications and future prospects. *Biotechnology Advances*, *31*(8), 1275–1291. https://doi.org/10.1016/j.biotechadv.2013.04.010

Andritsou, V., De Melo, E. M., Tsouko, E., Ladakis, D., Maragkoudaki, S., Koutinas, A. A., & Matharu, A. S. (2018). Synthesis and Characterization of Bacterial Cellulose from Citrus-Based Sustainable Resources. *ACS Omega*, *3*(8), 10365–10373. https://doi.org/10.1021/acsomega.8b01315

Azuma, Y., Hosoyama, A., Matsutani, M., Furuya, N., Horikawa, H., Harada, T., Hirakawa, H., Kuhara, S., Matsushita, K., Fujita, N., & Shirai, M. (2009). Whole-genome analyses reveal genetic instability of Acetobacter pasteurianus. *Nucleic Acids Research*, *37*(17), 5768–5783. https://doi.org/10.1093/nar/gkp612

Bassetti, M., Pecori, D., Sartor, A., Londero, A., Villa, G., Cadeo, B., Brillo, F., Bongiorno, D., Campanile, F., & Stefani, S. (2013). First report of endocarditis by Gluconobacter spp. in a patient with a history of intravenous-drug abuse. *Journal of Infection*, *66*(3), 285–287. https://doi.org/10.1016/j.jinf.2012.05.006

Battad-Bernardo, E., McCrindle, S. L., Couperwhite, I., & Neilan, B. A.

(2004). Insertion of an E. coli lacZ gene in Acetobacter xylinus for the production of cellulose in whey. *FEMS Microbiology Letters*, *231*(2), 253–260. https://doi.org/10.1016/S0378-1097(04)00007-2

Bell, E. L., Finnigan, W., France, S. P., Hepworth, L. J., Lovelock, S. L., Hayes, M. A., Osuna, S., Romero, E., Ryan, K. S., Turner, N. J., & Flitsch, S. L. (2021). *Biocatalysis 1 1 2*. *0123456789*, 1–21. https://doi.org/10.1038/s43586-021-00044-z

Blank, M., & Schweiger, P. (2018). Surface display for metabolic engineering of industrially important acetic acid bacteria. *PeerJ*, *2018*(4), 1–19. https://doi.org/10.7717/peerj.4626

Bolger, A. M., Lohse, M., & Usadel, B. (2014). Trimmomatic: a flexible trimmer for Illumina sequence data. *Bioinformatics*, *30*(15), 2114–2120. https://doi.org/10.1093/bioinformatics/btu170

Bron, P. A., & Kleerebezem, M. (2018). Lactic acid bacteria for delivery of endogenous or engineered therapeutic molecules. *Frontiers in Microbiology*, *9*(AUG), 1–4. https://doi.org/10.3389/fmicb.2018.01821

Caro-Astorga, J., Walker, K. T., Herrera, N., Lee, K. Y., & Ellis, T. (2021). Bacterial cellulose spheroids as building blocks for 3D and patterned living materials and for regeneration. *Nature Communications*, *12*(1), 1–9. https://doi.org/10.1038/s41467-021-25350-8

Carreira, P., Mendes, J. A. S., Trovatti, E., Serafim, L. S., Freire, C. S. R., Silvestre, A. J. D., & Neto, C. P. (2011). Utilization of residues from agro-forest industries in the production of high value bacterial cellulose. *Bioresource Technology*, *102*(15), 7354–7360. https://doi.org/10.1016/j.biortech.2011.04.081

Carvalho, R. D. D. O., do Carmo, F. L. R., Junior, A. de O., Langella, P., Chatel, J. M., Bermúdez-Humarán, L. G., Azevedo, V., & de Azevedo, M. S. (2017). Use of wild type or recombinant lactic acid bacteria as an alternative treatment for gastrointestinal inflammatory diseases: A focus on inflammatory bowel diseases and mucositis. *Frontiers in Microbiology*, *8*(MAY), 1–13. https://doi.org/10.3389/fmicb.2017.00800

Chavarrı, M., Silva-rocha, R., Martı, E., Heras, A. De, Pa, A. D., Arce-rodrı, A., Kim, J., Nikel, P. I., Durante-rodrı, G., & Lorenzo, D. (2013). *The Standard European Vector Architecture (SEVA): a coherent platform for the analysis and deployment of complex prokaryotic phenotypes*. *41*(November 2012), 666–675. https://doi.org/10.1093/nar/gks1119

Chhabra, S. R., & Keasling, J. D. (2019). Metabolic design and control for production in prokaryotes. *Comprehensive Biotechnology*, 217–230. https://doi.org/10.1016/B978-0-444-64046-8.00018-5

Collén, A., Saloheimo, M., Bailey, M., Penttilä, M., & Pakula, T. M. (2005). Protein production and induction of the unfolded protein response in Trichoderma reesei strain Rut-C30 and its transformant expressing endoglucanase I with a hydrophobic tag. *Biotechnology and Bioengineering*, *89*(3), 335–344. https://doi.org/10.1002/bit.20350

Deng, Y., Nagachar, N., Xiao, C., Tien, M., & Kao, T. H. (2013). Identification and characterization of non-cellulose-producing mutants of Gluconacetobacter hansenii generated by Tn5 transposon mutagenesis. *Journal of Bacteriology*, *195*(22), 5072–5083. https://doi.org/10.1128/JB.00767-13

Deppenmeier, U., Hoffmeister, M., & Prust, C. (2002). Biochemistry and biotechnological applications of Gluconobacter strains. *Applied Microbiology and Biotechnology*, *60*(3), 233–242. https://doi.org/10.1007/s00253-002-1114-5

Devine, P. N., Howard, R. M., Kumar, R., Thompson, M. P., Truppo, M. D., & Turner, N. J. (2018). Extending the application of biocatalysis to meet the challenges of drug development. *Nature Reviews Chemistry*, *2*(12), 409–421. https://doi.org/10.1038/s41570-018-0055-1

Elzer, P. H., Roop, R. M., Kovach, M. E., Robertson, G. T., Peterson, K. M., Steven Hill, D., & Farris, M. A. (2002). Four new derivatives of the broad-host-range cloning vector pBBR1MCS, carrying different antibiotic-resistance cassettes. *Gene*, *166*(1), 175–176. https://doi.org/10.1016/0378-1119(95)00584-1

Faber, K. (2011). Biocatalytic Applications. In *Biotransformations in Organic Chemistry*. https://doi.org/10.1007/978-3-642-17393-6_2

Florea, M., Hagemann, H., Santosa, G., Abbott, J., Micklem, C. N., Spencer-Milnes, X., De Arroyo Garcia, L., Paschou, D., Lazenbatt, C., Kong, D., Chughtai, H., Jensen, K., Freemont, P. S., Kitney, R., Reeve, B., & Ellis, T. (2016). Engineering control of bacterial cellulose production using a genetic toolkit and a new celluloseproducing strain. *Proceedings of the National Academy of Sciences of the United States of America*, *113*(24), E3431–E3440. https://doi.org/10.1073/pnas.1522985113

Florea, M., Reeve, B., Abbott, J., Freemont, P. S., & Ellis, T. (2016). Genome sequence and plasmid transformation of the model high-yield bacterial cellulose producer Gluconacetobacter hansenii ATCC 53582. *Scientific Reports*, *6*(September 2015), 1–9. https://doi.org/10.1038/srep23635

FREESE, E. B. (1961). *TRANSITIONS AND TRANSVERSIONS INDUCED BY DEPURINATING AGENTS*. 540–545.

Fukaya, M., & Iwata, T. (1985). *of Plasmids in cultivation and they suggested that a plasmid*. *49*(5), 1349–1355.

Fukaya, M., Tayama, K., Okumura, H., Masai, H., & Beppu, T. (2014). *Improved Transformation Method for Acetobacter with Plasmid DNA*. *1369*. https://doi.org/10.1080/00021369.1985.10867039

Fukaya, M., Tayama, K., Okumura, H., Masai, H., Uozumi, T., & Beppu, T. (1985). Improved transformation method for acetobacter with plasmid dna. *Agricultural and Biological Chemistry*, *49*(7), 2091–2097. https://doi.org/10.1080/00021369.1985.10867039

Gao, F., & Zhang, C.-T. (2008). Ori-Finder: A web-based system for finding oriC s in unannotated bacterial genomes. *BMC Bioinformatics*, *9*(1), 79. https://doi.org/10.1186/1471-2105-9-79

Gao, J. X., Li, P., Du, X. J., Han, Z. H., Xue, R., Liang, B., & Wang, S. (2017). A negative regulator of cellulose biosynthesis, bcsR, affects

biofilm formation, and adhesion/invasion ability of Cronobacter sakazakii. *Frontiers in Microbiology*, *8*(SEP), 1–11. https://doi.org/10.3389/fmicb.2017.01839

Gao, L., Wu, X., Zhu, C., Jin, Z., Wang, W., & Xia, X. (2020). Metabolic engineering to improve the biomanufacturing efficiency of acetic acid bacteria: advances and prospects. *Critical Reviews in Biotechnology*, *40*(4), 522–538. https://doi.org/10.1080/07388551.2020.1743231

Geng, Y., & Doberstein, B. (2010). *Developing the circular economy in China : Challenges and opportunities for achieving ' leapfrog development ' Developing the circular economy in China : Challenges and opportunities for achieving ' leapfrog development .' 4509*. https://doi.org/10.3843/SusDev.15.3

Gerstel, U., & Römling, U. (2003). The csgD promoter, a control unit for biofilm formation in Salmonella typhimurium. *Research in Microbiology*, *154*(10), 659–667. https://doi.org/10.1016/j.resmic.2003.08.005

Gilbert, C., Tang, T. C., Ott, W., Dorr, B. A., Shaw, W. M., Sun, G. L., Lu, T. K., & Ellis, T. (2021). Living materials with programmable functionalities grown from engineered microbial co-cultures. *Nature Materials*. https://doi.org/10.1038/s41563-020-00857-5

Gomes, R. J., Hernan, R. J., & Spinosa, A. (2018). *Acetic Acid Bacteria in the Food Industry : Systematics , Characteristics and Applications*. *0262*, 0–2. https://doi.org/10.17113/ftb.56.02.18.5593

Goosens, V. J., Walker, K. T., Aragon, S. M., Singh, A., Senthivel, V. R., Caro-astorga, J., Buat, M. L. A., Song, W., Lee, K., & Ellis, T. (2021). *Komagataeibacter tool kit (KTK): a modular cloning system for multigene constructs and programmed protein secretion from cellulose producing bacteria 3*. 1–21.

Guizelini, D., Raittz, R. T., Cruz, L. M., Souza, E. M., Steffens, M. B. R., & Pedrosa, F. O. (2016). GFinisher: a new strategy to refine and finish bacterial genome assemblies. *Scientific Reports*, *6*(1), 34963. https://doi.org/10.1038/srep34963

Gullo, M. (2018). *Biotechnological production of cellulose by acetic acid bacteria : current state and perspectives*. 6885–6898.

Güzel, M., & Akpınar, Ö. (2019). Production and Characterization of Bacterial Cellulose from Citrus Peels. *Waste and Biomass Valorization*, *10*(8), 2165–2175. https://doi.org/10.1007/s12649-018-0241-x

Ha, J. H., Shehzad, O., Khan, S., Lee, S. Y., Park, J. W., Khan, T., & Park, J. K. (2008). Production of bacterial cellulose by a static cultivation using the waste from beer culture broth. *Korean Journal of Chemical Engineering*, *25*(4), 812–815. https://doi.org/10.1007/s11814-008-0134-y

Hanke, T., Nöh, K., Noack, S., Polen, T., Bringer, S., Sahm, H., Wiechert, W., & Bott, M. (2013). Combined fluxomics and transcriptomics analysis of glucose catabolism via a partially cyclic pentose phosphate pathway in Gluconobacter oxydans 621H. *Applied and Environmental Microbiology*, *79*(7), 2336–2348. https://doi.org/10.1128/AEM.03414-12

Hattori, H., Yakushi, T., Matsutani, M., Moonmangmee, D., Toyama, H., Adachi, O., & Matsushita, K. (2012). High-temperature sorbose fermentation with thermotolerant Gluconobacter frateurii CHM43 and its mutant strain adapted to higher temperature. *Applied Microbiology and Biotechnology*, *95*(6), 1531–1540. https://doi.org/10.1007/s00253-012-4005-4

Hayata, Y. (2002). NII-Electronic Library Service. *Chemical Pharmaceutical Bulletin*, *43*, 2091.

Hu, S. Q., Gao, Y. G., Tajima, K., Sunagawa, N., Zhou, Y., Kawano, S., Fujiwara, T., Yoda, T., Shimura, D., Satoh, Y., Munekata, M., Tanaka, I., & Yao, M. (2010). Structure of bacterial cellulose synthase subunit D octamer with four inner passageways. *Proceedings of the National Academy of Sciences of the United States of America*, *107*(42), 17957–17961. https://doi.org/10.1073/pnas.1000601107

Hu, Y., Wan, H., Li, J., & Zhou, J. (2015). Enhanced production of l-sorbose in an industrial Gluconobacter oxydans strain by identification of a

strong promoter based on proteomics analysis. *Journal of Industrial Microbiology and Biotechnology*, *42*(7), 1039–1047. https://doi.org/10.1007/s10295-015-1624-7

Hungund, B. S., & Gupta, S. G. (2010). Strain improvement of Gluconacetobacter xylinus NCIM 2526 for bacterial cellulose production. *African Journal of Biotechnology*, *9*(32), 5170–5172. https://doi.org/10.5897/AJB09.1877

Hussain, Z., Sajjad, W., Khan, T., & Wahid, F. (2019). Production of bacterial cellulose from industrial wastes: a review. *Cellulose*, *26*(5), 2895–2911. https://doi.org/10.1007/s10570-019-02307-1

Inoue, T., Sunagawa, M., Mori, A., Imai, C., Fukuda, M., Takagi, M., & Yano, K. (1989). Cloning and sequencing of the gene encoding the 72-kilodalton dehydrogenase subunit of alcohol dehydrogenase from Acetobacter aceti. *Journal of Bacteriology*, *171*(6), 3115–3122. https://doi.org/10.1128/jb.171.6.3115-3122.1989

Ishikawa, A., Matsuoka, M., Tsuchida, T., & Yoshinaga, F. (1995). Increase in Cellulose Production by Sulfaguanidine-Resistant Mutants Derived from Acetobacter Xylinum Subsp. Sucrofermentans. *Bioscience, Biotechnology, and Biochemistry*, *59*(12), 2259–2262. https://doi.org/10.1271/bbb.59.2259

Iyer, P. R., Geib, S. M., Catchmark, J., Kao, T. H., & Tien, M. (2010). Genome sequence of a cellulose-producing bacterium, Gluconacetobacter hansenii ATCC 23769. *Journal of Bacteriology*, *192*(16), 4256–4257. https://doi.org/10.1128/JB.00588-10

Jacek, P., Ryngajłło, M., & Bielecki, S. (2019). Structural changes of bacterial nanocellulose pellicles induced by genetic modification of Komagataeibacter hansenii ATCC 23769. *Applied Microbiology and Biotechnology*, *103*(13), 5339–5353. https://doi.org/10.1007/s00253-019-09846-4

Jakob, F., Pfaff, A., Novoa-Carballal, R., Rübsam, H., Becker, T., & Vogel, R. F. (2013). Structural analysis of fructans produced by acetic acid

bacteria reveals a relation to hydrocolloid function. *Carbohydrate Polymers*, *92*(2), 1234–1242. https://doi.org/10.1016/j.carbpol.2012.10.054

Jun, H., Kieselbach, T., & Jönsson, L. J. (2011). Enzyme production by filamentous fungi: Analysis of the secretome of Trichoderma reesei grown on unconventional carbon source. *Microbial Cell Factories*, *10*, 1–10. https://doi.org/10.1186/1475-2859-10-68

Kallnik, V., Meyer, M., Deppenmeier, U., & Schweiger, P. (2010). Construction of expression vectors for protein production in Gluconobacter oxydans. *Journal of Biotechnology*, *150*(4), 460–465. https://doi.org/10.1016/j.jbiotec.2010.10.069

KAWANO, S., TAJIMA, K., KONO, H., ERATA, T., MUNEKATA, M., & TAKAI, M. (2002). Effects of Endogenous Endo-β-1,4-Glucanase on Cellulose Biosynthesis in Acetobacter xylinum ATCC23769. *Journal of Bioscience and Bioengineering*, *94*(3), 275–281. https://doi.org/10.1263/jbb.94.275

Kiefler, I., Bringer, S., & Bott, M. (2015). SdhE-dependent formation of a functional Acetobacter pasteurianus succinate dehydrogenase in Gluconobacter oxydans—a first step toward a complete tricarboxylic acid cycle. *Applied Microbiology and Biotechnology*, *99*(21), 9147–9160. https://doi.org/10.1007/s00253-015-6972-8

Kiefler, I., Bringer, S., & Bott, M. (2017). Metabolic engineering of Gluconobacter oxydans 621H for increased biomass yield. *Applied Microbiology and Biotechnology*, *101*(13), 5453–5467. https://doi.org/10.1007/s00253-017-8308-3

Kim, Y.-J., Kim, J.-N., Wee, Y.-J., Park, D.-H., & Ryu, H.-W. (2007). Bacterial Cellulose Production by Gluconacetobacter sp. RKY5 in a Rotary Biofilm Contactor. *Applied Biochemistry and Biotecnology*, *136*(4), 529–537. https://doi.org/10.1007/978-1-60327-181-3_44

Kondo, K., & Horinouchi, S. (1997). A new insertion sequence IS1452 from Acetobacter pasteurianus. *Microbiology*, *143*(2), 539–546.

https://doi.org/10.1099/00221287-143-2-539

Kosciow, K., Zahid, N., Schweiger, P., & Deppenmeier, U. (2014). Production of a periplasmic trehalase in gluconobacter oxydans and growth on trehalose. *Journal of Biotechnology*, *189*, 27–35. https://doi.org/10.1016/j.jbiotec.2014.08.029

Kovach, M. E., Elzer, P. H., Hill, D. S., Robertson, G. T., Farris, M. A., Roop, R. M., & Peterson, K. M. (1995). Four new derivatives of the broad-host-range cloning vector pBBR1MCS, carrying different antibiotic-resistance cassettes. *Gene*, *166*(1), 175–176. http://www-ab.informatik.uni-tuebingen.de/toolbox/index.php?view=domainpred

Krystynowicz, A., Koziołkiewicz, M., Wiktorowska-Jezierska, A., Bielecki, S., Klemenska, E., Masny, A., & Płucienniczak, A. (2005). Molecular basis of cellulose biosynthesis disappearance in submerged culture of Acetobacter xylinum. *Acta Biochimica Polonica*, *52*(3), 691–698. https://doi.org/10.18388/abp.2005_3432

Kubiak, K., Kurzawa, M., Jedrzejczak-Krzepkowska, M., Ludwicka, K., Krawczyk, M., Migdalski, A., Kacprzak, M. M., Loska, D., Krystynowicz, A., & Bielecki, S. (2014). Complete genome sequence of Gluconacetobacter xylinus E25 strain-Valuable and effective producer of bacterial nanocellulose. *Journal of Biotechnology*, *176*(1), 18–19. https://doi.org/10.1016/j.jbiotec.2014.02.006

Kuo, C. H., Teng, H. Y., & Lee, C. K. (2015). Knock-out of glucose dehydrogenase gene in Gluconacetobacter xylinus for bacterial cellulose production enhancement. *Biotechnology and Bioprocess Engineering*, *20*(1), 18–25. https://doi.org/10.1007/s12257-014-0316-x

Le Loir, Y., Azevedo, V., Oliveira, S. C., Freitas, D. A., Miyoshi, A., Bermúdez-Humarán, L. G., Nouaille, S., Ribeiro, L. A., Leclercq, S., Gabriel, J. E., Guimaraes, V. D., Oliveira, M. N., Charlier, C., Gautier, M., & Langella, P. (2005). Protein secretion in Lactococcus lactis: An efficient way to increase the overall heterologous protein production. *Microbial Cell Factories*, *4*, 1–13. https://doi.org/10.1186/1475-2859-4-2

Lee, K. Y., Buldum, G., Mantalaris, A., & Bismarck, A. (2014). More than meets the eye in bacterial cellulose: Biosynthesis, bioprocessing, and applications in advanced fiber composites. *Macromolecular Bioscience*, *14*(1), 10–32. https://doi.org/10.1002/mabi.201300298

Legastelois, I., Buffin, S., Peubez, I., Mignon, C., Sodoyer, R., & Werle, B. (2017). Non-conventional expression systems for the production of vaccine proteins and immunotherapeutic molecules. *Human Vaccines and Immunotherapeutics*, *13*(4), 947–961. https://doi.org/10.1080/21645515.2016.1260795

Li, Y., Tian, J., Tian, H., Chen, X., Ping, W., Tian, C., & Lei, H. (2016). Mutation-based selection and analysis of Komagataeibacter hansenii HDM1-3 for improvement in bacterial cellulose production. *Journal of Applied Microbiology*, *121*(5), 1323–1334. https://doi.org/10.1111/jam.13244

Liu, M., Li, S., Xie, Y., Jia, S., Hou, Y., Zou, Y., & Zhong, C. (2018). Enhanced bacterial cellulose production by Gluconacetobacter xylinus via expression of Vitreoscilla hemoglobin and oxygen tension regulation. *Applied Microbiology and Biotechnology*, *102*(3), 1155–1165. https://doi.org/10.1007/s00253-017-8680-z

Lynch, K. M., Zannini, E., Wilkinson, S., Daenen, L., & Arendt, E. K. (2019). Physiology of Acetic Acid Bacteria and Their Role in Vinegar and Fermented Beverages. *Comprehensive Reviews in Food Science and Food Safety*, *18*(3), 587–625. https://doi.org/10.1111/1541-4337.12440

M. Iguchi;, S. Yamanaka;, & A. Budhiono; (2000). Bacterial cellulose - a masterpiece of nature's arts. *Journal of Materials Science*, *35*(2), 261–270. https://doi.org/10.1023/A

TOWARDS THE CIRCULAR ECONOMY.

Macauley-Patrick, S., Fazenda, M. L., McNeil, B., & Harvey, L. M. (2005). Heterologous protein production using the Pichia pastoris expression system. *Yeast*, *22*(4), 249–270. https://doi.org/10.1002/yea.1208

Mangayil, R., Rajala, S., Pammo, A., Sarlin, E., Luo, J., Santala, V., Karp,

M., & Tuukkanen, S. (2017). Engineering and Characterization of Bacterial Nanocellulose Films as Low Cost and Flexible Sensor Material. *ACS Applied Materials and Interfaces*, *9*(22), 19048–19056. https://doi.org/10.1021/acsami.7b04927

Marchler-Bauer, A., Derbyshire, M. K., Gonzales, N. R., Lu, S., Chitsaz, F., Geer, L. Y., Geer, R. C., He, J., Gwadz, M., Hurwitz, D. I., Lanczycki, C. J., Lu, F., Marchler, G. H., Song, J. S., Thanki, N., Wang, Z., Yamashita, R. A., Zhang, D., Zheng, C., & Bryant, S. H. (2015). CDD: NCBI's conserved domain database. *Nucleic Acids Research*, *43*(D1), D222–D226. https://doi.org/10.1093/nar/gku1221

Martínez-García, E., Calles, B., Arévalo-Rodríguez, M., & De Lorenzo, V. (2011). PBAM1: An all-synthetic genetic tool for analysis and construction of complex bacterial phenotypes. *BMC Microbiology*, *11*(1), 38. https://doi.org/10.1186/1471-2180-11-38

Martínez, L. C., & Vadyvaloo, V. (2014). Mechanisms of post-transcriptional gene regulation in bacterial biofilms. *Frontiers in Cellular and Infection Microbiology*, *5*(MAR), 1–15. https://doi.org/10.3389/fcimb.2014.00038

Matsushita K., Toyama H., Tonouchi N., O.-K. A. (eds). (2016). Industrial Application of Acetic Acid Bacteria (Vitamin C and Others). In *Acetic Acid Bacteria.: Vol. 1호* (Issue May, pp. 31–48).

Matsutani, M., Nishikura, M., Saichana, N., Hatano, T., Masud-Tippayasak, U., Theergool, G., Yakushi, T., & Matsushita, K. (2013). Adaptive mutation of Acetobacter pasteurianus SKU1108 enhances acetic acid fermentation ability at high temperature. *Journal of Biotechnology*, *165*(2), 109–119. https://doi.org/10.1016/j.jbiotec.2013.03.006

Merfort, M., Herrmann, U., Bringer-Meyer, S., & Sahm, H. (2006). High-yield 5-keto-D-gluconic acid formation is mediated by soluble and membrane-bound gluconate-5-dehydrogenases of Gluconobacter oxydans. *Applied Microbiology and Biotechnology*, *73*(2), 443–451. https://doi.org/10.1007/s00253-006-0467-6

Merfort, M., Herrmann, U., Ha, S. W., Elfari, M., Bringer-Meyer, S., Görisch, H., & Sahm, H. (2006). Modification of the membrane-bound glucose oxidation system in Gluconobacter oxydans significantly increases gluconate and 5-keto-D-gluconic acid accumulation. *Biotechnology Journal*, *1*(5), 556–563. https://doi.org/10.1002/biot.200600032

Meyer, M., Schweiger, P., & Deppenmeier, U. (2013). Effects of membrane-bound glucose dehydrogenase overproduction on the respiratory chain of Gluconobacter oxydans. *Applied Microbiology and Biotechnology*, *97*(8), 3457–3466. https://doi.org/10.1007/s00253-012-4265-z

Mientus, M., Kostner, D., Peters, B., Liebl, W., & Ehrenreich, A. (2017). Characterization of membrane-bound dehydrogenases of Gluconobacter oxydans 621H using a new system for their functional expression. *Applied Microbiology and Biotechnology*, *101*(8), 3189–3200. https://doi.org/10.1007/s00253-016-8069-4

Mostafa, H. E., Mostafa, H. E., Geis, A., & Geis, A. (2002). Cloning of. *Society*, *68*(5), 2619–2623. https://doi.org/10.1128/AEM.68.5.2619

Murooka, Y., Takizawa, N., & Harada, T. (1981). Introduction of bacteriophage mu into bacteria of various genera and intergeneric gene transfer by RP4::Mu. *Journal of Bacteriology*, *145*(1), 358–368. https://doi.org/10.1128/jb.145.1.358-368.1981

Nakai, T., Tonouchi, N., Konishi, T., Kojima, Y., Tsuchida, T., Yoshinaga, F., Sakai, F., & Hayashi, T. (1999). Enhancement of cellulose production by expression of sucrose synthase in Acetobacter xylinum. *Proceedings of the National Academy of Sciences of the United States of America*, *96*(1), 14–18. https://doi.org/10.1073/pnas.96.1.14

Ninla Elmawati Falabiba, Anggaran, W., Mayssara A. Abo Hassanin Supervised, A., Wiyono, B. ., Ninla Elmawati Falabiba, Zhang, Y. J., Li, Y., & Chen, X. (2014). Central Carbon Metabolism and Respiration in Gluconobacter oxydans. In *Acetic Acid Bacteria: Ecology and Physiology* (Vol. 5, Issue 2, pp. 40–51).

Ohmori, S., Uozumi, T., & Beppu, T. (1982). Loss of acetic acid resistance

and ethanol oxidizing ability in an Acetobacter strain. *Agricultural and Biological Chemistry*, *46*(2), 381–389. https://doi.org/10.1080/00021369.1982.10865082

Okonechnikov, K., Golosova, O., & Fursov, M. (2012). Unipro UGENE: a unified bioinformatics toolkit. *Bioinformatics*, *28*(8), 1166–1167. https://doi.org/10.1093/bioinformatics/bts091

Okumura, H., Tagami, H., Fukaya, M., Masai, H., Kawamura, Y., Horinouchi, S., & Beppu, T. (1988). Cloning of the β-Isopropylmalate Dehydrogenase Gene from Acetobacter aceti and Its Use for Construction of a New Host-Vector System for Acetobacter. *Agricultural and Biological Chemistry*, *52*(12), 3125–3129. https://doi.org/10.1271/bbb1961.52.3125

Omadjela, O., Narahari, A., Strumillo, J., Mélida, H., Mazur, O., Bulone, V., & Zimmer, J. (2013). BcsA and BcsB form the catalytically active core of bacterial cellulose synthase sufficient for in vitro cellulose synthesis. *Proceedings of the National Academy of Sciences of the United States of America*, *110*(44), 17856–17861. https://doi.org/10.1073/pnas.1314063110

Onouchi, N. T., Ugiyama, M. S., & Okozeki, K. Y. (2003). *Construction of a Vector Plasmid for Use in Gluconobacter oxydans*. *67*(1), 211–213.

Park, S., Baker, J. O., Himmel, M. E., Parilla, P. A., & Johnson, D. K. (2010). Cellulose crystallinity index: measurement techniques and their impact on interpreting cellulase performance. *Biotechnology for Biofuels*, *3*(1), 10. https://doi.org/10.1186/1754-6834-3-10

Pasteur, L. P. (1864). *Mémoire sur la fermentation acétique Annales*. *1*.

Patel, R. N. (2016). Green biocatalysis. In *Hoboken, New Jersey : John Wiley & Sons*. https://doi.org/10.1201/9781482269802-30

Peterbauer, C., Maischberger, T., & Haltrich, D. (2011). Food-grade gene expression in lactic acid bacteria. *Biotechnology Journal*, *6*(9), 1147–1161. https://doi.org/10.1002/biot.201100034

Peters, B., Junker, A., Brauer, K., Mühlthaler, B., Kostner, D., Mientus, M.,

Liebl, W., & Ehrenreich, A. (2013). Deletion of pyruvate decarboxylase by a new method for efficient markerless gene deletions in Gluconobacter oxydans. *Applied Microbiology and Biotechnology*, *97*(6), 2521–2530. https://doi.org/10.1007/s00253-012-4354-z

Peters, B., Mientus, M., Kostner, D., Junker, A., Liebl, W., & Ehrenreich, A. (2013). Characterization of membrane-bound dehydrogenases from Gluconobacter oxydans 621H via whole-cell activity assays using multideletion strains. *Applied Microbiology and Biotechnology*, *97*(14), 6397–6412. https://doi.org/10.1007/s00253-013-4824-y

Qi, Z., Wang, W., Yang, H., Xia, X., & Yu, X. (2014). Mutation of Acetobacter pasteurianus by UV irradiation under acidic stress for high-acidity vinegar fermentation. *International Journal of Food Science and Technology*, *49*(2), 468–476. https://doi.org/10.1111/ijfs.12324

Saichana, N., Matsushita, K., Adachi, O., Frébort, I., & Frebortova, J. (2015). Acetic acid bacteria: A group of bacteria with versatile biotechnological applications. *Biotechnology Advances*, *33*(6), 1260–1271. https://doi.org/10.1016/j.biotechadv.2014.12.001

Saito, Y., Ishii, Y., Hayashi, H., Imao, Y., Akashi, T., Yoshikawa, K., Noguchi, Y., Soeda, S., Yoshida, M., Niwa, M., Hosoda, J., & Shimomura, K. (1997). Cloning of genes coding for L-sorbose and L-sorbosone dehydrogenases from Gluconobacter oxydans and microbial production of 2-keto-L-gulonate, a precursor of L-ascorbic acid, in a recombinant G. oxydans strain. *Applied and Environmental Microbiology*, *63*(2), 454–460. https://doi.org/10.1128/aem.63.2.454-460.1997

Sauer, U., & Eikmanns, B. J. (2005). The PEP—pyruvate—oxaloacetate node as the switch point for carbon flux distribution in bacteria: We dedicate this paper to Rudolf K. Thauer, Director of the Max-Planck-Institute for Terrestrial Microbiology in Marburg, Germany, on the occasion of his 65th. *FEMS Microbiology Reviews*, *29*(4), 765–794. https://doi.org/10.1016/j.femsre.2004.11.002

Saxena, I. M., Kudlicka, K., Okuda, K., & Brown, R. M. (1994). Characterization of genes in the cellulose-synthesizing operon (acs operon) of Acetobacter xylinum: Implications for cellulose crystallization. *Journal of Bacteriology*, *176*(18), 5735–5752. https://doi.org/10.1128/jb.176.18.5735-5752.1994

Schleyer, U., Bringer-meyer, S., & Sahm, H. (2008). *An easy cloning and expression vector system for Gluconobacter oxydans*. *125*, 91–95. https://doi.org/10.1016/j.ijfoodmicro.2007.04.016

Schmidt, F. R. (2004). Recombinant expression systems in the pharmaceutical industry. *Applied Microbiology and Biotechnology*, *65*(4), 363–372. https://doi.org/10.1007/s00253-004-1656-9

Scott Williams, W. S., & Cannon, R. E. (1989). Alternative environmental roles for cellulose produced by Acetobacter xylinum. *Applied and Environmental Microbiology*, *55*(10), 2448–2452. https://doi.org/10.1128/aem.55.10.2448-2452.1989

Shi, L., Li, K., Zhang, H., Liu, X., Lin, J., & Wei, D. (2014). Identification of a novel promoter gHp0169 for gene expression in Gluconobacter oxydans. *Journal of Biotechnology*, *175*(1), 69–74. https://doi.org/10.1016/j.jbiotec.2014.01.035

Shi, Y. Y., Li, K. F., Lin, J. P., Yang, S. L., & Wei, D. Z. (2015). Engineered Expression Vectors Significantly Enhanced the Production of 2-Keto-D-gluconic Acid by Gluconobacter oxidans. *Journal of Agricultural and Food Chemistry*, *63*(22), 5492–5498. https://doi.org/10.1021/acs.jafc.5b01652

Siemen, A., Kosciow, K., Schweiger, P., & Deppenmeier, U. (2018). Production of 5-ketofructose from fructose or sucrose using genetically modified Gluconobacter oxydans strains. *Applied Microbiology and Biotechnology*, *102*(4), 1699–1710. https://doi.org/10.1007/s00253-017-8699-1

Solieri Lisa, G. P. (2009). Vinegars of the World. In *Spiringer*.

Spohner, S. C., Müller, H., Quitmann, H., & Czermak, P. (2015). Expression

of enzymes for the usage in food and feed industry with Pichia pastoris. *Journal of Biotechnology*, *202*, 118–134. https://doi.org/10.1016/j.jbiotec.2015.01.027

STEEL, R., & WALKER, T. K. (1957). A comparative study of cellulose-producing cultures and celluloseless mutants of certain Acetobacter spp. *Journal of General Microbiology*, *17*(2), 445–452. https://doi.org/10.1099/00221287-17-2-445

Steiner, P., & Sauer, U. (2003). Long-term continuous evolution of acetate resistant Acetobacter aceti. *Biotechnology and Bioengineering*, *84*(1), 40–44. https://doi.org/10.1002/bit.10741

Taweecheep, P., Naloka, K., Matsutani, M., Yakushi, T., Matsushita, K., & Theeragool, G. (2019a). Superfine bacterial nanocellulose produced by reverse mutations in the bcsC gene during adaptive breeding of Komagataeibacter oboediens. *Carbohydrate Polymers*, *226*(September), 115243. https://doi.org/10.1016/j.carbpol.2019.115243

Taweecheep, P., Naloka, K., Matsutani, M., Yakushi, T., Matsushita, K., & Theeragool, G. (2019b). Superfine bacterial nanocellulose produced by reverse mutations in the bcsC gene during adaptive breeding of Komagataeibacter oboediens. *Carbohydrate Polymers*, *226*(May), 115243. https://doi.org/10.1016/j.carbpol.2019.115243

Tayama, K., Fukaya, M., Okumura, H., Kawamura, Y., Horinouchi, S., & Beppu, T. (1994). Transformation of acetobacter polyoxogenes with plasmid dna by electroporation. *Bioscience, Biotechnology and Biochemistry*, *58*(5), 974–975. https://doi.org/10.1080/bbb.58.974

Teh, M. Y., Ooi, K. H., Danny Teo, S. X., Bin Mansoor, M. E., Shaun Lim, W. Z., & Tan, M. H. (2019). An Expanded Synthetic Biology Toolkit for Gene Expression Control in Acetobacteraceae [Research-article]. *ACS Synthetic Biology*, *8*(4), 708–723. https://doi.org/10.1021/acssynbio.8b00168

Tonouchi, N., Sugiyama, M., & Yokozeki, K. (2003). Construction of a vector plasmid for use in gluconobacte. *Bioscience, Biotechnology and*

Biochemistry, *67*(1), 211–213. https://doi.org/10.1271/bbb.67.211

Umeda, Y., Hirano, A., Ishibashi, M., Akiyama, H., Onizuka, T., Ikeuchi, M., & Inoue, Y. (1999). Cloning of cellulose synthase genes from Acetobacter xylinum JCM 7664: Implication of a novel set of cellulose synthase genes. *DNA Research*, *6*(2), 109–115. https://doi.org/10.1093/dnares/6.2.109

Uozumi, T., & Beppu, T. (1985). Construction of Plasmid Vectors and a Genetic Transformation System for Acetobacter aceti. *Agricultural and Biological Chemistry*, *49*(4), 1011–1017. https://doi.org/10.1271/bbb1961.49.1011

Verma, V., Qazi, G. N., & Parshad, R. (1992). Intergeneric protoplast fusion between Gluconobacter oxydans and Corynebacterium species. *Journal of Biotechnology*, *26*(2–3), 327–330. https://doi.org/10.1016/0168-1656(92)90016-3

Walsh, G. (2018). Biopharmaceutical benchmarks 2018. *Nature Biotechnology*, *36*(12), 1136–1145. https://doi.org/10.1038/nbt.4305

Wang, P., Zeng, W., Xu, S., Du, G., Zhou, J., & Chen, J. (2018). Current challenges facing one-step production of L-ascorbic acid. *Biotechnology Advances*, *36*(7), 1882–1899. https://doi.org/10.1016/j.biotechadv.2018.07.006

Watanabe, K., Tabuchi, M., Morinaga, Y., & Yoshinaga, F. (1998). Structural features and properties of bacterial cellulose produced in agitated culture. *Cellulose*, *5*(3), 187–200. https://doi.org/10.1023/A:1009272904582

Watanabe, K., & Yamanaka, S. (1995). Effects of Oxygen Tension in the Gaseous Phase on Production and Physical Properties of Bacterial Cellulose Formed Under Static Culture Conditions. *Bioscience, Biotechnology, and Biochemistry*, *59*(1), 65–68. https://doi.org/10.1271/bbb.59.65

Weinhouse, H., Sapir, S., Amikam, D., Shilo, Y., Volman, G., Ohana, P., & Benziman, M. (1997). C-di-GMP-binding protein, a new factor

regulating cellulose synthesis in Acetobacter xylinum. *FEBS Letters*, *416*(2), 207–211. https://doi.org/10.1016/S0014-5793(97)01202-7

Wilkins, M. R., Suryawati, L., Maness, N. O., & Chrz, D. (2007). Ethanol production by Saccharomyces cerevisiae and Kluyveromyces marxianus in the presence of orange-peel oil. *World Journal of Microbiology and Biotechnology*, *23*(8), 1161–1168. https://doi.org/10.1007/s11274-007-9346-2

Wong, H. C., Fear, A. L., Calhoon, R. D., Eichinger, G. H., Mayer, R., Amikam, D., Benziman, M., Gelfand, D. H., Meade, J. H., Emerick, A. W., Bruner, R., Ben-Bassat, A., & Tal, R. (1990). Genetic organization of the cellulose synthase operon in Acetobacter xylinum. *Proceedings of the National Academy of Sciences of the United States of America*, *87*(20), 8130–8134. https://doi.org/10.1073/pnas.87.20.8130

Woodley, J. M. (2020). New frontiers in biocatalysis for sustainable synthesis. *Current Opinion in Green and Sustainable Chemistry*, *21*, 22–26. https://doi.org/10.1016/j.cogsc.2019.08.006

Wu, R. Q., Li, Z. X., Yang, J. P., Xing, X. H., Shao, D. Y., & Xing, K. L. (2010). Mutagenesis induced by high hydrostatic pressure treatment: A useful method to improve the bacterial cellulose yield of a Gluconoacetobacter xylinus strain. *Cellulose*, *17*(2), 399–405. https://doi.org/10.1007/s10570-009-9388-8

Wu, S., Snajdrova, R., Moore, J. C., Baldenius, K., & Bornscheuer, U. T. (2021). Biocatalysis: Enzymatic Synthesis for Industrial Applications. *Angewandte Chemie - International Edition*, *60*(1), 88–119. https://doi.org/10.1002/anie.202006648

Zdobnov, E. M., & Apweiler, R. (2001). InterProScan - an integration platform for the signature-recognition methods in InterPro. *Bioinformatics*, *17*(9), 847–848. https://doi.org/10.1093/bioinformatics/17.9.847

Zhang, L., Lin, J., Ma, Y., Wei, D., & Sun, M. (2010). Construction of a novel shuttle vector for use in gluconobacter oxydans. *Molecular*

Biotechnology, *46*(3), 227–233. https://doi.org/10.1007/s12033-010-9293-2

Zhang, Y. X., Perry, K., Vinci, V. A., Powell, K., Stemmer, W. P. C., & Del Cardayré, S. B. (2002). Genome shuffling leads to rapid phenotypic improvement in bacteria. *Nature*, *415*(6872), 644–646. https://doi.org/10.1038/415644a

Zheng, Y., Zhang, K., Su, G., Han, Q., Shen, Y., & Wang, M. (2015). The evolutionary response of alcohol dehydrogenase and aldehyde dehydrogenases of Acetobacter pasteurianus CGMCC 3089 to ethanol adaptation. *Food Science and Biotechnology*, *24*(1), 133–140. https://doi.org/10.1007/s10068-015-0019-x

Zheng, Y., Zhang, K., Wang, C., Liu, H., Luo, J., & Wang, M. (2010). Improving acetic acid production of Acetobacter pasteurianus AC2005 in hawthorn vinegar fermentation by using beer for seed culture. *International Journal of Food Science and Technology*, *45*(11), 2394–2399. https://doi.org/10.1111/j.1365-2621.2010.02413.x

Zhong, C. (2020). Industrial-Scale Production and Applications of Bacterial Cellulose. In *Frontiers in Bioengineering and Biotechnology* (Vol. 8, p. 605374). Frontiers Media S.A. https://doi.org/10.3389/fbioe.2020.605374

Conclusions and future prospects

The major objective of this PhD thesis was to develop new biocatalytic and fermentative methods for the valorization of agricultural and industrial waste residues. In particular, the work has been designed to exploit the citrus pulp industry and biorefinery wastes for the production of added-value compounds. In the second chapter we characterized a cytochrome P450 CYP153A6 monooxygenase employing *E. coli* as host strain. P450 CYP153A6 monooxygenase was chosen for AAB transformation as a promising enzyme due to its high regioselectivity especially on limonene. We demonstrated the employment of CYP153A6 for the hydroxylation of the allylic methyl group of limonene and other terpenes to the corresponding alcohols. Then in the third chapter, we cloned the CYP153A6 operon into acetic acid bacteria (*Komagataeibacter xylinus* and *Acetobacter malorum*) employing different molecular approaches. The work was aimed at optimizing the biocatalytic conditions for the biotransformation of limonene to perillic acid. Furthermore, in the same chapter, we proposed a molecular GFP biosensor, called “cumate induction system”, to detect in the culture media the presence of perillic acid, derived from limonene biotransformation. In chapter four we demonstrated how the *Komagataeibacter xylinus* engineered strains might be used as effective biocatalysts for the valorization of orange peel wastes. We optimized the fermentation conditions employing orange peel juice as culture media to transform the limonene, naturally contained in the OPJ, into perillic acid. Future investigation should be focused on the scale up of OPJ in large scale fermenters, to achieve a significant amount of perillic acid production. In the last chapter we isolated and characterized a novel bacterial cellulose producer strain namely *Komagataeibacter rhaeticus ENS9b.* Differently from other BC producers, we showed that *ENS9b* was able to produce BC from acetate and crude glycerol, both by-products from the biodiesel production process.

From our perspective, the main novelties of this PhD thesis are related to the employment of recombinant AAB for biocatalysis. Another important outcome

worth to be mentioned is the utilization of the cumate induction system for the detection of perillic acid.

Scientific production

Papers included in this PhD thesis

Whole recombinant cells of E. coli harboring cytochrome CYP153A as biocatalyst for regioselective hydroxylation of monoterpene derivatives (Preprint).

Expression of cytochrome CYP153A6 in acetic acid bacteria: preparation of new biocatalysts for converting hydrocarbons into aldehydes and carboxylic acids (Preprint).

Optimization of molecular and fermentative approaches for the valorisation of limonene from orange peel wastes employing *K. xylinus* (Preprint).

Characterization of Komagataeibacter isolate reveals new prospects on waste stream valorization for bacterial cellulose production. Cannazza, P., Rissanen, A. J., Guizelini, D., Losoi, P., Sarlin, E., & Romano, D. August, 2021. https://doi.org/10.20944/preprints202108.0312.v1

Papers not included in this PhD thesis

Contente, M. L., Annunziata, F., **Cannazza, P.** et al., 2021. Biocatalytic Approaches for an Efficient and Sustainable Preparation of Polyphenols and Their Derivatives. Journal of Agricultural and Food Chemistry.

Rabuffetti, Marco, **Cannazza P.**, Martina Letizia, Andrea Pinto, Diego Romano, Pilar Hoyos, Andres R. Alcantara, Ivano Eberini, Tommaso Laurenzi, Louise Gourlay, Flavio Di Pisa and Francesco Molinari. 2021. “Bioorganic Chemistry Structural Insights into the Desymmetrization of Bulky 1 , 2-Dicarbonyls through Enzymatic Monoreduction.” Bioorganic Chemistry 108.

Contente, Martina L., Noemi Fiore, **Cannazza P.**, David Roura Padrosa, Francesco Molinari, Louise Gourlay, and Francesca Paradisi. 2020. “Uncommon Overoxidative Catalytic Activity in a New Halo-Tolerant Alcohol Dehydrogenase.” ChemCatChem 1–8.

Laurent, Christophe V. F. P., Peicheng Sun, Stefan Scheiblbrandner, Florian Csarman, **Cannazza P.**, Matthias Frommhagen, Willem J. H. van Berkel, Chris Oostenbrink, Mirjam A. Kabel, and Roland Ludwig. 2019. “Influence of Lytic Polysaccharide Monooxygenase Active Site Segmentson Activity and Affinity.” International Journal of Molecular Sciences 20(24).

Poster communications

Cannazza P. Biocatalytic and fermentative approaches for the production of added value compounds from food wastes using recombinant bacteria. International Synthetic & Systems Biology Summer School – SSBSS 2019 at Scuola Normale Superiore, Pisa – Tuscany – Italy / July 22-26, 2019. Summer school e Workshop.

Cannazza P. XXIV Workshop on the developments in the Italian PhD Research on food science, technology and biotechnology, Florence, 11-13 September 2019. Poster.

Christophe V.F.P. Laurent, P. Sun, **P. Cannazza**, et al. Structural modifications to *Neurospora crassa* LPMO9C and their effect on the catalytic activity, 4th International Symposium on Biocatalysis and Biotransformations (BioTrans 2019), July 7-11, 2019, Groningen, The Netherlands. Poster.

Oral communications

Cannazza P., Romano D, Molinari F: "Biocatalytic approaches for the production of added value compounds using genetically modified acetic acid bacteria". “The Next Generation of Biocatalysis” Bern 27-28 may, 2021

Cannazza P. “Biocatalytic and fermentative approaches for the production of added value compounds using wild type and genetically modified acetic acid bacteria”. First Virtual Workshop on the Developments in Italian PhD Research on Food Science, Technology and Biotechnology 15th September 2021– Palermo, Italy